

School of Doctoral Studies in Biological Sciences
University of South Bohemia in České Budějovice
Faculty of Science



Role of IDGFs and adenosine signaling in cell survival and energy homeostasis

Ph.D. Thesis

Mgr. Václav Brož

Supervisor: Prof. RNDr. Michal Žurovec, CSc.

Faculty of Science, University of South Bohemia

Biology Centre of the Czech Academy of Sciences, Institute of Entomology

České Budějovice 2017

This thesis should be cited as:

Broz, V., 2017: Role of IDGFs and adenosine signaling in cell survival and energy homeostasis. Ph.D. Thesis. University of South Bohemia, Faculty of Science, School of Doctoral Studies in Biological Sciences, České Budějovice, Czech Republic, 167 pp.

■ Annotation

Two groups of growth regulators were described in *Drosophila* imaginal disc cell culture Cl.8+ - Imaginal disc growth factors (IDGFs) belonging to chitinase-like protein family of carbohydrate binding proteins and Adenosine deaminase-related growth factors (ADGFs), which are active adenosine deaminases influencing homeostasis of key cellular metabolite adenosine. The functions of two of the IDGFs, as well as the effects of extracellular adenosine and its receptor were studied primarily in *in vitro* cell culture. The results supported the role in the regulation of cell survival and energy homeostasis especially in imaginal disc cells. Both the IDGFs and adenosine also seem to play important roles in organismal responses to stress and infection and may interact *in vivo*.

■ Declaration [in Czech]

Prohlašuji, že svoji disertační práci jsem vypracoval samostatně pouze s použitím pramenů a literatury uvedených v seznamu citované literatury.

Prohlašuji, že v souladu s § 47b zákona č. 111/1998 Sb. v platném znění souhlasím se zveřejněním své disertační práce, a to v úpravě vzniklé vypuštěním vyznačených částí archivovaných Přírodovědeckou fakultou elektronickou cestou ve veřejně přístupné části databáze STAG provozované Jihočeskou univerzitou v Českých Budějovicích na jejích internetových stránkách, a to se zachováním mého autorského práva k odevzdanému textu této kvalifikační práce. Souhlasím dále s tím, aby toutéž elektronickou cestou byly v souladu s uvedeným ustanovením zákona č. 111/1998 Sb. zveřejněny posudky školitele a oponentů práce i záznam o průběhu a výsledku obhajoby kvalifikační práce. Rovněž souhlasím s porovnáním textu mé kvalifikační práce s databází kvalifikačních prací Theses.cz provozovanou Národním registrem vysokoškolských kvalifikačních prací a systémem na odhalování plagiátů.

České Budějovice, 2. 5. 2017

.....

Václav Brož

This thesis originated from a partnership of Faculty of Science, University of South Bohemia, and Institute of Entomology, Biology Centre of the CAS, supporting doctoral studies in the Molecular and Cell Biology and Genetics study programme.



Přírodovědecká
fakulta
Faculty
of Science

Jihočeská univerzita
v Českých Budějovicích
University of South Bohemia
in České Budějovice



BIOLOGICKÉ
CENTRUM
AV ČR, v. v. i.



Entomologický ústav
Institute of Entomology

■ Financial support

This work was supported by:

The Grant Agency of the ASCR, grant KJB501410801

The Grant Agency of the Czech Republic, grant P305/10/2406

The Czech Science Foundation, grant P305/14-27816S and 14-07172S

The European Community's Seventh Framework Program (FP7/2007-2013)
under grant agreement No. 229518

The Research Center Program MSMT– LC06077

The Grant Interreg Bayern - Tschechische Republik Ziel ETZ 2014-2020 No. 123

■ Acknowledgements

I would like to thank to my supervisor, Michal Zurovec, for the opportunity to work on such a challenging topic. I appreciate his never-ending enthusiasm for science. I also thank my colleagues and friends for supporting my. Finally, I would like to express many thanks to Iveta, for pushing me to finish this work.

■ List of publications and author's contribution

The thesis is based on the following publications:

- I. **Vaclav Broz, Lucie Kucerova, Lenka Rouhova, Jana Fleischmannova, Hynek Strnad, Peter J. Bryant & Michal Zurovec (2017) *Drosophila* imaginal disc growth factor 2 is a trophic factor involved in energy balance, detoxification, and innate immunity. *Scientific Reports* 7:43273**

Vaclav Broz produced recombinant IDGF2 protein, performed cell culture experiments and assays, measured concentration of IDGF2 in the haemolymph and prepared transgenic fly line carrying fused IDGF2 protein with GFP. He prepared the manuscript for publication in cooperation with Michal Zurovec.

- II. **Lucie Kucerova, Vaclav Broz, Md. Badrul Arefin, Houda Ouns Maaroufi, Jana Hurychova, Hynek Strnad, Michal Zurovec & Ulrich Theopold. (2015) The *Drosophila* Chitinase-Like Protein IDGF3 is involved in protection against nematodes and in wound healing. *Journal of Innate Immunity* 8(2):199-210**

Vaclav Broz prepared transgenic fly line carrying fused IDGF3 protein with GFP.

- III. **Jana Fleischmannova, Lucie Kucerova, Katerina Sandova, Veronika Steinbauerova, Vaclav Broz, Petr Simek and Michal Zurovec (2012) Differential response of *Drosophila* cell lines to extracellular adenosine. *Insect Biochemistry and Molecular Biology* 42: 321-331**

Vaclav Broz cultivated *Drosophila* cell lines and performed some in vitro experiments

- IV. **Lucie Kucerova, Vaclav Broz, Jana Fleischmannova, Roman Sidorov, Vladimir Dolezal and Michal Zurovec (2012) Effects of adenosine analogs on *Drosophila* adenosine receptor: the effect of adenosine analogs on cAMP signaling in *Drosophila* cells and their utility for in vivo experiments. *Journal of Neurochemistry* 121: 383–395**

Vaclav Broz cultivated *Drosophila* cell lines and performed measurements of cAMP response to adenosine agonist and antagonists.

Michal Zurovec, the corresponding author of the manuscripts, confirms the contribution of Vaclav Broz in these publications as described above.



prof. RNDr. Michal Žurovec, CSc.

■ Contents

1.	Introduction	1
1.1.	Regulation of cellular homeostasis in insect cells	1
1.2.	Adenosine signaling	2
1.2.1	Adenosine as a growth regulator.....	2
1.2.2	Adenosine receptor	4
1.3.	Chitinases and chitinase-like proteins	5
1.3.1.	Structure of CLPs and their binding of glycans	6
1.3.2.	Mammalian CLPs.....	8
1.3.3.	IDGFs	8
2.	Aims	12
3.	Summary	13
4.	Results	17
4.1.	Publication I	17
4.2.	Publication II	60
4.3.	Publication III	126
4.4.	Publication IV	142
5.	Conclusion and future perspectives	159
6.	References	161
7.	Curriculum vitae	166

List of abbreviations

ADA	adenosine deaminase
ADGF	Adenosine Deaminase-related Growth Factors
Ado	adenosine
AdoR	Adenosine receptor
cAMP	cyclic adenosine monophosphate
CLP	chitinase-like protein
CM	complete medium
CNT	Concentrative Nucleoside Transporters
dAdo	2-deoxyadenosine
dAkt/PKB	protein kinase B
ENT	Equilibrative Nucleoside Transporters
EPN	entomo pathogenic nematodes
GalN	galactoseamine
GFP	green fluorescent protein
GH18	family 18 chitinases or glycoside hydrolase 18 proteins
GlcN	glucosamine
GlcNAc	<i>N</i> -acetylglucosamine
IDGF	Imaginal Disc Growth Factors
Imd	Immune deficiency signaling pathway
JAK-STAT	The Janus kinase and signal transducers and activators of transcription signaling pathway
JNK	c-Jun N-terminal kinases
MAP	mitogen-activated protein kinase
MM	chemically defined medium or minimal medium
PI3K	Phosphatidylinositol-4,5-bisphosphate 3-kinase
RNAi	RNA interference
SFM	supplement-free medium

TIM	triose-phosphate isomerase
TMRE	tetramethylrhodamine ethyl ester
Wg/Wnt	Wingless signaling pathways
$\Delta\Psi_m$	mitochondrial membrane potential

1. Introduction

1.1. Regulation of cellular homeostasis in insect cells.

Drosophila is the most important model organism in biological research, particularly in genetics and developmental biology. The current diabetes pandemic as well as the importance of metabolic homeostasis in cancer etiology aroused high interest in studies of body metabolism and its control. The conservation of organ systems and basic metabolic regulatory circuits predetermine *Drosophila* as an excellent model for studying metabolic homeostasis. Improved understanding of the control of organ specific metabolism can prevent failures and dysregulation of these pathways, which can lead to disease.

Insects have organ systems that carry out basically the same metabolic function as their counterparts in vertebrates (Leopold and Perrimon, 2007). For example, insect fat body and vertebrate livers are reservoirs of triglycerides, which can be mobilized when needed. Muscles and neural tissue consume high amounts of energy, however, unlike muscles, neural tissue cannot fluctuate during periods of energy shortages (Ellison, 2001). Sugars are the most important source of metabolic fuel and their cellular import and export are tightly regulated. Energy homeostasis occurs through tight regulation by numerous local factors. Many of the basic metabolic regulatory circuits are conserved between insects and vertebrates. Hence, for example, in response to elevated levels of circulating sugar, flies secrete insulin. Flies also mobilize stored energy in response to a hormone related to glucagon. In addition, flies can even develop similar metabolic conditions as people, and thus can develop type 2 diabetes if exposed to a high-sugar food (Barry and Thummel, 2016).

Research on mammalian *in vitro* cell cultures provided key information on tissue specific growth requirements of various cell types including mitogenic growth factors, hormones or serum proteins. Interestingly, studies of insect cells *in vitro* were scarce because of a lack of defined *in vitro* systems or growth media composition and gene products with mitogenic or other biochemical activities. After sequencing of *Drosophila* genome the insect cell cultures became important tool for whole genome RNAi screenings focused on morphological changes, interactions with pathogens or missing components of various signaling pathways (Baeg et al., 2005; D'Ambrosio and Vale, 2010; Foley and O'Farrell, 2004).

Several important *Drosophila* cell lines became widely used, including S2 cells derived from *Drosophila* whole embryos. (Schneider, 1971); Mbn-2 are haematopoietic cells derived from the now lost mutant *l(3)mbn* (Samakovlis et al., 1992). Bg2-c2 neuroblasts, derived from *Drosophila* larval central nervous system (Ui et al., 1994), Cl.8+ cells were derived by cloning from third instar wing imaginal disc cell line originally designated CME W1 (Currie et al., 1988). The Cl.8+ imaginal disc cell line seems to be the most interesting, because they perform extensive morphological changes depending on growth conditions.

Two groups of growth regulators were described in insect imaginal disc cell line Cl.8+. The first group has six members named Adenosine deaminase-related growth factors (ADGF-A, -A2, -B, -C and -D) representing active adenosine deaminase enzymes influencing homeostasis of key cellular metabolite adenosine (Zurovec et al., 2002). The second group also contains six members and is called Imaginal disc growth factors (IDGF-1-6) belonging to chitinase-like protein family and are able to bind numerous proteins on cell surface (Kawamura et al., 1999). Functions of both types of these growth regulators seem to be evolutionary conserved, but mechanisms of their function are not fully understood.

1.2. Adenosine signaling

1.2.1. Adenosine as a growth regulator

Adenosine (Ado) is a ubiquitous metabolite and a widespread signaling molecule that is generated and released from cells following injury or stress. It promotes processes important in both metabolic imbalance and tissue protection. Although it is difficult to observe Ado effects during normal physiological conditions, its role is more evident in various pathological situations, including neurological, cardiovascular, inflammatory diseases, and cancer (Fredholm et al., 2011). Physiological concentrations of Ado are relatively low ranging from 0.06-0.3 μM in *Drosophila* and 0.05-0.4 μM in humans, however it may locally increase to the micromolar range under stressful conditions (Dolezelova et al., 2007). Changes in cytosolic Ado concentrations also affect mitochondrial adenosine level and mitochondrial bioenergetics (Boison et al., 2002).

Several proteins modulate the extracellular concentration of adenosine, including nucleoside transporters, ecto-5'-nucleotidases and Ado deaminases (Dolezelova et al., 2005; Fenckova et al., 2011; Hirsh et al., 2007). Elevated level of extracellular Ado in *Drosophila* hemolymph is lethal, as shown in the mutants in the *Adgf-A* gene (Dolezal et al., 2005;

Dolezal et al., 2003). Ado transfer across the plasma membrane is mediated by equilibrative nucleoside transporters (ENTs) and concentrative nucleoside transporters (CNTs), respectively (Pastor-Anglada et al., 2007). The transporters function in the salvage pathways of nucleotide synthesis. Null mutants in the *Drosophila* Equilibrative nucleoside transporter 2 (*Ent2*) are also homozygous lethal, while *Ent2* hypomorphs show defects in synaptic transmission and associative learning (Knight et al., 2010).

Ado signaling and metabolism are conserved among phyla, but the number of genes involved in flies is lower than in mammals. *Drosophila* has a single adenosine receptor, three ENTs, and two CNTs (Fleischmannova et al., 2012). The closest human homolog of *Drosophila* Ado receptor (*AdoR*) is *A2A AR*, having 38% identity within 350 N-terminal amino acids. Given the conservation of Ado signaling studies on *Drosophila* will contribute both conceptually and practically to our understanding of the role of Ado in organisms.

There is a large amount of literature reporting Ado-induced growth arrest or cell death (Henderson and Scott, 1980; Merighi et al., 2002; Ohkubo et al., 2007; Peyot et al., 2000; Schrier et al., 2001). Numerous reports also described cytoprotective effects of Ado, especially on myocardial and neural cells during ischemia (Barankiewicz et al., 1997; Ely and Berne, 1992). Consistently, mammalian receptor subtypes were shown to have antiproliferative and apoptotic, as well as prosurvival function depending on the cell type and applied Ado concentration (Ohana et al., 2001). Activation of AdoR may negatively influence cell survival via activation of cAMP, Ca²⁺, or MAP kinase cascades (Kizaki et al., 1990; Merighi et al., 2005; Szondy, 1994). It was recently shown that Ado transporters might play an important role in cellular metabolism independent of Ado receptor signaling. (Ohkubo et al., 2007; Wu et al., 2006). Moreover, synergistic effect of both Ado uptake and signalling in apoptosis induction has also been reported in some cell lines (Di Iorio et al., 2002).

The research on *Drosophila* also shows that elevated level of extracellular Ado can have both cytotoxic or cytoprotective effects. In my thesis we have studied effects of Ado on several cell lines. Our results are described in the publication "*Differential response of Drosophila cell lines to extracellular adenosine*".

1.2.2. Adenosine receptor

Most physiological effects of Ado are mediated by cell surface G protein-coupled Ado receptors (AdoRs). Four well-characterized AdoR (A1, A2A, A2B, and A3) with partially overlapping functions are known in mammals. Two of the receptors, A1 and A3, inhibit cyclic adenosine monophosphate (cAMP) production, whereas A2A and A2B stimulate adenylyl cyclase (Fredholm, 2010). The normal physiological roles of Ado receptors in mice were studied using knockouts of relevant genes. These experiments revealed relatively small differences between mutant and wild-type mice, suggesting there might be some compensatory changes in Ado signal. However, this was not studied systematically, and a mouse with the knockout of all four Ado receptors has not yet been prepared. Detecting the pathophysiological roles of Ado receptors has been more difficult because it requires models of disease in genetically modified organisms (Pandey and Nichols, 2011).

The AdoR studies in mammals are focused on determining which Ado receptor mediates the particular physiological function. In addition, a number of AdoR ligands display much better metabolic stability than adenosine and selectivity for individual receptor subtypes were characterized. A detailed structure of the human A2AR has been solved and co-crystallization was performed with adenosine or some agonists and antagonists (Jaakola et al., 2008; Lebon et al., 2011; Xu et al., 2011). Contact amino acid residues for binding of these adenosine analogs were elucidated.

Drosophila has a single AdoR and *AdoR* null mutants, which are viable and show no obvious phenotypic changes (Dolezelova et al., 2007; Wu et al., 2009). *Drosophila* genetic methods and lower complexity of this model having only a single AdoR subclass provides unique opportunity to investigate local Ado signaling, its role in maintaining tissue integrity and homeostasis, as well as its cross talk with systemic organismal responses.

In my thesis we focused on the problem of identifying a specific second messenger pathway that is activated by the AdoR in *Drosophila* cells and establishing a general pharmacological profile of the receptor. It was also important for further research to find AdoR analogs with higher metabolic stability than adenosine. Our results are described in the publication “ Effects of adenosine analogs on *Drosophila* adenosine receptor: the effect of adenosine analogs on cAMP signaling in *Drosophila* cells and their utility for in vivo experiments”.

1.3. Chitinases and chitinase-like proteins

Chitinases are enzymes that hydrolyze chitin - the linear polymer of β -1,4-linked N-acetylglucosamines. Chitinases are classified into two families, family 18 and family 19, based on the conservation of amino acid sequences (Coutinho and Henrissat, 1999). The family 18 chitinases, or glycoside hydrolase 18 (GH18) proteins, characterized by an enzyme core, which has 8 strands of parallel β sheets, creating a barrel forming a ring, so called $(\alpha\beta)_8$ TIM barrel fold (Rathore and Gupta, 2015). The family 18 chitinases are evolutionary old proteins, widely distributed in all kingdoms, including bacteria, plants and animals. The family 18 chitinases consists of active enzymes as well as chitinase-like proteins (CLPs) with abrogated enzymatic activity, but still able to bind carbohydrates. It was proposed that CLPs may have evolved from chitinases and acquired new properties as carbohydrate binding proteins activating some surface glycoproteins (Varela et al., 2002). The most extensive expansion of the number of GH18 genes with distinctive TIM barrel modular architecture seems to occur within the protostomes highly metabolizing chitin including nematodes and insects (Arakane and Muthukrishnan, 2010; Funkhouser and Aronson, 2007).

Human genome contains at least three of the GH18 proteins with demonstrated enzymatic activity - including di-N-acetylchitobiase, chitotriosidase and acidic mammalian chitinase (AMCase), as well as another gene closely related to the AMCase, but carrying a truncated GH18 domain (Kuranda and Aronson, 1986). In addition, human genome also has four CLPs, including chitinase 3-like 1 protein (CHI3L1 or YKL-40 or HC gp-39), chitinase 3-like 2 protein (CHI3L2 or YKL-39), oviduct-specific glycoprotein (oviductin or Mucin 9) and stabilin-1 interacting chitinase-like protein (SI-CLP) (Ranok et al., 2015). The CLP group seems to undergo expansion in late deuterostomes (Funkhouser and Aronson, 2007).

The *D. melanogaster* GH18 protein family contains sixteen members including ten active chitinase enzymes and six CLP proteins called Imaginal disc growth factors (IDGFs) (Zhu et al., 2008). It seems that *Drosophila*, like other higher Diptera, contains more CLP genes than other insects. Clustering of related Idgf genes on chromosomes and their mutual sequence identity of approximately 50% suggest their recent duplication in this insect group. All *D. melanogaster* Idgfs carry an amino acid substitution that is known to abrogate chitinase catalytic activity. This substitution involves the terminal glutamate for glutamine in

the conserved active site sequence motif DXXDXDXE (Kawamura et al., 1999; Watanabe et al., 1992).

For comparison, a search for the GH18 family members in the *C. elegans* genome identified 37 genes or predicted genes encoding chitinases and related CLPs (Funkhouser and Aronson, 2007). Interestingly, three members of the CLPs (Cg-Clp1, Cg-Clp2 and Cg-Clp3) were reported in the bivalve mollusc *Crassostrea gigas* (Badariotti et al., 2007). It seems that human and mollusc CLPs also evolved from active chitinases independently by convergent evolution, but they have the same function and the human homolog YKL-40 can be substituted for the mollusc Clp1 (Badariotti et al., 2007, 2011).

Despite the fact that mammalian and insect CLPs have similar structural features and biological function, they seem to have evolved from chitinases independently (Funkhouser and Aronson, 2007). Interestingly, no CLPs were found in the nearly complete *D. discoideum* genome suggesting that the expansion of CLPs and other GH18 genes must have occurred in protostomes *C. elegans* and *D. melanogaster*, together with the appearance of chitinous structures in these species (Funkhouser and Aronson, 2007), while in vertebrates their presence in gastric juices suggests their association with chitin digestion (Hamid et al., 2013). Interestingly, part of the family members in both invertebrates and vertebrates lost their enzymatic function and are associated with cell growth.

1.3.1. Structure of CLPs and their binding of glycans

The crystal structure of several CLP is known (*Drosophila* IDGF2, murine Ym1 and human YKL-40, YKL-39 and SI-CLP) (Fusetti et al., 2003; Meng et al., 2010; Schimpl et al., 2012; Sun et al., 2001; Varela et al., 2002). All members of the family 18 Glycosyl Hydrolases have the classical $(\alpha\beta)_8$ barrel-fold, also called the TIM (triose-phosphate isomerase) barrel with eight-stranded parallel β sheets surrounded by eight α helices antiparallel to the β barrel. Moreover, there is an additional domain with an $\alpha\beta$ fold, which is between the strand $\beta 7$ and helix $\alpha 7$. Interestingly, this motif is found in most of the chitinase-like proteins described to date. There are two *cis* peptide bonds, which are conserved in all family 18 chitinases and none of them involves a proline residue. They seem to be necessary for correct barrel folding. There are two disulfide bridges in the molecule of all CLPs as well as the Cys residues are conserved in all CLPs (Varela et al., 2002).

In ($\alpha\beta$)₈ barrel enzymes, the β sheets and the α helices are doing the scaffold of the enzyme. The active side or the sugar binding pocket is formed by the loops between them. These loops can be variable in length and amino acid composition. In all CLPs, the sugar binding groove is located across the C-terminal ends of the β -strands of the TIM barrel. The sugar binding is done by the hydrophobic stacking interactions of the aromatic residues located around the surface of the binding pocket with the hydrophobic sides of the bound sugar rings (Fusetti et al., 2003).

The human CLP members, as well as *Drosophila* IDGF6 protein and the *Tribolium* homologs of IDGF2 and IDGF4 bind to chitin. It was shown by x-ray crystallography and by glycan screen method that YKL-40, YKL-39 and SI-CLP bind to oligomers of *N*-acetylglucosamine (Fusetti et al., 2003; Meng et al., 2010; Ranok et al., 2015; Zhu et al., 2007). Unfortunately, *Drosophila* and *Tribolium* members were examined only by colloidal chitin binding assay. More rigorous assays would be needed in order to examine exact binding specificity, for example by glycan screen involving hundreds of glycans in an array.

It was shown, that YKL-40 and SI-CLP interact with membrane receptors, YKL-40 with Syndecan-1 and SI-CLP with Stabilin-1 (Bharadwaj et al., 2009; Kzhyshkowska et al., 2006). It would be interesting to look at the glycosylation of these proteins, if they contain a chitin moiety. It was also shown, that human CLPs preferentially bind to chitin polymers composed of four or more GlcNAc residues by occupying the central part of the groove, whereas shorter oligosaccharides bind preferentially at the more distant subsites on the protein surface (Fusetti et al., 2003). Although YKL-40 was shown to bind chitin, an affinity chromatography experiment demonstrated specific binding of YKL-40 to collagen types I, II, and III, thus identifying collagens as its potential ligands (Bigg et al., 2006). Furthermore, YKL-40 was reported to bind heparin or heparan sulfate. This is accomplished by the cluster of basic amino acid residues, which are also found in other heparin binding proteins. This putative heparin-binding site is located elsewhere than the sugar binding groove and it was not possible to prove the binding to heparin with co-crystallization experiments (Fusetti et al., 2003).

Interestingly, the murine member of the CLP family, Ym1, has a different saccharide-binding specificity and prefers the moieties with a free amine group, such as GlcN or GalN polymers instead of chitin. Specific binding of Ym1 to heparin indicates that heparin or heparan sulfate may represent the preferred *in vivo* ligands (Sun et al., 2001).

1.3.2. Mammalian CLPs

Mammalian and insect CLPs seem have similar biological roles in cell growth regulation and innate immune response. Human YKL-40 is the most studied member of these enzymatically-inactive CLPs. YKL-40 was reported to regulate responses to bacteria, cell death, inflammation and tissue remodeling by a mechanism that is still poorly understood (He et al., 2013; Johansen et al., 1995; Zhou et al., 2014). Its closely related homologue YLK-39 is a non-glycosylated, secretory protein discovered in the primary culture of human articular chondrocytes. However, its expression pattern indicates a role in autoimmune response and connective tissue remodeling. Oviductin is the most distant member of the human CLPs and is suggested to play a role in fertilization. It is exclusively expressed and secreted by oviductal epithelium (Arias et al., 1994; Malette et al., 1995). SI-CLP is the last described member of the human CLP family. SI-CLP has a known binding partner, the receptor Stabilin-1. It is suggested, that its role will be close to YKL-40 in tissue remodeling. Elevated levels of YKL-40 and also other human CLPs have been associated with numerous autoimmune diseases and also in a broad spectrum of cancers. YKL-40 became a biomarker for poor prognosis of survival in cancer patients. Human CLPs have been shown to affect cancer development and could be a good treatment choice (Shao et al., 2010). Because the serum levels of CLPs are elevated in multiple pathological events their function is speculated to be associated with tissue homeostasis and remodeling.

It seems that vertebrate CLPs influence cell homeostasis by binding to carbohydrate moieties of a number of surface receptors. This binding seems to be necessary for their function. CLPs are sometimes called “chitolectins” and are included among 15 presently known families of animal lectins, which mediate a variety of biological processes, including cell-cell and host-pathogen interactions, serum-glycoprotein turnover, and innate immunity responses (Gupta et al., 2012).

1.3.3. IDGFs

1.3.3.1. Effects of *Drosophila* IDGFs in tissue culture *in vitro*

Drosophila IDGF proteins were described as secretory proteins produced by larval fat body and haemocytes, able to cooperate with insulin to stimulate proliferation, polarization and motility of imaginal disc cells Cl.8+ *in vitro* (Kawamura et al., 1999). It seems that various

IDGFs are secreted by many different cell types in culture suggesting that they play important roles as mitogenic factors (Kirkpatrick et al., 1995). The mechanism of their effect is not known. Kawamura et al. suggested that IDGF2 and other IDGFs support growth of imaginal disc Cl.8+ cells because it works as a cofactor of insulin, probably by binding to a glycan moiety of the insulin receptor (Kawamura et al., 1999).

In order to examine the effect of IDGFs on the proliferation of *Drosophila* Cl.8+ cells, we choose the IDGF2 as prototypical member of IDGF family with known crystal structure. We focused our experiments on the examination of the relationship of IDGF2 to insulin, measurement of physiological concentration of IDGF2 in *Drosophila* hemolymph and examination, whether IDGF2 could protect cells from death caused by serum deprivation, toxicity of xenobiotics or high concentrations of extracellular adenosine and deoxyadenosine. Our results are described in the publication "*Drosophila* imaginal disc growth factor 2 is a trophic factor involved in energy balance, detoxification and innate immunity".

1.3.3.2. IDGF expression in *Drosophila* in vivo under normal conditions

IDGFs are a family of six chitinase-like *Drosophila* hemolymph proteins with similar pattern of expression. They were localized in yolk and cephalic furrow of the early embryo and in the vicinity of embryonic larval tracheal system in later embryonic stage (Kawamura et al., 1999). In larval stage they are mainly produced by fat body and haemocytes. The highest expression in adults was detected in nurse cells.

The IDGFs make up 10 % of all hemolymph proteins. The expression pattern of larval haemocytes showed mainly the expression of *Idgf1*, *Idgf2* and *Idgf3*. Moreover, the lymph gland, the hematopoietic organ of *Drosophila* larvae, shows a strong expression of *Idgf1* (Irving et al., 2005). IDGF4 and IDGF6 were detected in imaginal discs (Irving et al., 2005; Karlsson et al., 2004) and *Idgf2* in the eye disc (Michaut et al., 2003).

1.3.3.3. IDGF responses to various stimuli in vivo

Idgfs transcriptionally respond to aseptic injury and also to challenge with gram negative and gram positive bacteria as shown by microarray experiments using the whole adult flies (De Gregorio et al., 2001). The expression profile of adult flies deficient in Toll, Imd or in both pathways in systematic response to microbial infection revealed the induction of *Idgf1* and *Idgf3*. *Idgf1* is an acute response gene, the up-regulation reach the maximum just

after one hour after injury and then the expression is dropping. Instead, *Idgf3* is a sustained response gene. The up-regulation is constant from the time of injury for the next 48 hours. Moreover, *Idgf3* expression is abolished in Imd and Toll double mutants, *Idgf3* seems to be regulated by both pathways independently. The expression of *Idgf1* is not dependent on these two immune pathways (De Gregorio et al., 2002).

Similarly, Idgfs were also detected in tissue responses by examining fly's intestine-responses to bacterial infection. The results suggested that the gut immune responses were regulated by the Imd and JAK-STAT pathways, but not by the Toll pathway. Moreover, gut response to the Gram-negative bacterium infection revealed the up-regulation of *Idgf1* and *Idgf3* (Buchon et al., 2014). Constitutive activation of the JAK/STAT pathway also up-regulates *Idgf1* (Kwon et al. 2008). Interestingly, the JAK-STAT pathway seems to regulate the expression of *Idgf1*, but a genome-wide RNAi analysis revealed that there is no positive feedback loop from *Idgf1* to JAK/STAT (Baeg et al., 2005). One more RNAi screen found no Idgf gene connected with the activation of the Imd pathway in *Drosophila* S2 cells. Knock-down of Idgf genes, one by one, was analyzed for their effect on Imd pathway activity in response to gram negative bacterium stimulus (Kleino et al., 2008).

No microarray analysis was performed on immune-stimulated *Drosophila* larvae, however, interesting data come from a proteome study. The hemolymph proteome of *Drosophila* larvae after immune challenge with Gram-positive bacteria or yeast showed the up-regulation of IDGF2 protein in the hemolymph (Vierstraete et al., 2003). In addition, the IDGFs are also found in the hemolymph clot, which is rapidly formed after injury (Karlsson et al., 2004).

The Idgfs respond to nutritional conditions. The transcriptional response to starvation stress involved the up-regulation of genes involved in growth and maintenance processes and protein biosynthesis, while defense and immunity proteins are down-regulated. Surprisingly, *Idgf1* and *Idgf3* are among genes up-regulated by starvation stress (Harbison et al., 2005). In *Bombyx mori*, we can see rather opposite effect. There seems to be only a single Idgf homolog in *Bombyx*, BmIDGF. The amount of BmIDGF in the hemolymph is high during the larval stage (feeding stage) and relatively low during the molting, wandering and pupal stages. In addition, the protein amount is also depended on feeding. Starvation caused a significant decline in expression, and after refeeding the transcripts increased again (Wang et al., 2009).

Idgf2 was found among the genes up-regulated after the induction of regeneration in *Drosophila* wing imaginal discs. *Drosophila* imaginal discs are the larval primordia of adult organs. Discs are capable to undergo regenerative growth after transplantation and in vivo culture into the adult abdomen. *Idgf2* expression was up-regulated during the first 24 hours of regeneration of the wing disc. Within this first class of up-regulated genes, there were also genes associated with dorsal closure, the JNK cascade, MAP kinase activity, and the Notch and Wg signaling pathways. In addition, other genes associated with imaginal disc development, immune response (like *Idgf2*), and apoptotic processes were detected (Blanco et al., 2010).

1.3.3.4. Genetic analysis of IDGF genes

The gene silencing experiments of individual Idgfs showed that some Idgfs are essential for larval and adult molting processes. Insect chitinases are present in molting fluid and are predicted to mediate the digestion of chitin present in the exoskeleton. *Tribolium castaneum*, the red flour beetle, became a model organism for high-throughput RNAi screening. By using gene specific RNAi the biological functions of individual members of the chitinase-like proteins family were examined. All chitinases with catalytic activity were found to be required for proper development. Also the homolog of *Idgf4* was essential for proper molting but there were no abnormalities in (*Tc*)*Idgf2* dsRNA treated beetles. Unfortunately, because of the large number of tested genes in this study, the authors pick just the homolog of *Idgf2* and *Idgf4* (Zhu et al., 2008). What would bring the knock-down of other family members is elusive. Similar results were obtained in *Drosophila* in which the individual *Idgfs* were knocked-down with the help of RNAi by using a cuticle specific driver. The results showed that *Idgfs* are needed for cuticle molting during larval as well as in pupal stages. The authors suggest that the *Idgfs* are involved in the protection of newly synthesized cuticle matrix against degradation (Pesch et al., 2016).

In our research we focused on the possible role of IDGF3 in immune responses. We have generated *Drosophila Idgf3* deletion and over expression mutants and examined them in standard infection and injury tests. We also conducted an extensive whole genome transcriptional analysis of IDGF3 mutant flies. Our results were included to the publication “*The Drosophila Chitinase-Like Protein IDGF3 is involved in protection against nematodes and in wound healing*”.

2. Aims of this thesis

IDGFs and adenosine are key factors affecting the growth and survival of *Drosophila* cells. The function of both types of these growth regulators seems to be evolutionary conserved, but their mechanisms of action are not fully understood. We used in our study genetic, biochemical, as well as cell biological approaches. In my dissertation I focused on the characterization of the prototypical IDGF family protein, IDGF2, in cell culture; the analysis of IDGF3 mutant flies by genetic methods; the pharmacological examination of adenosine receptor as a major molecule mediating the adenosine signal, and the comparison of adenosine effects on various types of cells *in vitro*.

The main aims of my work were as follows:

- 1) To prepare recombinant IDGF2 protein
- 2) To determine the concentration of IDGF2 in hemolymph *in vivo*.
- 3) To examine the relationship of IDGF2 to insulin
- 4) To compare the cytoprotective effects of IDGF2
- 5) To find some IDGF2 downstream target genes in wing disc cells
- 6) To characterize the phenotype of IDGF3 mutant flies with respect to the immune response
- 7) To find some IDGF3 downstream target genes *in vivo*
- 8) To identify preferred physiological second messenger system of Ado signaling in fly cells
- 9) To establish the pharmacological profile of AdoR and find metabolically stable analogs
- 10) To compare Ado toxicity in different cell lines

3. SUMMARY

Evolutionary conservation of organ systems and basic metabolic regulatory circuits predetermine *Drosophila* as an excellent model for studying metabolic homeostasis. In addition to unique genetic tools *Drosophila* also provides defined cell culture *in vitro* systems in which the effects of various growth regulators can be directly examined in defined growth conditions. The combination of the genetic methods of functional analysis with such *in vitro* approaches provides new important insights into our understanding of cellular and organismal survival.

Two groups of growth regulators were described in *Drosophila* imaginal disc cell culture Cl.8+ - Imaginal disc growth factors (IDGF-1-6) belonging to chitinase-like protein family of carbohydrate binding proteins and Adenosine deaminase-related growth factors (ADGF-A, -A2, -B, -C and -D), which are active adenosine deaminases influencing homeostasis of key cellular metabolite adenosine. Functions of both types of these growth regulators seem to be evolutionary conserved, and mechanisms of their function are not fully understood.

Publication I

***Drosophila* imaginal disc growth factor 2 is a trophic factor involved in energy balance, detoxification, and innate immunity.** [Vaclav Broz](#), Lucie Kucerova, Lenka Rouhova, Jana Fleischmannova, Hynek Strnad, Peter J. Bryant & Michal Zurovec (2017)

Scientific Reports 7:43273

In the first publication, we choose one of the IDGFs, the IDGF2 as a prototypical member of *Drosophila* CLPs and examined its effects on cell growth and survival. We show that the IDGF2 does not activate insulin receptor pathway, because it shows distinct effect on cell survival than insulin and it has no effect on downstream insulin phosphorylation targets PKB and S6K. IDGF2 is a protective factor in cultured insect cells and this cytoprotection seems to cover a wide range of harmful conditions and may involve several mechanisms. Recombinant IDGF2 saves the Cl.8+ cells from death caused by serum

deprivation, toxicity of xenobiotics or high concentrations of extracellular adenosine (Ado) and deoxyadenosine (dAdo). The IDGF2 is able to renew the mitochondrial and cellular energy homeostasis and prevent the dissipation of mitochondrial membrane potential ($\Delta\Psi_m$) in cultured cells. Transcriptional profiling also supports the protective role of IDGF2 and many of the induced genes were implicated in energy metabolism, detoxification and innate immunity. We show that the concentration of IDGF2 *Drosophila* hemolymph reaches 19 ± 3 ng/ μ l (approximately 400 nM), and it can be further induced by injury or infection. The highest IDGF2 accumulation was found at garland and pericardial nephrocytes further supporting its role in organismal detoxification. Taken together, IDGF2 has similar overall homeostatic and protective effect as mammalian serum and chitinase-like glycoproteins recently associated with pathogenic processes related to inflammation, extracellular tissue remodeling, fibrosis and solid carcinomas.

Publication II

The *Drosophila* Chitinase-Like Protein IDGF3 is involved in protection against nematodes and in wound healing. Lucie Kucerova, Vaclav Broz, Md. Badrul Arefin, Houda Ouns Maaroufi, Jana Hurychova, Hynek Strnad, Michal Zurovec & Ulrich Theopold (2015)

Journal of Innate Immunity 8(2):199-210

In the second article, we analyzed the function of another *Drosophila* IDGF family member, the IDGF3, in the organism *in vivo* using genetic approach. Because several genome-wide analyses of transcriptional responses to infections performed earlier in other laboratories implicated some of the IDGF proteins in the immune responses, we have focused on the IDGF3 role in immunity. We generated *Drosophila Idgf3* deletion and overexpression mutants and examined them in standard infection and injury tests. We show that IDGF3 mutant flies are more sensitive to gram-negative bacteria and entomopathogenic nematode (EPN) infections. We also show that the wound healing process is slower in the IDGF3 mutants. In addition, the IDGF3 protein is a component of the hemolymph clot formed after wounding, the null mutants have clotting defect, while the IDGF3-overexpressing flies have over-clotting phenotype. Finally, we identified the IDGF3-modulated genes by an extensive whole genome transcriptional analysis. The signal pathway

impact analysis (SPIA) as well as the Gene set enrichment analysis (GSEA) showed enrichment for genes involved in innate defense mechanisms and signal pathways connected to wound healing as well as regenerative processes including Wingless (Wg) and JAK/STAT signaling. The activation of Wingless and JAK/STAT signaling is also consistent with growth-promoting role of IDGF3 observed earlier by Kawamura et al. The phenotypes of the IDGF3 mutants show that at least some of the IDGF functions are not overlapping and are specific for the individual family members.

Publication III

Differential response of *Drosophila* cell lines to extracellular adenosine. Jana Fleischmannova, Lucie Kucerova, Katerina Sandova, Veronika Steinbauerova, Vaclav Broz, Petr Simek and Michal Zurovec (2012)

Insect Biochemistry and Molecular Biology 42: 321-331

In the third publication, we show the effect of an excess of cellular metabolite adenosine on the growth of different cell types *in vitro*. We show that different types of *Drosophila* cell lines may significantly differ by their ability to reutilize Ado which has a dramatic effect on their energy homeostasis. Adenosine is a crucial metabolite that affects a wide range of physiological processes. We show that imaginal disc Cl.8+ cells are very effective in Ado uptake. However, when the extracellular Ado concentration exceeds the physiological levels, it affects their viability, morphology, and mitochondrial polarity. High Ado uptake in these cells is followed by Ado conversion to AMP by Ado kinase and stimulation of ATP production in mitochondria, which may interfere with cellular homeostasis and leads to cell death. In contrast, hematopoietic cell line Mbn2 or neuroblast cells Bg2-c2 survive quite well even in high (100 μ M) Ado concentration, because they are characterized by lower Ado uptake and preferential conversion of Ado to inosine by adenosine deaminase as a part of the purine catabolic pathway. Our results show that different types of *Drosophila* cell lines use different pathways for Ado conversion and suggest that such differences may be an important part of complex mechanisms of tissue specific regulation of energy homeostasis in the fly body.

Publication IV

Characterization of the *Drosophila* adenosine receptor: the effect of adenosine analogs on cAMP signaling in *Drosophila* cells and their utility for *in vivo* experiments. Lucie Kucerova, Vaclav Broz, Jana Fleischmannova, Roman Sidorov, Vladimir Dolezal and Michal Zurovec (2012) Journal of Neurochemistry 121: 383–395

Because it is assumed that most of the physiological effects of adenosine signaling are mediated by adenosine receptors, we focused in our fourth publication on the characterization of the *Drosophila* adenosine receptor (DmAdoR). Adenosine receptors belong to G protein-coupled receptor family and are well conserved among species. *Drosophila* genome contains only one AdoR subtype, which was shown earlier to activate both cAMP and calcium second messenger pathways when overexpressed in heterologous Chinese Hamster (CHO) cells *in vitro*. Recent elucidation of human A2A Adenosine receptors structure showed conserved amino acids necessary for the contact with the adenosine moiety. However, the selectivity of adenosine analogs for AdoR subtypes is still not well understood. In this study we have characterized the second-messenger stimulation by endogenous DmAdoR in *Drosophila* neuroblast cell line Bg2-c2 and examined a number of adenosine analogs for their ability to interact with DmAdoR. We show that adenosine can stimulate cAMP but not calcium production in *Drosophila* cells. We found one full and four partial DmAdoR agonists, as well as two full and two partial antagonists. The employment of the full agonist, 2-chloroadenosine, in flies *in vivo* mimicked the phenotype of DmAdoR overexpression, whereas the full antagonist, SCH58261, rescued the flies from the lethality caused by DmAdoR overexpression. Our results support the emerging view of the amino acid residues necessary for ligand activity. Differences in pharmacological effect of the tested analogs between DmAdoR and human A2AR can be partially explained by the dissimilarity of specific key amino acid residues disclosed by the alignment of these receptors. Both identified agonists and antagonists of *Drosophila* AdoR are metabolically stable and will serve as important tools in further research.

4. Results

4.1.1. Publication I

Vaclav Broz, Lucie Kucerova, Lenka Rouhova, Jana Fleischmannova, Hynek Strnad, Peter J. Bryant & Michal Zurovec (2017) ***Drosophila* imaginal disc growth factor 2 is a trophic factor involved in energy balance, detoxification, and innate immunity.** *Scientific Reports* 7:43273

Abstract:

Drosophila imaginal disc growth factor 2 (IDGF2) is a member of chitinase-like protein family (CLPs) able to induce the proliferation of imaginal disc cells *in vitro*. In this study we characterized physiological concentrations and expression of IDGF2 *in vivo* as well as its impact on the viability and transcriptional profile of *Drosophila* cells *in vitro*. We show that IDGF2 is independent of insulin and protects cells from death caused by serum deprivation, toxicity of xenobiotics or high concentrations of extracellular adenosine (Ado) and deoxyadenosine (dAdo). Transcriptional profiling suggested that such cytoprotection is connected with the induction of genes involved in energy metabolism, detoxification and innate immunity. We also show that IDGF2 is an abundant hemolymph component, which is further induced by injury in larval stages. The highest IDGF2 accumulation was found at garland and pericardial nephrocytes supporting its role in organismal defense and detoxification. Our findings provide evidence that IDGF2 is an important trophic factor promoting cellular and organismal survival.

SCIENTIFIC REPORTS



OPEN

Drosophila imaginal disc growth factor 2 is a trophic factor involved in energy balance, detoxification, and innate immunity

Vaclav Broz^{1,2}, Lucie Kucerova¹, Lenka Rouhova², Jana Fleischmannova¹, Hynek Strnad³, Peter J. Bryant⁴ & Michal Zurovec^{1,2}

Drosophila imaginal disc growth factor 2 (IDGF2) is a member of chitinase-like protein family (CLPs) able to induce the proliferation of imaginal disc cells *in vitro*. In this study we characterized physiological concentrations and expression of IDGF2 *in vivo* as well as its impact on the viability and transcriptional profile of *Drosophila* cells *in vitro*. We show that IDGF2 is independent of insulin and protects cells from death caused by serum deprivation, toxicity of xenobiotics or high concentrations of extracellular adenosine (Ado) and deoxyadenosine (dAdo). Transcriptional profiling suggested that such cytoprotection is connected with the induction of genes involved in energy metabolism, detoxification and innate immunity. We also show that IDGF2 is an abundant haemolymph component, which is further induced by injury in larval stages. The highest IDGF2 accumulation was found at garland and pericardial nephrocytes supporting its role in organismal defence and detoxification. Our findings provide evidence that IDGF2 is an important trophic factor promoting cellular and organismal survival.

The cells of higher eukaryotes integrate mitogenic, differentiating, stress and defence signals with aging or nutrient status to regulate growth and proliferation. Several growth factors have been shown to be involved in the growth of *Drosophila* imaginal disc cells, including epidermal growth factor (EGF), proteins of the insulin family, adenosine deaminase growth factors (ADGFs)^{1,2} and imaginal disc growth factors (IDGFs)³. It is important to fill the current gaps in our knowledge of IDGFs, which are unusual among the growth factors since they are present in insect haemolymph in large concentrations and seem to integrate signals needed for growth, cell viability, and the innate immune response.

IDGFs comprise a small family of six secreted glycoproteins with a molecular weight of about 47 kDa and are identified as active growth factors from the conditioned media of the *Drosophila* cell lines^{4,5}. They belong to the chitinase-like proteins (CLPs), showing a mutual sequence identity of approximately 50%, and are produced by the larval fat body and haemocytes^{5,6}. IDGFs are structurally related to a large family of 18 glycosyl hydrolases known in both vertebrates and invertebrates (15–25% amino acid sequence identity), which include chitinases and chitinase-like proteins⁷. Unlike chitinases, IDGFs are not active enzymes since they carry an amino acid substitution that is known to abrogate chitinase catalytic activity, but they retain the ability to bind carbohydrates^{7–9}. CLPs have been reported to regulate responses to bacteria, cell growth, inflammation, and remodelling in various organisms by a mechanism that is still poorly understood^{10–12}.

IDGF2 is the best characterized *Drosophila* IDGF, having its crystal structure determined⁷. High levels of *Idgf2* mRNA expression have been reported in the yolk cytoplasm of the early embryo. High levels of IDGF2 protein have been detected in the haemolymph of *Drosophila* third instar larvae^{13,14} as well as in the larval fat body and salivary glands⁵. In adults, *Idgf2* mRNA has been detected in nurse cells and oocytes⁵. *Idgf2* was also identified as one of the genes upregulated in the early stages of imaginal disc regeneration¹⁵.

¹Institute of Entomology, Biology Centre CAS, Branisovska 31, 370 05 Ceske Budejovice, Czech Republic. ²Faculty of Science, University of South Bohemia, Branisovska 31, 370 05 Ceske Budejovice, Czech Republic. ³Institute of Molecular Genetics CAS, Videnska 1083, 142 20 Prague 4, Czech Republic. ⁴Developmental & Cell Biology, School of Biological Sciences, University of California, Irvine, USA. Correspondence and requests for materials should be addressed to M.Z. (email: zurovec@entu.cas.cz)

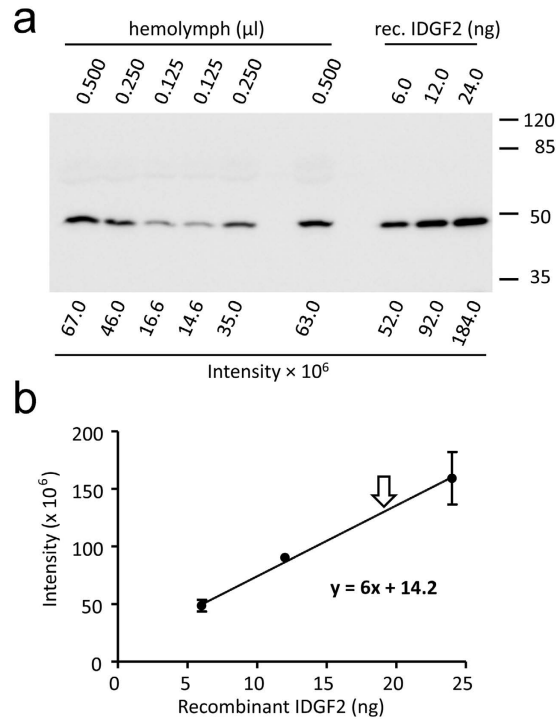


Figure 1. Quantification of IDGF2 protein in *Drosophila* haemolymph. (a) Representative western blot image showing 6–24 ng purified recombinant IDGF2 together with haemolymph samples separated on a 10% PAGE. IDGF2 was detected by anti-IDGF2 antibody. (b) Calibration curve derived by plotting the band density of haemolymph IDGF2 against known amounts of recombinant IDGF2 protein (based on three experiments). For haemolymph isolation, wandering L3 larvae were collected, larvae were surface sterilized in 70% ethanol and excess fluid was blotted off on paper towel. 10 larvae were used for isolation. The larvae were opened by gently pulling the epidermis apart with forceps. The haemolymph was collected with a fine glass pipette and immediately frozen. The haemocytes were not removed.

Recombinant IDGF2 showed a dose-dependent effect on the growth of imaginal disc Cl.8+ cells in supplement-free media (SFM) when used together with bovine insulin⁵. Vertebrate insulin has earlier been shown to activate the *Drosophila* insulin receptor¹⁶, and, based on the proposed cooperation between IDGF2 and insulin in stimulating imaginal disc cell growth, it has been suggested that IDGF2 might function as a cofactor of *Drosophila* insulin⁵.

Here, we examined the effects of IDGF2 on cell growth in tissue culture cells *in vitro* and searched for the mechanisms involved. We show that recombinant IDGF2 at levels corresponding to its haemolymph concentration supports the survival of Cl.8+ cells independently of insulin. The effects of recombinant IDGF2 include protection against cell death caused by serum deprivation, as well as against elevated levels of Ado, dAdo and some xenobiotics in serum-free conditions. We found that the highest accumulation of IDGF2 protein *in vivo* was in pericardial and garland nephrocytes that contribute to detoxification of the insect haemolymph. Furthermore, IDGF2 is induced by injury *in vivo* and activates the expression of a number of target genes involved in the energy metabolism, detoxification, and the innate immune response.

Results

Recombinant IDGF2 promotes the growth of Cl.8+ cells *in vitro*. In order to examine the effect of the growth factor IDGF2 on the proliferation of *Drosophila* Cl.8+ cells, we prepared a recombinant IDGF2 protein in a baculovirus expression system. First, we used the recombinant IDGF2 to determine the concentration of native IDGF2 in *Drosophila* haemolymph *in vivo* (Fig. 1). The results of three independent experiments indicated that the concentration of IDGF2 in the haemolymph is $19 \pm 3 \text{ ng}/\mu\text{l}$ (approximately 400 nM).

Kawamura *et al.*⁵ showed that the addition of recombinant IDGF2 promotes the survival and growth of Cl.8+ cells in a supplement-free medium (without FBS or fly extract), but containing yeast extract (SFM). To verify the function of recombinant IDGF2, we treated the Cl.8+ cells in SFM with physiologically-relevant IDGF2 concentrations and assessed their viability by monitoring changes in mitochondrial membrane potential ($\Delta\Psi\text{m}$) and morphology. As shown in Fig. 2a, the TMRE readouts of cell treated for 36 hrs with SFM were characterized by a small proportion (16.9%) of living cells (right peak in the plot, Fig. 2a). Consistently, increasing concentrations of IDGF2 dose dependently increased cell viability (Fig. 2a–h and Fig. S1a–g). Our results show that higher than physiological concentrations of IDGF2 are needed for the survival of the Cl.8+ cells for longer incubation in SFM or chemically defined minimal medium (MM) (Fig. 2 and S1). These results correlated with the cell morphology, such that the cell population with reduced TMRE staining also had a lower FSC signal corresponding to a smaller cell size and an increased SSC signal indicating higher density characteristic for apoptotic cells (Fig. S1a'–g').

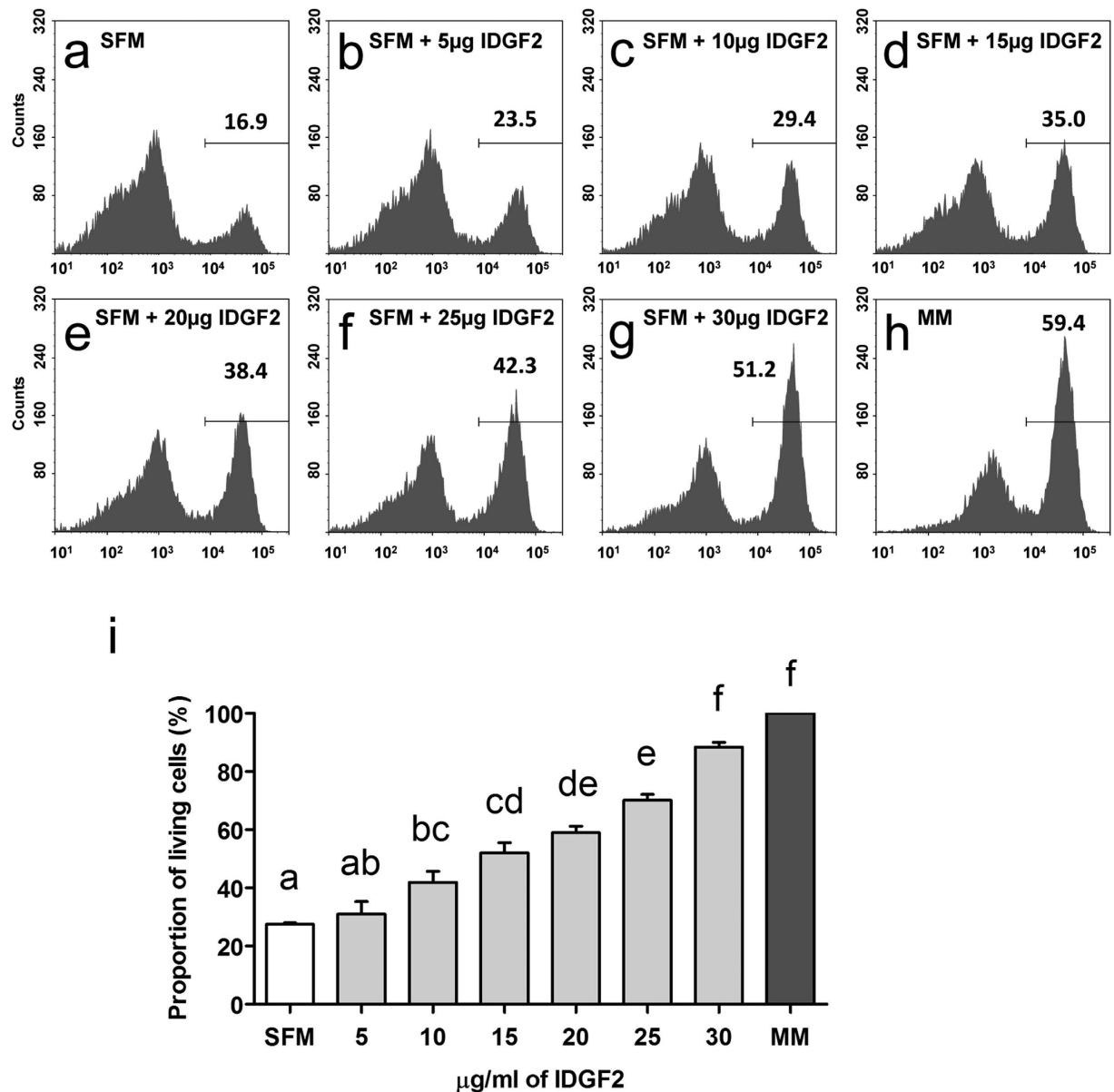


Figure 2. IDGF2 effect on the mitochondrial membrane potential ($\Delta\Psi_m$) of Cl.8+ cells incubated 36 hrs in SFM determined by TMRE staining and flow cytometry. Higher than physiological doses of IDGF2 (more than 20 $\mu\text{g/ml}$) are needed for Cl.8+ cell survival during a longer incubation period. (a) Control Cl.8+ cells in supplement free media (SFM); (b–g) Cl.8+ cells in increasing concentrations of recombinant IDGF2 (5, 10, 15, 20, 25 and 30 $\mu\text{g/ml}$, respectively). (h) Cl.8+ cells in chemically defined medium (MM). Living cells with active mitochondria sequester the TMRE stain (right peaks), while TMRE-negative cells undergo apoptosis (left peaks). Increasing concentrations of IDGF2 led to a higher proportion of living cells. The total cell population was gated on TMRE-positive cells, and the numbers represent the proportion of these cells. (i) Dose dependent effect of IDGF2 on Cl.8+ cell viability in SFM shown as the proportion of control cells in MM. The graph summarizes the three cell cytometry experiments and the data is presented as mean \pm SEM. Significant differences were evaluated by ANOVA followed by Tukey test and are indicated by different letters ($p < 0.05$).

Since the SFM contained an undefined component, yeast extract, we also prepared fully defined cell culture media (minimal media, MM) containing bovine insulin, but without yeast extract. Interestingly, as shown in Fig. S1, the Cl.8+ cells in MM survived better than in SFM showing a modest IDGF2 effect on both the $\Delta\Psi_m$ (Fig. S1h–n) and cell morphology (Fig. S1h'–n'). Our results show that IDGF2 has dose-dependent protective effects in both types of growth media, which prevent loss of $\Delta\Psi_m$ and morphological alterations.

We also compared the proliferation of Cl.8+ cells in SFM and SFM plus IDGF2 with the proliferation of these cells under standard conditions in complete media (CM, containing FBS, fly extract, yeast extract and insulin)¹⁷. We tested the effect of recombinant IDGF2 on cell division by direct cell counting (Fig. 3). The results show that Cl.8+ cells in SFM without IDGF2 did not grow and slowly died, while IDGF2 treatment (16 $\mu\text{g/ml}$) of such cells

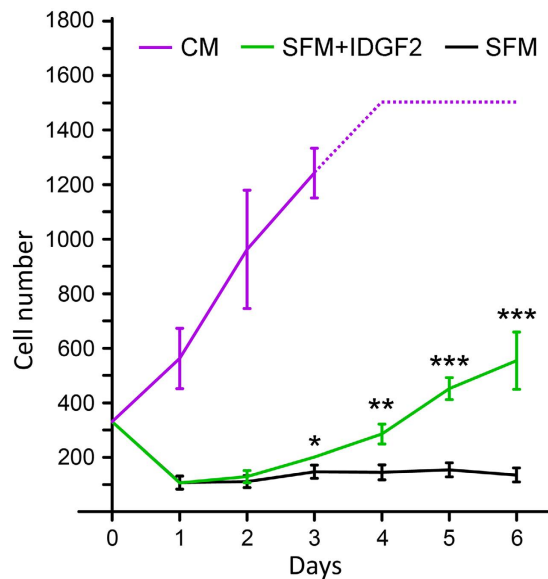


Figure 3. Effect of IDGF2 on the proliferation of *Drosophila* imaginal disc cells. The Cl.8+ were grown in different cell culture conditions. CM, complete medium; SFM - supplement-free medium (=medium containing yeast extract and insulin); SFM + IDGF2 - cells in SFM + IDGF2 (16 μ g/ml). The growth/survival rates of cells were measured by the direct counting of cells using digital photographs of identical areas (0.8 \times 0.8 mm) taken every 24 hrs. Each point represents the mean \pm SEM (n = 3). Significant differences (* p < 0.05, ** p < 0.01, *** p < 0.001) between SFM and SFM + IDGF2 treatments are indicated by asterisks and were evaluated by Student's t-test.

stimulated proliferation after a short lag phase in which about two thirds of the cells died but the rest grew with a doubling time of approximately 3 days. In contrast, the cells in the CM proliferated faster with a doubling time of approximately 2 days, most probably due to the nutrient-rich conditions.

Our results showed that the effect of recombinant IDGF2 on the survival and proliferation of Cl.8+ cells in SFM or MM was dose-dependent with concentrations of 10–30 μ g/ml. The Cl.8+ cells in SFM required higher than physiological IDGF2 concentrations to show similar viability as the cells in MM. Interestingly, the addition of IDGF2 to Cl.8+ cells in CM caused only a marginal increase in $\Delta\Psi_m$ (Fig. S2).

IDGF2 exerts cytoprotective effects on Cl.8+ cells independent of insulin. Earlier report suggested that IDGF2 is a cofactor of *Drosophila* insulin-like peptides⁵. We therefore compared the effects of insulin and IDGF2 on the viability of Cl.8+ cells in insulin-free minimal medium (MM) using TMRE staining. The results show that Cl.8+ cells treated with IDGF2 had a significantly higher proportion of living cells (Fig. 4) than the control. In an example shown in Fig. 4c, the IDGF2 increased cell viability by about 8% (from 58.2% to 65.0%) while insulin showed almost no effect by itself as well as no synergy with IDGF2. Interestingly, while insulin treatment did not affect the proportion of living and dying cells, it significantly shifted the position of the right peak further right (increased the $\Delta\Psi_m$) (Fig. 4b,f). These results suggest that the responses to both growth factors are distinct and probably mediated by separate mechanisms.

To examine whether IDGF2 is able to activate the insulin pathway we compared the ability of IDGF2 and insulin to phosphorylate the insulin downstream targets dS6K (S6 kinase) and dAkt/PKB (protein kinase B). The Cl.8+ cells in MM media poor in nutrients served as a negative control, while the cells in MM plus insulin or in nutrient-rich CM would have their insulin pathway activated. We treated Cl.8+ cells in MM with IDGF2, insulin or IDGF2 plus insulin (70 min or 3 h of exposure) and analysed the extracts by PAGE and western blotting. Cl.8+ cells in CM were used as the control. The western blots were probed with phosphospecific dS6K and dAkt/PKB antibodies. As shown in Fig. 4g,h, the P-Thr-398 dS6K antibody detected the phosphorylated form of dS6K exclusively in the insulin-stimulated cells or the cells in CM, whereas it was almost completely absent in the IDGF2 and control samples (cells starved in MM). Similarly, a high level of the phosphorylated form of dAkt/PKB was observed in insulin-stimulated cells or control cells in CM. The combination of IDGF2 plus insulin produced the same intensity signal for phosphorylated dS6K and dAkt/PKB as insulin alone, suggesting that IDGF2 has no role in the activation of the insulin pathway. Consistently, the pre-treatment of cells with rapamycin (TOR inhibitor) or LY294002 (PI3K inhibitor) abolished dS6K phosphorylation without decreasing the cell viability (Fig. S4).

Our data further confirmed that IDGF2 increases the survival of Cl.8+ cells in MM. The results also reveal that IDGF2 does not activate the insulin pathway. Interestingly, we did not observe any significant effect of insulin on Cl.8+ cell viability under these experimental conditions.

IDGF2 protects Cl.8+ cells from the deleterious effects of some metabolites and xenobiotics. It has also been shown that IDGF2 promotes the growth of Cl.8+ cells in SFM containing yeast extract⁵. We have

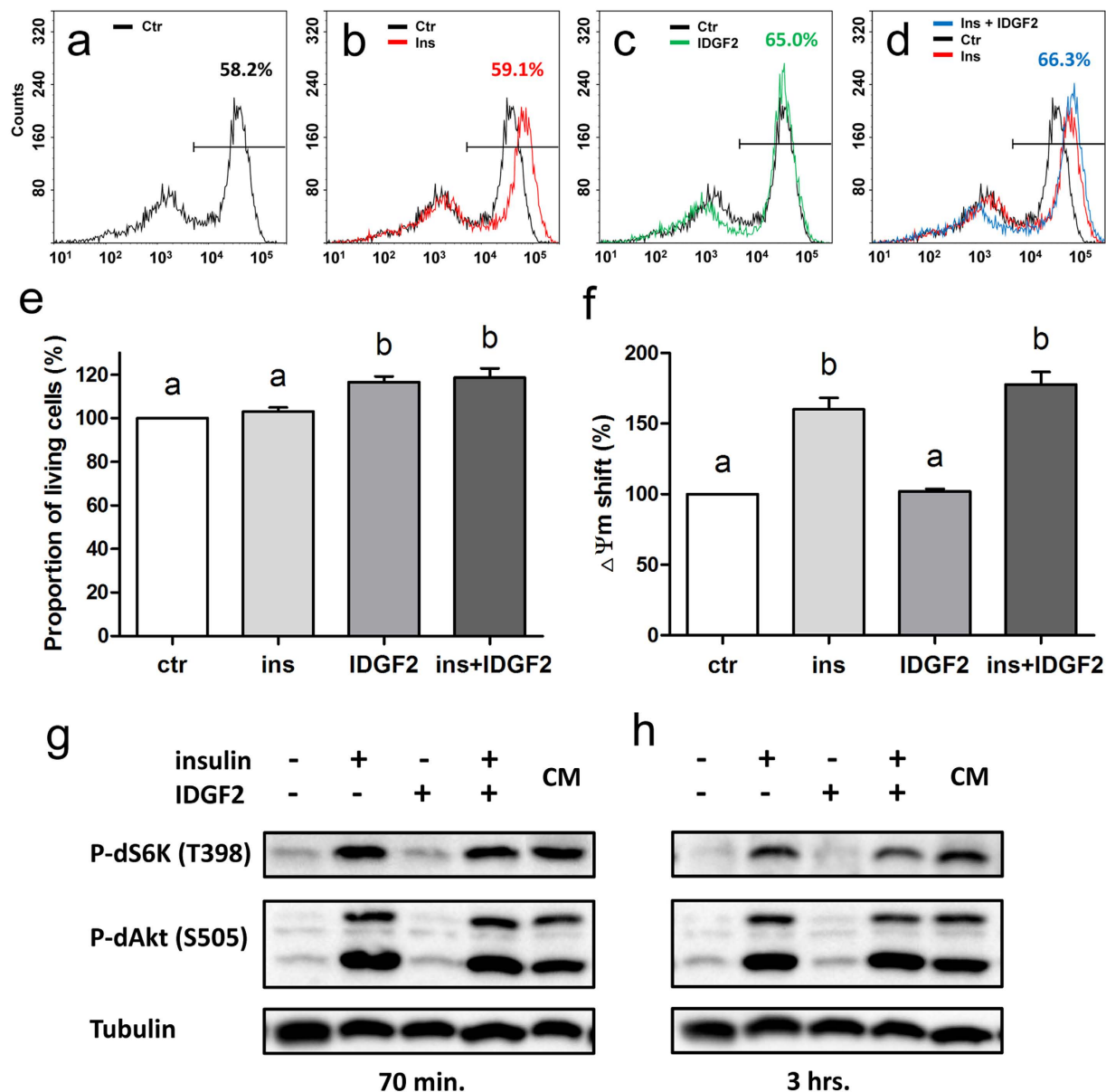


Figure 4. Effects of insulin and IDGF2 on Cl.8+ cells in chemically defined media. (a–d) Representative examples of flow cytometry plots of TMRE fluorescence of Cl.8+ cells incubated for 24 h in (a) MM (b) MM with insulin, (c) MM with IDGF2 and (d) MM with insulin and IDGF2. Numbers represent the proportion of viable cells. (e) The effects of insulin and IDGF2 on the proportion of living cells. Values represent the average percentage change in TMRE staining of living cells (right peaks) compared to control. The graph summarizes the three cell cytometry experiments shown in Fig. S3. (f) Effects of insulin and IDGF2 on the position of the right peak median. Values represent the average median increase in TMRE staining of living cells (right peaks) compared to control. The graph summarizes the three flow cytometry experiments shown in Fig. S3. Data in the graphs are presented as mean \pm SEM. Significant differences were evaluated by ANOVA followed by Tukey test and are indicated by different letters ($p < 0.05$). (g,h) Western blot analysis comparing the levels of phosphorylated dS6K (T398) and dAkt/PKB (S505) in Cl.8+ cells grown in MM for 24 hours, followed by insulin (0.125 IU/ml) or IDGF2 (16 μ g/ml) treatment. CM – cells grown in complete media. The cells were harvested after 70 min (g) and 3 hrs (h) incubation. The phosphorylation of dS6K and dAkt/PKB was significantly increased in insulin-treated cells, but not in IDGF2-treated cells. Tubulin detected with anti-alpha tubulin antibody was used as a loading control. Full-length blots are shown in Fig. S11.

previously shown that the proliferation of these cells in such media is blocked by a high level of Ado or dAdo, which are present in the yeast extract, and requires detoxification by bovine adenosine deaminase (ADA) or ADGFs¹⁸. To test the hypothesis that IDGF2 can protect Cl.8+ cells from high levels of these nucleosides, we examined the effects of Ado and dAdo with and without IDGF2, and assessed cell viability using MTS and TMRE staining. The MTS staining results showed that Ado and dAdo treatment ($\geq 15 \mu$ M and $\geq 70 \mu$ M, respectively)

caused cell death in MM, while the simultaneous treatment of Cl.8+ cells with 30 μ M Ado or 70 μ M dAdo together with IDGF2 (16 μ g/ml) protected the viability of these cells (Fig. S5a). Similarly, flow-cytometric analysis of TMRE stained cells showed that the Ado treatment increased the number of cells that lost $\Delta\Psi_m$ (left peak, Fig. S5d) thus reduced the number of viable cells by about half (right peak), while IDGF2 protected these cells. Consistently, the negative effect of dAdo on $\Delta\Psi_m$ was also reduced by IDGF2 (Fig. S5c,e,g,h).

The toxicity of Ado and dAdo has previously been reported in other cell types to have different mechanisms of action; while Ado has been implicated in apoptosis by receptor-dependent or independent mechanisms, dAdo has been associated with the block of DNA synthesis followed by progressive cell death¹⁹. As shown in Fig. 5a, the addition of 15 μ M Ado to Cl.8+ cells in MM led to a high proportion of cells with positive TUNEL staining, while co-treatment with IDGF2 brought the rate of TUNEL-positive cells back to normal. Similarly, the BrdU staining showed the inhibition of DNA synthesis at dAdo concentrations of 30 μ M and higher, while such cells co-treated with IDGF2 (16 μ g/ml) still retained a considerable proportion of cells incorporating BrdU (Fig. 5b). As expected, the effect of 30 μ M dAdo on the proportion of TUNEL-positive cells (Fig. 5c) as well as the effect of 20 μ M Ado on BrdU-stained cells were not significant (Fig. 5d,e), thus confirming their different mechanisms of action.

Our previous experiments with Ado-treated Cl.8+ cells showed that the excess of extracellular Ado in MM is transported into cells and caused a massive accumulation of ATP followed by the loss of $\Delta\Psi_m$ and apoptosis²⁰. To test whether IDGF2 influences Ado uptake from the cytoplasm via nucleoside transporters, we compared the uptake of Ado-treated Cl.8+ cells with or without IDGF2. The results showed that IDGF2 had no effect on Ado uptake (Fig. S6a). We also tested whether IDGF2 would decrease the deleterious level of ATP accumulation in Ado-treated Cl.8+ cells (Fig. S6b). Surprisingly, the concentration of ATP was significantly higher in Cl.8+ cells treated with Ado together with IDGF2 than in the Ado-treated controls. However, despite the high level of ATP the IDGF2-treated cells (unlike with the cells treated only with Ado) did not display a dissipation of $\Delta\Psi_m$ and survived (Fig. S5e).

To examine, whether IDGF2 could act as a protective agent against more types of toxic substances, we tested three xenobiotics, which have previously been studied in *Drosophila*, including rotenone (an inhibitor of mitochondrial respiratory complex I)²¹, resveratrol (an AMPK activator that confers cytoprotection in various models of oxidative injury)²² and SP600125 (a JNK inhibitor)²³. We assessed the toxic effects of these chemicals and chose the concentrations, close to the threshold dose levels at which toxicity first appears. The Cl.8+ cells with or without IDGF2 (16 μ g/ml) co-treatment were incubated in MM with the respective xenobiotic for 16 hrs. The resulting cell viability was assessed by TMRE staining and flow cytometry. As shown in Fig. 6, the co-treatment of Cl.8+ cells with IDGF2 dramatically reduced the effect of examined xenobiotics on $\Delta\Psi_m$.

Interestingly, we observed the cytoprotective effects of IDGF2 on Cl.8+ cells treated with the xenobiotics or metabolites only in minimal media, but not in cells cultured under more physiological conditions in complete culture media containing FBS, fly extracts and yeast extracts. For comparison we also tested the effects of Ado and xenobiotics in MM supplemented with 2% FBS, 2.5% fly extracts, or both (Fig. S7). The results show that FBS and partly also fly extract stabilize $\Delta\Psi_m$ to a similar extent and reduce the toxicity of low doses of xenobiotics and metabolites. It is not clear whether FBS and IDGF2 work via similar mechanisms (fly extracts contain a mix of IDGF proteins).

Taken together, our results further suggest that IDGF2 effectively stabilizes $\Delta\Psi_m$ and inhibits the $\Delta\Psi_m$ dissipation induced by a wide range of agents. The cytoprotective effect of IDGF2 was shown to be of a similar extent to that of FBS.

Downstream targets of IDGF2. To better understand the mechanism of IDGF2 action, we performed genome-wide transcriptional analysis to identify genes that were differentially expressed in Cl.8+ cells in response to IDGF2. Treatment of Cl.8+ cells with IDGF2 altered the expression of 81 genes, which passed our filtering criteria (p-value < 0.05 and |logFC| > 0.8) for statistical significance (Table S2). Microarray data classification based on functional groupings (gene ontology, GO) showed that most of the induced genes are involved in innate immunity (22.2%), morphogenesis (22.2%), metabolic process (14.8%), various transporters (14.8%), cytoskeleton organization (11%) and response to stimulus (10%) (Table S2). Interestingly, at least seven of the induced genes (8.6%) were implicated earlier in the response to xenobiotics²⁴.

We verified the IDGF2-mediated upregulation of several genes in Cl.8+ cells using real-time RT-PCR. They included *Attacin A* and *D*, *Cecropin A1*, *PGRP-LB* and *Rel* from the *Imd* immune pathway and *Homeodomain interacting protein kinase (hipk)* from the *Wnt* pathway, as well as *Zfh1* implicated in the activation of nephrocytes (Fig. 7a). In addition, the kinetics of induction of several IDGF2-inducible immune genes, including *Drosocin*, *Cecropin A2* and *Attacin B* was examined by northern blot analysis. As shown in Fig. 7b, the induction of these transcripts occurred within 30 min after IDGF treatment, suggesting that they represent the primary response genes.

For comparison, we extended our microarray analysis and included the expression profiles of Cl.8+ cells treated with the combination of IDGF2 (16 μ g/ml) and 50 μ M Ado as well as with 50 μ M Ado only. The treatment with a combination of IDGF2 and Ado significantly changed the transcript levels of 196 genes while the treatment with Ado-only altered the expression rates of 117 genes fulfilling our filtering criteria (p-value < 0.05 and |logFC| > 0.8). The proportions of genes in functional GO groups are shown in Tables S3 and S4.

To compare the lists of differentially expressed genes for the three treatments we constructed a Venn diagram (Fig. S8). We inspected in more detail the genes expressed exclusively in the cells simultaneously treated with Ado+IDGF2, since they might be involved in the compensatory homeostatic mechanisms allowing the survival of Ado-treated Cl.8+ cells. Candidate genes for such compensatory changes may include the upregulated trehalose transporters *Tret1-1* and *Tret1-2* or predicted sugar transporter-like gene *CG3168*, presumably needed for energy mobilization. Among other candidates, which may also influence energy homeostasis, we noticed down-regulated *ATPase (V0 complex)* and upregulated *5'-nucleotidase CG32549* (Table S4).

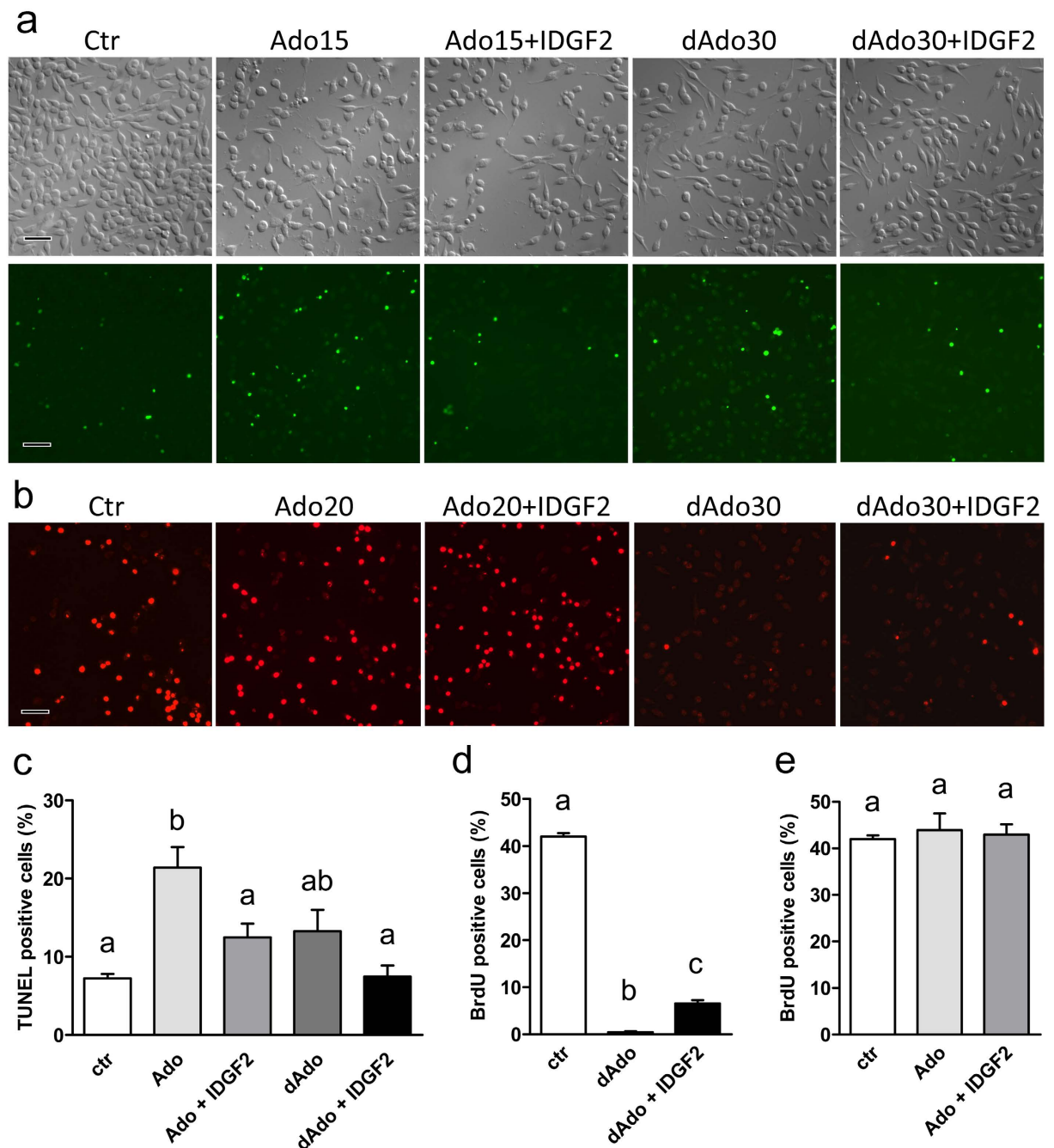


Figure 5. Cytoprotective effects of IDGF2 on CL8+ cells in MM treated with Ado and dAdo. **(a)** Effect of Ado (15 μ M), IDGF2 (16 μ g/ μ l) plus Ado (15 μ M), dAdo (30 μ M), and IDGF2 (16 μ g/ μ l) plus dAdo (30 μ M) on CL8+ cell morphology in the top panels and DNA fragmentation (TUNEL staining) in the bottom panels. Green spots represent the nuclei of apoptotic cells. The addition of IDGF2 reduced the number of apoptotic cells in Ado-treated CL8+ cells. Bar = 100 μ m. **(b)** BrdU staining (red). The cells were treated with dAdo (30 μ M), IDGF2 (16 μ g/ μ l) plus dAdo (30 μ M), Ado (20 μ M), IDGF2 (16 μ g/ μ l) plus Ado (20 μ M). dAdo-treated cells were essentially negative for BrdU incorporation. The addition of IDGF2 to dAdo increased the number of BrdU-positive cells. dAdo treated CL8+ cells did not show morphological changes connected with apoptosis, but they did not proliferate. **(c)** Effects of Ado, dAdo and IDGF2 on the relative proportion of the TUNEL-positive (apoptotic cells) CL8+ cells. Concentrations: Ado (15 μ M), IDGF2 (16 μ g/ μ l), dAdo (30 μ M). **(d,e)** Effects of Ado, dAdo and IDGF2 on the relative proportion of the BrdU-positive CL8+ cells. Concentrations: Ado (20 μ M), IDGF2 (16 μ g/ μ l), dAdo (30 μ M). Data in the graphs are presented as mean \pm SEM (n = 3). Significant differences were evaluated by ANOVA followed by Tukey test and are indicated by different letters (p < 0.05).

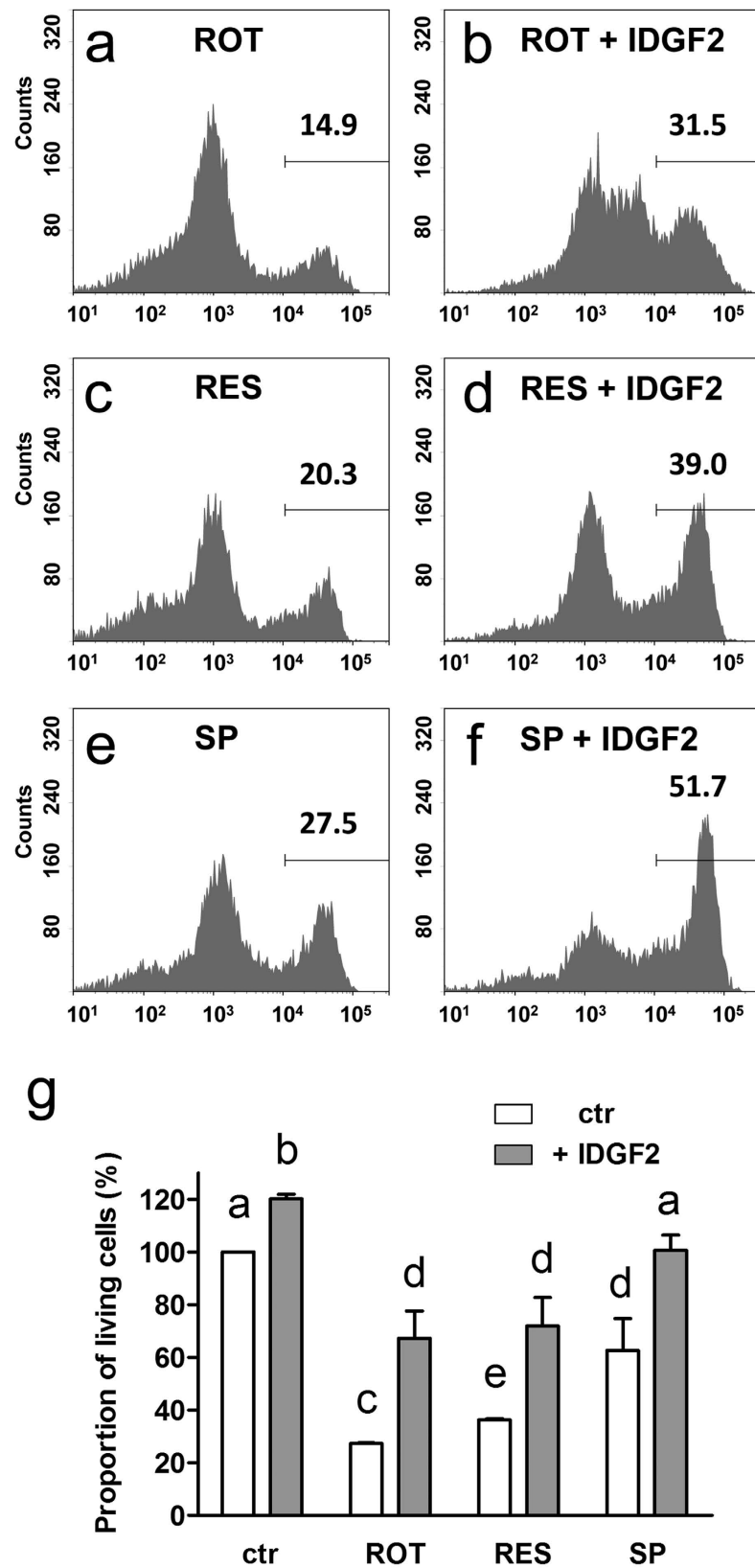


Figure 6. Cytoprotective effects of IDGF2 on Cl.8+ cells treated with xenobiotics. The cells were treated with 0.01 μ M rotenone (ROT) (a,b), 100 μ M resveratrol (RES) (c,d), 25 μ M SP600125 (SP) (e,f) for 16 hrs. Mitochondrial polarity was assessed by flow cytometric analysis of TMRE stained cells. The co-treatment with IDGF2 (16 μ g/ml) partially rescued cell viability (b,d,f). (g) Effects of IDGF2 on the viability of cells treated by xenobiotics. The graph summarizes three cell cytometry experiments. Data in the graphs are presented as mean \pm SEM. Significant differences were evaluated by ANOVA followed by Tukey test and are indicated by different letters ($p < 0.05$).

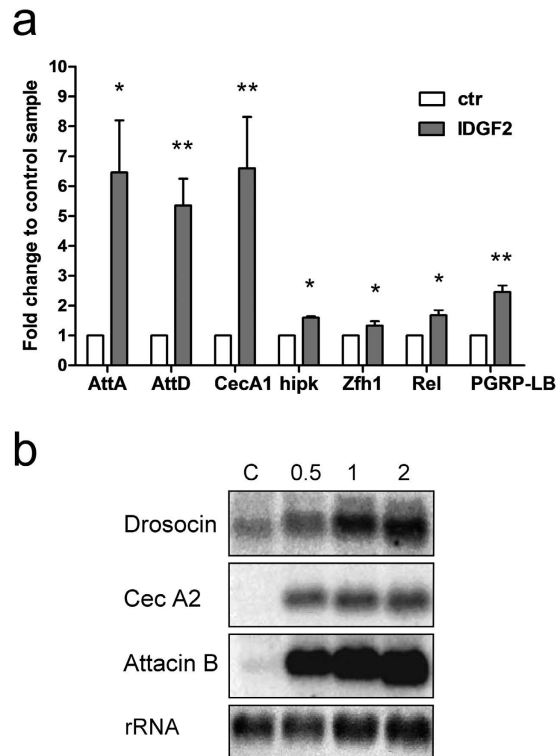


Figure 7. Validation of microarray gene expression changes induced by IDGF2 in Cl.8+ cells. (a) The Cl.8+ cells were induced by the addition of IDGF2 (16 µg/ml) and relative changes in gene expression were analysed by real-time reverse transcription PCR (RNA was isolated 4 h after treatment). $n = 3$. *AttA* - *Attacin A*; *AttD* - *Attacin D*; *CecA1* - *Cecropin A1*; *hipk* - *Homeodomain interacting protein kinase*; *Zfh1* - *Zn finger homeodomain 1*; *Rel* - *Relish*; *PGRP-LB* - *Peptidoglycan recognition protein LB*. Data in the graph are presented as mean \pm SEM ($n = 3$). Significant differences ($*p < 0.05$, $**p < 0.01$) between control and IDGF2 treatment are indicated by asterisks and were evaluated by Student's *t*-test. (b) *Drosocin* (CG10816), *cecropin A2* (CG1367) and *attacin B* (CG18372) transcripts in IDGF2-treated Cl.8+ cells were examined by northern analysis. Numbers on top denote time intervals following IDGF2 addition in h. The bottom panel shows methylene blue-stained rRNA as a loading control. Full-length blots are shown in Fig. S11.

The results of gene-enrichment analysis are shown in Table S5. The major significantly enriched KEGG pathway of differentially expressed genes for IDGF2 is a phagosome pathway, which is an important counterpart of the defence mechanisms. In contrast, Ado treatment had the largest impact on the downregulation of pantothenate and CoA biosynthesis, key precursors required for many biosynthetic reactions involved in lipogenesis²⁵. Interestingly, the simultaneous treatment of Cl.8+ cells with Ado+IDGF2 lead to the strong upregulation of three overlapping pathways involved in organismal detoxification containing glutathione as well as cytochrome P450 gene family members (Table S5).

Our data suggest that IDGF2 is involved in several biological processes. The IDGF2 treatment of Cl.8+ cells activates the immune response and its component phagocytosis as indicated by GO annotation and GSEA-KEGG analyses, respectively. Interestingly, the simultaneous treatment of Cl.8+ cells with IDGF2 and Ado lead to the up-regulation of multiple genes involved in stress and detoxification as well as energy metabolism.

IDGF2 is localized in pericardial and garland cells *in vivo* and is induced by aseptic or septic injury.

In order to obtain information on the function of IDGF2 *in vivo*, we examined the developmental expression patterns of IDGF2 by qPCR. The results showed that IDGF2 is expressed at all stages assessed, and the highest expression levels were detected in pupae and adult males (Fig. 8a).

The tissue distribution of the IDGF2 transcript in *Drosophila* larvae was examined by *in situ* hybridization, and confirmed the fat body as major sites of IDGF2 expression⁵ (Fig. S9a). We also examined the IDGF2 protein distribution in *Drosophila* larvae of first and third instar using transgenic flies carrying the *Idgf2::GFP* construct and immunostaining with an anti-GFP antibody. As shown in Fig. 8b–f, a high amount of IDGF2 protein was present in garland and pericardial cells, *Drosophila* nephrocytes that are an important part of the excretory system and are implicated in the detoxification of the insect body²⁶. Interestingly, we did not detect any *Idgf2* transcripts in garland cells by *in situ* hybridization (Fig. S9c), suggesting that proteins accumulate in garland cells after being secreted into the haemolymph. To verify this idea, we also expressed the *UAS-IDGF2-myc* transgene under the fat body-specific driver (*Lsp2-Gal4*) and examined the localization of the recombinant IDGF2. While the strongest

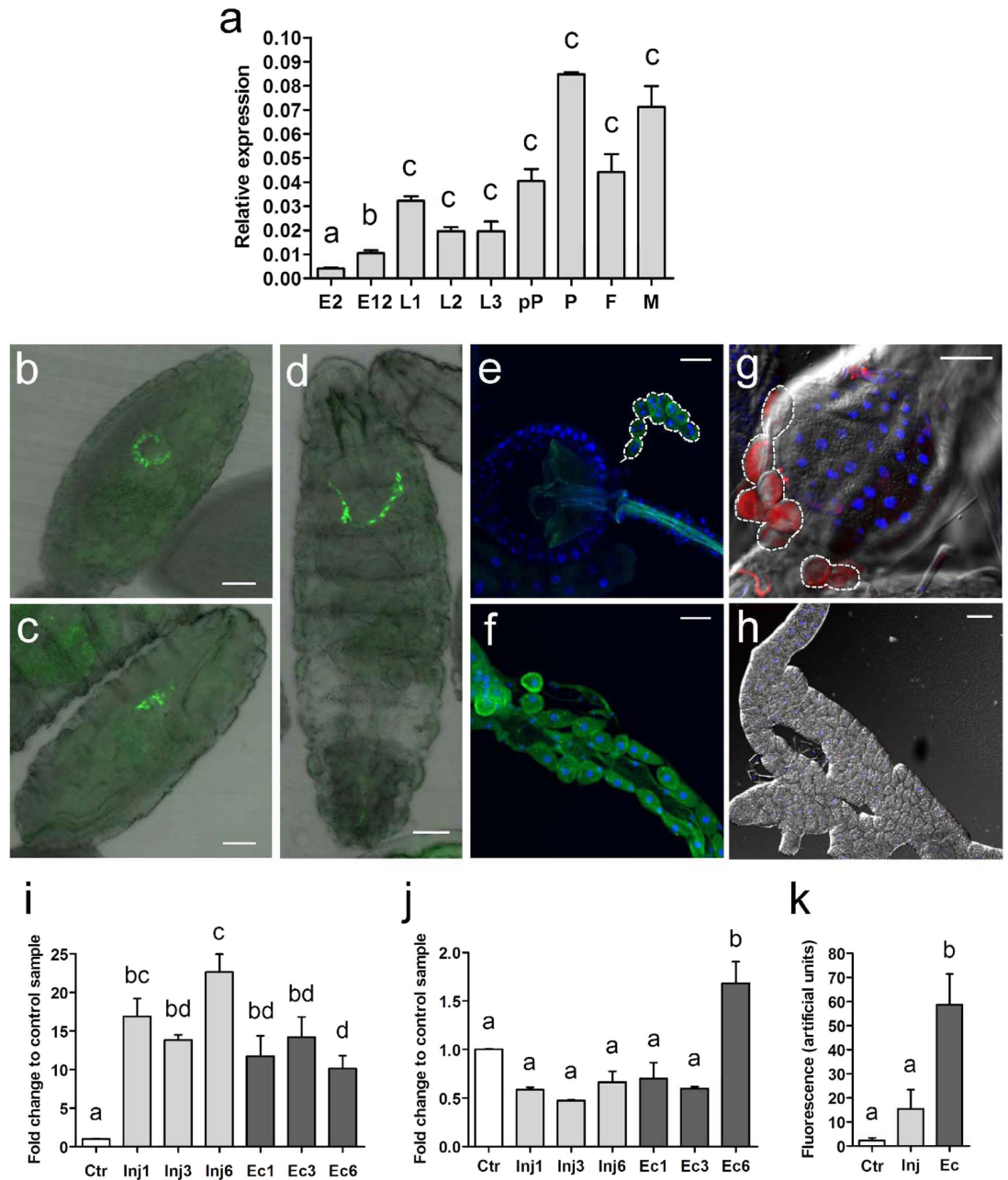


Figure 8. Expression and localization profile of IDGF2 in development and by septic and aseptic injury. (a) Developmental expression profile of *Idgf2* assayed by qRT-PCR. E2 - embryos 2 h, E12 - embryos 12 h, L1 - first instar larvae, L2 - second instar larvae, L3 - third instar larvae, pP - white prepupae, P - pupae (stage P10), F - females, M - males. *rp49* mRNA was used as an internal control. Data in the graphs are presented as mean \pm SEM ($n = 3$). (b–f) Localization of IDGF2::GFP (green) driven by the IDGF2 promoter. (b,c) - embryo, stage 16, dorsal and lateral view, (d) - first instar larva, (e) - proventriculus with attached garland cells (tracing line) from third instar larva, (f) - aorta from third instar larva. IDGF2::GFP fusion protein was detected by anti-GFP antibody. Cell nuclei were stained with DAPI (blue). Scale bar 50 μ m. IDGF2 protein was mostly localized in garland cells (b–e) and pericardial cells (f). (g–h) IDGF2-myc was expressed in the fat body (by *UAS-Gal4* system) and detected with anti-myc antibody (red). Strongest IDGF2-myc signal was accumulated in garland cells (tracing line), scale bar 50 μ m (g). While almost no signal was observed in the fat body, scale bar 100 μ m (h). *Idgf2* expression change in third instar larvae (i) and imagoes (j) after aseptic (light gray columns) or septic injury (dark gray columns) with *E. coli*. Non-wounded larvae and flies served as controls. In both sets of experiments, total RNA was extracted 1, 3 and 6 h after injury from whole animals. *rp49* mRNA was used as an internal control ($n = 3$). (k) Fluorescence signal from *Idgf2*::GFP in garland cells in L3 larva responds to infection after aseptic (light gray columns) or septic injury (dark gray columns) with *E. coli*. The values were derived from fluorescence images using the ImageJ analysis program. Non-wounded larvae served as controls ($n = 4$). Data in the graphs are presented as mean \pm SEM. Significant differences were evaluated by ANOVA followed by Tukey test and are indicated by different letters ($p < 0.05$).

IDGF2-myc signal detected with anti-myc antibody was again observed in garland cells (Fig. 8g), the fat body contained almost no signal (Fig. 8h) probably because of its rapid release into the haemolymph.

Since various CLPs were earlier implicated in responses to bacteria and tissue remodelling²⁷, we tested *Idgf2* expression in response to aseptic as well as septic injury in third instar larvae and adult male flies. Septic injury was performed with a syringe needle dipped in a culture of Gram-negative bacteria (*E. coli*). Changes in relative *Idgf2* transcript levels were determined 1, 3 and 6 h after the injury by qRT-PCR. The results confirmed that *Idgf2* expression is induced after both septic and aseptic injury in the larval stage but not in adults, except for a modest induction observed 6 h after septic injury. Interestingly, in larvae, *Idgf2* mRNA induction after 6 h was greater in the aseptic injury experiment than under septic conditions (Fig. 8i,j). In contrast, the staining of IDGF2 in larval garland cells increased dramatically after septic injury (Fig. 8k).

Our results show that IDGF2 is activated by septic and aseptic injury at the larval stage and to some extent also in adults. The accumulation of IDGF2 in garland and pericardial nephrocytes is consistent with its role in organismal detoxification.

Discussion

IDGF2 seems to be an unusual invertebrate mitogen from several points of view. It was discovered in the conditioned media of *Drosophila* cells, it is present in *Drosophila* haemolymph in high concentrations, and it has a carbohydrate-binding capacity. IDGF2 has been reported earlier to have a synergistic effect with insulin, potentially functioning as its cofactor⁵. However, our results show that IDGF2 does not act through the *Drosophila* insulin receptor, and that it has a different effect on cells. Taken together, our data strongly suggest that IDGF2 and insulin activate different pathways, however, we cannot exclude that some of the native *Drosophila* insulin-like peptides play a cooperative or moderating role on IDGF2 *in vivo*. The relatively weak effect of insulin on Cl.8+ cell proliferation in Shields and Sang M3-based growth medium has previously been observed and ascribed to the specific composition of this medium²⁸.

The cytoprotective function of IDGF2 is best seen in Cl.8+ cells, but we also observed the subtle effects of IDGF2 on other cell types, including the embryonic cell line S2 (Fig. S10). IDGF2 enhances the survival of Cl.8+ cells in serum-free conditions of SFM or MM, but it shows only a marginal effect in CM (Fig. S2). Despite of the high concentration of IDGF2 used in our experiments only relatively few cells show a response. For example, only about 30% of Cl.8+ cells survived and continued to divide in SFM at physiological IDGF2 concentration (Fig. 3). The variability in the IDGF2 response did not seem to be caused by the potential heterogeneity of Cl.8+ cells. The cell survival seemed to be a stochastic process, and the surviving cells did not become more resistant to Ado or to other deleterious conditions. The effect of IDGF2 rather suggested that it can renew homeostatic equilibrium only in part of the cell population.

IDGF2-induced cytoprotection seems to cover a wide range of harmful conditions and may involve several mechanisms. IDGF2 enhanced the survival of Cl.8+ cells in the serum-free and low nutrient MM conditions as well as protecting them from cytotoxic levels of Ado, dAdo and certain xenobiotics. Interestingly, it has previously been suggested that the cytotoxic effects of some treatments and chemicals disappear in the presence of serum proteins, which keep the cells in a more physiological state²⁹. We found that IDGF2 affected Cl.8+ cells in a similar way to FBS, with the 2% FBS showing similar cytoprotective effects on the toxicity of Ado and xenobiotics. However, in contrast to IDGF2, FBS was also shown to have some adenosine deaminase activity, specific to the detoxification of Ado and dAdo¹⁸. FBS is routinely added to insect culture media at similar concentrations as in vertebrate cell cultures³⁰, but its role is poorly understood. Our data suggest that Cl.8+ cells require the binding of IDGF2 for their proliferation, and FBS may be a substitute for this requirement.

Our differential expression profiling of genes involved in IDGF2-induced cytoprotection suggested that the Cl.8+ cell response against Ado involves the mobilization of energy-providing carbohydrates as well as the adjustment of purine metabolism. We have previously reported that Ado treatment caused the excessive uptake and recycling of extracellular Ado and a subsequent high ATP production and followed by the loss of $\Delta\Psi_m$, which were considered to be hallmarks of Cl.8+ cell apoptosis²⁰. Here, we show that the Cl.8+ cells treated simultaneously with Ado and IDGF2 reach even higher ATP levels than do cells treated only with Ado, but that such an increase was not accompanied by the loss of $\Delta\Psi_m$ and cell death. It therefore seems that the depolarization of $\Delta\Psi_m$ in Cl.8+ cells is a key event for the initiation of Ado-induced apoptosis and IDGF2 might be able to renew the mitochondrial and cellular energy homeostasis. Interestingly, earlier reports on mouse cells showed that the increase of cytosolic Ado affects mitochondrial adenosine production and disrupts mitochondrial bioenergetics³¹.

Our results also revealed that IDGF2 is able to increase BrdU incorporation in dAdo-treated cells (Fig. 5b). Since it has been earlier reported that, in mammalian cells, the dAdo toxicity is caused by the imbalance in purine metabolism leading to the block of DNA synthesis and cell death¹⁹, it seems that the IDGF2-induced cytoprotection against dAdo toxicity in Cl.8+ cells might also be connected with homeostasis in the purine metabolism.

Alternatively, the cytoprotective effects of IDGF2 might be related to the regulation of detoxification. Our transcriptional profiling of Cl.8+ cells simultaneously treated with IDGF2 and Ado revealed the induction of a number of detoxification enzymes, including glutathione-S-transferases and members of the cytochrome P450 family. We suggest that the induction of detoxification mechanisms may play important role, especially in the protection of Cl.8+ cells from the toxicity of some xenobiotics.

Our experiments indicated that IDGF2 also plays protective roles at the level of the organism. Our expression profiling analysis revealed the activation of genes involved in organismal detoxification including the genes specific to the function of *Drosophila* nephrocytes (garland and pericardial cells)³², such as *Zn finger homeodomain 1* (involved in the differentiation of garland cells) and *Mec2* (a podocin homolog involved in nephrocyte filtration). This observation is further supported by the *in vivo* localization of IDGF2 in garland and pericardial cells.

Moreover, IDGF2 might also have an important protective immune function. It was shown for the closely related IDGF3 protein that *Drosophila* IDGF3 mutants are more susceptible to infection with the nematodes or

Gram-negative bacteria²⁷. IDGF1 and 3 have been previously suggested as pattern recognition molecules³³ able to recognize chitin or related carbohydrates on the surface of nematodes and other parasites and thus activate immune effector mechanisms²⁷. We observed IDGF2 induction by aseptic or septic injury and confirmed its ability to induce the transcription of a number of defence-related genes, including the key NF- κ B transcription factor *relish*³⁴ and many antibacterial peptides (Fig. 7a,b). IDGF2 might be involved in wound healing rather than in the response to infection, since the *Idgf2* induction after 6 h was greater in the aseptic injury experiment than under septic conditions (Fig. 8i).

Taken together, there is an interesting parallel between the effects of IDGF2 and some mammalian members of the 18 glycosyl hydrolase family. The prototypical YKL-40 protein has been reported in normal human serum at concentrations in the nanomolar range and is increased in the serum of patients with arthritis or asthma³⁵. Recent reports have demonstrated the role of YKL-40 in diabetes and the promotion of tumour expansion^{36,37}. This all suggests that vertebrate and insect CLPs are involved in similar cellular and organismal functions; they bind to the carbohydrate components of a number of cell surface receptors and regulate multiple signalling pathways^{10–12}. Thus, further investigation of the downstream signalling pathways and exact biological function of IDGF2 and other CLPs require more studies. IDGF2 can serve as a suitable model for the research on other CLPs.

In summary, our research fills an important gap in the knowledge of *Drosophila* growth factors. We show that IDGF2 does not activate the insulin pathway but rather is involved in the enhancement of cellular survival under starvation conditions, and elevated levels of extracellular Ado, dAdo and xenobiotics *in vitro*. It seems that the IDGF2 keeps the cells in more physiological state, so that they can devote more resources to the detoxification or elimination of a toxic agent or for the renewal of homeostasis. *Drosophila* IDGF2 is an important trophic factor with similar overall homeostatic effect as mammalian serum proteins. Recombinant IDGF2 may serve as an important additive to *in vitro* cell and organ cultures.

Materials and Methods

Drosophila stocks. All flies were reared at 25 °C on a standard cornmeal-yeast-agar diet. Oregon-R flies (from The Bloomington *Drosophila* Stock Center, BDSC) were used for the determination of *Idgf2* expression profile and injury experiments. Transgenic flies carrying *Idgf2::GFP* constructs were generated as described earlier²⁷. The oligonucleotides containing 50-bp homology arms for recombineering followed by the linker region of amplification are shown in Table S1. For generation of *UAS-Idgf2-myc* fly strains we followed the protocol published previously²⁷. cDNA from *Idgf2* was amplified from EST-clone *GH12581* by primers listed in Table S1. Stable stocks with *UAS-Idgf2-myc* were produced using standard P-element transformation of the w^{1,18} flies. A homozygous-viable double insertion on the 2nd and 3rd chromosome was used for further experiments together with *Lsp2-Gal4* (BDSC).

Recombinant protein isolation. The Bac-to-Bac (Invitrogen) method was used for the production of histidine-tagged recombinant IDGF2. First, *Idgf2* cDNA was subcloned into the transfer vector and used for recombination with baculovirus DNA according to the manufacturer's instructions. Sf9 cells were used for transfections and virus amplification. Hi5 cells, used for protein production, were infected with a multiplicity of infection of 10 plaque-forming units (pfu) per cell. Three days post-infection, the medium was harvested, dialyzed against binding buffer and used for protein purification. Recombinant proteins were purified using a Ni-nitrilotriacetic acid (NTA) column (Qiagen). Fractions containing recombinant proteins were pooled and dialyzed in PBS. The IDGF2 concentrations were determined by Bradford assay (Sigma-Aldrich).

Cell culture. The *Drosophila* imaginal disc cell line Cl.8+¹⁷ was grown at 25 °C in complete medium (CM) containing Shields and Sang M3 Insect Medium (Sigma-Aldrich) supplemented with 2% fetal bovine serum (FBS), 2.5% fly extract, and 0.125 IU/mL insulin. The “supplement-free medium” (SFM) was Shields and Sang medium (Sigma-Aldrich, S8398) containing yeast extract (1 g/l). The “minimal medium” (MM) was Shields and Sang medium (Sigma-Aldrich, S8523) lacking yeast extract, supplemented with L-leucine, L-methionine, fumaric acid, folic acid, myo-inositol, pyridoxine, riboflavin, thiamine and insulin (0.125 IU/mL). Since this medium was fully chemically defined, it was used in most experiments. Embryonic S2 cells were maintained in Shields and Sang medium supplemented with 10% FBS.

Lepidopteran cells Sf9 and Hi5 used for baculovirus expression were maintained at 27 °C in TNM-FH medium (Sigma-Aldrich) supplemented with 10% FBS. Hi5 cells were maintained in EX-CELL Serum-Free medium (Sigma-Aldrich).

Functional *in vitro* assays. Cell viability was assessed using the CellTiter 96 Aqueous One Solution cell kit (Promega), which contains a tetrazolium compound MTS. Cl.8+ cells were seeded at a concentration of 1×10^6 /ml in a flat-bottomed 96-well plate in minimal medium (MM) with or without recombinant IDGF2 (16 μ g/ml), Ado and dAdo and incubated for 22 h. Next, 20 μ l of MTS solution was added to each well and the plate was incubated for an additional 3 h at 25 °C. The absorbance at 490 nm was recorded with a 96-well plate reader. The assay was performed with five replicates for each sample.

Proliferation of Cl.8+ cells in SFM and CM was also measured by the direct counting of cells using digital photographs of identical areas (0.8 \times 0.8 mm) taken every 24 hrs. Each value represents an average of three fields per plate.

TUNEL staining, BrdU incorporation, the ATP assay and the Ado uptake assay were performed as described previously²⁰. For TUNEL staining, we used the *In Situ* Cell Death Detection kit with fluorescein (Roche), and for BrdU incorporation, we used the *In Situ* Cell Proliferation Kit, FLUOS (Roche). ATP was measured by The CellTiter-Glo[®] Luminescent Cell Viability Assay (Promega). The Ado uptake assay was performed using H³-Ado in MM.

Cell cytometry. The $\Delta\Psi_m$ analysis is based on the property of living cells with active mitochondria to sequester the TMRE stain (right peaks), while TMRE-negative cells lose their $\Delta\Psi_m$ and undergo apoptosis (left peaks). To stain for mitochondrial polarity, Cl.8+ cells were incubated with 600 nM tetramethyl rhodamine ethyl ester (TMRE, Molecular Probes), for 30 min at 25 °C in culture medium. The dye was taken up by mitochondria and mitochondrial staining was analysed by flow cytometry in the 585/40 channel using ACEA NovoCyte™ 3000. At least 12,000 events were used for analysis. Morphological analysis is based on the measurement of cell size and granularity as indicated by the flow cytometry forward scatter versus side scatter (FSC/SSC) intensity plots.

The Cl.8+ cells were grown in 12-well plates at a concentration of 5×10^5 /ml in MM or CM and treated with recombinant IDGF2 (16 µg/ml), Ado (30–100 µM) and dAdo (70–100 µM). Rotenone (0.01 µM, Sigma-Aldrich), resveratrol (100 µM, Tocris Bioscience) and SP600125 (25 µM, Tocris Bioscience) were used at the threshold dose level at which the toxicity was low but detectable. In all these experiments, the same volumes of the corresponding solvents were used in the controls.

Western blotting and immunostaining. For IDGF2 protein quantification, hemolymph collected from wandering third instar larvae or known amounts of recombinant IDGF2 were subjected to SDS PAGE. SDS-PAGE and western blotting were performed as described earlier³⁸. Samples of recombinant IDGF2 were electrophoresed in parallel. Proteins were transferred to PVDF membranes and detected using an antibody against IDGF2. The anti-IDGF2 rabbit polyclonal antibody was developed using a KLH-coupled synthetic peptide IYHPDGSKDRLAH (Genscript). HRP-conjugated goat anti-rabbit IgG were used as the secondary antibody (1:5000, Jackson ImmunoResearch). The immunocomplexes were detected using a chemiluminescence reagent kit (Thermo Scientific). Protein bands were quantified with a LAS-3000 imaging system (Fuji Corp.). A standard curve was constructed from the readouts of recombinant IDGF2 protein. The resulting value was obtained by averaging the data from three independent experiments.

For the dS6K and dAkt/PKB phosphorylation assay, Cl.8+ cells were grown in 12-well plates at a concentration of 5×10^5 /ml, starved (in a 4:1 dilution ratio of MM to CM media) for 24 h and treated with recombinant IDGF2 (16 µg/ml) or insulin (0.125 IU/mL) for 70 min or 3 h in MM. The cells were also pretreated for 30 min with 15 µM LY294002 (PI3K inhibitor) or for 15 min with 20 nM rapamycin (TOR inhibitor). The rabbit anti-phospho-dS6K (Thr398) and anti-phospho-dAkt/PKB (S505) antibodies were from Cell Signaling Technology (1:1000); the monoclonal anti- α -tubulin antibody (T9026) was from Sigma-Aldrich (1:2000).

A rabbit polyclonal anti-GFP (1:500 dilution, Invitrogen) antibody was used to detect the IDGF2::GFP fusion protein, with subsequent detection using an AlexaFluor 488-conjugated anti-rabbit antibody (1:2000 dilution, Abcam). IDGF2-myc was detected with mouse anti-myc antibody (1:500 dilution, Sigma Aldrich) and goat anti-mouse antibody conjugated with Cy3 (1:2000 dilution, Jackson ImmunoResearch). DAPI (1:1000, Sigma-Aldrich) was used for the visualization of cell nuclei. Fluorescent images were acquired using a confocal microscope (Olympus Fluoview FV1000). Images were analysed with the ImageJ graphics program.

Northern blotting and microarray analysis. Northern blotting was performed as described earlier³⁸. Total RNA was isolated from control and IDGF2-treated cells (16 µg/ml for 4 h), using TRIZOL (Life Technologies). Cl.8+ cells were lysed in TRIZOL and the aqueous phase was used for further purification on RNeasy spin columns (Qiagen RNeasy kit).

The Affymetrix GeneChip® *Drosophila* Genome Array System was used for the microarray analysis following the standard protocol (100 ng RNA was amplified with GeneChip 3' IVT Express Kit (Affymetrix) and 10 µg of labeled cRNA was hybridized onto the chip according to the protocols provided by the manufacturer. Labelled cDNA was hybridized to an Affymetrix GeneChip *Drosophila* Genome Array. The analysis was performed using three replicates. Data were pre-processed in the Partek Genomic Suite (Partek Incorporated), as described previously³⁹ and various Bioconductor packages, including Limma⁴⁰. In short, the transcription profiles were background corrected using the GCRMA method, quantile normalized and variance stabilized using the base-2 logarithmic transformation. Limma was used for differential expression analysis. Deregulated genes were selected based on FDR (false discovery rate) < 0.05. FDR was calculated by BH (Benjamini-Hochberg) procedure. The transcription data are MIAME compliant and deposited in the ArrayExpress database (accession E-MTAB-5007). All statistical analyses were performed in R software (<http://www.R-project.org>) via Bioconductor. Gene set enrichment analysis and determination of gene functions were performed using DAVID Bioinformatics Resources web service⁴¹ and AmiGO2⁴².

Real-Time RT-PCR. Total RNA isolation, subsequent reverse transcription and real-time RT-PCR from different time points of *Drosophila* development or from larvae with septic or aseptic injury was performed as described previously²⁷. For real-time RT-PCR from Cl.8+ cells, we followed a protocol described previously²⁰. The primers are shown in Table S1.

***Drosophila* septic and aseptic injury assays.** Injury experiments were performed according to DeGregorio *et al.*⁴³. We used the wandering third instar larvae or 3 day old adult males. The aseptic injury was performed by pricking the larvae or fly thorax with a sterile 0.2 mm syringe needle, while for septic injury the needle was first dipped into a concentrated *Escherichia coli* K12 culture. The puncture wounds were small, and no discernible amount of body fluid was lost from the injured animals. The flies were then kept at 25 °C and collected at specific time points after injury (1, 3 and 6 h).

References

- Dolezelova, E., Zurovec, M., Dolezal, T., Simek, P. & Bryant, P. J. The emerging role of adenosine deaminases in insects. *Insect Biochem Mol Biol* **35**, 381–389 (2005).
- Dolezal, T., Dolezelova, E., Zurovec, M. & Bryant, P. J. A role for adenosine deaminase in Drosophila larval development. *PLoS Biol* **3**, e201 (2005).
- Hipfner, D. R. & Cohen, S. M. New growth factors for imaginal discs. *Bioessays* **21**, 718–720 (1999).
- Kirkpatrick, R. B., Matico, R. E., McNulty, D. E., Strickler, J. E. & Rosenberg, M. An abundantly secreted glycoprotein from *Drosophila melanogaster* is related to mammalian secretory proteins produced in rheumatoid tissues and by activated macrophages. *Gene* **153**, 147–154 (1995).
- Kawamura, K., Shibata, T., Saget, O., Peel, D. & Bryant, P. J. A new family of growth factors produced by the fat body and active on *Drosophila* imaginal disc cells. *Development* **126**, 211–219 (1999).
- Irving, P. *et al.* New insights into *Drosophila* larval haemocyte functions through genome-wide analysis. *Cell Microbiol* **7**, 335–350 (2005).
- Varela, P. F., Llera, A. S., Mariuzza, R. A. & Tormo, J. Crystal structure of imaginal disc growth factor-2. A member of a new family of growth-promoting glycoproteins from *Drosophila melanogaster*. *J Biol Chem* **277**, 13229–13236 (2002).
- Watanabe, T., Oyanagi, W., Suzuki, K., Ohnishi, K. & Tanaka, H. Structure of the gene encoding chitinase D of *Bacillus circulans* WL-12 and possible homology of the enzyme to other prokaryotic chitinases and class III plant chitinases. *J Bacteriol* **174**, 408–414 (1992).
- Zhu, Q., Arakane, Y., Beeman, R. W., Kramer, K. J. & Muthukrishnan, S. Characterization of recombinant chitinase-like proteins of *Drosophila melanogaster* and *Tribolium castaneum*. *Insect Biochem Mol Biol* **38**, 467–477 (2008).
- He, C. H. *et al.* Chitinase 3-like 1 regulates cellular and tissue responses via IL-13 receptor alpha2. *Cell Rep* **4**, 830–841 (2013).
- Johansen, J. S., Cinton, C., Jorgensen, M., Kamby, C. & Price, P. A. Serum YKL-40: a new potential marker of prognosis and location of metastases of patients with recurrent breast cancer. *Eur J Cancer* **31A**, 1437–1442 (1995).
- Zhou, Y. *et al.* Chitinase 3-like 1 suppresses injury and promotes fibroproliferative responses in Mammalian lung fibrosis. *Sci Transl Med* **6**, 240ra276 (2014).
- Karlsson, C. *et al.* Proteomic analysis of the *Drosophila* larval hemolymph clot. *J Biol Chem* **279**, 52033–52041 (2004).
- Vierstraete, E. *et al.* Proteomics in *Drosophila melanogaster*: first 2D database of larval hemolymph proteins. *Biochem Biophys Res Commun* **304**, 831–838 (2003).
- Blanco, E. *et al.* Gene expression following induction of regeneration in *Drosophila* wing imaginal discs. Expression profile of regenerating wing discs. *BMC Dev Biol* **10**, 94 (2010).
- Fernandez-Almonacid, R. & Rosen, O. M. Structure and ligand specificity of the *Drosophila melanogaster* insulin receptor. *Molecular and Cellular Biology* **7**, 2718–2727 (1987).
- Peel, D. J., Johnson, S. A. & Milner, M. J. The ultrastructure of imaginal disc cells in primary cultures and during cell aggregation in continuous cell lines. *Tissue Cell* **22**, 749–758 (1990).
- Zurovec, M., Dolezal, T., Gazi, M., Pavlova, E. & Bryant, P. J. Adenosine deaminase-related growth factors stimulate cell proliferation in *Drosophila* by depleting extracellular adenosine. *Proc Natl Acad Sci USA* **99**, 4403–4408 (2002).
- Hershfield, M. S. & Kredich, N. M. Resistance of an adenosine kinase-deficient human lymphoblastoid cell line to effects of deoxyadenosine on growth, S-adenosylhomocysteine hydrolase inactivation, and dATP accumulation. *Proc Natl Acad Sci USA* **77**, 4292–4296 (1980).
- Fleischmannova, J. *et al.* Differential response of *Drosophila* cell lines to extracellular adenosine. *Insect Biochem Mol Biol* **42**, 321–331 (2012).
- Coulom, H. & Birman, S. Chronic exposure to rotenone models sporadic Parkinson's disease in *Drosophila melanogaster*. *J Neurosci* **24**, 10993–10998 (2004).
- Ivanov, V. N. *et al.* Resveratrol sensitizes melanomas to TRAIL through modulation of antiapoptotic gene expression. *Exp Cell Res* **314**, 1163–1176 (2008).
- Moon, D. O. *et al.* JNK inhibitor SP600125 promotes the formation of polymerized tubulin, leading to G2/M phase arrest, endoreduplication, and delayed apoptosis. *Exp Mol Med* **41**, 665–677 (2009).
- Misra, J. R., Horner, M. A., Lam, G. & Thummel, C. S. Transcriptional regulation of xenobiotic detoxification in *Drosophila*. *Genes Dev* **25**, 1796–1806 (2011).
- Swinnen, J. V., Brusselmans, K. & Verhoeven, G. Increased lipogenesis in cancer cells: new players, novel targets. *Curr Opin Clin Nutr Metab Care* **9**, 358–365 (2006).
- Crossley, A. C. In *Comprehensive Insect Physiology Biochemistry and Pharmacology* Vol. 3 (eds Kerkut, G. A. & Gilbert, L. I.) 487–516 (Pergamon Press, 1985).
- Kucerova, L. *et al.* The *Drosophila* Chitinase-Like Protein IDGF3 Is Involved in Protection against Nematodes and in Wound Healing. *J Innate Immun* (2015).
- Zartman, J., Restrepo, S. & Basler, K. A high-throughput template for optimizing *Drosophila* organ culture with response-surface methods. *Development* **140**, 667–674 (2013).
- Lehrer, R. I. & Ganz, T. Defensins: endogenous antibiotic peptides from human leukocytes. *Ciba Found Symp* **171**, 276–290, discussion 290–273 (1992).
- Echalier, G. *Drosophila Cells in Culture*. (Academic Press, 1997).
- Boison, D. *et al.* Neonatal hepatic steatosis by disruption of the adenosine kinase gene. *Proc Natl Acad Sci USA* **99**, 6985–6990 (2002).
- Weavers, H. *et al.* The insect nephrocyte is a podocyte-like cell with a filtration slit diaphragm. *Nature* **457**, 322–326 (2009).
- De Gregorio, E., Spellman, P. T., Tzou, P., Rubin, G. M. & Lemaitre, B. The Toll and Imd pathways are the major regulators of the immune response in *Drosophila*. *EMBO J* **21**, 2568–2579 (2002).
- Buchon, N., Silverman, N. & Cherry, S. Immunity in *Drosophila melanogaster*—from microbial recognition to whole-organism physiology. *Nat Rev Immunol* **14**, 796–810 (2014).
- Hoover, D. J. *et al.* Expression of the chitinase family glycoprotein YKL-40 in undifferentiated, differentiated and trans-differentiated mesenchymal stem cells. *PLoS One* **8**, e62491 (2013).
- Di Rosa, M. & Malaguarnera, L. Chitinase 3 Like-1: An Emerging Molecule Involved in Diabetes and Diabetic Complications. *Pathobiology* **83**, 228–242 (2016).
- Low, D. *et al.* Chitinase 3-like 1 induces survival and proliferation of intestinal epithelial cells during chronic inflammation and colitis-associated cancer by regulating S100A9. *Oncotarget* **6**, 36535–36550 (2015).
- Zurovec, M., Kodrik, D., Yang, C., Sehna, F. & Scheller, K. The P25 component of *Galleria* silk. *Mol Gen Genet* **257**, 264–270 (1998).
- Arefin, B. *et al.* Genome-wide transcriptional analysis of *Drosophila* larvae infected by entomopathogenic nematodes shows involvement of complement, recognition and extracellular matrix proteins. *J Innate Immun* **6**, 192–204 (2014).
- Smyth, G. K. *Limma: linear models for microarray data*. 397–420 (Springer, 2005).
- Huang da, W., Sherman, B. T. & Lempicki, R. A. Systematic and integrative analysis of large gene lists using DAVID bioinformatics resources. *Nat Protoc* **4**, 44–57 (2009).
- Carbon, S. *et al.* AmiGO: online access to ontology and annotation data. *Bioinformatics* **25**, 288–289 (2009).
- De Gregorio, E., Spellman, P. T., Rubin, G. M. & Lemaitre, B. Genome-wide analysis of the *Drosophila* immune response by using oligonucleotide microarrays. *Proc Natl Acad Sci USA* **98**, 12590–12595 (2001).

Acknowledgements

We thank Ruzenka Kuklova for technical assistance. We also thank Thomas Radimerski and Robert Farkas for critical reading of the manuscript. This research was supported by grant P305/14-27816S from the Czech Science Foundation and Grant Interreg Bayern - Tschechische Republik Ziel ETZ 2014-2020 no. 123. V.B. was partially supported by grant 14-07172S from the Czech Science Foundation.

Author Contributions

V.B., L.K., L.R., H.S. and M.Z. performed experiments. All authors commented on the results and manuscript.

Additional Information

Supplementary information accompanies this paper at <http://www.nature.com/srep>

Competing financial interests: The authors declare no competing financial interests.

How to cite this article: Broz, V. *et al.* *Drosophila* imaginal disc growth factor 2 is a trophic factor involved in energy balance, detoxification, and innate immunity. *Sci. Rep.* 7, 43273; doi: 10.1038/srep43273 (2017).

Publisher's note: Springer Nature remains neutral with regard to jurisdictional claims in published maps and institutional affiliations.



This work is licensed under a Creative Commons Attribution 4.0 International License. The images or other third party material in this article are included in the article's Creative Commons license, unless indicated otherwise in the credit line; if the material is not included under the Creative Commons license, users will need to obtain permission from the license holder to reproduce the material. To view a copy of this license, visit <http://creativecommons.org/licenses/by/4.0/>

© The Author(s) 2017

Supplementary information

***Drosophila* imaginal disc growth factor 2 is a trophic factor involved in energy balance, detoxification, and innate immunity**

Vaclav Broz^{1,2}, Lucie Kucerova¹, Lenka Rouhova², Jana Fleischmannova¹, Hynek Strnad³, Peter J. Bryant⁴ and Michal Zurovec^{1,2}

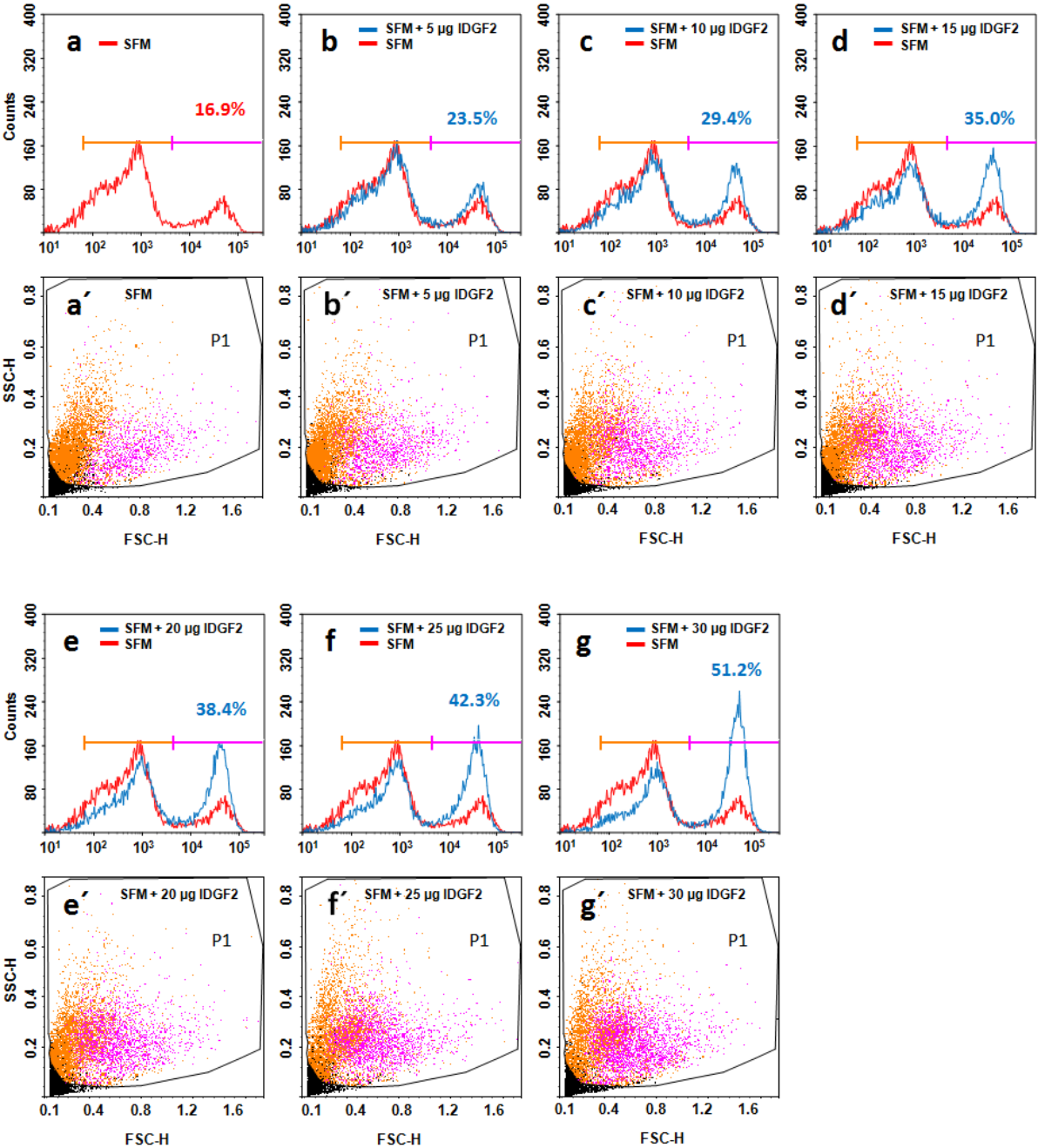
¹Institute of Entomology, Biology Centre CAS, Branisovska 31, 370 05 Ceske Budejovice, Czech Republic;

²Faculty of Science, University of South Bohemia, Branisovska 31, 370 05 Ceske Budejovice, Czech Republic;

³Institute of Molecular Genetics CAS, Videnska 1083, 142 20 Prague 4; Czech Republic;

⁴Developmental & Cell Biology, School of Biological Sciences, University of California, Irvine, USA.

Figure S1. Dose effect of IDGF2 treatment on *Drosophila* Cl.8+ cells. Histograms (a-n) and FSC/SSC plots (a'-n') show mitochondrial polarity assessed by flow cytometric analysis of TMRE stained cells in SFM (a-g) and chemically defined media MM (h-n). The cells with active mitochondria (sequestering TMRE) correspond to right peaks in histograms (a-n) and to pink cell populations shown in scatter plots (a'-n'). The left peaks in histograms (a-n) and orange cell populations in scatter plots (a'-n') consist of TMRE-negative cells undergoing apoptosis. Apoptotic cells are clearly distinguishable from normal Cl.8+ cells in scatter plots by having reduced cell size (low FSC) and enhanced density (high SSC).



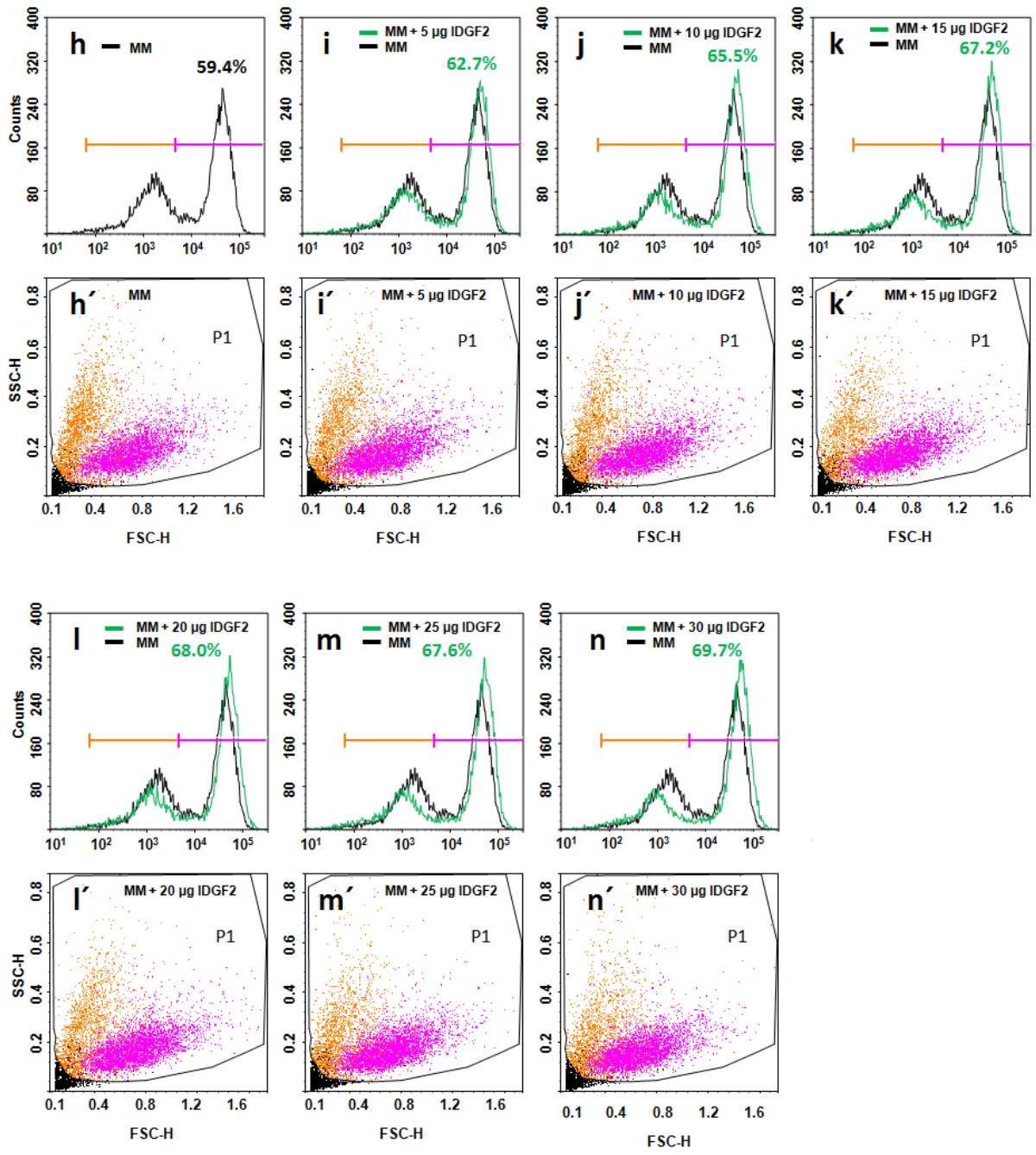


Figure S2. IDGF2 has only a marginal effect on Cl.8+ in the complete media (CM).

Mitochondrial polarity was assessed by flow cytometric analysis of TMRE stained cells. Numbers represent the proportion of viable cells.

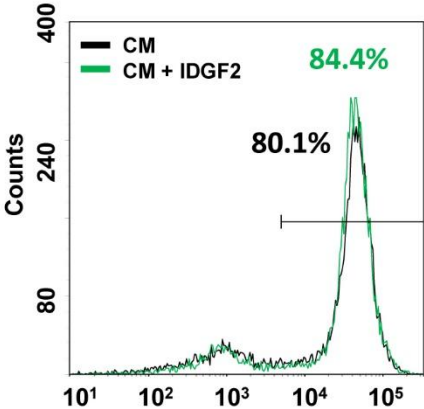


Figure S3. Results of three separate experiments comparing the effects of insulin and IDGF2 on CI.8+ cells in chemically defined media. The figure shows histograms of mitochondrial membrane potential assessed by TMRE fluorescence. The cells were analyzed 24 h after the transfer from CM to MM (black) or to MM supplemented with insulin (red), IDGF2 (green) or both (blue). Numbers represent the proportion of viable cells. IDGF2 (16 $\mu\text{g}/\text{ml}$) treated cells had a higher proportion of living cells (panels C, G and K compared to the TMRE-control cells). Insulin treatment (0.125 IU/ml) led to a shift of the right peak further to the right (panels B, F and J), suggesting an increase in $\Delta\Psi_m$.

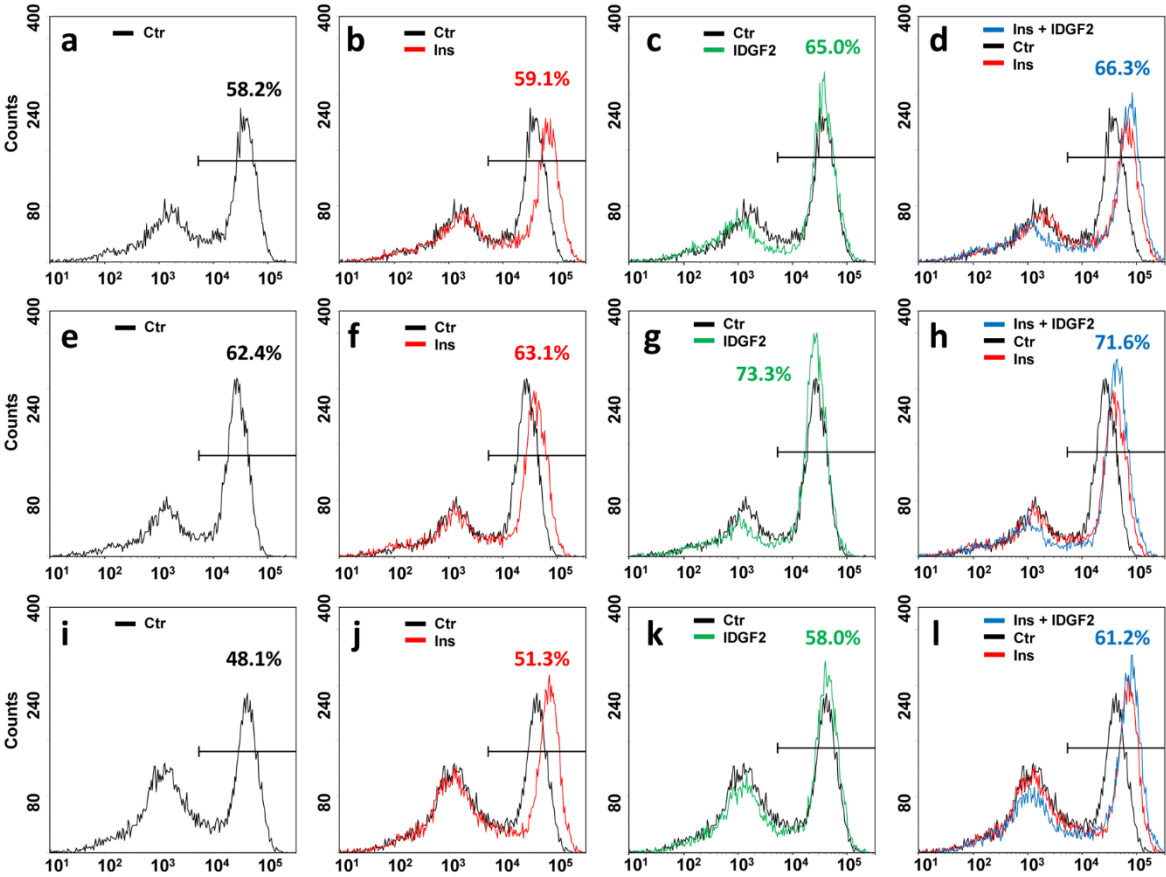
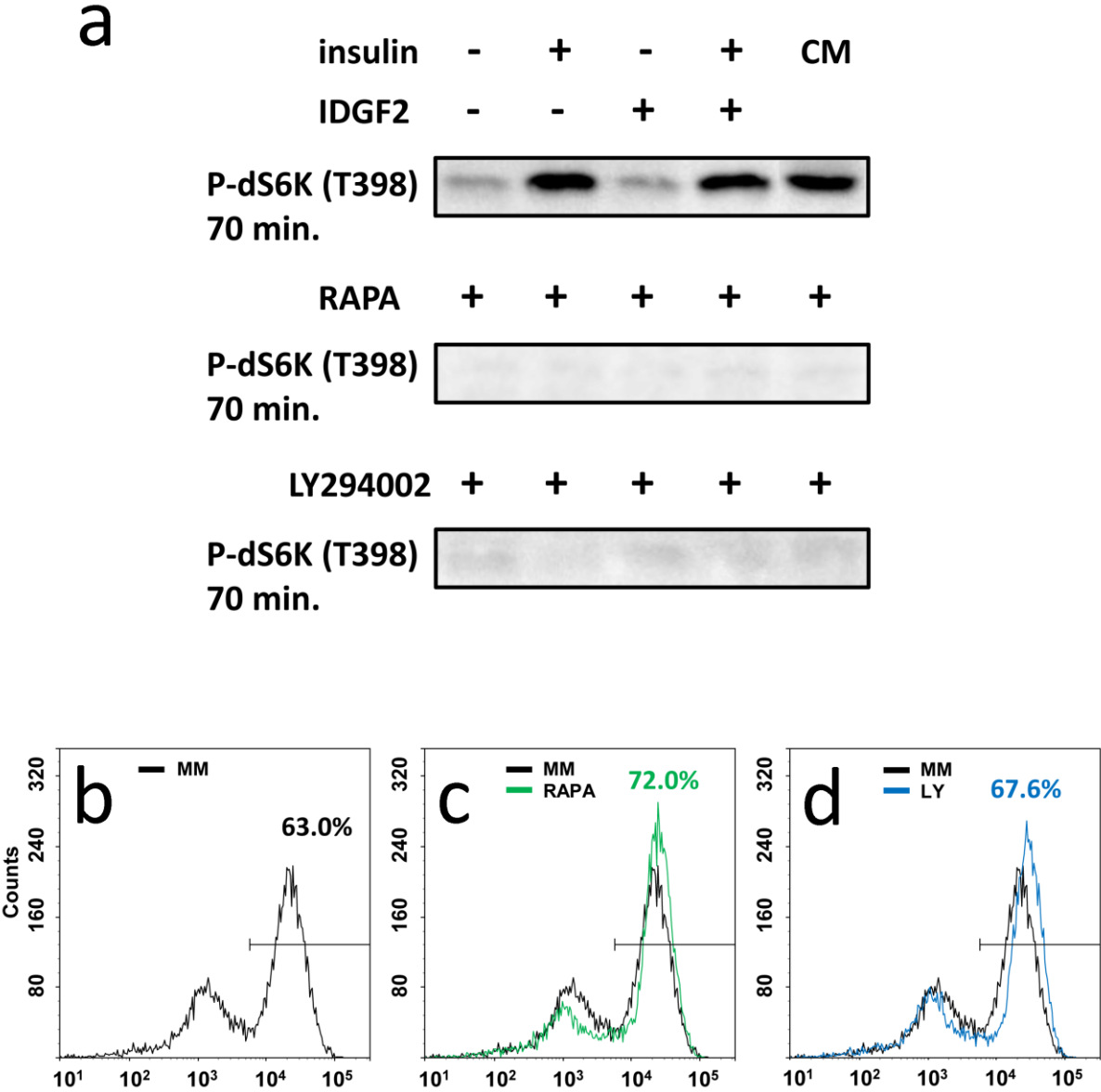


Figure S4. Western blot analysis comparing the levels of phosphorylated dS6K (T398) in Cl.8+ cells pretreated with Rapamycin or LY294002. (a) Rapamycin (20 nM) and LY294002 (15 μM) abolished dS6K phosphorylation. Both drugs did not affect cell viability determined by TMRE staining and flow cytometry (c,d). The cells were treated for 16 h in MM (b); MM + 20 nM rapamycin (c) and MM + 15 μM LY294002 (d). Numbers represent the proportion of viable cells.



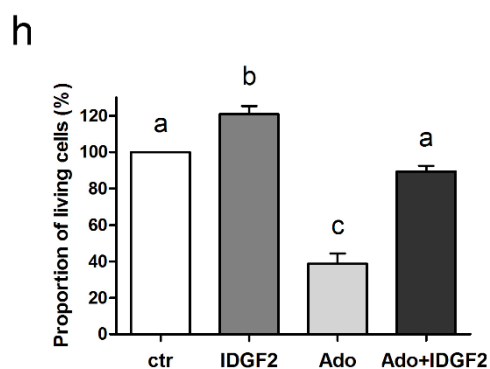
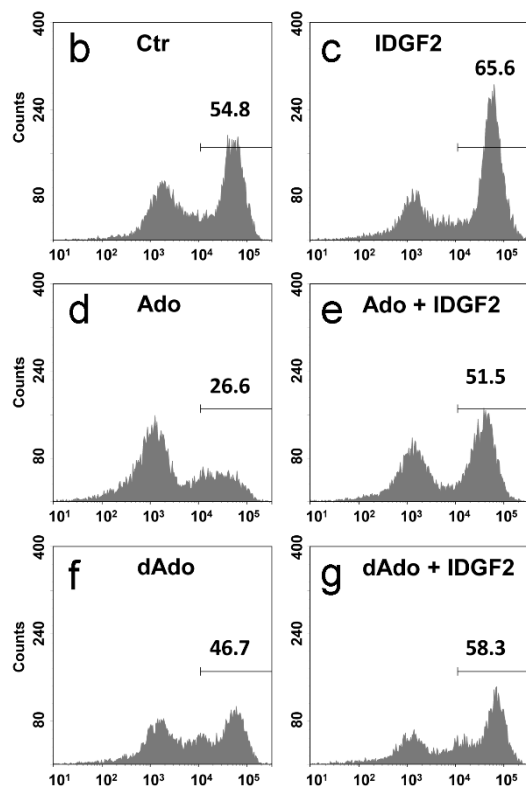
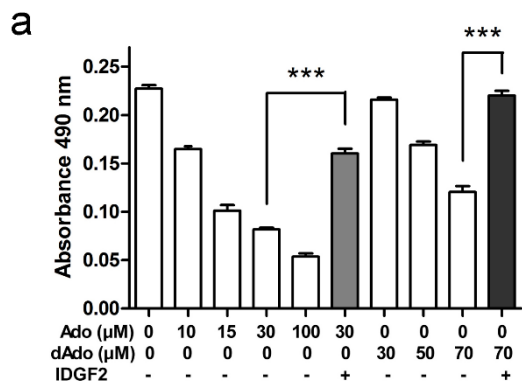


Figure S5. Cytotoxic effect of Ado and dAdo can be antagonized by IDGF2. (a)

MTS cell viability assay performed on cells treated with 0, 10, 15, 30 or 100 μM Ado or with 0, 30, 50 or 70 μM dAdo show a concentration-dependent decrease in MTS staining as well as the rescue of 30 μM Ado (grey bar) or 70 μM dAdo (black bar) treated Cl.8+ cells with IDGF2 (16 μg/ml). Data in the graphs are presented as mean ± SEM (n = 5). Significant differences (***) p < 0.001 between highlighted treatments are indicated by asterisk and was evaluated by Student's t-test. (b-g) mitochondrial polarity was assessed by flow cytometric analysis of TMRE stained cells. Cl.8+ cells in MM (b and c) or MM plus Ado (30 μM) (d and e) and dAdo (70 μM) (f, g) in the absence (b, d, f) or presence (c, e, g) of IDGF2 (16 μg/ml). The total cell population was gated on TMRE positive cells; the numbers represent the proportion of these cells. (h) Effects of IDGF2 on the viability of cells treated by Ado. The graph summarizes three cell cytometry experiments. Significant differences were evaluated by ANOVA followed by Tukey test and are indicated by different letters (p < 0.05).

Figure S6. Effect of IDGF2 on Ado uptake and ATP synthesis and deleterious effects of dAdo and resveratrol on ATP synthesis. (a) IDGF2 (5 or 20 $\mu\text{g/ml}$) does not influence $\text{H}^3\text{-Ado}$ (10 μM) uptake by Cl.8+ cells. Dipy (Dipyridamole) a known inhibitor of equilibrative Ado transport serve as positive control (b) IDGF2 (16 $\mu\text{g/ml}$) does not decrease ATP synthesis in Cl.8+ cells treated with Ado (30 μM). (c) Decrease of ATP synthesis in Cl.8+ cells treated with dAdo or resveratrol. Data in the graphs are presented as mean \pm SEM (n = 3). Significant differences were evaluated by ANOVA followed by Tukey test and are indicated by different letters ($p < 0.05$).

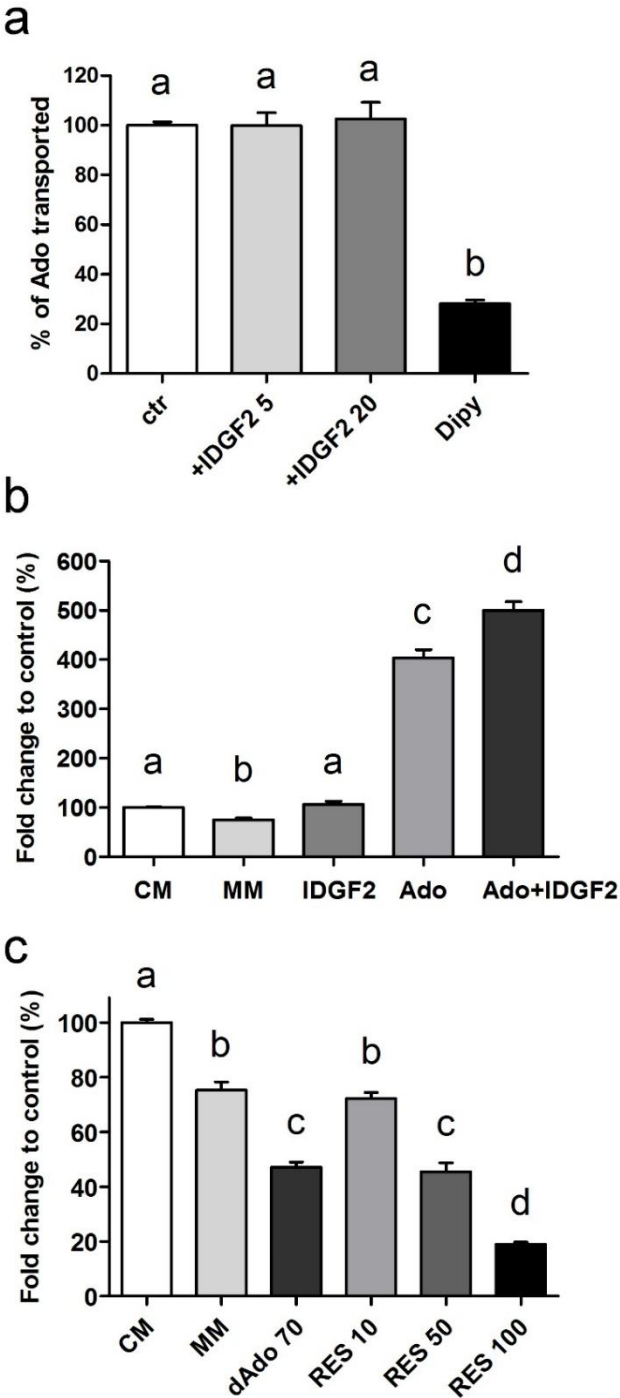


Figure S7. The effects of serum (2%) and fly extracts (2.5%) on Cl.8+ cells in MM treated with Ado (100 μM), resveratrol (RES, 100 μM) and rotenone (ROT, 0.01 μM). Mitochondrial polarity was assessed by flow cytometric analysis of TMRE stained cells. Numbers represent the proportion of viable cells.

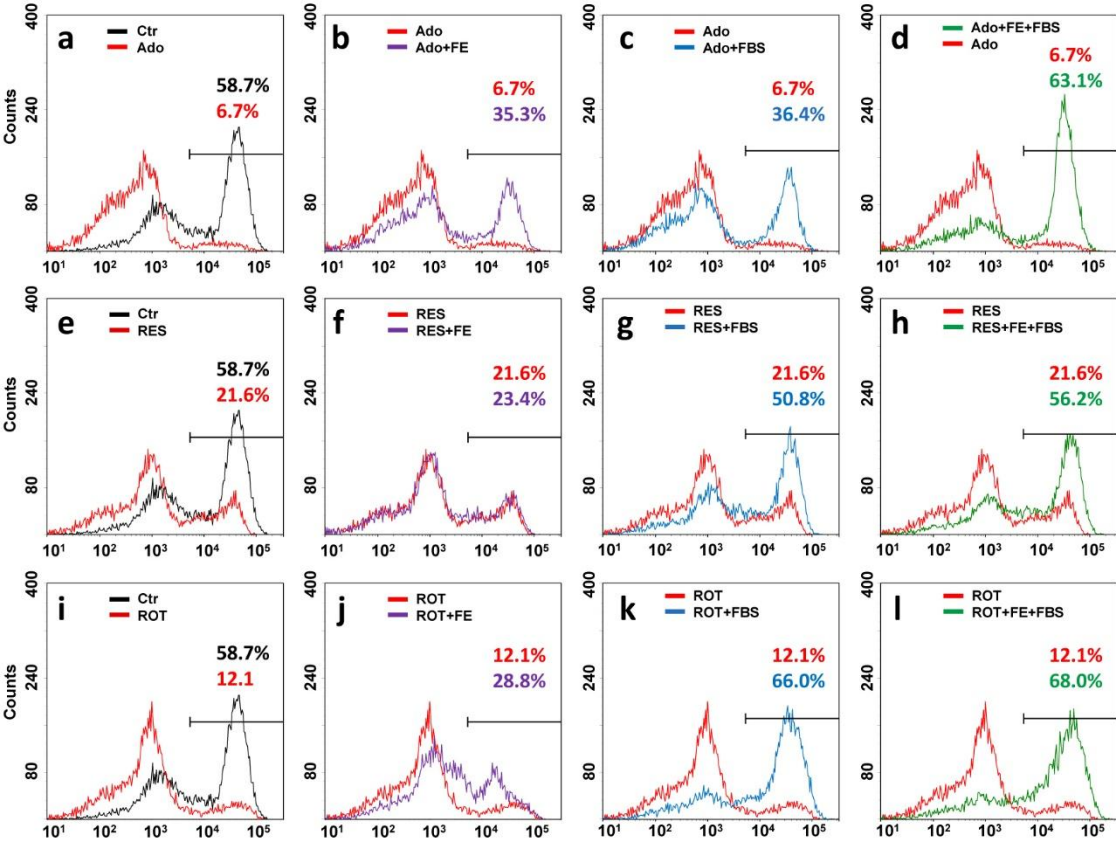


Figure S8. Venn diagram summarizing the results of microarray analysis. Diagram compares numbers of significantly ($p < 0.05$, $|\logFC| > 0.8$) regulated genes in Cl.8+ cells treated with IDGF2 (16 $\mu\text{g/ml}$), Ado (50 μM) or IDGF2 (16 $\mu\text{g/ml}$) + Ado (50 μM). Lists of genes are shown in Tables S2-4.

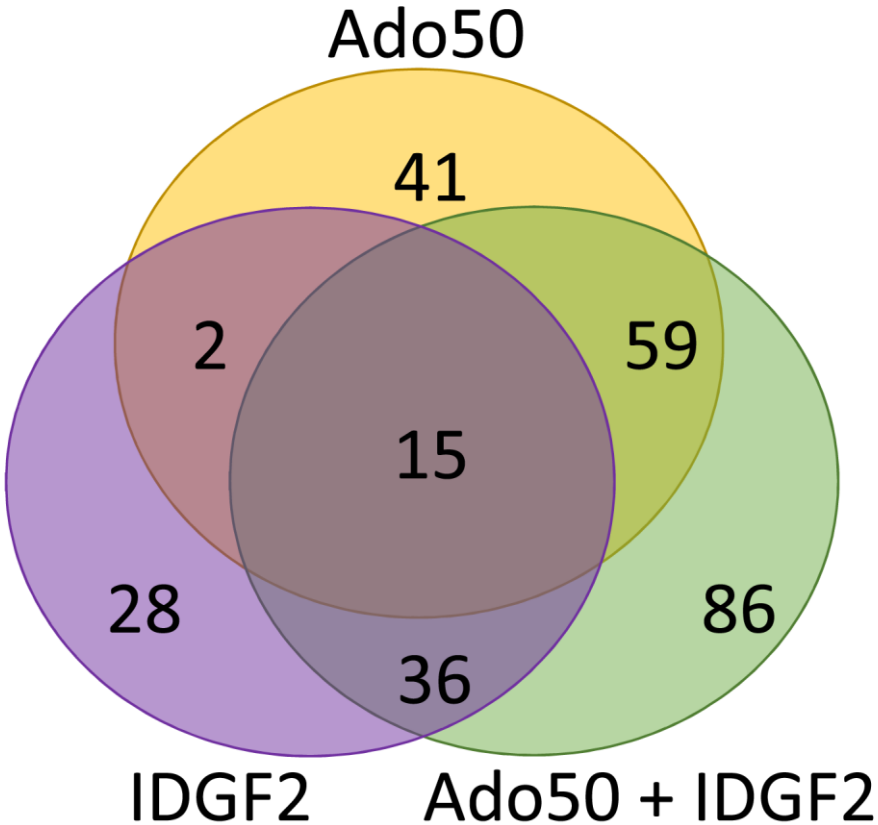


Figure S9. *Idgf2* transcript expression. Wild-type third instar larval tissues showing in situ hybridization with digoxigenin-labeled antisense RNA probe (**a, c**), for *Idgf2*. Strongest expression signal was detected in fat body (**a**), whereas garland cells (red tracing line) attached to proventriculus do not show any signal (**c**). Corresponding negative control with sense RNA probes are shown in (**b, d**). Scale bars: 50 μ m.

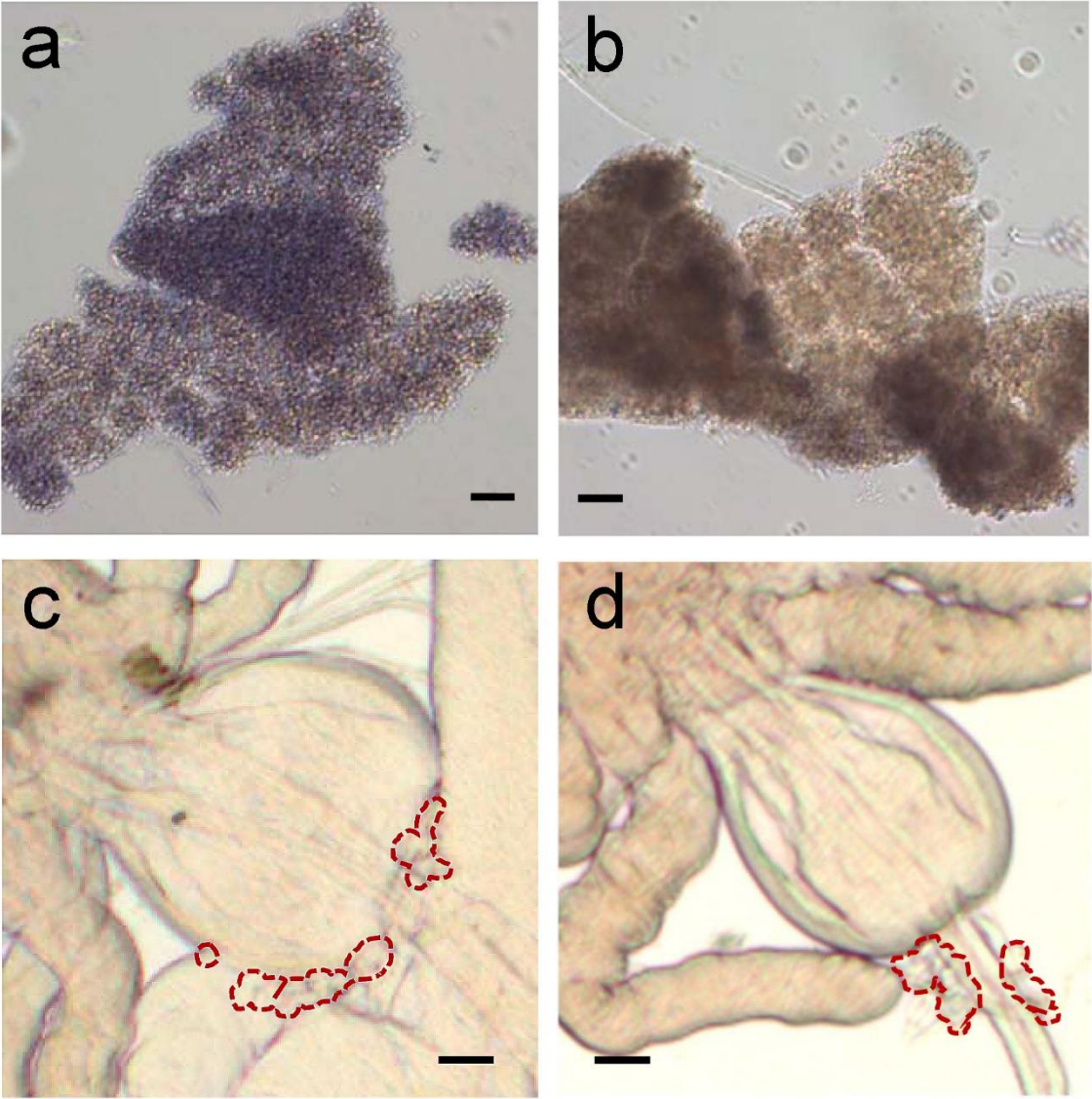


Figure S10. The effects of IDGF2 on S2 cells. The cells were grown in chemically defined media (a, b), or treated with Ado 50 μ M (c, d) and Ado 100 μ M (e, f). Mitochondrial membrane potential was assessed by flow cytometric analysis of TMRE stained cells. Numbers represent the proportion of viable cells.

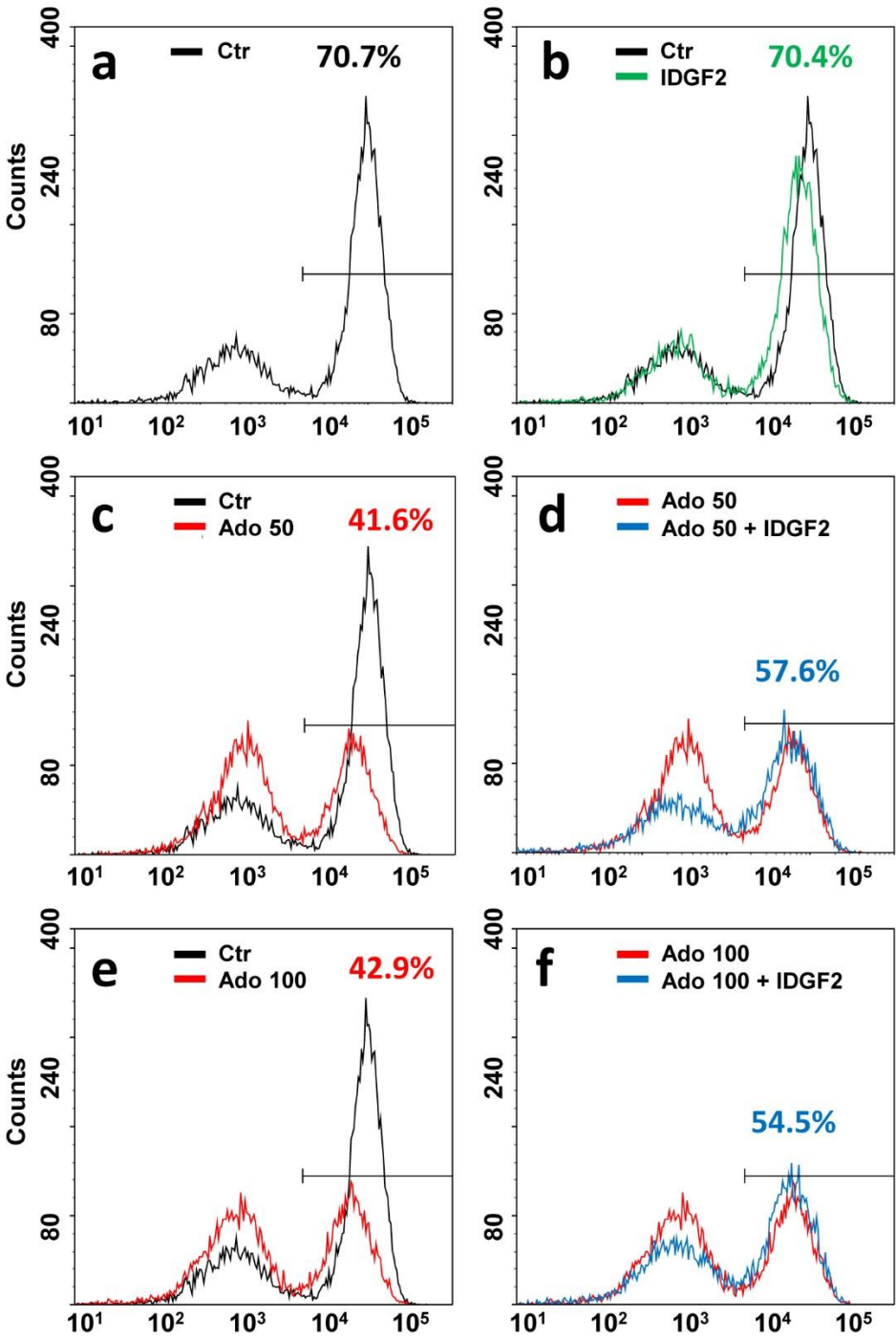


Figure S11. Representative full-length western blot images from Fig. 4g. and northern blot images from Fig. 7b (a) cropped western blot from Fig. 4g.; (b, c, d and e) full-length western blots; (f) cropped northern blots (Fig7b); (g, h and i) full length northern blots.

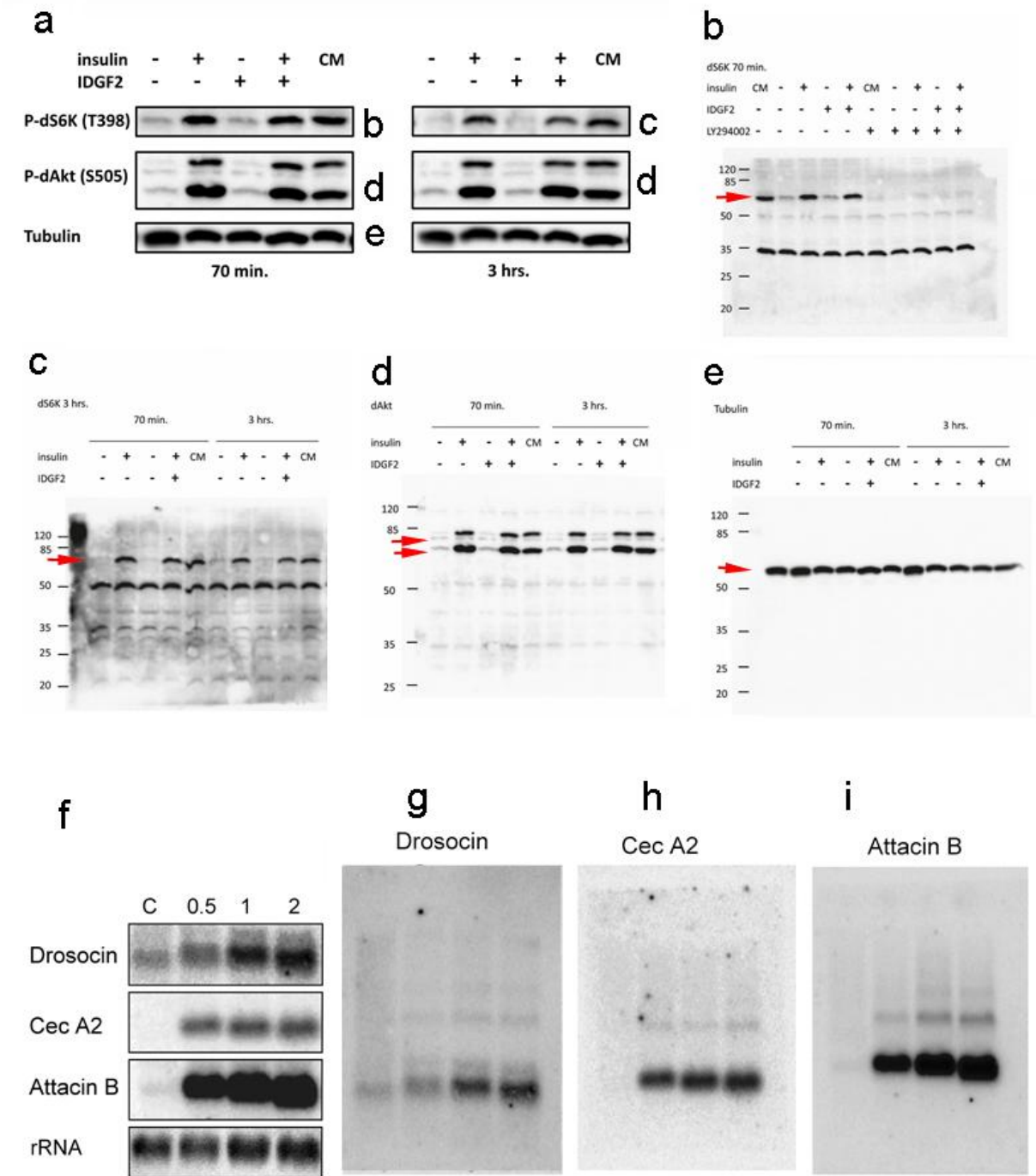


Table S1. List of primers used in this study

Gene	Primer name	Sequence	Reference
Idgf2	forward Idgf2::GFP recombineering	AGTGCTCAGGCGATAAGTATCCCATTCTGC GAGCCATCAAATATCGTCTAGAAGTGCAT ACCAATCAGGACCCGC	This study
	reverse Idgf2::GFP recombineering	ATAATTGATAATTGTTTATTTAAAGTATTA ATGTTATGTTTCGTTTACTTGTCGTCGTCA TCCTGTAGTCA	This study
	Idgf2EcoF	TGAATTCATCATGAAGGCGTGGATCTGGTT	This study
	Idgf2R1	CTTCTGAGATGAGTTTTTGTCTAGACGAT ATTTGATGGCTCG	This study
	MycXba	GTTCTAGATCACAGATCCTCTTCTGAGATG AGTTTTTGTTT	This study
Ribosomal protein L32	rp49 fw	CTTCATCCGCCACCAGTC	Kucerova et al., 2015
	rp49 rev	GGCGACGCACTCTGTTGT	Kucerova et al., 2015
Imaginal disc growth factor 2	Idgf2 fw	GCTACTATGACTCTTCGAGTTACACC	This study
	Idgf2 rev	TCCAGATCGGGATTGAGC	This study
Attacin-A	AttA fw	TGGTCATGGTGCCTCTTTG	Arefin et al. 2014
	AttA rev	GATTGTGTCTGCCATTGTTGA	Arefin et al. 2014
Attacin-D	AttD fw	CGGAGTAAGGGTTCGGTGAT	This study
	AttD rev	GCCATGCTGCAGTGAGAGT	This study
Cecropin A1	CecA1 fw	CTTCGTTTTTCGTCGCTCTC	This study
	CecA1 rev	TTTTCTTGCCAATTTTCTTCAG	This study
Homeodomain interacting protein kinase	Hipk fw	AGTCGCCGGCTCATCATA	This study
	Hipk rev	CCTTCACCCGCTTCTTCAC	This study
Zn finger homeodomain 1	Zfh1 fw	ATCCCGATCTGCCCTATG	This study
	Zfh1 rev	GCCTTCGGACACTCTATGC	This study
Relish	Rel fw	CTATGTGGCGCAATTTATCAAC	This study
	Rel rev	TGGCCTCACGCTCTGTCTC	This study
Peptidoglycan recognition protein LB	PGRP-LB fw	GGCGATGGCATGATTTACA	This study
	PGRP-LB rev	GCGGCAGTTCGGTTCTC	This study

Table S2. List of 81 genes differentially expressed upon IDGF2 treatment of Cl.8+ cells. The genes are arranged into classes according to their GO terms. The statistical threshold was set to $p < 0.05$ and the threshold of induction was set to 1.74.

SYMBOL	GENE NAME	logFC	GO term
--------	-----------	-------	---------

immune response

AttA	Attacin-A	2.91 / 6.54	antibacterial humoral response
AttC	Attacin-C	3.44	antibacterial humoral response
AttD	Attacin-D	5.22	antibacterial humoral response
CecA1	Cecropin A1	6.22	antibacterial humoral response
CecA2	Cecropin A2	5.08	antibacterial humoral response
CecB	Cecropin B	2.09	antibacterial humoral response
CecC	Cecropin C	5.18 / 5.79	antibacterial humoral response
Dpt	Diptericin	1.18	antibacterial humoral response
DptB	Diptericin B	4.91	antibacterial humoral response
Dro	Drosocin	4.15	antibacterial humoral response
FBgn0030309	CG1572	1.14	hemocyte proliferation
Mtk	Metchnikowin	2.08	humoral immune response
PGRP-LB	Peptidoglycan recognition protein LB	4.17	response to bacterium
PGRP-SA	Peptidoglycan recognition protein SA	1.43	response to bacterium
PGRP-SD	Peptidoglycan recognition protein SD	3.21	response to bacterium
pirk	poor Imd response upon knock-in	2.1	negative regulation
Rel	Relish	1.25	innate immune response
vir-1	virus-induced RNA 1	0.83	response to virus

metabolic process

FBgn0033388	CG8046	1.06	metabolic process
FBgn0037344	CG2926	0.8	regulation of gene expression
FBgn0037482	CG10055	0.9	primary metabolic process
Gclc	Glutamate-cysteine ligase	0.99	biosynthetic process;
gish	gilgamesh	1.2	protein phosphorylation
GstD2	Glutathione S transferase D2	0.99	metabolic and cellular process
Psa	Puromycin sensitive aminopeptidase	0.84	regulation of proteolysis
qin	qin	0.85	regulation of gene expression
scaf	scarface	1.18	protein metabolic process
Spn4	Serine protease inhibitor 4	1.12	regulation of proteolysis
Sulf1	Sulfated	1.02	metabolic and cellular process
y	yellow	0.86	biosynthetic process

localization - transport

AnnIX	Annexin IX	1.06	endosomal transport
CASK	CASK ortholog	0.97	protein localization
CG4928	UNC93-like protein	1.34	transport
FBgn0038414	CG6901	1.04	transmembrane transport
FBgn0039644	CG11897	0.84	transport
Mec2	CG7635	1.06	nephrocyte filtration
Mvl	Malvolio	1.56	metal ion transport
Oatp74D	Organic anion transporting polypeptide 74D	0.97	transport
Pmp70	Peroxisomal Membrane Protein 70 kDa	0.9	transmembrane transport
RabX1	RabX1	1.35	vesicle-mediated transport
spri	sprint	1.23	vesicle-mediated transport
Trn	Transportin	0.96	intracellular protein transport

morphogenesis and development

CAP	CG18408	0.95	system development
CrebA	Cyclic-AMP response element binding protein A	1.4	system development
FBgn0033889	CG6701	1.09	nervous system development
FBgn0260965	CG42588	0.97	nervous system development
FBgn0263346	CG43427	0.92	wing disc development
FBgn0263993	CG43736	0.88	morphogenesis and development
fng	fringe	-0.8	imaginal disc morphogenesis
foi	fear-of-intimacy	2.09	system development
fra	frazzled	0.84	nervous system development
glec	glilectin	1.19	nervous system development
hipk	homeodomain interacting protein kinase	1.51	imaginal disc morphogenesis
kug	kugelei	1.08	system development
Mob2	CG11711	0.97	system development
Nrg	Neuroglian	0.95	nervous system development
pyd	polychaetoid	0.85	morphogenesis and development
spen	split ends	1.48	imaginal disc morphogenesis
Wnk	CG7177	0.81	system development
zfh1	Zn finger homeodomain 1	1.12	garland nephrocyte differentiation

cellular component organization or biogenesis

Jupiter	CG31363	0.99	cytoskeleton organization
Map205	Microtubule-associated protein 205	0.86	cytoskeleton organization
mask	multiple ankyrin repeats single KH domain	1.82	cytoskeleton organization
Mmp1	Matrix metalloproteinase 1	2.51	membrane organization
nuf	nuclear fallout	0.92	cytoskeleton organization
Rac2	CG8556	0.97	cytoskeleton organization
RhoGAP18B	Rho GTPase activating protein at 18B	0.87	cytoskeleton organization
spir	spire	1.47	cytoskeleton organization
trio	CG18214	0.81	cytoskeleton organization

response to stimulus

Ect4	Ectoderm-expressed 4	0.87	signal transduction
FBgn0046763	CG17278	1.05	signal transduction
FBgn0263706	CG43658	1.34	signal transduction
FBgn0264339	CG43795	0.81	signal transduction
for	foraging	1.21	response to food
Gprk2	G protein-coupled receptor kinase 2	1.09	signal transduction
Rtnl1	Reticulon-like1	0.94	response to chemicals
sda	slamdance	1.82	mechanical stimulus

unknown

FBgn0036419	CG13482	2.36	unknown
FBgn0052436	CG32436	-0.89	unknown
FBgn0266101	CG44838	1.24	unknown
SP1173	CG10121	0.82	unknown

Table S3. List of 117 genes differentially expressed upon 50 μ M Ado treatment of Cl.8+ cells. The genes are arranged into classes according to their GO terms. The statistical threshold was set to $p < 0.05$ and the threshold of induction was set to 1.74.

SYMBOL	GENE NAME	logFC	GO term
--------	-----------	-------	---------

immune response

FBgn0033459	CG12744	0.87	response to fungus
pirk	poor lmd response upon knock-in	0.8	negative regulation
vir-1	virus-induced RNA 1	1.26	response to virus

metabolic process

bip2	CG2009	1.01	biosynthetic process
bun	bunched	1.89	primary metabolic process
crp	cropped	1.74	biosynthetic process
ctp	cut up	1.09	metabolic or cellular process
dm	diminutive	1.71	biosynthetic process
DOR	Diabetes and obesity regulated	0.99	biosynthetic process
exba	extra bases	0.82	protein dephosphorylation
FBgn0015351	CG14906	0.91	biosynthetic process
FBgn0028540	CG9008	0.91	metabolic and cellular process
FBgn0030316	CG11695	-0.82	biosynthetic process
FBgn0033204	CG2065	0.85	protein phosphorylation
FBgn0036403	CG6661	1.06	oxidation-reduction process
FBgn0036556	CG5830	1.18	protein acetylation
FBgn0037973	CG18547	0.8	oxidation-reduction process
FBgn0038595	CG7142	1.17	proteolysis
FBgn0038730	CG6300	1.43	primary metabolic process
FBgn0051633	CG31633	1.57	proteolysis
gem	gemini	0.81	biosynthetic process
gish	gilgamesh	1.36	protein phosphorylation
GLS	Glutaminase	0.99	biosynthetic process
GstE1	Glutathione S transferase E1	1.09	metabolic and cellular process
GstO3	Glutathione S transferase O3	0.82	metabolic and cellular process
Hsp26	Heat shock protein 26	1.07	protein folding
Hsp27	Heat shock protein 27	0.94	protein folding
Hsp67Bc	Heat shock gene 67Bc	1.15	protein folding
Hsp68	Heat shock protein 68	1.06	protein folding
Hsp70Ba	Heat-shock-protein-70Ba	1.6	protein folding
chm	chameau	1.38	protein acetylation
lolal	lola like	0.9	regulation of gene expression

MED10	Mediator complex subunit 10	0.82	biosynthetic process
MED26	Mediator complex subunit 26	1.04	biosynthetic process
Mocs1	Molybdenum cofactor synthesis 1 ortholog	0.86	biosynthetic process
Paip2	polyA-binding protein interacting protein 2	1.11	biosynthetic process
Pka-C3	cAMP-dependent protein kinase 3	1.66	primary metabolic process
Ppat-Dpck	Bifunctional Phosphopantetheine adenyltransferase - Dephospho-CoA kinase	-1.03	regulation of growth
PRL-1	PRL-1 phosphatase	1.23	metabolic process
rho	rhomboid	0.97	protein metabolic process
Spn4	Serine protease inhibitor 4	0.86	regulation of proteolysis
tws	twins	0.87	regulation of proteolysis

localization - transport

Best1	Bestrophin 1	0.87	transport
corn	cornetto	1.41	vesicle-mediated transport
FBgn0031645	CG3036	1.68	transport
FBgn0039644	CG11897	0.93	transport
FBgn0051272	CG31272	0.89	transport
glob1	globin 1	1.57	vesicle-mediated transport
Nup153	Nucleoporin 153	1.06	transport
Rala	Ras-related protein	1.42	transport
rin	rasputin	1.08	transport
sky	skywalker	1.21	vesicle-mediated transport
Syx1A	Syntaxin 1A	1.17	vesicle-mediated transport
Vap-33-1	VAMP-associated protein 33kDa	1	transport
yin	CG44402	-0.88	vesicle-mediated transport
ZnT77C	Zinc transporter 77C	1.16	transport

morphogenesis and development

a	arc	1	morphogenesis and development
Akap200	A kinase anchor protein 200	0.9	system development
akirin	CG8580	1.49	morphogenesis and development
CAP	CG18408	1.05	system development
comm2	CG7554	0.88	nervous system development
Cul-2	Cullin-2	0.87	morphogenesis and development
dlp	dally-like	1.45	cell development
fax	failed axon connections	1.51	nervous system development
FBgn0036814	CG14073	0.8	morphogenesis and development
FBgn0039316	CG11893	0.87	morphogenesis and development
FBgn0263346	CG43427	0.86	wing disc development

FBgn0263993	CG43736	0.94	morphogenesis and development
glec	gliolectin	1.33	nervous system development
hig	hikaru genki	1.28	system development
hipk	homeodomain interacting protein kinase	1.56	imaginal disc morphogenesis
kay	kayak	0.95	morphogenesis and development
lama	lamina ancestor	1.13	cell development
Nrt	Neurotactin	0.97	nervous system development
pnt	pointed	0.96	cell differentiation
S	Star	1.11	system development
Socs36E	Suppressor of cytokine signaling at 36E	1.07	embryonic morphogenesis
sprt	sprite	1.35	garland nephrocyte differentiation
stau	staufen	0.85	oocyte development
Swip-1	Swiprosin-1	1.11	morphogenesis and development
Ten-m	Tenascin major	1.15	morphogenesis and development
uzip	unzipped	0.95	nervous system development

cellular component organization or biogenesis

Fhos	Formin homology 2 domain containing	1.17	cellular component movement
mask	multiple ankyrin repeats single KH domain	1.59	cytoskeleton organization
Mmp1	Matrix metalloproteinase 1	1.33	membrane organization
nuf	nuclear fallout	1	cytoskeleton organization
pyd	polychaetoid	0.95	cytoskeleton organization
Rcd2	Reduction in Cnn dots 2	1.79	cell cycle process
spir	spire	1.07	cytoskeleton organization

response to stimulus

Btk29A	Btk family kinase at 29A	0.82	signal transduction
dsd	distracted	0.87	signal transduction
FBgn0039419	CG12290	0.92	signal transduction
FBgn0046763	CG17278	0.89	signal transduction
FBgn0051694	CG31694	1.14 / 1.19	signal transduction
itp	ion transport peptide	0.95	defense response
pes	peste	1.16	defense response
Piezo	CG44122	0.93	signal transduction
Traf4	TNF-receptor-associated factor 4	0.87	signal transduction

unknown

bip1	CG7574	0.9	unknown
FBgn0031474	CG2991	1.06	unknown
FBgn0032197	CG5694	1.22	unknown
FBgn0032400	CG6770	2.18	unknown
FBgn0032805	CG10337	0.8	unknown
FBgn0033458	CG18446	0.8	unknown
FBgn0033945	CG12868	1.21	unknown
FBgn0035996	CG3448	1.32	unknown
FBgn0036419	CG13482	0.91	unknown
FBgn0038682	CG5835	0.84	unknown
FBgn0040837	CG8620	1.17	unknown
FBgn0050460	CG30460	0.9	unknown
FBgn0250869	CG42240	2.04	unknown
FBgn0259711	CG42365	0.91	unknown
FBgn0266101	CG44838	1.47	unknown
fok	fledgling of Klp38B	1.35	unknown
l(1)G0469	lethal (1) G0469	1.1	unknown
Uhg1	U snoRNA host gene 1	1.57	unknown
Xrp1	CG17836	0.95	unknown

Table S4. List of 196 genes differentially expressed upon simultaneous treatment of IDGF2 plus 50 μ M Ado in Cl.8+ cells. The genes are arranged into classes according to their GO terms. The statistical threshold was set to $p < 0.05$ and the threshold of induction was set to 1.74. Genes exclusively expressed upon simultaneous treatment of IDGF2 plus 50 μ M Ado are shown in gray.

SYMBOL	GENENAME	logFC	GO term
--------	----------	-------	---------

immune response

AttA	Attacin-A	2.3 / 6.0	antibacterial humoral response
AttC	Attacin-C	3.86	antibacterial humoral response
AttD	Attacin-D	5.33	antibacterial humoral response
cact	cactus	1.06	immune response
CecA1	Cecropin A1	6.52	antibacterial humoral response
CecA2	Cecropin A2	5.98	antibacterial humoral response
CecB	Cecropin B	2.32	antibacterial humoral response
CecC	Cecropin C	5.1 / 5.7	antibacterial humoral response
Dpt	Diptericin	1.34	antibacterial humoral response
DptB	Diptericin B	4.82	antibacterial humoral response
Dro	Drosocin	3.66	antibacterial humoral response
FBgn0030309	CG1572	0.9	hemocyte proliferation
FBgn0033459	CG12744	0.99	response to fungus
FBgn0259735	CG42389	0.81	immune response
LysX	Lysozyme X	0.89	humoral immune response
Mtk	Metchnikowin	1.77	humoral immune response
PGRP-LB	Peptidoglycan recognition protein LB	3.13	response to bacterium
PGRP-SA	Peptidoglycan recognition protein SA	0.97	response to bacterium
PGRP-SD	Peptidoglycan recognition protein SD	2.88	response to bacterium
pirk	poor Imd response upon knock-in	2.63	negative regulation
Rel	Relish	1.09	innate immune response
TepIV	Thiolester containing protein IV	1.2	antibacterial humoral response
vir-1	virus-induced RNA 1	1.94	response to virus

metabolic process

alph	alphabet	1.04	primary metabolic process
bun	bunched	2.02	primary metabolic process
CalpB	Calpain-B	0.9 / 1.1	proteolysis
Clamp	Chromatin-linked adaptor for MSL proteins	0.84	regulation of gene expression
crp	cropped	1.83	biosynthetic process
Cyp6w1	CG8345	-1.21	oxidation-reduction process
dm	diminutive	1.74	biosynthetic process
DOR	Diabetes and obesity regulated	0.91	biosynthetic process
EloA	Elongin A	0.8	regulation of gene expression
Ets21C	Ets at 21C	0.97	regulation of gene expression

FBgn0015351	CG14906	1.38	biosynthetic process
FBgn0029856	CG11700	1.07	protein metabolic process
FBgn0030332	CG9360	0.97	biosynthetic process
FBgn0033204	CG2065	1.36	protein phosphorylation
FBgn0034583	CG10527	0.87	methylation
FBgn0036403	CG6661	1.68	oxidation-reduction process
FBgn0036828	CG6841	0.9	regulation of gene expression
FBgn0036837	CG18135	-0.95	lipid metabolic process
FBgn0037973	CG18547	0.82	oxidation-reduction process
FBgn0038381	CG3303	0.9	proteolysis
FBgn0038470	CG18213	0.87	regulation of gene expression
FBgn0038595	CG7142	1.08	proteolysis
FBgn0038730	CG6300	0.84	primary metabolic process
FBgn0051633	CG31633	1.34	proteolysis
FBgn0052369	CG32369	0.81	proteolysis
FBgn0052549	CG32549	0.88	primary metabolic process
Fur1	Furin 1	1.03	proteolysis
gem	gemini	0.85	biosynthetic process
gish	gilgamesh	1.34	protein phosphorylation
GLS	Glutaminase	1.21	biosynthetic process
GstD2	Glutathione S transferase D2	1.16	metabolic and cellular process
GstD3	Glutathione S transferase D3	0.92	metabolic and cellular process
GstD4	Glutathione S transferase D4	1.51	metabolic and cellular process
GstE1	Glutathione S transferase E1	1.55	metabolic and cellular process
GstO3	Glutathione S transferase O3	1.27	metabolic and cellular process
Hsc70Cb	CG6603	0.98	protein folding
Hsp26	Heat shock protein 26	1.42	protein folding
Hsp27	Heat shock protein 27	1.32	protein folding
Hsp67Bc	Heat shock gene 67Bc	1.55	protein folding
Hsp68	Heat shock protein 68	1.86	protein folding
Hsp70Bbb	Heat-shock-protein-70Bb	2.09	protein folding
chm	chameau	1.68	protein acetylation
Kr-h1	Kruppel homolog 1	0.83	regulation of gene expression
kuz	kuzbanian	1.4	proteolysis
Mocs1	Molybdenum cofactor synthesis 1 ortholog	1.26	biosynthetic process
mus201	mutagen-sensitive 201	0.85	metabolic process - DNA repair
Naam	Nicotinamide amidase	1.08	metabolic process
Oda	Ornithine decarboxylase antizyme	0.92	biosynthetic process
Pde8	Phosphodiesterase 8	0.95	metabolic process
PRL-1	PRL-1 phosphatase	1.14	metabolic process
Psa	Puromycin sensitive aminopeptidase	1.36	regulation of proteolysis
qin	qin	0.88	regulation of gene expression
rho	rhomboid	1.17	protein metabolic process
scaf	scarface	1.08	protein metabolic process
Spn4	Serine protease inhibitor 4	1.84	regulation of proteolysis
Spn6	Serine protease inhibitor 6	1.21	regulation of proteolysis

stv	starvin	0.81	protein metabolic process
y	yellow	1.4	biosynthetic process;
δTry	deltaTrypsin	0.82	proteolysis

localization - transport

AnnIX	Annexin IX	1.22	endosomal transport
Best1	Bestrophin 1	1.25	transport
corn	cornetto	1.59	vesicle-mediated transport
FBgn0026875	CG3638	1.46	transport
FBgn0027556	CG4928	1.64	transport
FBgn0029896	CG3168	0.85	transport
FBgn0031645	CG3036	1.5	transport
FBgn0032026	CG7627	0.87	transport
FBgn0036043	CG8177	1.62	transport
FBgn0038414	CG6901	1.14	transmembrane transport
FBgn0039644	CG11897	1.43	transport
FBgn0051272	CG31272	1.39	transport
FBgn0052103	CG32103	0.99	transport
Gie	GTPase indispensable for equal segregation of chromosomes	1.09	vesicle-mediated transport
glob1	globin 1	1.3	vesicle-mediated transport
Klp61F	Kinesin-like protein at 61F	-0.8	vesicle-mediated transport
Mvl	Malvolio	1.45	metal ion transport
nrv1	nervana 1	0.89	transport
Prestin	CG5485	0.96	transport
Rab1	Rab-protein 1	0.81	vesicle-mediated transport
RabX1	RabX1	1.02	vesicle-mediated transport
subdued	subdued	0.86	transport
Tret1-1	Trehalose transporter 1-1	1.07	transport
Tret1-2	Trehalose transporter 1-2	0.87	transport
Trn	Transportin	0.86	intracellular protein transport
Vha100-2	Vacuolar H[+] ATPase subunit 100-2	-0.82	proton transport
Zip99C	CG7816	0.97	transport
ZnT77C	Zinc transporter 77C	1.21	transport

morphogenesis and development

CAP	CG18408	0.8 / 1.5	morphogenesis and development
comm2	CG7554	1.32	nervous system development
cv-2	crossveinless 2	1.0	nervous system development
dally	division abnormally delayed	0.94	nervous system development
dlp	dally-like	1.46	cell development
fax	failed axon connections	1.72	nervous system development
FBgn0051534	CG43427	1.02	wing disc development
foi	fear-of-intimacy	1.79	system development
glec	glilectin	1.58	nervous system development

hig	hikaru genki	1.42	system development
hipk	homeodomain interacting protein kinase	1.48	imaginal disc morphogenesis
lama	lamina ancestor	1.65	cell development
Nrt	Neurotactin	1.7	nervous system development
Psc	Posterior sex combs	0.8	system development
S	Star	1.34	system development
Socs36E	Suppressor of cytokine signaling at 36E	1.84	embryonic morphogenesis
sprt	sprite	1.41	garland nephrocyte differentiation
Swip-1	Swiprosin-1	0.97	morphogenesis and development
trbl	tribbles	0.82	imaginal disc morphogenesis
Tsp42Ef	Tetraspanin 42Ef	1.03	nervous system development
zfh1	Zn finger homeodomain 1	0.81	garland nephrocyte differentiation

cellular component organization or biogenesis

caps	capricious	0.95	cell adhesion
Dg	Dystroglycan	0.84	cytoskeleton organization
FBgn0034160	CG5550	1.36	cytoskeleton organization
Fhos	Formin homology 2 domain containing	1.04	cellular component movement
Gli	Glilotactin	1.03	cytoskeleton organization
Incenp	Inner centromere protein	-0.86	mitotic cell cycle process
Kmn1	kinetochore Mis12-Ndc80 network component 1	-0.82	cell cycle process
LamC	Lamin C	0.89	cytoskeleton organization
Lasp	CG3849	0.97	cytoskeleton organization
Mcm7	Minichromosome maintenance 7	-0.82	cell cycle process
Mmp1	Matrix metalloproteinase 1	3.28	membrane organization
nuf	nuclear fallout	1.12	cytoskeleton organization
pav	pavarotti	-0.83	cell cycle process
polo	polo	-0.86	cell cycle process
Rcd2	Reduction in Cnn dots 2	2.21	cell cycle process
rhea	CG6831	0.92	cytoskeleton organization
rols	rolling pebbles	0.84	cytoskeleton organization
spir	spire	1.2 / 1.7	cytoskeleton organization
trio	CG18214	0.86	cytoskeleton organization

response to stimulus

14-3-3zeta	14-3-3zeta	0.81	signal transduction
Akt1	CG4006	0.82	signal transduction
Ars2	CG7843	0.91	response to chemicals
Cam	Calmodulin	1.67	signal transduction
drk	downstream of receptor kinase	0.81	signal transduction
Ect4	Ectoderm-expressed 4	0.9 / 1.0	signal transduction

FBgn0039419	CG12290	1.01	signal transduction
FBgn0046763	CG17278	0.98	signal transduction
FBgn0051694	CG31694	1.3 / 1.4	signal transduction
for	foraging	1.46	response to food
Galpha73B	G protein alpha 73B	1.0	signal transduction
G-oalpha47A	G protein oalpha 47A	1.34	signal transduction
MESR3	Misexpression suppressor of ras 3	-1.35	signal transduction
pes	peste	1.43	defense response
Pvf3	PDGF- and VEGF-related factor 3	1.12	signal transduction
Rtnl1	CG33113	0.8 / 1.2	response to stimulus
sda	slamdance	1.85	mechanical stimulus

unknown

Arc2	CG13941	0.82	unknown
bip1	CG7574	1.19	unknown
FBgn0029766	CG15784	0.89	unknown
FBgn0031474	CG2991	1.03	unknown
FBgn0032022	CG14275	0.86	unknown
FBgn0032400	CG6770	2.1	unknown
FBgn0032587	CG5953	0.8	unknown
FBgn0032805	CG10337	1.35	unknown
FBgn0033458	CG18446	1.18	unknown
FBgn0033945	CG12868	0.97	unknown
FBgn0035237	CG13917	0.87	unknown
FBgn0035996	CG3448	1	unknown
FBgn0036419	CG13482	2.74	unknown
FBgn0037016	CG13252	0.89	unknown
FBgn0037746	CG8478	-1.08	unknown
FBgn0038638	CG7702	1.87	unknown
FBgn0038682	CG5835	1.83	unknown
FBgn0040837	CG8620	1.5	unknown
FBgn0052541	CG43759	0.87	unknown
FBgn0250869	CG42240	2.03	unknown
FBgn0265185	CG44250	1.46	unknown
FBgn0266101	CG44838	1.21	unknown
fok	fledgling of Klp38B	1.26	unknown
l(1)G0469	lethal (1) G0469	1.4	unknown
NijA	Ninjurin A	0.85	unknown
Nop17l	Nop17 like	0.88	unknown
sip2	septin interacting protein 2	-1.1	unknown
SP1173	CG10121	1.25	unknown
Xrp1	CG17836	0.83	unknown

Table S5. The enriched KEGG pathways of differentially expressed genes in Cl.8+ cells treated with Ado, IDGF and Ado + IDGF2 (FDR-value < 0.05 and |logFC| > 0.4). gSIG = number of differentially expressed genes in pathway; gDET = number of genes in pathway verified in our microarrays; FDR = Fisher's exact test, FDR value; Direction = direction of change: "Up" - mostly upregulated genes were detected, "Down" - mostly downregulated genes were detected.

KEGG	Name	gSIG	gDET	FDR	Direction
------	------	------	------	-----	-----------

IDGF2

dme04145	Phagosome	3	29	0.0116	Up
----------	-----------	---	----	--------	----

Ado

dme00770	Pantothenate and CoA biosynthesis	2	7	0.0193	Down
----------	-----------------------------------	---	---	--------	------

Ado+IDGF2

dme00480	Glutathione metabolism	7	24	0.000062	Up
dme00980	Metabolism of xenobiotics by cytochrome P450	7	21	0.00028	Up
dme00982	Drug metabolism - cytochrome P450	7	20	0.00028	Up

4.2. Publication II

Lucie Kucerova, Vaclav Broz, Md. Badrul Arefin, Houda Ouns Maaroufi, Jana Hurychova, Hynek Strnad, Michal Zurovec & Ulrich Theopold. (2015) **The Drosophila Chitinase-Like Protein IDGF3 is involved in protection against nematodes and in wound healing.** *Journal of Innate Immunity* 8(2):199-210

Abstract:

Chitinase-like proteins (CLPs) of the 18 glycosyl hydrolase family retain structural similarity to chitinases but lack enzymatic activity. Although CLPs are upregulated in several human disorders that affect regenerative and inflammatory processes, very little is known about their normal physiological function. We show that an insect CLP (*Drosophila* imaginal disc growth factor 3, IDGF3) plays an immune-protective role during entomopathogenic nematode (EPN) infections. During these infections, nematodes force their entry into the host via border tissues, thus creating wounds. Whole-genome transcriptional analysis of nematode-infected wild-type and *Idgf3* mutant larvae have shown that, in addition to the regulation of genes related to immunity and wound closure, IDGF3 represses Jak/STAT and Wingless signaling. Further experiments have confirmed that IDGF3 has multiple roles in innate immunity. It serves as an essential component required for the formation of hemolymph clots that seal wounds, and *Idgf3* mutants display an extended developmental delay during wound healing. Altogether, our findings indicate that vertebrate and invertebrate CLP proteins function in analogous settings and have a broad impact on inflammatory reactions and infections. This opens the way to further genetic analysis of *Drosophila* IDGF3 and will help to elucidate the exact molecular context of CLP function.

The *Drosophila* Chitinase-Like Protein IDGF3 Is Involved in Protection against Nematodes and in Wound Healing

Lucie Kucerova^{a, b} Vaclav Broz^b Badrul Arefin^a Houda Ouns Maaroufi^a
Jana Hurychova^{a, c} Hynek Strnad^d Michal Zurovec^b Ulrich Theopold^a

^aDepartment of Molecular Biosciences, Wenner-Gren Institute, Stockholm University, Stockholm, Sweden; ^bBiology Centre of the ASCR, Institute of Entomology and Faculty of Science, University of South Bohemia, Ceske Budejovice, ^cDepartment of Animal Physiology and Immunology, Institute of Experimental Biology, Masaryk University, Brno, and ^dInstitute of Molecular Genetics of the ASCR, Prague, Czech Republic

Key Words

Chitinase-like proteins · Imaginal disc growth factor · Hemolymph clot · Wound healing · Nematode infection · Insect immunity

Abstract

Chitinase-like proteins (CLPs) of the 18 glycosyl hydrolase family retain structural similarity to chitinases but lack enzymatic activity. Although CLPs are upregulated in several human disorders that affect regenerative and inflammatory processes, very little is known about their normal physiological function. We show that an insect CLP (*Drosophila* imaginal disc growth factor 3, IDGF3) plays an immune-protective role during entomopathogenic nematode (EPN) infections. During these infections, nematodes force their entry into the host via border tissues, thus creating wounds. Whole-genome transcriptional analysis of nematode-infected wild-type and *Idgf3* mutant larvae have shown that, in addition to the regulation of genes related to immunity and wound closure, IDGF3 represses Jak/STAT and Wingless signaling. Further experiments have confirmed that IDGF3 has multiple roles in innate immunity. It serves as an essential component

required for the formation of hemolymph clots that seal wounds, and *Idgf3* mutants display an extended developmental delay during wound healing. Altogether, our findings indicate that vertebrate and invertebrate CLP proteins function in analogous settings and have a broad impact on inflammatory reactions and infections. This opens the way to further genetic analysis of *Drosophila* IDGF3 and will help to elucidate the exact molecular context of CLP function.

© 2015 The Author(s)
Published by S. Karger AG, Basel

Introduction

Tissue repair and regeneration are fundamental processes required for the replacement of dead or damaged cells after injury and during inflammatory processes. Normal healing in mammals, which leaves no permanent traces, is tightly regulated and requires a strict balance between the de novo production of and degradation of extracellular matrix. In case this balance is disturbed or

M.Z. and U.T. share senior authorship.

KARGER

E-Mail karger@karger.com
www.karger.com/jin

© 2015 The Author(s)
Published by S. Karger AG, Basel
1662–811X/15/0082–0199\$39.50/0

Karger
Open access

This article is licensed under the Creative Commons Attribution-NonCommercial-NoDerivatives 4.0 International License (CC BY-NC-ND) (<http://www.karger.com/Services/OpenAccessLicense>). Usage and distribution for commercial purposes as well as any distribution of modified material requires written permission.

Dr. Ulrich Theopold
Department of Molecular Biosciences
Wenner-Gren Institute, Stockholm University
SE-106 91 Stockholm (Sweden)
E-Mail uli.theopold@su.se

the stimulus persists, this leads to a fibroblastic stage which involves the sustained formation of extracellular matrix and tissue remodeling, and may leave a permanent scar (fibrosis). In addition to their involvement during regenerative processes, fibroses may also be part of immune reactions that involve the formation of larger inflammatory cell aggregates (granulomas) against abiotic objects and parasites, such as nematodes [1, 2]. When left unchecked, fibrosis formation potentially leads to permanent damage, resulting in morbidity and mortality [1]. Examples of the latter situation include cardiovascular diseases and organ-wide lesions affecting the skin, liver, kidney and lung [1] as well as aberrant tissue repair in cancers [3]. Tissue regeneration and immune responses against certain nematodes are dominated by a T-helper 2 cell (Th2)-based response, which includes the Th2 cytokines IL-4, IL-5 and IL-13 [2]. During both fibrosis formation and the response against nematodes, members of the 18 glycosyl hydrolase family are strongly induced.

Insect innate immune systems use effector mechanisms that resemble mammalian granulomas. They include capsules which are made against larger intruders, such as parasitoid eggs, nodules against large quantities of bacteria and hemolymph clots that form at the entry site of insect (entomo)pathogenic nematodes (EPNs) [4]. During all 3 reactions, blood cells (hemocytes) aggregate and release cytokines and extracellular matrix components. This may attract additional hemocytes or, in some cases, lead to the differentiation of additional hemocyte types. Subsequently, a cellular aggregate forms, which ultimately melanizes.

The 18 glycosyl hydrolase family is well conserved across animal orders. It comprises enzymatically active members that degrade chitin as well as chitinase-like proteins (CLPs), which may still bind to chitin or related polysaccharides but lack enzymatic activity (e.g. human Chi3l1/YKL40 and mouse Ym1) [2]. CLPs are often dysregulated in patients with various disorders such as asthma, chronic obstructive pulmonary disease (COPD), rheumatoid arthritis, cancer, diabetes and atherosclerosis; they effect inflammatory responses and tissue remodeling, and can serve as useful diagnostic markers [5]. Despite their association with disease, molecular insight into their physiological function and their contribution to disease etiology emerged only recently. Human Chi3l1 contributes to the augmentation of bacterial killing, the regulation of cell death, inflammation and remodeling [6, 7]. This involves the formation of a complex of IL-13, the IL-13 receptor alpha 2 and Chi3l1 [6]. Dysregulation of CLPs may influence the Th1/Th2 balance, shifting mac-

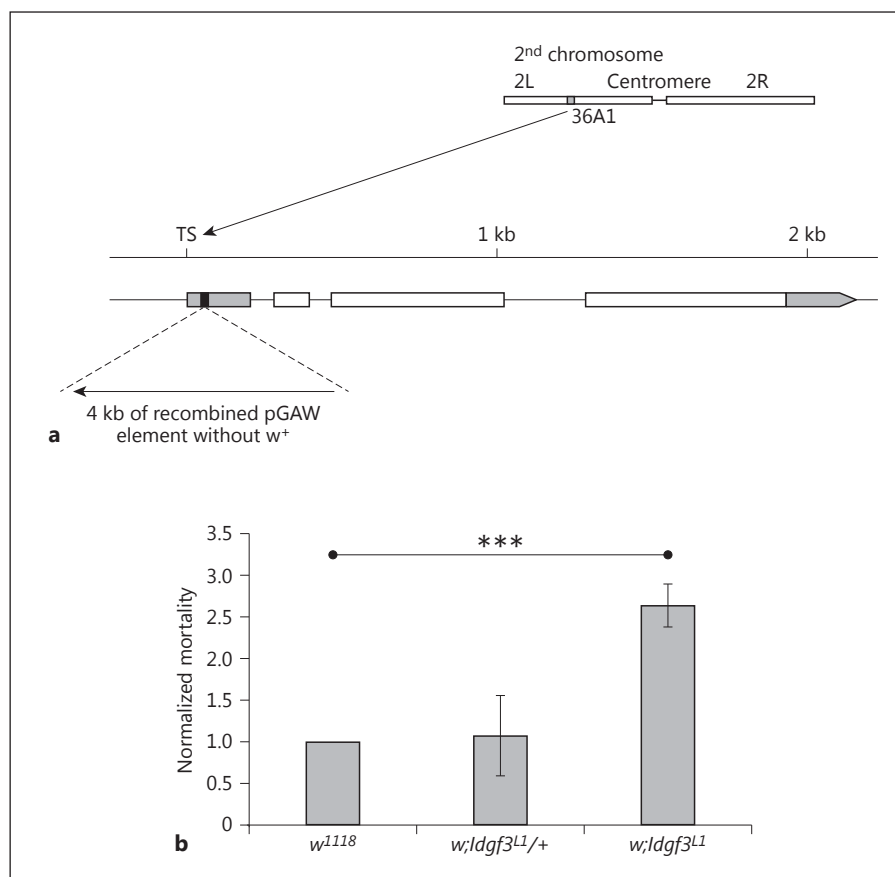
rophages towards the M2 phenotype and activating MAP kinase and Akt signaling as well as the Wnt pathway [6]. A complex regulatory role for Chi3l1 in the progression of idiopathic pulmonary fibrosis was recently revealed [7]. Chi3l1 levels were increased in patients with idiopathic pulmonary fibrosis, which is associated with distortion of the lung architecture and compromised lung function. Importantly, the Chi3l1 levels correlated with the disease progression. The specific role of Chi3l1 was further studied in a mouse fibrosis model involving bleomycin-treatment and inducible expression of human Chi3l1. YKL-40 induction after bleomycin treatment had a protective role early on after injury, but at later stages, elevated Chi3l1 levels had profibrotic effects [7]. The 3 mouse CLP members were recently studied in an infection model that involved migration of a nematode through the lung epithelia. CLPs were found to limit parasite survival, although this came at the expense of the host and led to an increase in lung damage [8]. Both innate immune cells and γ/δ T cells were involved [8] (review [9]).

Drosophila imaginal disc growth factors (IDGFs) comprise a small family of 6 secreted glycoproteins with sequence similarity (approx. 56%) to mammalian CLPs [10]. Like mammalian CLPs, they lack the amino acids required for enzymatic activity, resulting in the loss of chitinase activity [11]. The founding member of this family, named DS47, was identified by Kirkpatrick et al. [10] in 1995 as a secreted product of S2 cells, a cell line exhibiting macrophage-like properties. The in vivo function of this family is not known, but IDGF1 and IDGF2 were implicated in the stimulation of growth and motility of *Drosophila* cells in vitro [12].

Drosophila IDGFs are produced in the fat body and hemocytes, the two major immune tissues in flies [10, 12, 13]. Their concentration in the hemolymph increases after infection or parasitization [4, 14]. Strong transcriptional upregulation of IDGF family members was detected in several published microarray studies of the response to infection and injury [13, 15]. *Micrococcus luteus* and *Escherichia coli* infection (but not fungal infection) induces *Idgf3* expression in adults [13, 16]. These findings indicate that IDGFs contribute to immune responses.

In this study, we analyzed the function of *Drosophila* IDGF3, with a special focus on immunity. We found that *Idgf3* mutants are homozygous-viable, and have defects in hemolymph clotting, which is the earliest response of *Drosophila* larvae after injury and upon nematode entry. Transcription profiling suggested that IDGF3 is involved in the regulation of innate defense mechanisms and signal pathways connected to wound healing as well as regenerative

Fig. 1. IDGF3 mutants are more sensitive to EPN infection. **a** Schematic diagram of the *Idgf3* gene in the mutant *Idgf3^{L1}*, which was generated by imprecise excision of NP2446, a P-element located 45 bp after transcription start of *Idgf3*. TS = Transcription start of the *Idgf3* gene. Black box represents the 8 bp duplication at the P-element insertion site, the gray boxes represent the nontranslated region and the white boxes represent the coding regions. **b** *Idgf3* mutant larvae (*w;Idgf3^{L1}*) are sensitive to EPN infections 48 h after infection. Heterozygotes in the *Idgf3* mutation (*w;Idgf3^{L1}/+*) have similar mortality to the control (*w¹¹¹⁸*). Differences compared to control genotype were analyzed using the Student t test. *** $p < 0.001$, only significant results are shown; error bars represent SEM.



processes including Wingless (Wg) and Jak/STAT signaling, both implicated in the formation of fibrotic lesions in mammals. In addition, IDGF3 has further effects on the fly immune and regenerative response: *Idgf3* mutants show an increased mortality after nematode infections and increased time requirements during wound healing. This is consistent with the proposed immune and regenerative function of mammalian CLPs. Altogether, this suggests that, similar to human Chi3l1, *Drosophila* IDGF3 is a key regulator of the epithelial response to injury and infection.

Materials and Methods

Drosophila Strains and Production of Transgenic Lines

For standard procedures, flies were raised on a cornmeal-yeast-agar-sugar diet with 0.3% Nipagin at 25°C. Transgenic flies carrying *Idgf3::GFP* and *UAS-Idgf3-myc* constructs were generated (see below).

The *Idgf3^{L1}* mutant was generated by mobilization of the P-element, NP2446, which is located at +45 bp after transcription start of the *Idgf3* gene. The *Idgf3^{L1}* mutant contains a partially excised and recombined P-element which has lost the *w⁺* marker and con-

tains a small duplication of 8 bp in transcription start of the *Idgf3* gene (fig. 1a), leading to a complete loss of transcription (online suppl. fig. S1; www.karger.com/doi/10.1159/000442351 for all online suppl. material). The *Idgf3^{L1}* mutants are viable under homozygous conditions. The recessive lethal *dac⁷* mutant [17], which covers the *Idgf1-3* cluster and the 3' end of the *Dachshund* gene, was kindly provided by Graeme Mardon (Baylor College of Medicine, Houston). The following fly lines were obtained from the Bloomington Stock Center: *Idgf3^{NP2446}*, *Act-Gal4::PR/TM6BTb* [18], *hmlΔ-Gal4* (III) and the wild-type lines *Canton S* and *w¹¹¹⁸*, which served as our controls.

For overexpression and rescue experiments, either *hml-Gal4* driver was used (it mimics the natural expression of *Idgf3* in hemocytes) or progesterone-inducible *Act-Gal4::PR* driver (it mimics inducible expression of *Idgf3* as a response to infections). For activation of *Act-Gal4::PR* driver larvae of the experimental genotype *w;Act-Gal4::PR/UAS-Idgf3-myc* and control genotype *w;Act-Gal4::PR/+* (driver only) were transferred for 12 h to fly food containing 5 µg/ml of mifepristone (Sigma-Aldrich) according to Rogulja and Irvine [18].

Transgenic Constructs

To produce a *UAS-Idgf3-myc* construct wild-type cDNA for the *Idgf3* gene from the EST-clone, GH07453 from the pOT2 vector was amplified by PCR using Pfu DNA polymerase (Fermentas)

and the following primers, Idgf3EcoF: TGAATTCATCATGACTGGCTCTCTTTGGCTC and Idgf3R1: CTTCTGAGATGAGTTTTTGTTCGAGAAGTCGATACTTGATGGCG in the first step. The PCR product was used as a template in a subsequent PCR reaction with the same forward primers Idgf3EcoF and MycXba: GTTCTAGATCACAGATCCTCTTCTGAGATGAGTTTTTGTTC as reverse primers, extending the sequence for the myc tag and XbaI cutting site. The final PCR product was cut using EcoR/XbaI and cloned into the pUAST vector. Stable stocks with *UAS-Idgf3-myc* were produced using standard P-element transformation of the *w¹¹¹⁸* fly strain. A homozygous-viable insertion on the 3rd chromosome was used for further experiments.

Recombineering of GFP into Idgf3 in Flyfos Construct

The *Idgf3::GFP* fusion construct is based on a fosmid library clone pFlyFos (ID = 026931) obtained from Pavel Tomancak [19] which contains the *Idgf1-3* gene cluster including regulatory elements. The genomic region of the *Idgf3* gene was modified by recombineering in *E. coli* in vivo by use of the Red/ET recombination technology according to the protocol in Ejsmont et al. [19], with the following modifications: the GFP protein was connected to the C-terminus of *Idgf3* via a 2 × TY1 tag. The PCR cassette for tagging was amplified with Phusion polymerase (NEB). The plasmid containing the tagging cassette (2 × TY1 tag, C-terminus GFP and KanR) was used as a template. For the generation of the PCR cassette, oligonucleotides containing 50-bp homology arms for recombineering followed by the linker region of amplification were used; forward: GCACAAACGATCGCTTCCCCATGCTGCGC-GCCATCAAGTATCGACTTCTCGAAGTGCATACCAAT-CAGGACCCGC and reverse: TGGACTGGAGAAGTTGGCTT-AGAGAAGTTGGCTTAGAGAAGTCGGCTTACTTGTTCGT-CGTCATCCTTGTAGTCA. The recombined fosmid was purified with a Plasmid Midiprep kit (Macherey-Nagel). Since pFlyfos contains an attB site, a stable stock with an extra copy of the *Idgf3::GFP* fusion gene using the native promoter was produced using PhiC31 integrase-mediated transgenesis into the attP40 insertion site on the left arm of the 2nd chromosome.

Real Time RT-PCR

Total RNA from 15 flies per sample was isolated using the RNA Blue reagent (Top-Bio). The RNA was further purified with the NucleoSpin RNA II kit (Macherey-Nagel) including an on-column digestion step with rDNase I. One microgram of total RNA was reverse-transcribed at 42°C using oligo(dT)₁₇ and PrimeScript reverse transcriptase (Takara). The PCR reaction volume was 20 µl, containing 5 µl of diluted cDNA and reaction mix [ExTaq Hot Start polymerase (0.75 units; Takara), ExTaq buffer and dNTPs (200 µM each), Cyber green 1:25,000 and the primers (400 nM each)]. The amplification was carried out on a Rotor-Gene 3000 (Corbet Research) for 40 cycles (94°C for 20 s; 60°C for 30 s; 72°C for 30 s) following an initial denaturation/Taq activation step (95°C for 2 min). Each sample was analyzed in triplicate. Primers (sequences shown in online suppl. table S5) were designed with Lasergene PrimerSelect software (DNASTAR) to assure that each amplicon encompassed an exon/intron boundary. The product size was confirmed by melting analysis. Data were analyzed and quantified with Rotor-Gene 6 analysis software. Relative values were normalized to the rp49 cDNA and standardized to the *w¹¹¹⁸* sample. All results are presented with means and SEM from 4 independent biological samples.

Nematode Infections

Nematode infections were performed in duplicate in 96-well plates as described previously, and analyzed using the Student t test [4].

Experimental Design and Preparation of Microarray Samples

We analyzed 2 different genotypes, i.e. a control and a null mutation in the *Idgf3* gene. All genotypes were generated as progeny from the shared parental genotype *w;Idgf3^{-1/+};UAS-Idgf3-myc/UAS-Idgf3-myc*, which should minimize genetic background variation in our samples. All samples (*Idgf3* mutant and control) and replicates were processed in 1 experiment. Age-matched third-instar larvae (96 h after egg-laying) were analyzed. For the control and mutant genotypes, we used samples infected by EPNs for 2 h and analyzed these 6 h afterwards as described in the study by Arefin et al. [4]. The summary of the microarray analysis is shown in online supplementary table S6. Samples were frozen and stored at -80°C till RNA extraction.

Total RNA from whole larvae was extracted using RiboZol RNA extraction reagent (Amresco) according to the manufacturer's protocol, and subsequently cleaned with the NucleoSpin RNA II kit (Macherey-Nagel). The quality and concentration of the RNA were measured with a NanoDrop 2000 spectrophotometer (Thermo Scientific). RNA integrity was analyzed in an Agilent 2100 bioanalyzer. We included only samples with an intact RNA profile.

Expression Profiling

The Affymetrix GeneChip® *Drosophila* genome 2.0 array system was used for microarray analysis following the standard protocol: 100 ng RNA was amplified with GeneChip 3' IVT express kit (Affymetrix), and 10 µg of labeled cRNA was hybridized to the chip according to the manufacturer's instructions.

Statistical Analysis of Array Data

Analysis was performed in triplicate and analyzed as previously described [4]. Although all data were processed in parallel, the transcriptome of the control larvae was already available in a previous study [4] and that of the *Idgf3* mutants is made available as part of this study. The transcription data are MIAME-compliant and deposited in the ArrayExpress database (www.ebi.ac.uk/arrayexpress; accession Nos. E-MTAB-1542 [4] and E-MTAB-3478). To identify significantly perturbed pathways, we performed signal pathway impact analysis (SPIA) [20] on Kyoto Encyclopedia of Genes and Genomes (KEGG) pathways [21]: genes with |logFC| > 2 and a p value < 0.05 were considered differentially transcribed. Twelve genes had significantly changed after nematode infection in the controls had been validated before by quantitative RT-PCR [4].

Bead Aggregation Assay

The bead aggregation assay was performed according to Lesch et al. [22] with slight modifications. Briefly, 2.5 µl of hemolymph was collected from 6 late third-instar larvae (120 h after egg collection) and mixed for 30 s with 10 µl of *Drosophila* Ringer and 5 µl of bead suspension (tosylactivated Dynabeads M-280, Dynal Biotech ASA) at a concentration of approximately 2.0 × 10⁹ beads/ml. Prior to usage, the beads were washed in 10× PBS and blocked in 0.1% BSA in 1× PBS overnight according to the manufacturer's instructions. Pictures were taken with a Leica MZ FLIII fluores-

cence stereomicroscope associated with a Panasonic DMC-G2 camera, and analyzed and quantified with the ImageJ graphics program with the module Analyze Particles.

Clotting and Wounding Assays

Clots were prepared using the 'hanging drop' method [22] and stained either natively with FITC-conjugated peanut agglutinin (PNA, Sigma-Aldrich) or fixed with 4% p-formaldehyde and stained with antibodies and other fluorescent dyes. The following antibodies and dyes were used: rabbit anti-IDGF3 (1:50 dilution, for a further description see below), rabbit polyclonal anti-GFP (1:2,000 dilution, Life Technologies), AlexaFluor 568-conjugated anti-rabbit (1:1,000 dilution, Invitrogen), FITC-conjugated anti-rabbit (1:200 dilution, Life Technologies) and DAPI (1:1,000 dilution, Sigma-Aldrich). Confocal images were taken with a Zeiss LSM 780 microscope.

Wounding assays were performed according to Burra et al. [23]. Feeding third-instar larvae (96 h after egg-laying) were injured with a tungsten needle (125 μ m in diameter). For the survival experiment, wounded larvae were transferred to vials with fly food and the number of dead and pupated larvae was scored approximately every 12 h. Results were analyzed in R statistical software with the log-rank test. For localization of IDGF3:GFP, the wound site was observed under a Leica MZ FLIII fluorescence stereomicroscope and scored every hour for a period of 8 h. Images were taken with a Hamamatsu ORCA-ER camera (C4742-95) attached to a Zeiss Axioplan 2 microscope.

The anti-IDGF3 antibody was raised in rabbits against 14 amino acid long peptide C-EQRHLAQITSMKER (cysteine linked to the carrier protein), which was specific for IDGF3, by the GenScript company.

Results

IDGF3 Mutants Are More Sensitive to EPN Infection

Idgf1-3 were identified as immune response genes by several microarray studies [4, 13, 15]. In order to elucidate the role of IDGFs in immunity, we generated an *Idgf3* mutant for which a P-element, integrated close to transcription start of *Idgf3* gene, was available (fig. 1a; see Materials and Methods). RT-PCR analysis of a mutant obtained by imprecise excision of the P-element showed that the mutant did not express the *Idgf3* gene (online suppl. fig. S1). Mutant larvae showed a normal phenotype. *Idgf3* adult flies were viable but showed wing defects, in line with the proposed function as a growth factor (online suppl. fig. S2). Adult males were also sterile and females exhibited lower fecundity (online suppl. fig. S3). To test whether *Idgf3* has an immune function, we followed the survival of *Idgf3* mutants after infection with EPNs (*Heterorhabditis bacteriophora* and their symbiotic bacteria *Photorhabdus luminescens*) [4]. Mutant larvae infected with EPNs had a 2.5-fold higher mortality rate at day 2 after infection when

compared to the control larvae (fig. 1b). These results showed that IDGF3 has a protective function against nematodes.

Transcriptome Analysis Identifies Pathways That Are Regulated by IDGF3 during EPN Infection

In order to map IDGF3-regulated genes, we compared the transcriptome of nematode-infected and naïve *Idgf3* mutants to controls with an identical genetic background (online suppl. fig. S4) [4]. The underlying rationale was to identify genes and pathways that contribute to the difference in susceptibility towards nematodes between normal and mutant larvae. Analysis of the biological process gene ontology terms (AmiGO 2) for genes that were differentially regulated when comparing naïve wild-type and mutant larvae did not detect any enriched terms, in line with the lack of any dramatic phenotype of the mutants at this stage. In contrast, the infection of both mutant and normal larvae led to a highly significant induction of immune-related genes (fig. 2: overlapping group in the Venn diagram; online suppl. table S1: complete list of 150 induced genes and 51 downregulated ones). Enriched GO categories in this group almost exclusively included those with a function in immunity (fig. 2; online suppl. tables S1, S2). Most nematode-regulated genes shared directionality of their regulation and even showed similar levels of induction when compared in EPN-infected controls and mutant larvae (online suppl. table S1: genes shared after infection). The only exceptions were 2/201 genes (CG32379 and CG10621), a carboxypeptidase and a homocysteine S-methyltransferase, respectively, which were regulated in opposite directions. Altogether, this confirmed our previous findings that EPN infection induces a strong immune response [4], and showed at the same time that most of the immune response does not depend on the presence of IDGF3. However, there are some notable exceptions, namely 3 antimicrobial peptides which are amongst the 5 most strongly induced genes in infected control larvae but are not induced in *Idgf3* mutants (fig. 2: category A; for a complete list, see online suppl. table S1: ctr infection-specific). They include 2 small peptides (immune-induced peptides, recently named Bomanins [24]) and, most significantly, *Drosomycin*, the signature gene for the Toll pathway. The dataset from infected *Idgf3* mutants allowed us to comprehensively identify those genes that are induced in an IDGF3-dependent manner upon EPN infections (online suppl. tables S3, S4). GSEA analysis of this group showed enrichment for pathways that are involved in developmental processes in *Drosophila*. In flies, many of the pro-

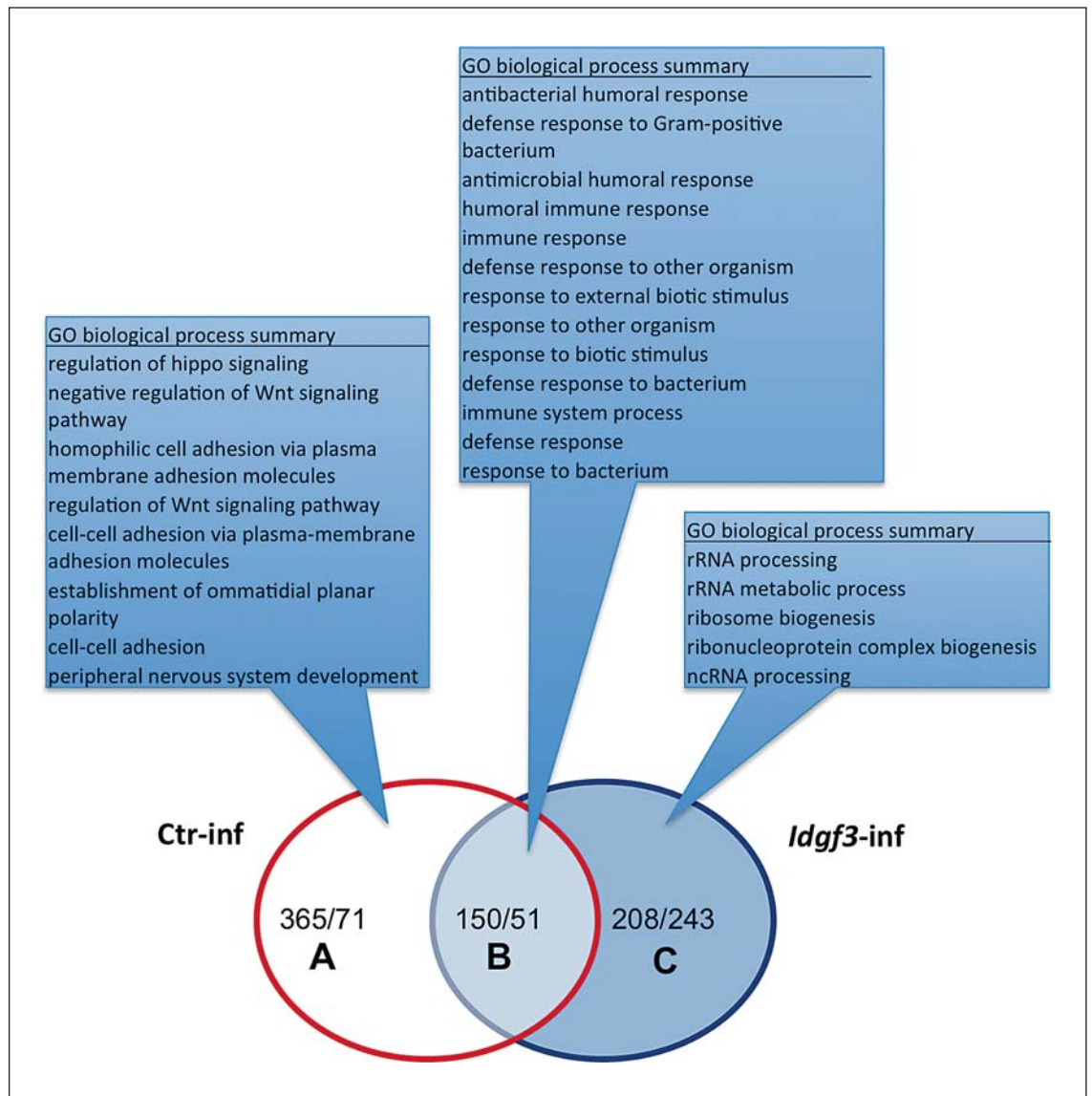


Fig. 2. Microarray expression analysis after nematode infections of *Idgf3* mutants and control larvae. *Idgf3* mutants and control larvae were infected with *H. bacteriophora* containing GFP-labeled *P. luminescens* (Materials and Methods) and differentially expressed genes classified using GO term enrichment analysis in AmiGO 2.

RNA samples were analyzed with Affymetrix expression arrays (genome 2.0). The Venn diagram shows the number of significantly regulated genes ($|\log_2FC| > 1$, $q < 0.05$) compared to noninfected control (Ctr-inf) samples of the corresponding genotype.

Table 1. SPIA of KEGG pathways

Group	KEGG ID	Title	gDET	gALL	gSIG_P	pG_P	Status_P
EPNi in controls	dme04630	Jak-STAT signaling pathway	18	21	6	0.00206	inhibited
	dme04310	Wnt signaling pathway	78	92	9	0.0198	inhibited
EPNi in <i>Idgf3</i> mutants	n.s.						

gALL = Known number of genes defined in *Drosophila* genome; gDET = number of genes belonging to a given pathway; gSIG = number of significantly regulated genes ($|\logFC| > 2$ and $p < 0.05$); n.s. = no significant pathway detected.

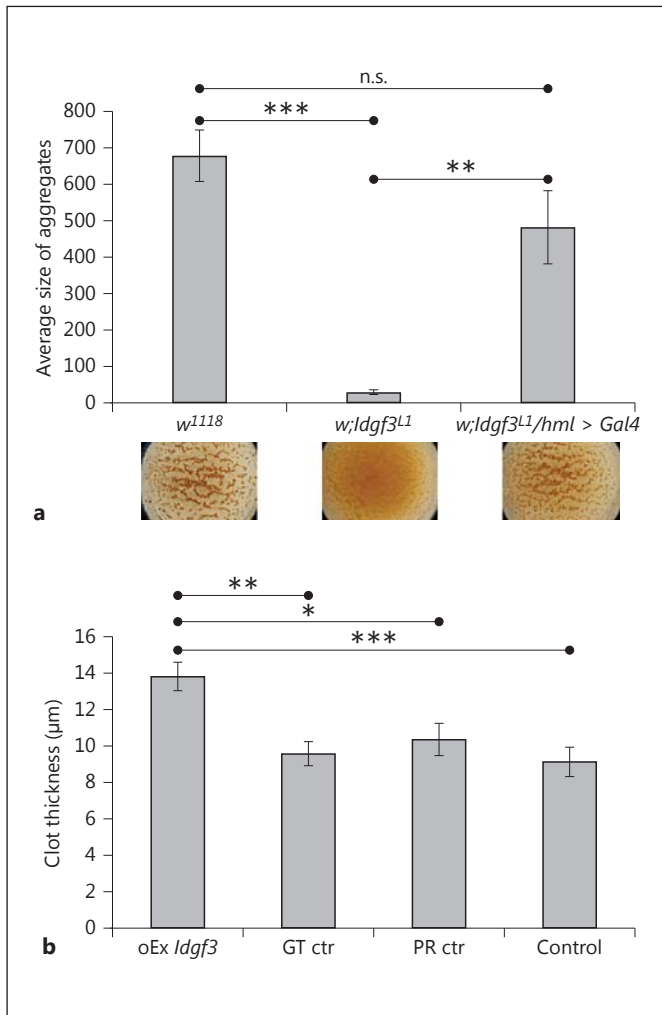


Fig. 3. IDGF3 mutants show defects in clot formation. **a** Hemolymph preparations were used to detect clot formation using a previously described bead aggregation assay [22]. *Idgf3^{L1}* mutants lacked clot formation visible through a lack of bead aggregation (middle part of the figure underneath the diagram and quantification in the diagram) compared to controls (*w¹¹¹⁸*). The clotting defect was rescued by ectopic expression of *Idgf3* in hemocytes (*Idgf3^{L1}/hml > Idgf3*). Data were analyzed using one-way ANOVA and the Tukey test. n.s. = Not significant. ** $p < 0.01$, *** $p < 0.001$; error bars represent SEM from 4 independent preparations. **b** Ubiquitous inducible overexpression of *Idgf3* leads to more extensive clot formation measured as thickness of the clot. Control larvae (GT ctr = nontreated genotype control, PR ctr = mifepristone-treated driver control and Control = nontreated driver control) and overexpression larvae (oEx *Idgf3*) preparations of clots were stained with FITC-conjugated PNA and the thickness of the clots was measured using a confocal microscope. Experimental genotype: *w;UAS-Idgf3/Act-Gal4:PR*; driver control genotype: *w;Act-Gal4:PR/+*. The flies were treated 12 h with mifepristone (5 µg/ml) for 12 h. Data were analyzed using one-way ANOVA and the Tukey test. * $p < 0.05$, ** $p < 0.01$, *** $p < 0.001$; error bars represent SEM from 5 independent preparations measured repeatedly at multiple spots of the grid.

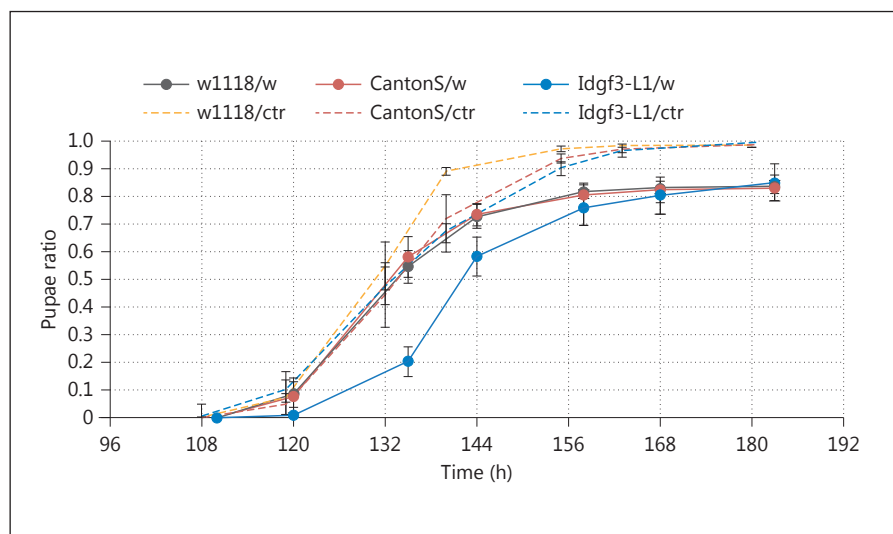
cesses identified regulate cellular activities that are required during the development of the nervous system and/or the imaginal discs. Several of these have been implicated in regenerative processes in mammals including Wg signaling (Wnt or Wg in flies), Hedgehog (Hh) and Jak/STAT signaling. SPIA (table 1) showed that Wg and Jak/STAT signaling are significantly downregulated upon EPN infection in control larvae but not in infected mutants. Completely in line with this, individual inspection of the genes that were induced after infection of wild-type larvae identified several negative regulators of both Wg and Jak/STAT signaling (online suppl. table S4). The Wg pathway includes *naked cuticle* [25], *sulfated* [26], *shifted* [27], *nemo* [28] and *Rho1* [29], whereas the Jak/STAT signaling involves 2 members of the SOCS family [30] and a PI3-kinase (CG4141), which acts in a regulatory loop upon axonal injury [31].

Additional induced genes were also notable, including *myoblast city (Mbc)*, which functions during syncytium formation in other contexts and may support the formation of the epithelial syncytia found at the wound edges [32]. Altogether, these results establish IDGF3 as a novel regulator of EPN-induced immune and regenerative processes.

IDGF3 Mutants Have Clotting Defects

Many of the genes previously identified to protect *Drosophila* from nematode infection are involved in clotting, wound sealing or encoding extracellular matrix components [4, 33, 34]. To determine whether *Idgf3* mutants exhibit clotting defects, we used a previously established bead aggregation assay [22]. Compared to the controls, the mutant hemolymph showed very poor bead aggregation (compare the lower part of fig. 3a and the quantification above). When we verified the ultrastructure of clots from the mutant hemolymph, we found that it completely lacked the fibrous clot matrix observed in normal larvae (online suppl. fig. S5). The ectopic expression of IDGF3 in hemocytes in the mutant background rescued the ability to aggregate beads (fig. 4a) and restored clot fiber formation (online suppl. fig. S5C), showing that although IDGF3 is expressed in other organs especially in the fat body, its expression in hemocytes is sufficient to drive clot formation. To further confirm a role for IDGF3 in clotting, we used an inducible system to overexpress the protein (details in Materials and Methods). Clot samples from overexpressing larvae showed increased lectin staining and extended fiber formation (online suppl. fig. S6). This also led to larger aggregates of clot matrix, which were not detected in normal clots (online suppl. fig. S6B).

Fig. 4. IDGF3 mutant larvae exhibit delayed development and pupate later after wounding in comparison with control larvae. Wounded *Idgf3^{L1}* mutant larvae (*Idgf3-L1/w*, solid blue line) delayed pupation for approximately 10 h and differed significantly (log-rank test; $p < 0.01$) compared to other wounded control larvae *w¹¹¹⁸* (*w1118/w*, solid grey line) and *Canton S* (*CantonS/w*, solid red line). Survival of all genotypes after wounding was equal at around 85%. The fraction of pupated nonwounded controls (*/ctr*) is shown as dashed lines.



In addition, the average thickness of the clots prepared from larvae overexpressing IDGF3 was increased compared to all the controls (fig. 3b). Altogether, this indicates that the extent of clot formation correlates with the level of IDGF3 expression.

IDGF3 Promotes Wound Healing

To test the effects of IDGF3 on wound healing, we injured mutant and wild-type larvae with a tungsten needle and followed their recovery (fig. 4). Both groups survived wounding equally well in the long term, in line with previous observations that the absence of a hemolymph clot has limited effects on survival after wounding, even in mutants where immunity is clearly affected [34]. They also both showed a developmental delay due to wounding, similar to that observed after the induction of wounds upon irradiation or in genetically induced wounds as well as in a *Drosophila* tumor model [35, 36]. Strikingly, though, the developmental delay was more pronounced in the mutant, showing that IDGF3 supports a swift recovery after wounding (fig. 4). Most likely as a consequence of reduced clotting, the scab in *Idgf3* mutants was also less confined (online suppl. fig. S7). Altogether, this provides functional proof for the contribution of IDGF3 to wound healing, in line with our GO analysis of the transcriptome data.

IDGF3 Is Part of Hemolymph Clots and Is Present at Wound Sites

Since the extent of clot formation seemed to depend on the concentration of IDGF3 in the hemolymph, we

wondered whether IDGF3 itself was present in the clot. Clots from wild-type larvae, prepared using previously established methods [37], were labeled with an antibody against IDGF3 (fig. 5a). Double staining of the clot using PNA (which binds several clot components via their carbohydrate moiety [22]) and the IDGF3-specific antibody showed partial overlap including both clot fibers and hemocytes. Similarly, a GFP-tagged version of IDGF3 both localized to clot fibers and accumulated in wounds afflicted by mechanical injury (fig. 5b, c). The pattern that we observed is compatible with the idea that IDGF3 is an integral part of hemolymph clots, which form after wounding. Altogether, our results suggest that IDGF3 has an important role in *Drosophila* wound closure and contributes to wound healing and regenerative reactions that protect *Drosophila* larvae against nematode infections.

Discussion

We describe a novel and unanticipated function for IDGF3, one of the *Drosophila* members of the CLPs. We show that IDGF3 is an integral part of the hemolymph clot and contributes to the protection against EPNs. The latter finding provides further support for the clot's function in immunity [38, 39]. Notably, the mouse CLP member *Ym1* is amongst the most strongly induced proteins upon nematode infections in mice [40], and its function in the protection against nematodes was strongly suggested in recent studies of the 3 mouse CLP members [8].

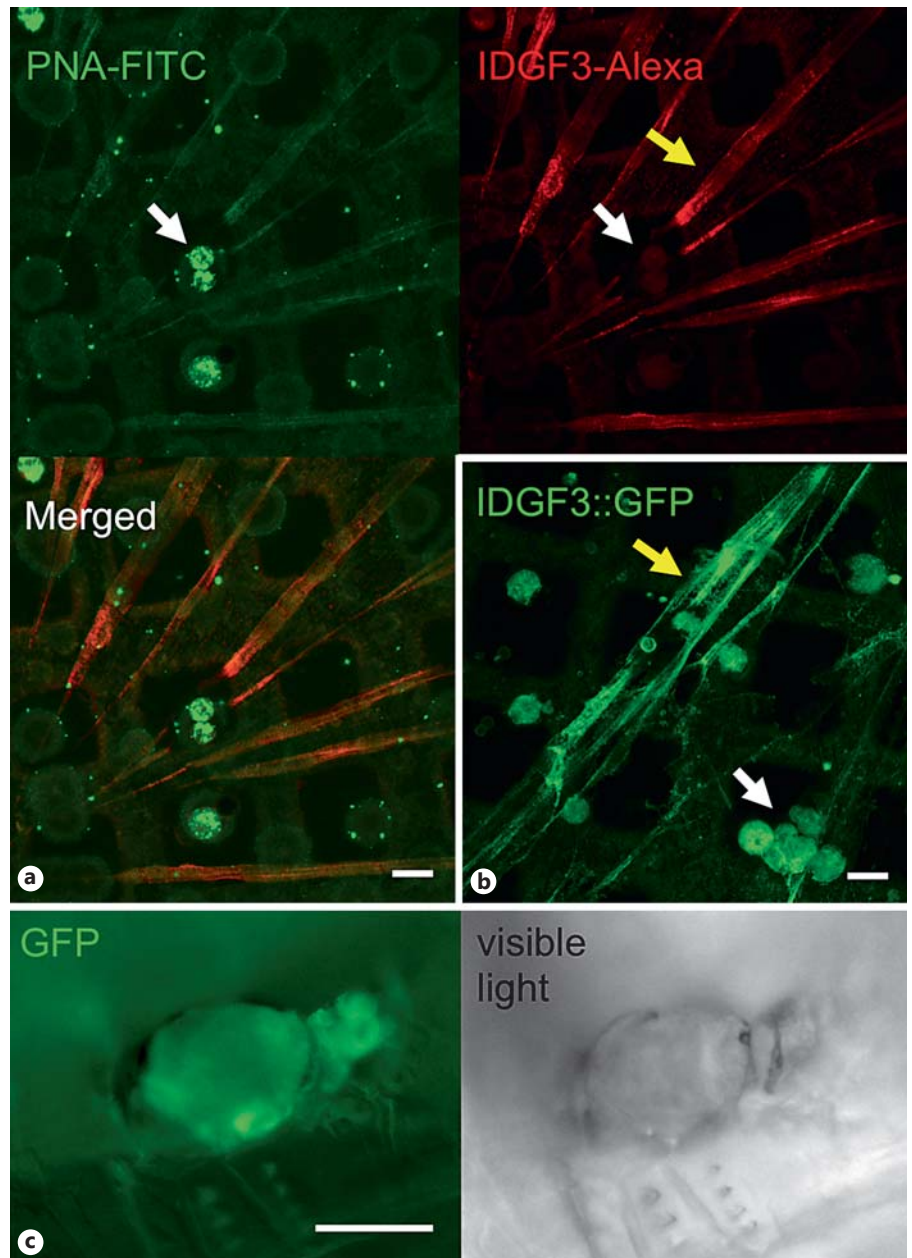


Fig. 5. IDGF3 is part of the hemolymph clot and is present in wounds. **a** Clot fibers were prepared as described before [52]. They were caught on grids, fixed, and without any prior detergent treatment, stained with PNA-FITC (upper left), and an IDGF3-specific antibody (IDGF3-Alexa; upper right). Pictures were recorded using confocal microscopy. Scale bar: 15 μ m. Both PNA and IDGF3 were detected on the surface of hemocytes (white arrows) and in clot fibers (yellow arrows). In a double-staining, the PNA signal on the surface of hemocytes is stronger, but IDGF3 staining is stronger in the fibers (Merged). **b** Clot fibers and hemocytes visualized using an IDGF3-GFP fusion protein show a stronger signal in hemocytes because of the presence of intracellular IDGF3. Scale bar: 15 μ m. **c** IDGF3 accumulates in clots at the wound site. GFP-tagged IDGF3 was followed using fluorescence microscopy of larvae 6 h after wounding with tungsten needles. Scale bar: 50 μ m.

To study the effects of IDGF3 in larvae infected with EPNs in an unbiased way, we performed transcriptional profiling of infected wild-type and mutant *Drosophila* larvae. We found a large set of genes that are induced during nematode infection in both cases. Many of these are immune genes including antimicrobial peptides; this confirms previous results [4] and suggests that at least part of the protection against EPNs is caused by antibacterial activity, which acts upon the nematodes' symbiotic bacteria that are released during the infection. A subfrac-

tion of immune genes is induced in an IDGF3-dependent manner, in line with the proposed immune modulatory role of chitinase family members [8].

Enrichment analysis using SPIA identified additional pathways that are regulated via IDGF3. Amongst these, Wg and Jak/STAT, which are downregulated, are notable. Both pathways have been linked to fibrotic lesions in mammals and we show clearly that they are modulated by CLP signaling. Using AmiGO analysis of the array data, manual analysis of individual regulated genes and

SPIA, we found a number of negative regulators of Wg signaling that were induced and additional genes that have antiproliferative effects. This is in line with results from previous studies of wound healing in *Drosophila* and other insects where proliferation was not observed [41]. Of note, among the Wg regulators induced, we identified *shifted*, the *Drosophila* ortholog of mammalian Wnt inhibitory factor, which, in the fruit fly, has been shown to control the activity of Hh rather than Wg [27]. Thus, IDGF signaling may lead to both Wg repression and Hh activation. In vertebrates, Wg and Hh have dual functions during development and skin repair [42]. Our findings suggest that there is a different function for Wg and Jak/STAT signaling during EPN infections when compared to other *Drosophila* models of injury such as during gut regeneration. Both upon feeding bacteria and chemical irritants (including bleomycin), canonical Wg and Jak/STAT signaling in gut epithelia are required to induce stem cell proliferation [43, 44], indicating that, although the dual use of the pathways may be conserved between epithelia, the outcome appears to depend on the tissue and/or regulation via IDGF3 and the clot. An example for a potential key regulator is provided by *nejjre*, the *Drosophila* homolog of histone acetyltransferase CREB-binding protein, which we found to be induced, and which acts as a bimodal regulator of Wg signaling [45]. Taken together, the pattern of induction that we observed after nematode infection is compatible with previous findings, i.e. that cuticular wounding in flies activates cellular activities that help to close the wound rather than activate cell proliferation [41]. Future work will enable us to localize the differential regulation of genes/pathways to individual cells/tissues. The site of damage, neighboring tissues [46] and more distant sites [47, 48] are potential targets.

Our functional analysis shows that IDGF3 supports a swift recovery after wounding. This means that, upon wounding and in the context of nematode infections, IDGF3 plays a positive role, similar to mammalian CLPs at an early stage of regeneration after wounding or upon infection. It will be of great interest to study how *Drosophila* IDGF3 affects the development of fibrotic lesions and the reaction against chronic states such as tumors; *Drosophila* models are available for both of these [49–51]. For the mechanism of action of IDGF3, we envisage the following 3, not necessarily exclusive, scenarios. (1) Based on its carbohydrate (chitin)-binding activity, it may mediate the interaction between the clot and the wound edges where chitin has become exposed due to damage to the underlying basement membrane and the epithelia; this

idea is supported by the accumulation of IDGF3 that we observed at the wound edges (fig. 5c). (2) Since *Drosophila* IDGFs are known to act as cytokines, IDGF3 may bind to carbohydrate moieties present on hemocytes, and, similar to vertebrate Chi311, regulate cellular activities. (3) Similar to what has been proposed for mouse CLPs, *Drosophila* IDGFs may act as pattern recognition molecules that bind chitin or related carbohydrates on the surface of nematodes and other parasites, activating immune effector mechanisms [8]. Combinations of these mechanisms can be envisaged, e.g. while present as a soluble protein in the hemolymph, IDGF3 may act as a cytokine, and upon incorporation into the clot, it may act as a structural component.

Our results have the potential to aid our understanding of the dual role mammalian CLPs play during chronic states such as the development of fibrotic lesions [7]. Our list of IDGF3-dependent genes that are induced upon infection provides a genome-wide source of further targets for the functional analysis of wound healing and subsequent regenerative processes.

Taken together, the work presented here provides experimental evidence for a protective function of CLPs during wounding and immune reactions. This opens the way for using the genetically tractable *Drosophila* model to study these processes in normal and pathological contexts and also their contribution to resistance against parasites.

Acknowledgements

We thank Dr. Michael Williams from Uppsala University for critical reading of the manuscript. We are grateful to the service laboratory at IMG and especially to Martina Chmelikova for technical assistance. The authors' work is supported by the Swedish Research Council (VR-2010-5988 to U.T.), the Swedish Foundation for International Cooperation in Research and Higher Education (STINT, IG2011-2042 to U.T.), the Knut and Alice Wallenberg Foundation (KAW2012.0058), the Swedish Cancer Foundation (CAN 2010/553 to U.T.) and the Czech Science Foundation (grant No. GA14-27816S to M.Z.).

Disclosure Statement

The authors declare no competing interests.

References

- Meneghin A, Hogaboam CM: Infectious disease, the innate immune response, and fibrosis. *J Clin Invest* 2007;117:530–538.
- Anthony RM, Rutitzky LI, Urban JF Jr, Stadecker MJ, Gause WC: Protective immune mechanisms in helminth infection. *Nat Rev Immunol* 2007;7:975–987.
- Franco C, Hess S: Recent proteomic advances in developmental, regeneration, and cancer governing signaling pathways. *Proteomics* 2015;15:1014–1025.
- Arefin B, Kucerova L, Dobes P, Markus R, Strnad H, Wang Z, Hyrsl P, Zurovec M, Theopold U: Genome-wide transcriptional analysis of *Drosophila* larvae infected by entomopathogenic nematodes shows involvement of complement, recognition and extracellular matrix proteins. *J Innate Immunol* 2014;6:192–204.
- Lee CG, Da Silva CA, Dela Cruz CS, Ahangari F, Ma B, Kang MJ, He CH, Takyar S, Elias JA: Role of chitin and chitinase/chitinase-like proteins in inflammation, tissue remodeling, and injury. *Annu Rev Physiol* 2011;73:479–501.
- He CH, Lee CG, Dela Cruz CS, Lee CM, Zhou Y, Ahangari F, Ma B, Herzog EL, Rosenberg SA, Li Y, Nour AM, Parikh CR, Schmidt I, Modis Y, Cantley L, Elias JA: Chitinase 3-like 1 regulates cellular and tissue responses via IL-13 receptor alpha2. *Cell Rep* 2013;4:830–841.
- Zhou Y, Peng H, Sun H, Peng X, Tang C, Gan Y, Chen X, Mathur A, Hu B, Slade MD, Montgomery RR, Shaw AC, Homer RJ, White ES, Lee CM, Moore MW, Gulati M, Geun Lee C, Elias JA, Herzog EL: Chitinase 3-like 1 suppresses injury and promotes fibroproliferative responses in mammalian lung fibrosis. *Sci Transl Med* 2014;6:240ra276.
- Sutherland TE, Logan N, Ruckerl D, Humbles AA, Allan SM, Papayannopoulos V, Stockinger B, Maizels RM, Allen JE: Chitinase-like proteins promote IL-17-mediated neutrophilia in a tradeoff between nematode killing and host damage. *Nat Immunol* 2014;15:1116–1125.
- Muallem G, Hunter CA: Paradigm shift: Ym1 and Ym2 as innate immunological regulators of IL-17. *Nat Immunol* 2014;15:1099–1100.
- Kirkpatrick RB, Matico RE, McNulty DE, Strickler JE, Rosenberg M: An abundantly secreted glycoprotein from *Drosophila melanogaster* is related to mammalian secretory proteins produced in rheumatoid tissues and by activated macrophages. *Gene* 1995;153:147–154.
- Varela PF, Llera AS, Mariuzza RA, Tormo J: Crystal structure of imaginal disc growth factor-2. A member of a new family of growth-promoting glycoproteins from *Drosophila melanogaster*. *J Biol Chem* 2002;277:13229–13236.
- Kawamura K, Shibata T, Saget O, Peel D, Bryant PJ: A new family of growth factors produced by the fat body and active on *Drosophila* imaginal disc cells. *Development* 1999;126:211–219.
- Irving P, Troxler L, Heuer TS, Belvin M, Koczynski C, Reichhart JM, Hoffmann JA, Hetru C: A genome-wide analysis of immune responses in *Drosophila*. *Proc Natl Acad Sci USA* 2001;98:15119–15124.
- Vierstraete E, Verleyen P, Sas F, Van den Bergh G, De Loof A, Arcakens L, Schoofs L: The instantly released *Drosophila* immune proteome is infection-specific. *Biochem Biophys Res Commun* 2004;317:1052–1060.
- De Gregorio E, Spellman PT, Rubin GM, Lemaitre B: Genome-wide analysis of the *Drosophila* immune response by using oligonucleotide microarrays. *Proc Natl Acad Sci USA* 2001;98:12590–12595.
- De Gregorio E, Spellman PT, Tzou P, Rubin GM, Lemaitre B: The Toll and IMD pathways are the major regulators of the immune response in *Drosophila*. *EMBO J* 2002;21:2568–2579.
- Mardon G, Solomon NM, Rubin GM: Dachshund encodes a nuclear protein required for normal eye and leg development in *Drosophila*. *Development* 1994;120:3473–3486.
- Rogulja D, Irvine KD: Regulation of cell proliferation by a morphogen gradient. *Cell* 2005;123:449–461.
- Ejsmont RK, Sarov M, Winkler S, Lipinski KA, Tomancak P: A toolkit for high-throughput, cross-species gene engineering in *Drosophila*. *Nat Methods* 2009;6:435–437.
- Tarca AL, Draghici S, Khatri P, Hassan SS, Mittal P, Kim JS, Kim CJ, Kusanovic JP, Romero R: A novel signaling pathway impact analysis. *Bioinformatics* 2009;25:75–82.
- Kanehisa M, Goto S, Sato Y, Furumichi M, Tanabe M: KEGG for integration and interpretation of large-scale molecular data sets. *Nucleic Acids Res* 2012;40:D109–D114.
- Lesch C, Goto A, Lindgren M, Bidla G, Dushay MS, Theopold U: A role for hemolectin in coagulation and immunity in *Drosophila melanogaster*. *Dev Comp Immunol* 2007;31:1255–1263.
- Burra S, Wang Y, Brock AR, Galenko MJ: Using *Drosophila* larvae to study epidermal wound closure and inflammation. *Methods Mol Biol* 2013;1037:449–461.
- Clemmons AW, Lindsay SA, Wasserman SA: An effector peptide family required for *Drosophila* Toll-mediated immunity. *PLoS Path* 2015;11:e1004876.
- Yang L, Meng F, Ma D, Xie W, Fang M: Bridging Decapentaplegic and Wntless signaling in *Drosophila* wings through repression of naked cuticle by Brinker. *Development* 2013;140:413–422.
- You J, Belenkaya T, Lin X: Sulfated is a negative feedback regulator of Wntless in *Drosophila*. *Dev Dyn* 2011;240:640–648.
- Glise B, Miller CA, Crozatier M, Halbisen MA, Wise S, Olson DJ, Vincent A, Blair SS: Shifted, the *Drosophila* ortholog of Wnt inhibitory factor-1, controls the distribution and movement of Hedgehog. *Dev Cell* 2005;8:255–266.
- Zeng YA, Verheyen EM: Nemo is an inducible antagonist of Wntless signaling during *Drosophila* wing development. *Development* 2004;131:2911–2920.
- Greer ER, Chao AT, Bejsovec A: Pebble/ECT2 RhoGEF negatively regulates the Wntless/Wnt signaling pathway. *Development* 2013;140:4937–4946.
- Stec WJ, Zeidler MP: *Drosophila* SOCS proteins. *J Signal Transduct* 2011;2011:894510.
- Doherty J, Sheehan AE, Bradshaw R, Fox AN, Lu TY, Freeman MR: PI3K signaling and Stat92E converge to modulate glial responsiveness to axonal injury. *PLoS Biol* 2014;12:e1001985.
- Losick VP, Fox DT, Spradling AC: Polyploidization and cell fusion contribute to wound healing in the adult *Drosophila* epithelium. *Curr Biol* 2013;23:2224–2232.
- Hyrsl P, Dobes P, Wang Z, Hauling T, Wilhelmsson C, Theopold U: Clotting factors and eicosanoids protect against nematode infections. *J Innate Immunol* 2011;3:65–70.
- Wang Z, Wilhelmsson C, Hyrsl P, Loof TG, Dobes P, Klupp M, Loseva O, Morgelin M, Ikle J, Cripps RM, Herwald H, Theopold U: Pathogen entrapment by transglutaminase-A conserved early innate immune mechanism. *PLoS Path* 2010;6:e1000763.
- Halme A, Cheng M, Hariharan IK: Retinoids regulate a developmental checkpoint for tissue regeneration in *Drosophila*. *Curr Biol* 2010;20:458–463.
- Hauling T, Krautz R, Markus R, Volkenhoff A, Kucerova L, Theopold U: A *Drosophila* immune response against Ras-induced overgrowth. *Biol Open* 2014;3:250–260.
- Scherfer C, Karlsson C, Loseva O, Bidla G, Goto A, Havemann J, Dushay MS, Theopold U: Isolation and characterization of hemolymph clotting factors in *Drosophila melanogaster* by a pullout method. *Curr Biol* 2004;14:625–629.
- Loof TG, Schmidt O, Herwald H, Theopold U: Coagulation systems of invertebrates and vertebrates and their roles in innate immunity: the same side of two coins? *J Innate Immunol* 2011;3:34–40.
- Theopold U, Krautz R, Dushay MS: The *Drosophila* clotting system and its messages for mammals. *Dev Comp Immunol* 2014;42:42–46.
- Nair MG, Gallagher IJ, Taylor MD, Loke P, Coulson PS, Wilson RA, Maizels RM, Allen JE: Chitinase and Fizz family members are a generalized feature of nematode infection with selective upregulation of Ym1 and Fizz1 by antigen-presenting cells. *Infect Immunol* 2005;73:385–394.

- 41 Razzell W, Wood W, Martin P: Swatting flies: Modelling wound healing and inflammation in *Drosophila*. *Dis Model Mech* 2011;4:569–574.
- 42 Bielefeld KA, Amini-Nik S, Alman BA: Cutaneous wound healing: recruiting developmental pathways for regeneration. *Cell Mol Life Sci* 2013;70:2059–2081.
- 43 Takashima S, Mkrtchyan M, Younossi-Hartenstein A, Merriam JR, Hartenstein V: The behaviour of *Drosophila* adult hindgut stem cells is controlled by Wnt and Hh signaling. *Nature* 2008;454:651–655.
- 44 Lin G, Xu N, Xi R: Paracrine Wingless signaling controls self-renewal of *Drosophila* intestinal stem cells. *Nature* 2008;455:1119–1123.
- 45 Li J, Sutter C, Parker DS, Blauwkamp T, Fang M, Cadigan KM: CBP/p300 are bimodal regulators of Wnt signaling. *EMBO J* 2007;26:2284–2294.
- 46 Kux K, Pitsouli C: Tissue communication in regenerative inflammatory signaling: lessons from the fly gut. *Front Cell Infect Microbiol* 2014;4:49.
- 47 Nam HJ, Jang IH, You H, Lee KA, Lee WJ: Genetic evidence of a redox-dependent systemic wound response via Hyan protease-phenoxidase system in *Drosophila*. *EMBO J* 2012;31:1253–1265.
- 48 Takeishi A, Kuranaga E, Tonoki A, Misaki K, Yonemura S, Kanuka H, Miura M: Homeostatic epithelial renewal in the gut is required for dampening a fatal systemic wound response in *Drosophila*. *Cell Rep* 2013;3:919–930.
- 49 Zang Y, Wan M, Liu M, Ke H, Ma S, Liu LP, Ni JQ, Carlos Pastor-Pareja J: Plasma membrane overgrowth causes fibrotic collagen accumulation and immune activation in *Drosophila* adipocytes. *Elife* 2015;4:e07187.
- 50 Pastor-Pareja JC, Xu T: Dissecting social cell biology and tumors using *Drosophila* genetics. *Ann Rev Gen* 2013;47:51–74.
- 51 Wang L, Kounatidis I, Ligoxygakis P: *Drosophila* as a model to study the role of blood cells in inflammation, innate immunity and cancer. *Front Cell Infect Microbiol* 2013;3:113.
- 52 Lindgren M, Riazhi R, Lesch C, Wilhelmsson C, Theopold U, Dushay MS: Fondue and transglutaminase in the *Drosophila* larval clot. *J Insect Physiol* 2008;54:586–592.

Supplementary material:

Fig S1. Verification of the *Idgf3^{L1}* mutant. *Idgf3* expression was measured by qRT-PCR. Lower expression levels compared to white control (*w¹¹¹⁸*) were detected in *dac⁷* (*w; dac⁷/+*) and *Idgf3^{L1}* (*w; Idgf3^{L1}/+*) heterozygotes, whereas no expression was detected in transheterozygous mutant flies (*w; dac⁷/Idgf3^{L1}*). The *dac⁷* is deletion mutant was generated by Mardon (Mardon et al., 1994), which covers the end of the *dachshund* gene and part of the *Idgf 1-3* cluster. Data were compared using a t-test to control expression, **p* < 0.05, ****p* < 0.001, error bars represents SEM from four independent biological replicates.

Fig. S2. *Idgf3^{L1}* adult flies show wing defects. ~52% of adult flies homozygous for the *Idgf3^{L1}* mutation exhibit partially missing wing vein 5 (A) at least in one wing. B: The phenotype is more common to observe in females (f) than in males (m). 100 flies/sex were analyzed. Error bars represents SEM. Data were analyzed using a t-test, **p* < 0.05.

Fig. S3. *Idgf3^{L1}* females exhibit lower fecundity. 8 females/genotype (*w; Idgf3^{L1}* – homozygotes for *Idgf3* mutation and *w; Idgf3^{L1}/+* - heterozygotes for *Idgf3* mutation) were crossed with 3 *w¹¹¹⁸* males in one vial. After mating females were transferred to new vial with fly food for 48 hours. The number of progeny was counted subsequently. Data were compared using a t-test, ****p* < 0.001, error bars represents SEM from four replicates.

Fig. S4. PCA of the transcriptome data: a principal component analysis is shown for the *Idgf3* mutants and controls with and without infection with EPNs (*Heterorhabditis/Photorhabdus*).

Fig. S5. IDGF3 mutant lacked the fibrous clot matrix. Clot preparations were made as described before (Lindgren et al., 2008), caught on glass coverslip and shown in phase contrast (left) and after labeling with PNA-FITC (right). In control (A) PNA strongly stain hemocytes (white arrows) and clot fibers (yellow arrow). In *Idgf3^{L1}* mutant (B) the fibrous clot matrix is not detectable after PNA staining as well as in phase contrast exposures, only hemocytes (white arrows) are labeled with PNA. Ectopic expression of IDGF3 with the *hml* driver (C) restores formation of clot fibers (yellow arrows) in the *Idgf3^{L1}* mutant background. The scale bar corresponds to 50 μm.

Fig. S6. IDGF3 overexpression leads to thicker clots. Ubiquitous inducible overexpression of IDGF3 (with a progesterone inducible *Act* driver) leads to more extensive clot formation visualized in clot preparations (**B**, oEx *Idgf3*) as compared to wild type (**1A**, non-induced driver control). Note the stronger PNA signal (quantified in **C**) and the formation of foci of clot formation in the preparations from overexpression larvae (yellow arrow). The scale bar corresponds to 50 μ m. **C**: The strength of green fluorescence from PNA-FITC labeled clot preparations was measured with ImageJ. Data were compared using a t-test, * $p < 0.05$, error bars represents SEM from three replicates.

Fig. S7. Wounds from *Idgf3* mutants exhibit stronger melanization. Feeding stage 3rd instar larvae were wounded with tungsten needle according to (Burra et al., 2013). The wound site was examined after 1h. *Idgf3* mutants (**C**) show more extensive melanization similar to other mutants with bleeding defects (Goto et al., 2003) compared to control wild-type larvae *w¹¹¹⁸* (**A**) and *Canton S* (**B**). **D**: Quantification of melanin at the wound site. Data were analyzed using one-way ANOVA and Tukey's test, * $p < 0.05$, error bars represent SEM from five measurements.

Table S1. Gene list of significantly regulated probes ($|\log_2FC| > 1$, $q < 0.05$), comparison of the response to EPN infection in the control genotype and *Idgf3* mutants.

Table S2. GO term enrichment analysis for significantly regulated probes ($|\log_2FC| > 1$, $q < 0.05$) after EPN infection, in three groups **A: genes significantly changed only in infected control, **B**: genes shared in infected control and infected *Idgf3* mutant, **C**: genes significantly regulated only in *Idgf3* mutant.**

Table S3. GSEA of KEGG pathways. Significantly enriched pathways for nematode response in control (ctri x ctr) and mutant (m3i x m3).

Table S4. Enrichment analysis of KEGG pathways using DAVID. Significantly enriched pathways for nematode response in control (ctri x ctr) and mutant (m3i x m3).

Table S5. List of primers used in real-time RT-PCR.

Table S6. Genotypes and treatments of the lines used for the array study.

References:

Burra, S., Wang, Y., Brock, A. R. and Galko, M. J. (2013). Using *Drosophila* larvae to study epidermal wound closure and inflammation. *Methods Mol Biol* 1037, 449-61.

Goto, A., Kadowaki, T. and Kitagawa, Y. (2003). *Drosophila* hemolectin gene is expressed in embryonic and larval hemocytes and its knock down causes bleeding defects(1). *Dev Biol* 264, 582-91.

Lindgren, M., Riazi, R., Lesch, C., Wilhelmsson, C., Theopold, U. and Dushay, M. S. (2008). Fondue and transglutaminase in the *Drosophila* larval clot. *J Insect Physiol* 54, 586-92.

Mardon, G., Solomon, N. M. and Rubin, G. M. (1994). dachshund encodes a nuclear protein required for normal eye and leg development in *Drosophila*. *Development* 120, 3473-86.

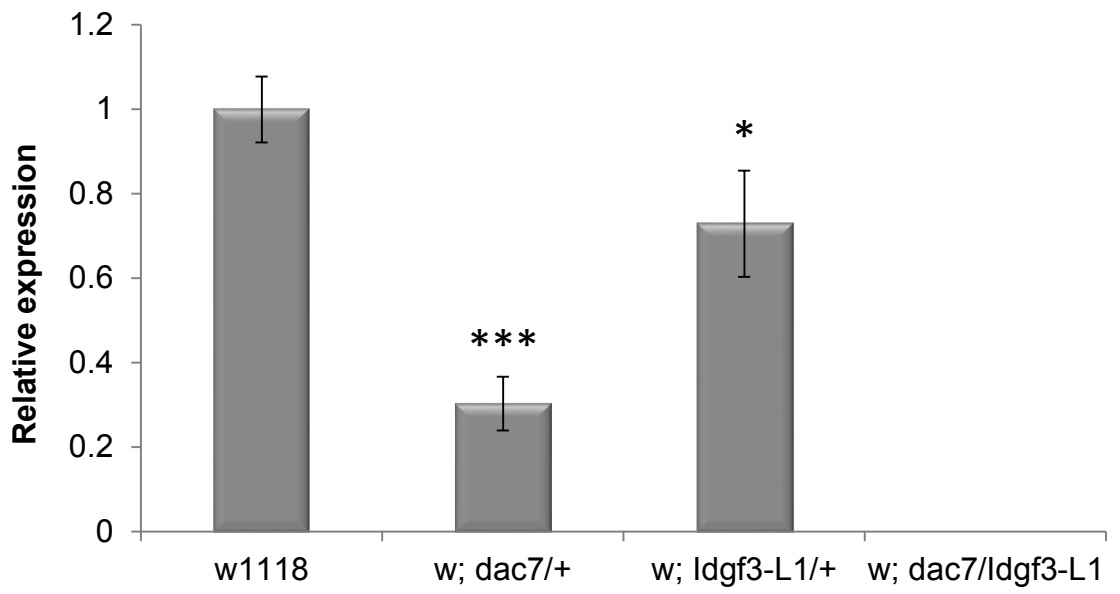


Figure S1

A



B

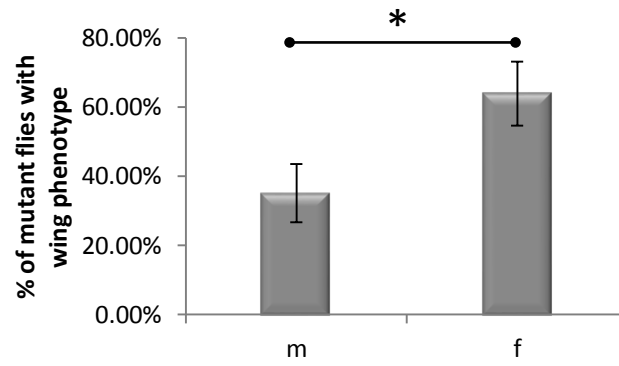


Figure S2

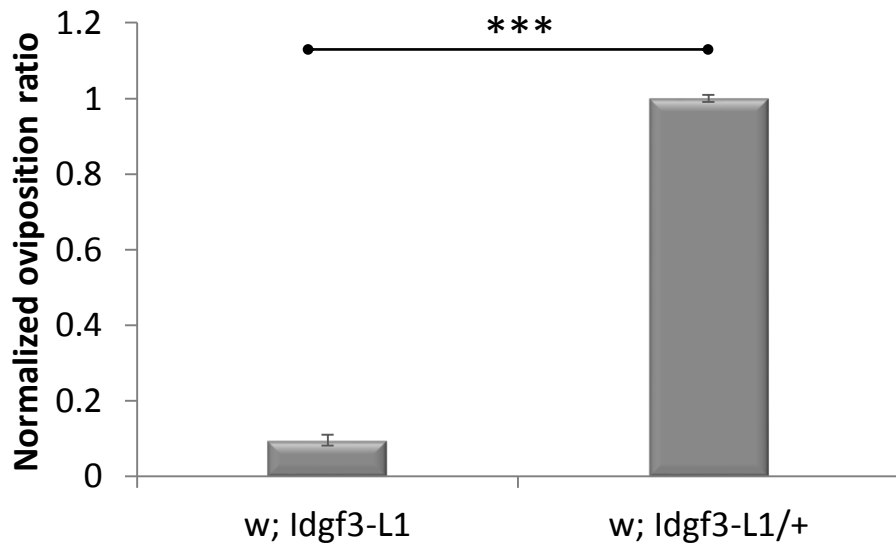


Figure S3

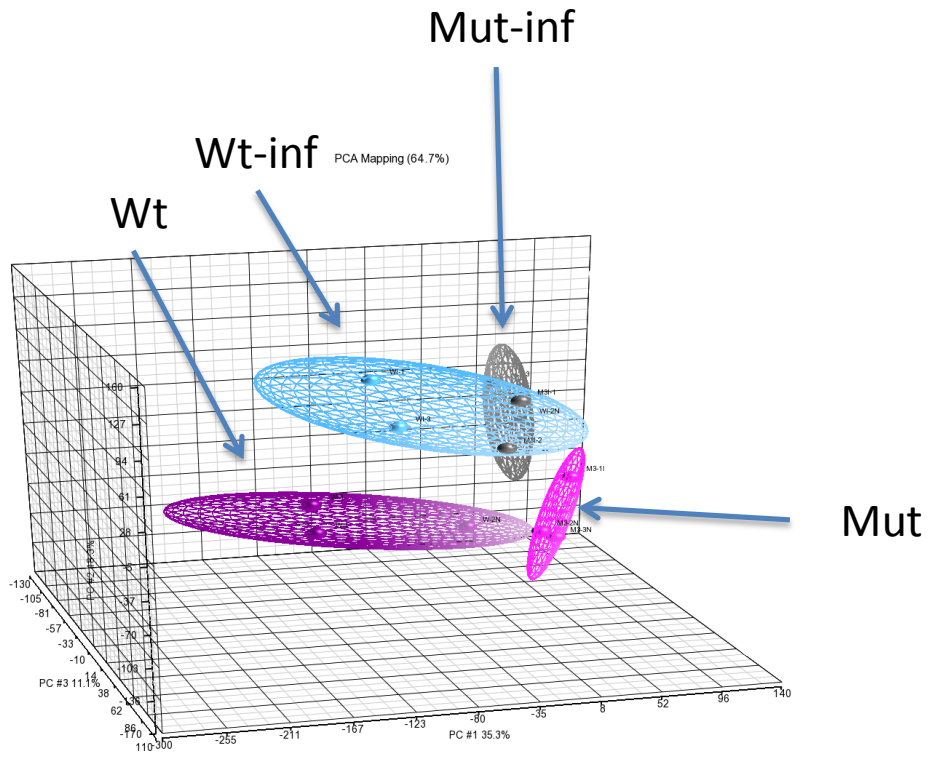


Figure S4

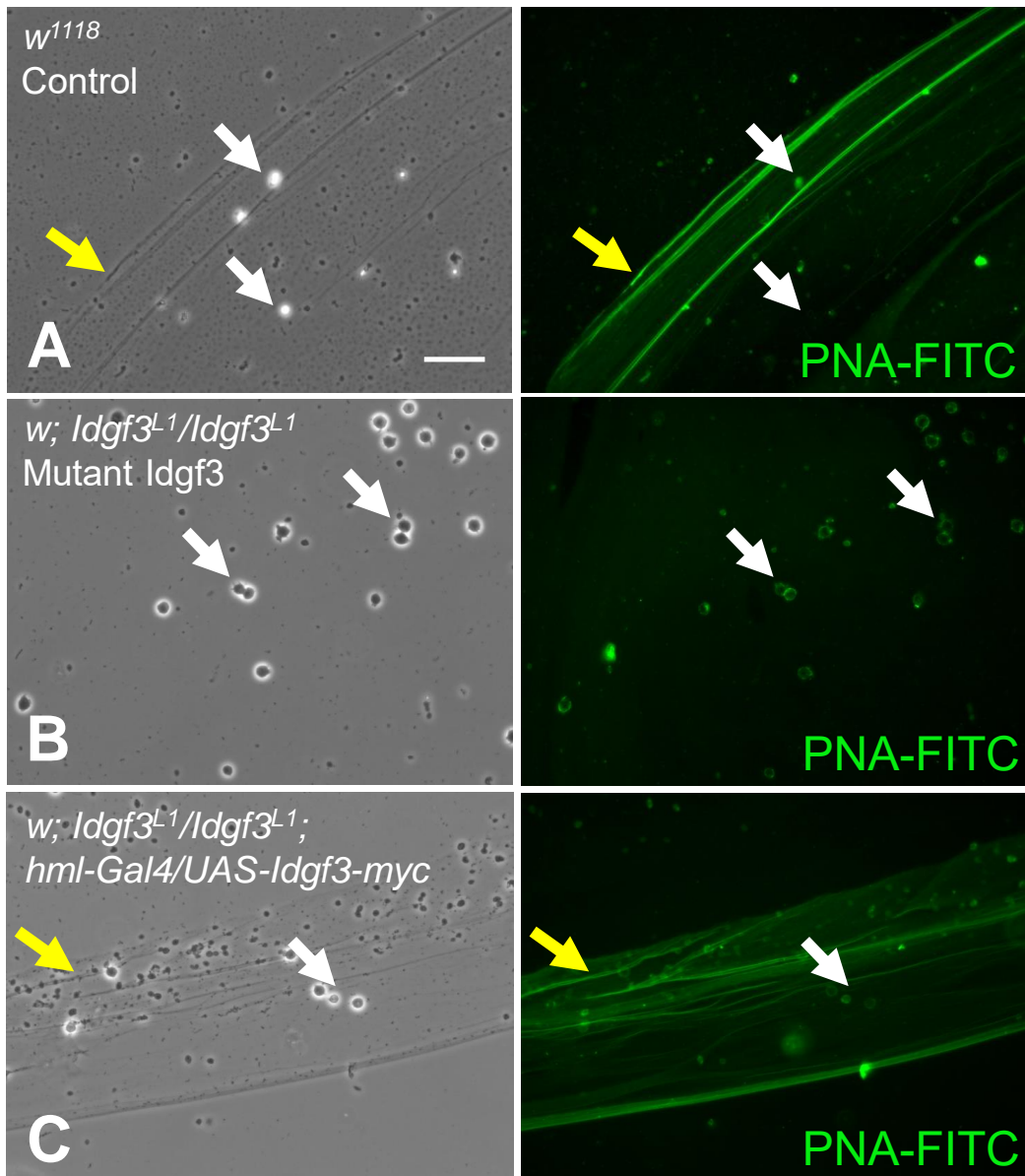


Figure S5

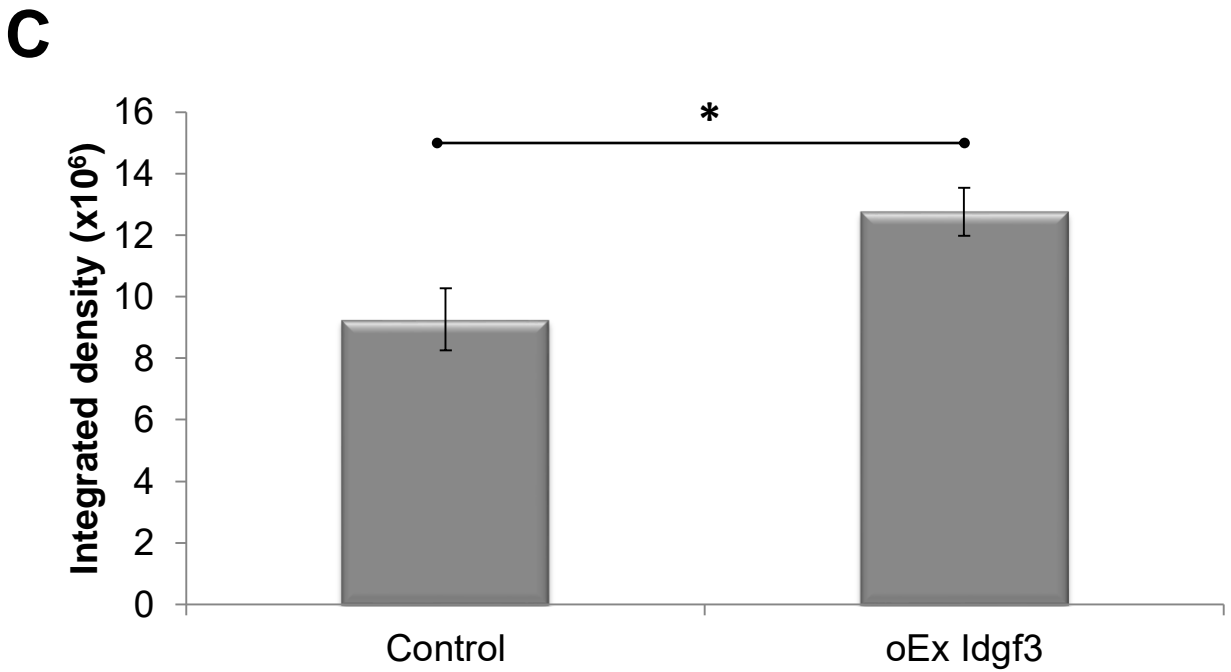
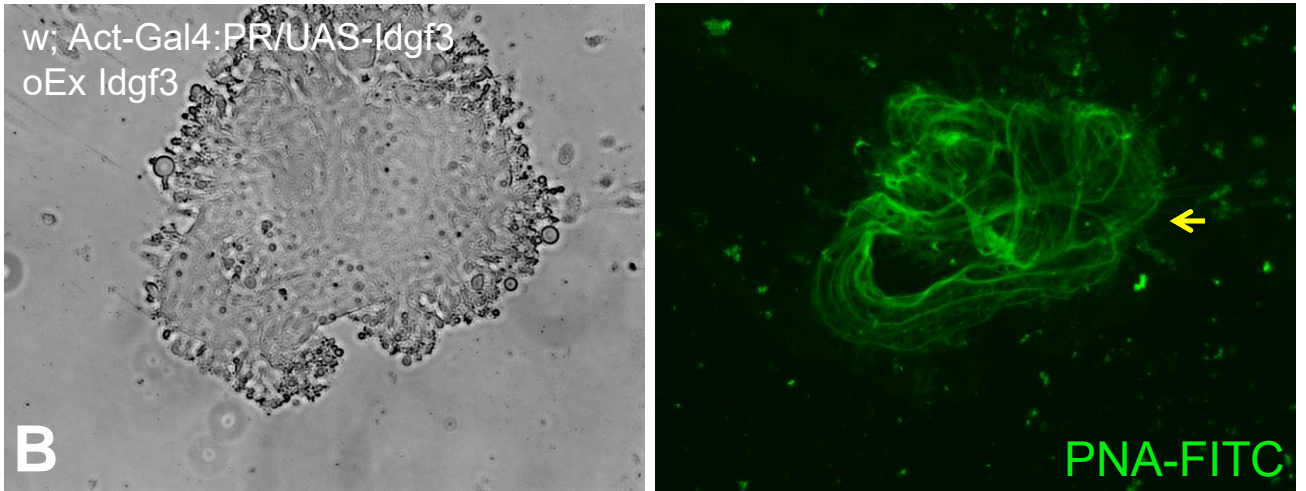
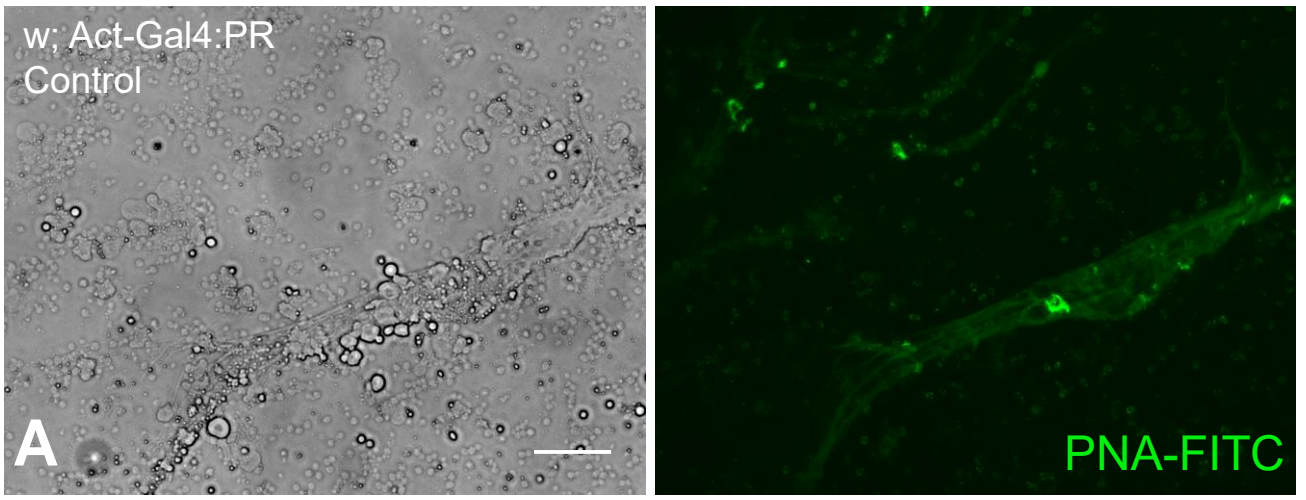


Figure S6

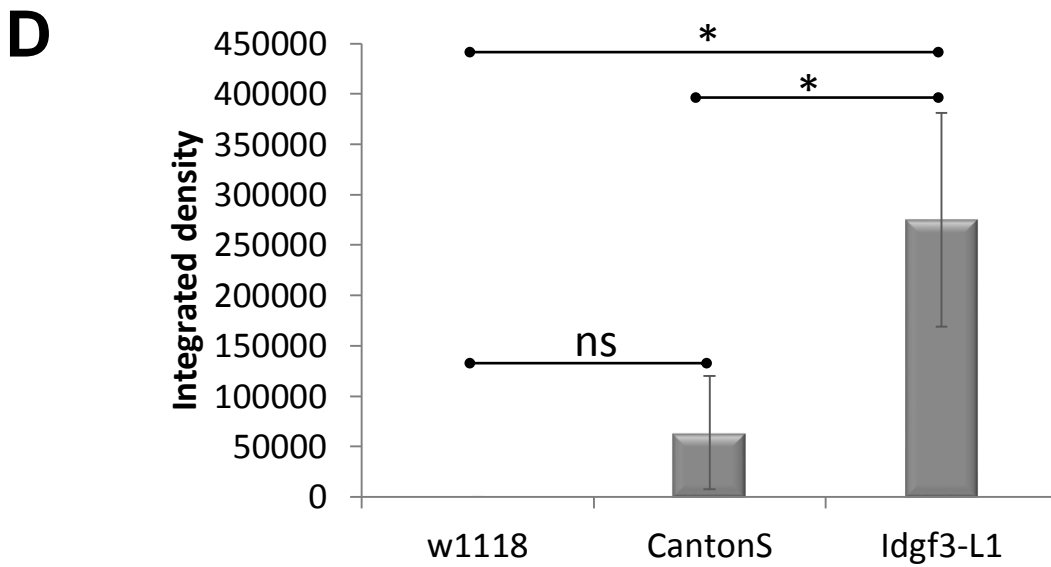
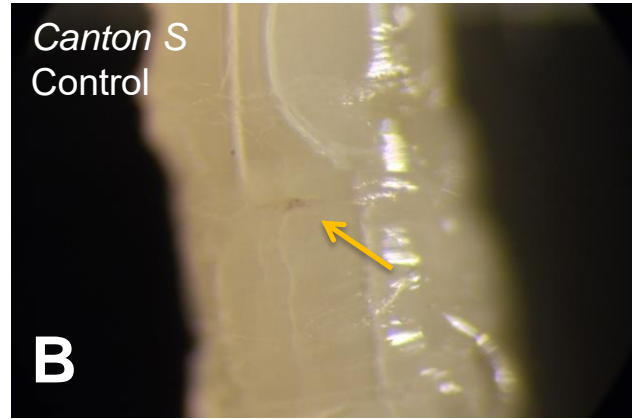
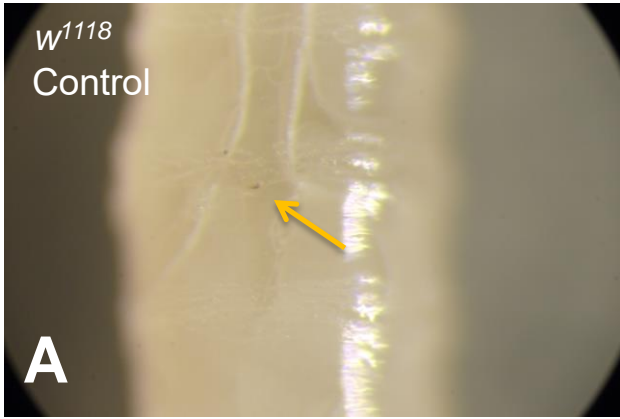


Figure S7

Shared genes	no.
upregulated	150
downregulated	51
upregulated in mutant downregulated in ctr	2

List of genes changed after infection shared in mutant and control:

ID	FLY	GENENAME	m3-m3i	ctr-ctrl
1627271_at		--- /// ---	9.5	7.1
1634366_at	•	elevated during infection	8.86	8.76
1638235_at	•	Diptericin B	8.26	7.29
1626345_at	•	Immune induced molecule 4	7.59	8.23
1641419_at	•	Attacin-C	7.35	7.94
1634271_at	•	Defensin	7.32	7.81
1629530_at	•	Immune induced molecule 23	7.22	6.75
1625174_at	•	CG15067 gene product from transcript CG15067-RA	7.19	6.95
1631370_at	•	CG30026 gene product from transcript CG30026-RB	7.08	5.29
1633053_at	•	Immune induced molecule 1	6.91	7.87
1622893_at	•	Immune induced molecule 3	6.88	8.99
1627613_at	•	Metchnikowin	5.92	5.5
1631660_at	•	CG15065 gene product from transcript CG15065-RA	5.66	7.81
1634477_at	•	CG42335 gene product from transcript CG42335-RC	5.64	3.53
1626319_a_at	•	Immune induced molecule 10	5.61	5.95
1634633_s_at		---	5.51	2.92
1627551_s_at		attacin /// attacin	5.5	5.46
1625124_at	•	Attacin-A	5.46	5.44
1623669_at	•	CG16836 gene product from transcript CG16836-RA	5.44	6.59
1639019_s_at		Immune induced molecule 10	5.39	6.93
1640360_at	•	Immune induced molecule 2	5.05	6.84
1636490_at	•	CG9681 gene product from transcript CG9681-RA	4.77	5.27
1631475_at	•	Attacin-D	4.77	3.84
1640757_at	•	CG33462 gene product from transcript CG33462-RA	4.56	4.49
1626530_at	•	Cecropin B	4.28	4.45
1632719_at	•	Cecropin C	4.26	5
1623884_at	•	CG16775 gene product from transcript CG16775-RB	4.12	3.57

unknown

1635601_at	CG42335 gene product from transcript CG42335-RC	3.96	1.95
1636293_at	CG2217 gene product from transcript CG2217-RA	3.55	2.87
1626392_s_at	Myocyte enhancer factor 2	3.52	1.46
1640144_at	CG18067 gene product from transcript CG18067-RA	3.32	3.28
1639704_at	CG14695 gene product from transcript CG14695-RA	3.06	2.29
1629201_at	CG5550 gene product from transcript CG5550-RB	2.77	2.81
1628355_at	CG32379 gene product from transcript CG32379-RB	2.75	-2.15
1632809_at	CG14762 gene product from transcript CG14762-RA	2.69	2.95
1624342_at	CG10911 gene product from transcript CG10911-RA	2.66	1.82
1641518_a_at	split ends	2.61	1.38
1629484_s_at	Chronologically inappropriate morphogenesis	2.49	2.45
1623455_s_at	IGF-II mRNA-binding protein	2.44	1.97
1638648_at	CG8160 gene product from transcript CG8160-RA	2.42	2.31
1628005_at	Chronologically inappropriate morphogenesis	2.4	2.16
1632017_at	Mucin 26B	2.38	2.44
1635959_at	CG13461 gene product from transcript CG13461-RA	2.37	2.06
1636521_at	CG1981 gene product from transcript CG1981-RA	2.34	1.54
1631700_at	Mucin 68Ca	2.34	1.89
1630067_a_at	Thiolester containing protein II	2.28	1.99
1625698_at	--- /// Regulator of G-protein signalling 7	2.22	2.47
1624587_at	CG13323 gene product from transcript CG13323-RA	2.19	1.91
1629307_s_at	headcase	2.17	1.96
1634920_at	Drosophila melanogaster LD07388 full insert cDNA.	2.16	1.86
1632945_at	Muscle-specific protein-300	2.12	2.02
1625048_at	neurofibromatosis type 1	2.06	2.03
1625139_at	CG11086 gene product from transcript CG11086-RA	2.04	1.24
1636798_at	CG13482 gene product from transcript CG13482-RA	2.02	2.22
1640884_at	CG15784 gene product from transcript CG15784-RA	2.01	1.22
1636205_at	CG42232 gene product from transcript CG42232-RB	2.01	2.47
1625445_s_at	schnurri	2	1.66
1638341_s_at	Mucin 68Ca	1.97	2.03
1636946_at	Serpins 88Eb	1.94	1.01
1622952_at	Immune induced molecule 18	1.93	1.83
1633145_at	Peptidoglycan recognition protein LF	1.85	1.8
1625269_at	CG9004 gene product from transcript CG9004-RA	1.85	1.09
1635580_at	CG7037 gene product from transcript CG7037-RB	1.82	1.93
1632430_at	Transferrin 1	1.82	1.18

1634992_s_at	CG9821 gene product from transcript CG9821-RB	1.8	1.74
1632958_a_at	CG42365 gene product from transcript CG42365-RA	1.79	1.5
1630088_at	CG16743 gene product from transcript CG16743-RA	1.74	1.7
1633821_at	CG10851 gene product from transcript CG10851-RM	1.71	1.39
1635030_at	CG12868 gene product from transcript CG12868-RB	1.69	1.39
1636297_at	Integrator 1	1.68	1.13
1625997_s_at	Drosophila melanogaster GH03753 full length cDNA.	1.68	1.58
1639321_s_at	Toll	1.67	1.18
1629113_a_at	Drosophila melanogaster GH15104 full insert cDNA.	1.67	1.32
1638708_s_at	cdna:known chromosome:BDGP5:3R:2232579:2271718:1	1.66	2.12
1640223_a_at	Perlecan	1.64	1.15
1624183_a_at	Fasciclin 1	1.63	1.95
1635168_at	CG5872 gene product from transcript CG5872-RA	1.61	1.14
1624619_s_at	--- /// ---	1.6	1.48
1634804_at	CG42533 gene product from transcript CG42533-RF	1.59	1.33
1629638_at	convoluted	1.59	1.13
1630207_at	CG16972 gene product from transcript CG16972-RA	1.57	1.52
1637712_at	CG30007 gene product from transcript CG30007-RB	1.55	1.06
1635282_at	CG7142 gene product from transcript CG7142-RA	1.55	1.35
1631109_at	CG13550 gene product from transcript CG13550-RA	1.55	1.32
1625999_at	asterless	1.52	1.23
1634447_at	CG31140 gene product from transcript CG31140-RB	1.47	1.17
1627376_at	Relish	1.47	1.82
1633846_at	CG15523 gene product from transcript CG15523-RA	1.46	1.14
1624252_s_at	--- /// slender lobes	1.44	1.23
1637703_a_at	Suppressor of cytokine signaling at 36E	1.43	1.15
1633313_at	Ankyrin 2	1.42	1.32
1636905_at	leak	1.41	1.82
1624719_at	CG10777 gene product from transcript CG10777-RB	1.4	1.24
1636653_at	necrotic	1.38	1.22
1632231_a_at	Myosin heavy chain-like	1.38	1.21
1624941_at	Breast cancer 2, early onset homolog	1.37	1.19
1635229_at	Elongase 68alpha	1.36	1.87
1634454_at	CG6303 gene product from transcript CG6303-RA	1.35	1.93
1629347_at	klumpfuss	1.35	2.08
1624533_s_at	trithorax	1.35	1.41
1623907_at	armitage	1.35	1.76

1635778_at	CG8771 gene product from transcript CG8771-RB	1.32	1.65	
1625970_at	expanded	1.32	1.15	
1639551_at	CG2009 gene product from transcript CG2009-RA	1.31	1.08	
1636061_at	cdna:known chromosome:BDGP5:3R:27050639:2705664	1.31	1.29	unknown
1633866_at	Suppressor of zeste 2	1.3	1.42	
1628423_at	Brahma associated protein 170kD	1.29	1.24	
1632287_at	CG32113 gene product from transcript CG32113-RB	1.28	1.4	
1631645_at	CG3363 gene product from transcript CG3363-RB	1.28	1.08	
1629398_at	CG10383 gene product from transcript CG10383-RA	1.28	1.46	
1633016_a_at	staufen	1.27	1.6	
1629295_at	Checkpoint suppressor homologue	1.27	1.48	
1628867_s_at	CG42390 gene product from transcript CG42390-RB	1.27	1.45	
1625530_at	CG10462 gene product from transcript CG10462-RB	1.27	1.14	
1634654_at	purity of essence	1.26	1.39	
1632210_at	CG30091 gene product from transcript CG30091-RA	1.24	1.47	
1626086_at	CG10621 gene product from transcript CG10621-RA	1.24	-1.36	
1622939_at	embargoed	1.23	1.03	
1639435_at	CG12359 gene product from transcript CG12359-RA	1.2	1.12	
1634092_at	Jumonji, AT rich interactive domain 2	1.2	1.52	
1627694_at	CG9715 gene product from transcript CG9715-RA	1.2	1.29	
1641272_at	CG42611 gene product from transcript CG42611-RA	1.19	1.29	
1628548_at	APC-like	1.19	1.46	
1639297_at	CG9568 gene product from transcript CG9568-RA	1.18	1.17	
1634174_at	CG9702 gene product from transcript CG9702-RA	1.17	1.02	
1633237_at	Imaginal disc growth factor 1	1.17	1.18	
1640747_s_at	CG8547 gene product from transcript CG8547-RC	1.16	1.39	
1638560_a_at	CG34407 gene product from transcript CG34407-RG	1.16	1.47	
1637539_a_at	hibris	1.16	1.37	
1631013_at	myoblast city	1.15	1.37	
1638352_at	CG16896 gene product from transcript CG16896-RA	1.13	1.31	
1632712_s_at	CG17836 gene product from transcript CG17836-RB	1.13	1.1	
1631696_s_at	CG3167 gene product from transcript CG3167-RA	1.13	1.15	
1624644_a_at	CG5514 gene product from transcript CG5514-RC	1.13	1.4	
1628159_a_at	CG32206 gene product from transcript CG32206-RB	1.12	1.06	
1633855_s_at	little imaginal discs	1.11	1.13	
1626478_at	windei	1.11	1.15	
1637542_s_at	Drosophila melanogaster DNA repair endonuclease (XPG)	1.09	1.21	

1624727_s_at	Ubiquitin-specific protease 64E	1.09	1.13
1636998_at	scabrous	1.07	1.62
1641048_a_at	toucan	1.06	1.18
1641226_a_at	multiple ankyrin repeats single KH domain	1.05	1.29
1631940_s_at	Centrosomal protein 190kD	1.04	1.32
1624620_at	Kinesin-like protein at 61F	1.04	1.12
1637478_s_at	hephaestus	1.03	1.03
1636939_at	Transport and Golgi organization 6	1.03	1.08
1641089_s_at	CG1815 gene product from transcript CG1815-RA	1.02	1.17
1640945_at	longitudinals lacking	1.02	1.41
1637619_s_at	Down syndrome cell adhesion molecule	1.01	1.16
1628172_at	mini spindles	1.01	1.16
1639072_at	hopscotch	1	1.33
1636126_at	CG8290 gene product from transcript CG8290-RA	1	1.11
1629685_at	CG16986 gene product from transcript CG16986-RA	-1	-1.13
1627354_at	--- /// ---	-1.03	-1.09
1624012_at	mitochondrial ribosomal protein L10	-1.03	-1.04
1626684_at	CG7607 gene product from transcript CG7607-RA	-1.08	-1.01
1623959_at	CG1532 gene product from transcript CG1532-RA	-1.08	-1.38
1637129_at	Glutathione S transferase E3	-1.09	-1.01
1632406_at	CG9117 gene product from transcript CG9117-RA	-1.11	-1.08
1634245_at	CG34229 gene product from transcript CG34229-RA	-1.13	-1.03
1633171_at	CG13690 gene product from transcript CG13690-RA	-1.13	-1.13
1629259_at	CG4186 gene product from transcript CG4186-RA	-1.2	-1.13
1625166_at	CG15456 gene product from transcript CG15456-RA	-1.22	-1.31
1640365_s_at	fuseless	-1.24	-1.29
1638634_at	CG32448 gene product from transcript CG32448-RC	-1.24	-1.16
1640584_at	Cyp9f3Psi	-1.25	-1.35
1639196_at	Jonah 25Bii	-1.27	-1.07
1633949_at	CG15152 gene product from transcript CG15152-RA	-1.29	-1.17
1639368_at	CG10505 gene product from transcript CG10505-RA	-1.32	-1.24
1638845_at	CG18643 gene product from transcript CG18643-RB	-1.37	-1.43
1638764_at	CG13516 gene product from transcript CG13516-RA	-1.38	-1.04
1634197_at	CG11576 gene product from transcript CG11576-RA	-1.42	-1.32
1630725_at	CG14572 gene product from transcript CG14572-RA	-1.42	-1.45
1634436_at	Allatostatin C	-1.5	-1.26
1634977_at	Tetraspanin 42Er	-1.54	-1.37

1633333_a_at	CG7231 gene product from transcript CG7231-RE	-1.65	-1.01
1631382_at	CG13085 gene product from transcript CG13085-RA	-1.67	-1.55
1635525_at	CG9672 gene product from transcript CG9672-RA	-1.71	-1.36
1636460_at	Jonah 65Ai	-1.73	-1.75
1641102_at	CG14141 gene product from transcript CG14141-RA	-1.8	-1.61
1623556_at	CG32669 gene product from transcript CG32669-RA	-1.81	-1.26
1637889_at	CG5883 gene product from transcript CG5883-RA	-1.89	-1.95
1625861_at	CG13012 gene product from transcript CG13012-RB	-1.93	-2.17
1632970_at	CG15336 gene product from transcript CG15336-RC	-1.99	-1.65
1632584_at	CG3344 gene product from transcript CG3344-RA	-1.99	-2.31
1637833_at	Juvenile hormone esterase	-2	-1.49
1627943_at	Insulin-like peptide 3	-2	-1.61
1634029_at	CG15902 gene product from transcript CG15902-RA	-2.01	-1.51
1632359_at	Tak1-like 2	-2.04	-1.45
1623817_at	CG7916 gene product from transcript CG7916-RA	-2.13	-1.24
1635371_at	CG31323 gene product from transcript CG31323-RA	-2.15	-1.24
1625203_at	CG9826 gene product from transcript CG9826-RB	-2.26	-2.22
1630740_at	CG4363 gene product from transcript CG4363-RA	-2.34	-2.33
1630218_at	CG13227 gene product from transcript CG13227-RA	-2.43	-1.31
1630404_at	CG34112 gene product from transcript CG34112-RB	-2.44	-1.77
1630977_at	CG16771 gene product from transcript CG16771-RC	-2.48	-1.84
1623229_at	CG7881 gene product from transcript CG7881-RA	-2.96	-2.4
1627321_x_at	--- /// Glutathione Synthetase	-3.04	-2.35
1636970_at	CG9394 gene product from transcript CG9394-RA	-3.16	-1.83
1631816_at	Adipokinetic hormone	-3.26	-2.26
1634445_at	CG32750 gene product from transcript CG32750-RA	-3.54	-2.41
1637326_at	CG15773 gene product from transcript CG15773-RB	-3.6	-2.85
1624333_at	CG9903 gene product from transcript CG9903-RA	-5.42	-2.55

only in ctr infection	no.
upregulated	365
downregulated	71

List of genes changed after infection specific for control:

ID	FLY	GENENAME	ctr-ctri	
1635189_at	•	Drosomycin	6.02	AMP
1635060_at	•	CG15068 gene product from transcript CG15068-RA	5.15	AMP-Bomanin
1638021_at	•	CG4757 gene product from transcript CG4757-RA	4.66	Carboxylesterase
1638772_at	•	CG18107 gene product from transcript CG18107-RA	2.95	AMP-Bomanin
1629046_a_at	•	CG4716 gene product from transcript CG4716-RA	2.94	methylenetetrahydrofolate dehydrogenase [NAD(P)+] activity
1636492_at		Drosophila melanogaster LP05669 full insert cDNA.	2.92	
1628963_at	•	CG4716 gene product from transcript CG4716-RA	2.7	
1637734_at	•	Thiolester containing protein I	2.66	
1628262_a_at	•	Zn finger homeodomain 1	2.54	
1636058_at	•	Mucin 96D	2.44	Chitin-binding domain
1637322_at	•	polychaetoid	2.4	guanylate kinase activity
1635733_x_at	•	Mucin 96D	2.4	
1629141_at	•	Insulin-like receptor	2.35	
1626087_at	•	starry night	2.32	transmembrane signaling receptor activity
1632295_s_at		cdna:novel chromosome:BDGP5:Uextra:8300480:830078	2.31	
1624033_at	•	beta amyloid protein precursor-like	2.31	
1623710_at	•	CG5847 gene product from transcript CG5847-RA	2.31	structural constituent of chitin-based cuticle
1631303_s_at	•	CG8524 gene product from transcript CG8524-RA	2.22	sequence-specific DNA binding;
1636576_s_at	•	no receptor potential A	2.21	GTPase activator activity; phosphatidylinositol phospholipase C activity;
1630502_at	•	anachronism	2.21	Transforming growth factor-beta, N-terminal
1635512_at	•	CG11893 gene product from transcript CG11893-RA	2.19	Protein kinase-like domain;
1633112_at	•	CG4322 gene product from transcript CG4322-RD	2.14	G-protein coupled receptor activity;
1624189_at	•	CG12236 gene product from transcript CG12236-RA	2.13	metal ion binding; nucleic acid binding
1624215_s_at	•	DISCO Interacting Protein 1	2.09	chromatin binding; double-stranded RNA binding
1625672_s_at		Drosophila melanogaster GH06422 full length cDNA.	2.08	
1638969_at	•	CG6279 gene product from transcript CG6279-RA	2.07	
1640472_at		Drosophila melanogaster GH06422 full length cDNA.	2.05	
1639785_s_at	•	wech	2.04	
1635730_at	•	CG30069 gene product from transcript CG30069-RA	2.02	
1634083_at	•	Neurofibromin 1	2.02	
1628632_at	•	polyA-binding protein interacting protein 2	2.01	
1624932_at	•	Odorant-binding protein 49a	2.01	
1627323_at	•	CG8388 gene product from transcript CG8388-RA	2	
1632130_s_at	•	CG8174 gene product from transcript CG8174-RA	1.98	

1633512_at	•	twin of eyeless	1.96
1624143_a_at	•	CG12071 gene product from transcript CG12071-RB	1.95
1629217_at	•	CG31258 gene product from transcript CG31258-RA	1.94
1624819_s_at		cdna:novel chromosome:BDGP5:Uextra:24197253:24212	1.93
1638359_s_at	•	CG14478 gene product from transcript CG14478-RA	1.92
1631691_at	•	CG16772 gene product from transcript CG16772-RA	1.92
1627796_s_at		cdna:known chromosome:BDGP5:3R:2232579:2271718:1	1.89
1634009_at	•	CG33957 gene product from transcript CG33957-RE	1.88
1631471_at	•	CG42342 gene product from transcript CG42342-RI	1.88
1627136_at	•	Kinesin-73	1.87
1629129_at	•	Tie-like receptor tyrosine kinase	1.85
1624565_a_at	•	CG16711 gene product from transcript CG16711-RB	1.85
1624297_at	•	derailed	1.85
1639894_at		Drosophila melanogaster LP21052 full insert cDNA.	1.8
1625511_at	•	CG34383 gene product from transcript CG34383-RE	1.79
1640598_s_at		lethal (3) neo38	1.78
1638060_at	•	CG10077 gene product from transcript CG10077-RA	1.77
1634075_at	•	dumpy	1.76
1637897_at	•	Cyclin T	1.75
1640892_a_at	•	Darkener of apricot	1.73
1636088_at	•	Distal-less	1.71
1636848_at	•	CG6024 gene product from transcript CG6024-RD	1.7
1639235_at	•	tartan	1.69
1637397_a_at		anastral spindle phenotype 1	1.69
1633303_at	•	CG43374 gene product from transcript CG43374-RC	1.69
1635900_at		insulin-stimulated eIF-4E binding protein	1.67
1632827_a_at	•	mutagen-sensitive 210	1.67
1635047_s_at	•	CG18214 gene product from transcript CG18214-RA	1.66
1624300_s_at	•	nemo	1.66
1630456_at	•	Myosin binding subunit	1.65
1636461_at	•	CG3630 gene product from transcript CG3630-RA	1.64
1639913_at	•	Connectin	1.63
1637079_at	•	CG5098 gene product from transcript CG5098-RA	1.63
1635684_a_at	•	CG2999 gene product from transcript CG2999-RD	1.63
1634084_at	•	CG4213 gene product from transcript CG4213-RA	1.63
1630729_at	•	telomere fusion	1.63
1640760_at	•	CG17838 gene product from transcript CG17838-RA	1.62

1639138_at	•	CG5524 gene product from transcript CG5524-RA	1.62
1625236_s_at	•	CG30483 gene product from transcript CG30483-RB	1.62
1634063_a_at	•	CG31317 gene product from transcript CG31317-RC	1.61
1641704_at	•	CG32176 gene product from transcript CG32176-RA	1.6
1641436_at	•	dim gamma-tubulin 5	1.6
1630570_at	•	CG13003 gene product from transcript CG13003-RB	1.6
1627191_a_at	•	enabled	1.59
1640805_at	•	anastral spindle 3	1.55
1637987_at	•	eukaryotic translation initiation factor 4G2	1.55
1636679_at	•	Myocardin-related transcription factor	1.55
1630361_at	•	naked cuticle	1.55
1629702_a_at	•	abrupt	1.55
1629325_at	•	mRNA-like ncRNA in embryogenesis 2	1.55
1625852_at	•	golden goal	1.55
1624970_s_at	•	Cullin-3	1.55
1639528_at	•	Nutrient Amino Acid Transporter 1	1.54
1627971_s_at	•	serrano	1.54
1627852_at	•	CG14655 gene product from transcript CG14655-RA	1.54
1637605_s_at	•	CG1146 gene product from transcript CG1146-RB	1.53
1632644_s_at	•	cdna:known chromosome:BDGP5:3R:13769829:1384150	1.52
1624378_at	•	enhanced adult sensory threshold	1.52
1630923_at	•	CG6945 gene product from transcript CG6945-RA	1.51
1637665_at	•	Drosophila melanogaster GH18144 full length cDNA.	1.5
1634039_at	•	nervous fingers 1	1.5
1633241_at	•	Drosophila melanogaster GH05922 full insert cDNA.	1.5
1626842_a_at	•	CG32464 gene product from transcript CG32464-RI	1.5
1640640_at	•	CG8639 gene product from transcript CG8639-RH	1.49
1632734_s_at	•	bangles and beads	1.49
1630376_at	•	CG1922 gene product from transcript CG1922-RA	1.49
1639582_at	•	Phosphodiesterase 11	1.47
1636526_at	•	CG9451 gene product from transcript CG9451-RA	1.46
1631059_at	•	Protein C kinase 98E	1.46
1630026_s_at	•	decapentaplegic	1.46
1623441_at	•	polyhomeotic proximal	1.46
1637710_at	•	karst	1.45
1636189_at	•	CG12306 gene product from transcript CG12306-RA	1.45
1630415_at	•	Alhambra	1.45

1626232_at	•	Calmodulin-binding transcription activator	1.45
1625687_at	•	kon-tiki	1.45
1635124_at	•	asense	1.44
1631516_s_at	•	skuld	1.44
1627151_at	•	CG4612 gene product from transcript CG4612-RC	1.44
1625921_at		mushroom body expressed	1.44
1624125_at	•	fat	1.44
1627394_s_at	•	anterior open	1.43
1633059_at	•	CG6357 gene product from transcript CG6357-RA	1.42
1629709_at	•	Meiotic central spindle	1.42
1626710_at	•	Stromalin	1.42
1638611_at		Drosophila melanogaster RE24931 full insert cDNA.	1.41
1625011_at	•	CG11206 gene product from transcript CG11206-RA	1.41
1624725_at	•	CG9626 gene product from transcript CG9626-RC	1.41
1624520_a_at	•	ftz transcription factor 1	1.41
1641738_a_at	•	CG13636 gene product from transcript CG13636-RB	1.4
1636974_at	•	dally-like	1.4
1631594_s_at	•	CG4141 gene product from transcript CG4141-RB	1.4
1631408_at	•	SoxNeuro	1.4
1627881_at		spalt major	1.4
1623863_a_at	•	Tis11 homolog	1.4
1623124_at	•	CG7376 gene product from transcript CG7376-RA	1.4
1638887_a_at	•	CG6339 gene product from transcript CG6339-RE	1.39
1633715_s_at	•	CG18769 gene product from transcript CG18769-RH	1.39
1632298_s_at	•	midline fasciclin	1.38
1629765_at	•	CG7715 gene product from transcript CG7715-RA	1.38
1628743_at	•	gliolectin	1.38
1626774_s_at	•	roundabout	1.38
1636092_a_at	•	wings apart-like	1.37
1632916_at	•	CG31357 gene product from transcript CG31357-RA	1.37
1631406_at	•	CG11414 gene product from transcript CG11414-RA	1.37
1627530_at	•	CG6700 gene product from transcript CG6700-RA	1.37
1637750_at	•	CG32139 gene product from transcript CG32139-RA	1.36
1631635_at	•	CG7294 gene product from transcript CG7294-RA	1.36
1629104_at	•	CG2258 gene product from transcript CG2258-RA	1.36
1626206_at	•	CG6947 gene product from transcript CG6947-RA	1.36
1625556_at	•	ariadne 2	1.36

1625447_at	•	CAP-D2 condensin subunit	1.36
1641548_at	•	CG10289 gene product from transcript CG10289-RA	1.35
1641475_at	•	Synaptotagmin 4	1.35
1640510_at	•	CG8600 gene product from transcript CG8600-RB	1.35
1639940_at	•	disconnected	1.35
1629290_at	•	Smad on X	1.35
1637481_at	•	CG6890 gene product from transcript CG6890-RA	1.34
1628849_at		cdna:novel chromosome:BDGP5:2R:15347450:15350135	1.34
1628420_s_at	•	CG6923 gene product from transcript CG6923-RC	1.34
1635127_at	•	CG34398 gene product from transcript CG34398-RF	1.33
1626352_at	•	scribbler	1.33
1624375_at	•	CG3227 gene product from transcript CG3227-RA	1.33
1638370_s_at	•	vielfaltig	1.32
1635123_at	•	gluon	1.32
1631222_at		pou domain motif 3	1.32
1630995_at	•	chiffon	1.32
1630010_a_at	•	pointed	1.32
1627122_at	•	CG32767 gene product from transcript CG32767-RD	1.32
1637365_at	•	CG31122 gene product from transcript CG31122-RA	1.31
1634291_at		cdna:known chromosome:BDGP5:3L:1950306:1964178:-	1.31
1630165_s_at	•	CG8815 gene product from transcript CG8815-RC	1.31
1623405_at	•	pavarotti	1.31
1639534_at	•	CG6792 gene product from transcript CG6792-RA	1.3
1628323_s_at	•	optic ganglion reduced	1.3
1637537_at	•	Leukocyte-antigen-related-like	1.29
1633852_at	•	found in neurons	1.29
1630772_at	•	squeeze	1.29
1630515_s_at	•	Glutactin	1.29
1630064_at	•	CG5639 gene product from transcript CG5639-RA	1.29
1635500_a_at	•	prospero	1.28
1630609_s_at	•	CG2225 gene product from transcript CG2225-RC	1.28
1640809_at	•	CG12105 gene product from transcript CG12105-RA	1.27
1634406_at	•	CG32982 gene product from transcript CG32982-RE	1.27
1632251_s_at	•	CG6181 gene product from transcript CG6181-RA	1.27
1625366_at	•	roughest	1.27
1625127_at	•	female sterile (1) homeotic	1.27
1622925_at		CREB binding protein	1.27

1640098_at	CG31132 gene product from transcript CG31132-RA	1.26
1627580_at	Dicer-1	1.26
1625768_s_at	longitudinals lacking	1.26
1622892_s_at	monkey-king	1.26
1636321_s_at	CG13624 gene product from transcript CG13624-RD	1.25
1633082_at	CG8449 gene product from transcript CG8449-RA	1.25
1628318_at	Spc105-related	1.25
1628243_at	debra	1.25
1636801_at	CG8232 gene product from transcript CG8232-RA	1.24
1636145_at	Serpin 28D	1.24
1624969_s_at	CG42319 gene product from transcript CG42319-RE	1.24
1641015_at	Bub1-related kinase	1.23
1639306_s_at	homeodomain interacting protein kinase	1.23
1623525_at	Polycomblike	1.23
1641024_at	Hybrid male rescue	1.21
1640020_at	CG10990 gene product from transcript CG10990-RB	1.21
1639266_at	CG15744 gene product from transcript CG15744-RA	1.21
1638956_at	Fasciclin 2	1.21
1630023_at	Daxx-like protein	1.21
1640838_s_at	A kinase anchor protein 200	1.2
1640627_at	dachsous	1.2
1640433_a_at	toutatis	1.2
1640096_at	CG17269 gene product from transcript CG17269-RA	1.2
1639703_s_at	CG10936 gene product from transcript CG10936-RB	1.2
1635037_at	CG4022 gene product from transcript CG4022-RC	1.2
1632554_at	CG9839 gene product from transcript CG9839-RA	1.2
1630975_at	CG2909 gene product from transcript CG2909-RA	1.2
1639798_at	mirror	1.19
1639396_s_at	Ceramidase	1.19
1627150_at	sister-of-Sex-lethal	1.19
1624463_s_at	CG3307 gene product from transcript CG3307-RC	1.19
1623755_at	Tenascin accessory	1.19
1623418_at	CG10244 gene product from transcript CG10244-RA	1.19
1641575_at	CG6977 gene product from transcript CG6977-RA	1.18
1640337_a_at	Ankyrin 2	1.18
1639438_at	male-specific lethal 1	1.18
1639411_at	lethal (1) G0148	1.18

1635378_at	•	CG7177 gene product from transcript CG7177-RA	1.18
1630390_at	•	DNA ligase I	1.18
1628865_at	•	odd paired	1.18
1625992_s_at	•	Na,K-ATPase Interacting	1.18
1639091_at	•	CG1100 gene product from transcript CG1100-RA	1.17
1638653_a_at		Elongation factor 4a	1.17
1637016_at		cdna:known chromosome:BDGP5:3R:2232579:2273729:1	1.17
1636182_a_at	•	CG10948 gene product from transcript CG10948-RB	1.17
1634061_a_at	•	retinal degeneration C	1.17
1629899_at	•	cactus	1.17
1627156_at	•	CG33225 gene product from transcript CG33225-RB	1.17
1641365_s_at		Drosophila melanogaster SD27140 full insert cDNA.	1.16
1641310_at	•	knockout	1.16
1639190_at	•	masquerade	1.16
1636887_s_at	•	CG11247 gene product from transcript CG11247-RC	1.16
1635007_at	•	Sulfated	1.16
1634125_at	•	CG30440 gene product from transcript CG30440-RA	1.16
1632308_at	•	ATAC complex component 2	1.16
1628418_at	•	abnormal oocyte	1.16
1623590_s_at	•	CG32438 gene product from transcript CG32438-RE	1.16
1639149_at		CG2989	1.15
1635619_a_at	•	centrosomin	1.15
1633390_at	•	tay bridge	1.15
1624263_at	•	Mta70 homologue	1.15
1639061_at	•	enoki mushroom	1.14
1637552_s_at	•	alan shepard	1.14
1631151_at	•	CG4951 gene product from transcript CG4951-RB	1.14
1629496_at	•	lethal (3) L1231	1.14
1628150_a_at	•	CG9449 gene product from transcript CG9449-RF	1.14
1626553_at	•	CG10376 gene product from transcript CG10376-RA	1.14
1641452_a_at	•	LIM-kinase1	1.13
1641352_at	•	CG7922 gene product from transcript CG7922-RA	1.13
1640764_at	•	RNA polymerase II 215kD subunit	1.13
1639494_at		cdna:known chromosome:BDGP5:2L:8525663:8528618:-	1.13
1639189_at	•	CG10255 gene product from transcript CG10255-RA	1.13
1635742_s_at	•	CG6445 gene product from transcript CG6445-RA	1.13
1634430_at		Drosophila melanogaster GM08142 full length cDNA.	1.13

1633752_at	•	Na,K-ATPase Interacting	1.13
1633020_at	•	unkempt	1.13
1626332_s_at	•	CG11486 gene product from transcript CG11486-RG	1.13
1641685_at	•	Enhancer of decapping 3	1.12
1641470_s_at	•	vestigial	1.12
1638839_at	•	relative of woc	1.12
1638568_s_at	•	Hairless	1.12
1634691_a_at	•	CG30020 gene product from transcript CG30020-RA	1.12
1634149_at	•	CG10212 gene product from transcript CG10212-RA	1.12
1631552_at	•	pyramus	1.12
1626090_at	•	pickled eggs	1.12
1625603_at	•	CG13604 gene product from transcript CG13604-RD	1.12
1623923_a_at	•	glass	1.12
1641445_s_at	•	CG7192 gene product from transcript CG7192-RA	1.11
1641333_s_at	•	CG7740 gene product from transcript CG7740-RD	1.11
1637684_at	•	CG8566 gene product from transcript CG8566-RB	1.11
1637111_a_at	•	Fak-like tyrosine kinase	1.11
1635403_at	•	shifted	1.11
1632602_s_at	•	Argonaute-1	1.11
1631768_at	•	quaking related 58E-1	1.11
1630717_s_at	•	combgap	1.11
1628866_at	•	nucampholin	1.11
1624543_s_at	•	Drosophila melanogaster SD01615 full length cDNA.	1.11
1624119_at	•	CG32486 gene product from transcript CG32486-RD	1.11
1640862_a_at	•	capsuleen	1.1
1637428_a_at	•	polychaetoid	1.1
1634562_s_at	•	Verprolin 1	1.1
1631094_s_at	•	skywalker	1.1
1628016_s_at	•	ariadne	1.1
1626147_s_at	•	withered	1.1
1640417_a_at	•	Protein kinase related to protein kinase N	1.09
1640083_at	•	CG1472 gene product from transcript CG1472-RA	1.09
1637947_s_at	•	CG30389 gene product from transcript CG30389-RA	1.09
1632666_at	•	Laminin B2	1.09
1631621_s_at	•	egghead	1.09
1629819_s_at	•	CG4700 gene product from transcript CG4700-RC	1.09
1627053_at	•	sloppy paired 2	1.09

1625243_a_at	Enhancer of bithorax	1.09
1631095_at	Posterior sex combs	1.08
1628901_at	Additional Sex Combs	1.08
1625578_at	Drosophila melanogaster GH12404 full length cDNA.	1.08
1622931_at	lethal (3) persistent salivary gland 2	1.08
1640541_at	fat facets	1.07
1639185_at	Myb-interacting protein 130	1.07
1637361_a_at	CG12179 gene product from transcript CG12179-RD	1.07
1636911_at	CG11352 gene product from transcript CG11352-RB	1.07
1630550_a_at	CG5674 gene product from transcript CG5674-RB	1.07
1628669_at	CG9754 gene product from transcript CG9754-RA	1.07
1628146_at	crumbs	1.07
1627649_at	CG7649 gene product from transcript CG7649-RC	1.07
1626494_at	CG7143 gene product from transcript CG7143-RA	1.07
1624304_s_at	Dorsal switch protein 1	1.07
1623100_at	CG6582 gene product from transcript CG6582-RA	1.07
1635909_at	Capicua	1.06
1634278_at	CG6409 gene product from transcript CG6409-RA	1.06
1633681_at	CG2519 gene product from transcript CG2519-RB	1.06
1633335_at	Son of sevenless	1.06
1633200_at	CG9449 gene product from transcript CG9449-RF	1.06
1632420_at	Reduction in Cnn dots 5	1.06
1631550_at	Negative elongation factor A	1.06
1626730_s_at	tonalli	1.06
1626018_a_at	crooked legs	1.06
1640311_s_at	Drosophila melanogaster batman protein mRNA, comple	1.05
1637774_s_at	CG8389 gene product from transcript CG8389-RB	1.05
1633021_s_at	Spinophilin	1.05
1630237_a_at	Distal-less	1.05
1628952_s_at	Furin 1	1.05
1628103_at	CG31496 gene product from transcript CG31496-RA	1.05
1625638_a_at	Hexokinase A	1.05
1639048_a_at	CG8229 gene product from transcript CG8229-RE	1.04
1634156_at	CG5604 gene product from transcript CG5604-RA	1.04
1633727_s_at	wallenda	1.04
1633387_at	CG32513 gene product from transcript CG32513-RA	1.04
1632471_at	CG12155 gene product from transcript CG12155-RA	1.04

1629160_s_at	Prosap	1.04
1628275_at	cdna:known chromosome:BDGP5:3L:14741029:1475105!	1.04
1626756_a_at	CG42378 gene product from transcript CG42378-RI	1.04
1626454_at	Cyclin B3	1.04
1625148_s_at	CG17870 gene product from transcript CG17870-RB	1.04
1623693_a_at	CG3365 gene product from transcript CG3365-RH	1.04
1636122_at	Suppressor of Cytokine Signaling at 16D	1.03
1632457_s_at	mastermind	1.03
1632161_at	lethal (3) 67BDr	1.03
1631919_at	CG17078 gene product from transcript CG17078-RB	1.03
1631502_at	worniu	1.03
1631481_a_at	Kruppel homolog 1	1.03
1629145_at	CG11734 gene product from transcript CG11734-RC	1.03
1627840_a_at	zipper	1.03
1627506_at	echinoid	1.03
1625515_a_at	scalloped	1.03
1623670_at	CG14562 gene product from transcript CG14562-RA	1.03
1638486_at	RNA-binding protein 1	1.02
1624301_at	CG10542 gene product from transcript CG10542-RA	1.02
1623133_a_at	CG10508 gene product from transcript CG10508-RK	1.02
1634309_at	CG14322 gene product from transcript CG14322-RA	1.01
1633876_at	CG7110 gene product from transcript CG7110-RB	1.01
1626738_at	mitochondrial RNA polymerase	1.01
1641639_at	escargot	1
1641620_s_at	CG4532 gene product from transcript CG4532-RA	1
1640054_at	CG10269 gene product from transcript CG10269-RA	1
1638681_at	piopio	1
1636248_at	CG15628 gene product from transcript CG15628-RA	1
1632519_at	CG8366 gene product from transcript CG8366-RA	1
1632381_at	domeless	1
1628791_at	CG13933 gene product from transcript CG13933-RA	1
1628342_s_at	ballchen	1
1627184_at	scaf6	1
1625945_a_at	CG1233 gene product from transcript CG1233-RB	1
1622949_at	pebbled	1
1632606_a_at	CG33169 gene product from transcript CG33169-RA	-1
1630830_a_at	Spermidine Synthase	-1

1629541_at	•	CG13018 gene product from transcript CG13018-RA	-1
1640452_at	•	CG2540 gene product from transcript CG2540-RA	-1.01
1637916_at	•	CG33013 gene product from transcript CG33013-RC	-1.01
1637379_at	•	CG14671 gene product from transcript CG14671-RA	-1.01
1641624_at	•	CG31957 gene product from transcript CG31957-RA	-1.03
1627349_at	•	Bekka	-1.03
1624635_at	•	CG14210 gene product from transcript CG14210-RA	-1.04
1627803_at	•	CG11875 gene product from transcript CG11875-RA	-1.05
1626658_at		--- /// ---	-1.06
1638047_at	•	cornichon related	-1.07
1633840_a_at	•	CG8026 gene product from transcript CG8026-RD	-1.07
1630821_at	•	CG2680 gene product from transcript CG2680-RB	-1.07
1633054_at	•	CG14057 gene product from transcript CG14057-RA	-1.08
1633691_at	•	CG32262 gene product from transcript CG32262-RA	-1.09
1630701_at	•	CG10778 gene product from transcript CG10778-RA	-1.11
1627432_at	•	CG6041 gene product from transcript CG6041-RA	-1.11
1624984_at	•	CG8021 gene product from transcript CG8021-RA	-1.11
1640917_at	•	CG15706 gene product from transcript CG15706-RA	-1.12
1635849_at	•	CG9804 gene product from transcript CG9804-RA	-1.12
1634023_at	•	CG14544 gene product from transcript CG14544-RA	-1.12
1624765_at	•	mitochondrial ribosomal protein L36	-1.12
1636630_s_at		--- /// garnysstan	-1.13
1626534_at	•	technical knockout	-1.13
1637118_at	•	CG30010 gene product from transcript CG30010-RA	-1.14
1640424_at	•	CG14463 gene product from transcript CG14463-RA	-1.15
1627633_at	•	CG42235 gene product from transcript CG42235-RE	-1.15
1630268_at	•	CG11781 gene product from transcript CG11781-RA	-1.16
1630505_a_at	•	CG1488 gene product from transcript CG1488-RB	-1.17
1630351_at	•	CG31229 gene product from transcript CG31229-RA	-1.17
1627438_at		Drosophila melanogaster RH74240 full insert cDNA.	-1.18
1631473_at	•	CG33170 gene product from transcript CG33170-RB	-1.19
1625149_at	•	CG7460 gene product from transcript CG7460-RB	-1.2
1636387_at	•	CG10300 gene product from transcript CG10300-RA	-1.21
1632145_a_at	•	CG31720 gene product from transcript CG31720-RC	-1.21
1628621_at	•	mitochondrial ribosomal protein S18C	-1.23
1639619_a_at	•	CG3994 gene product from transcript CG3994-RA	-1.24
1623464_at	•	CG13217 gene product from transcript CG13217-RA	-1.25

1631684_at	•	CG13014 gene product from transcript CG13014-RA	-1.26
1633989_at	•	CG1124 gene product from transcript CG1124-RA	-1.27
1633247_at	•	CG7006 gene product from transcript CG7006-RA	-1.27
1628221_at	•	CG17036 gene product from transcript CG17036-RA	-1.27
1631695_at	•	CG13066 gene product from transcript CG13066-RB	-1.29
1634158_at	•	Niemann-Pick type C-2f	-1.31
1632319_at	•	CG18598 gene product from transcript CG18598-RA	-1.32
1631002_at	•	cdna:known chromosome:BDGP5:3L:6141071:6141715:1	-1.32
1625901_s_at	•	CG34172 gene product from transcript CG34172-RB	-1.33
1633264_at	•	CG13024 gene product from transcript CG13024-RC	-1.34
1627723_at	•	CG14701 gene product from transcript CG14701-RA	-1.36
1630692_at	•	CG31789 gene product from transcript CG31789-RA	-1.43
1628284_at	•	CG3690 gene product from transcript CG3690-RA	-1.45
1640065_at	•	Glutathione S transferase E7	-1.46
1636683_at	•	CG14610 gene product from transcript CG14610-RB	-1.48
1625342_at	•	CG33282 gene product from transcript CG33282-RB	-1.53
1635263_at	•	CG11825 gene product from transcript CG11825-RB	-1.56
1626597_at	•	CG9521 gene product from transcript CG9521-RA	-1.58
1635878_s_at	•	CG17571 gene product from transcript CG17571-RA	-1.59
1628660_at	•	CG7130 gene product from transcript CG7130-RA	-1.63
1638742_at	•	Cuticular protein 67Fb	-1.7
1636604_at	•	CG12490 gene product from transcript CG12490-RB	-1.75
1634286_at	•	CG15554 gene product from transcript CG15554-RA	-1.78
1626025_at	•	CG34267 gene product from transcript CG34267-RA	-1.78
1633031_at	•	CG8299 gene product from transcript CG8299-RA	-1.84
1639350_at	•	cdna:known chromosome:BDGP5:3L:3934718:3935992:1	-1.85
1633142_at	•	CG17681 gene product from transcript CG17681-RA	-1.85
1639641_at	•	CG8560 gene product from transcript CG8560-RA	-1.87
1635274_at	•	CG34451 gene product from transcript CG34451-RA	-1.89
1623491_at	•	CG15155 gene product from transcript CG15155-RA	-2.15
1628500_at	•	CG32483 gene product from transcript CG32483-RA	-3.08
1625802_a_at	•	CG13135 gene product from transcript CG13135-RA	-3.58

only in mutant infection	no.
upregulated	309

List of genes changed after infection specific for mutant:

ID	FLY	GENENAME	m3-m3i
1629934_at	•	CG14219 gene product from transcript CG14219-RA	6.54
1635270_at		cdna:known chromosome:BDGP5:2R:14075227:1407579	6.01
1639571_s_at		heat shock 70 /// heat shock 70	5.42
1638238_at	•	CG5778 gene product from transcript CG5778-RB	4.57
1638003_at	•	CG14204 gene product from transcript CG14204-RA	4.33
1633812_at	•	CG9080 gene product from transcript CG9080-RA	4.2
1625235_at	•	CG13325 gene product from transcript CG13325-RA	3.79
1637229_a_at	•	CG11796 gene product from transcript CG11796-RA	3.77
1633009_a_at		Drosophila melanogaster GH19118 full length cDNA.	3.66
1629147_at	•	CG42633 gene product from transcript CG42633-RA	3.54
1627837_at	•	CG5527 gene product from transcript CG5527-RA	3.44
1635486_at	•	CG33468 gene product from transcript CG33468-RA	3.43
1641245_a_at		Drosophila melanogaster IP07237 full insert cDNA.	3.42
1634815_at	•	CG31104 gene product from transcript CG31104-RA	3.41
1634957_at	•	Diuretic hormone 44	3.4
1624283_at	•	Cuticular protein 47Eb	3.39
1623346_at	•	CG2861 gene product from transcript CG2861-RA	3.06
1623521_at		target of brain insulin	3.05
1636611_at	•	Trypsin 29F	2.82
1627807_at	•	world cup	2.8
1625557_at	•	CG34198 gene product from transcript CG34198-RA	2.77
1640657_at	•	CG42316 gene product from transcript CG42316-RD	2.61
1629905_s_at		IGF-II mRNA-binding protein	2.61
1636015_s_at	•	CG32850 gene product from transcript CG32850-RA	2.55
1626133_s_at		Drosophila melanogaster GH06606 full insert cDNA.	2.53
1633857_at	•	CG13659 gene product from transcript CG13659-RA	2.4
1635713_at	•	CG13185 gene product from transcript CG13185-RB	2.35
1627263_at	•	CG31601 gene product from transcript CG31601-RC	2.35
1641384_a_at	•	CG11327 gene product from transcript CG11327-RA	2.34
1636192_at	•	CG18178 gene product from transcript CG18178-RA	2.34
1633905_at	•	Ribosomal protein L28	2.29

1627936_s_at	cdna:novel chromosome:BDGP5:2L:22954463:22955770:	2.28
1630309_s_at	IGF-II mRNA-binding protein	2.26
1641534_at	CG11842 gene product from transcript CG11842-RA	2.24
1623247_at	CG10420 gene product from transcript CG10420-RA	2.24
1634962_s_at	hu li tai shao	2.22
1634020_at	CG12218 gene product from transcript CG12218-RA	2.22
1630934_at	cdna:novel chromosome:BDGP5:Uextra:15714903:15715	2.18
1640147_at	CG18518 gene product from transcript CG18518-RA	2.17
1640092_a_at	Ca[2+]-channel protein alpha[[1]] subunit D	2.14
1623415_at	dorsal	2.11
1631999_at	CG10710 gene product from transcript CG10710-RA	2.09
1624624_at	mushroom body defect	2.09
1626073_a_at	mushroom body defect	2.07
1626023_at	CG14932 gene product from transcript CG14932-RC	2.06
1631617_at	CG13742 gene product from transcript CG13742-RB	2.04
1631192_at	CG10887 gene product from transcript CG10887-RA	2.02
1635076_at	CG12674 gene product from transcript CG12674-RA	2
1630933_at	CG6738 gene product from transcript CG6738-RA	1.99
1623258_at	CG12493 gene product from transcript CG12493-RA	1.98
1635258_s_at	cdna:novel chromosome:BDGP5:3L:23166093:23171606:	1.96
1623825_s_at	CG17018 gene product from transcript CG17018-RC	1.96
1632870_at	CG32364 gene product from transcript CG32364-RA	1.95
1640903_at	CG4367 gene product from transcript CG4367-RA	1.92
1635893_at	alpha-Esterase-8	1.92
1634848_at	Spatzle-Processing Enzyme	1.92
1638991_at	CG5506 gene product from transcript CG5506-RA	1.91
1638331_s_at	CG4849 gene product from transcript CG4849-RA	1.91
1623784_at	CG5732 gene product from transcript CG5732-RB	1.91
1639218_s_at	CG15530 gene product from transcript CG15530-RB	1.9
1638849_a_at	CG2875 gene product from transcript CG2875-RB	1.9
1638053_at	Cytochrome P450-4p1	1.9
1636852_at	CG8939 gene product from transcript CG8939-RA	1.89
1628406_s_at	Drosophila melanogaster RH61266 full insert cDNA.	1.88
1637800_at	CG3347 gene product from transcript CG3347-RB	1.87
1634912_at	modulo	1.87
1629125_at	CG7897 gene product from transcript CG7897-RA	1.85
1627236_s_at	Drosophila melanogaster SD06908 full insert cDNA.	1.85

1633231_a_at	TBP-like factor	1.83
1633130_at	Drosophila melanogaster RT08037 full insert cDNA.	1.83
1630247_at	CG4554 gene product from transcript CG4554-RA	1.83
1637275_a_at	Drosophila melanogaster GH09427 full length cDNA.	1.8
1630938_a_at	CG14879 gene product from transcript CG14879-RB	1.8
1634724_at	CG12499 gene product from transcript CG12499-RA	1.79
1627847_s_at	yippee interacting protein 3	1.79
1635163_at	CG5731 gene product from transcript CG5731-RA	1.78
1623173_at	CG10013 gene product from transcript CG10013-RA	1.78
1639047_at	multiple ankyrin repeats single KH domain	1.77
1634520_at	vein	1.76
1640242_s_at	---	1.75
1630931_at	CG2843 gene product from transcript CG2843-RA	1.74
1625197_at	extra bases	1.74
1630119_s_at	no receptor potential A	1.73
1623855_s_at	CG11660 gene product from transcript CG11660-RA	1.72
1635886_s_at	Drosophila melanogaster SD06908 full insert cDNA.	1.71
1631087_a_at	CG9809 gene product from transcript CG9809-RB	1.7
1637386_at	retinal degeneration C	1.69
1635446_at	CG15043 gene product from transcript CG15043-RA	1.69
1631519_at	CG9143 gene product from transcript CG9143-RA	1.69
1641428_at	Cytochrome P450-9c1	1.68
1637658_at	methuselah-like 3	1.68
1636073_at	CG32344 gene product from transcript CG32344-RA	1.67
1633331_at	domino	1.67
1624809_s_at	cdna:novel chromosome:BDGP5:U:5573655:5575850:-1	1.67
1639408_a_at	shaking B	1.66
1638301_at	CG8157 gene product from transcript CG8157-RA	1.66
1625856_at	diminutive	1.66
1639442_a_at	Transferrin 1	1.64
1625195_s_at	schnurri	1.64
1624803_at	CG42316 gene product from transcript CG42316-RD	1.64
1634421_at	CG8414 gene product from transcript CG8414-RA	1.63
1623431_at	CG13423 gene product from transcript CG13423-RA	1.63
1630466_at	lethal (2) k09022	1.62
1625317_at	CG3735 gene product from transcript CG3735-RA	1.62
1634950_at	Maternal transcript 89Ba	1.6

1623852_at	CG10407 gene product from transcript CG10407-RA	1.6
1625046_at	RNA-binding motif protein 13	1.59
1639302_at	CG5645 gene product from transcript CG5645-RA	1.58
1635109_at	CG5888 gene product from transcript CG5888-RA	1.58
1639355_s_at	Female sterile (2) Ketel	1.57
1640080_at	CG9253 gene product from transcript CG9253-RA	1.56
1634712_s_at	Cytoplasmic linker protein 190	1.56
1632352_a_at	CG30007 gene product from transcript CG30007-RB	1.56
1624928_at	CG6064 gene product from transcript CG6064-RA	1.55
1623888_at	Caliban	1.55
1626818_at	CG13097 gene product from transcript CG13097-RA	1.54
1625316_s_at	protein phosphatase from PCR fragment D27	1.54
1625263_at	CG33554 gene product from transcript CG33554-RE	1.54
1637060_a_at	CG7421 gene product from transcript CG7421-RB	1.53
1629964_at	CG4076 gene product from transcript CG4076-RA	1.53
1628174_at	nimrod B1	1.52
1639447_at	CG15561 gene product from transcript CG15561-RA	1.51
1637356_a_at	CG12864 gene product from transcript CG12864-RB	1.51
1624573_at	CG4998 gene product from transcript CG4998-RB	1.51
1629617_at	CG14893 gene product from transcript CG14893-RB	1.5
1639367_a_at	cdna:known chromosome:BDGP5:2R:4016859:4018837:-	1.48
1633944_at	CG17362 gene product from transcript CG17362-RA	1.48
1636346_at	CG7839 gene product from transcript CG7839-RA	1.47
1634364_s_at	starvin	1.47
1623790_at	Mucin related 29B	1.47
1636625_at	krimper	1.46
1632850_at	CG7338 gene product from transcript CG7338-RA	1.46
1641282_at	methuselah-like 4	1.45
1638153_at	CG7907 gene product from transcript CG7907-RB	1.45
1623782_at	SREBP cleavage activating protein	1.45
1635894_at	CG30148 gene product from transcript CG30148-RA	1.44
1631180_at	CG5728 gene product from transcript CG5728-RA	1.44
1630950_at	CG10206 gene product from transcript CG10206-RA	1.44
1641059_at	Calcium ATPase at 60A	1.42
1639810_at	Dead box protein 73D	1.42
1635854_s_at	CG40351 gene product from transcript CG40351-RF	1.42
1628344_at	Casein kinase II beta subunit	1.42

1626680_at	CG9305 gene product from transcript CG9305-RA	1.42
1625752_at	Troponin C at 41C	1.42
1625437_at	--- /// ---	1.42
1624779_at	CG11583 gene product from transcript CG11583-RA	1.42
1628160_a_at	domino	1.41
1625880_at	cdna:known chromosome:BDGP5:3R:18552691:1855808	1.41
1641298_at	Elongator complex protein 1	1.4
1638780_at	Glutamate receptor IIE	1.4
1636119_at	CG1468 gene product from transcript CG1468-RA	1.4
1633717_a_at	CG2199 gene product from transcript CG2199-RB	1.4
1631248_at	lethal (1) G0020	1.4
1630324_at	wicked	1.4
1627967_a_at	methuselah-like 4	1.4
1627682_at	CG14949 gene product from transcript CG14949-RA	1.4
1641576_a_at	CG5205 gene product from transcript CG5205-RA	1.39
1640595_at	CG12301 gene product from transcript CG12301-RA	1.39
1629924_at	CG10238	1.39
1626077_s_at	CG43143 gene product from transcript CG43143-RF	1.39
1624826_at	CG8552 gene product from transcript CG8552-RA	1.39
1626884_a_at	Ataxin-2 Binding Protein 1	1.38
1634623_a_at	Drosophila melanogaster IP16196 full insert cDNA.	1.37
1632639_at	CG13941 gene product from transcript CG13941-RA	1.37
1624750_at	CG8545 gene product from transcript CG8545-RA	1.37
1639509_at	CG12396 gene product from transcript CG12396-RA	1.36
1624269_at	glaikit	1.36
1640808_at	CG11180 gene product from transcript CG11180-RA	1.35
1630445_at	lethal (3) 07882	1.35
1625116_at	Perlecan	1.35
1624957_a_at	CG4821 gene product from transcript CG4821-RE	1.35
1635568_at	mahjong	1.34
1629605_at	CG15056 gene product from transcript CG15056-RA	1.34
1629405_s_at	twenty-four	1.34
1634304_a_at	CG17233 gene product from transcript CG17233-RG	1.33
1629950_at	CG1785 gene product from transcript CG1785-RA	1.33
1627571_at	Cyclic-AMP response element binding protein A	1.33
1623496_at	kurz	1.33
1637412_a_at	stranded at second	1.32

1625551_at	Juvenile hormone-inducible protein 1	1.32
1623926_at	mushroom body miniature	1.32
1628264_a_at	homolog of RecQ	1.31
1639632_at	CG1234 gene product from transcript CG1234-RA	1.3
1636496_at	Nucleoporin 153	1.3
1628629_at	Microcephalin	1.3
1627183_at	cdna:known chromosome:BDGP5:3R:12475703:1247802	1.3
1625972_at	CG31999 gene product from transcript CG31999-RA	1.3
1625646_at	CG11148 gene product from transcript CG11148-RD	1.3
1629471_at	CG10803 gene product from transcript CG10803-RA	1.29
1632821_a_at	CG3287 gene product from transcript CG3287-RB	1.28
1632791_at	CG32479 gene product from transcript CG32479-RA	1.28
1629356_at	RNA polymerase I subunit	1.28
1628691_at	CG17514 gene product from transcript CG17514-RF	1.27
1624138_at	CG5800 gene product from transcript CG5800-RA	1.27
1633163_at	nucleostemin 3	1.26
1629753_at	Kruppel	1.26
1625843_s_at	PFTAIRE-interacting factor 1B	1.26
1636780_at	CG14233 gene product from transcript CG14233-RA	1.25
1631356_at	scaf6	1.25
1639414_at	Sno oncogene	1.24
1634601_at	CG9684 gene product from transcript CG9684-RA	1.24
1633003_at	CG30349 gene product from transcript CG30349-RA	1.24
1623924_at	CG12325 gene product from transcript CG12325-RA	1.24
1637866_at	CG9246 gene product from transcript CG9246-RA	1.23
1630806_at	female sterile (1) K10	1.23
1641032_at	unconventional prefoldin RPB5 interactor	1.22
1638614_at	CG18273 gene product from transcript CG18273-RA	1.21
1635664_at	Buzidau	1.21
1635441_at	CG33337 gene product from transcript CG33337-RB	1.21
1627492_at	lethal (3) 72Dn	1.21
1626444_at	Fibrillarlin	1.21
1639719_at	CG2163 gene product from transcript CG2163-RA	1.2
1638445_a_at	Secretory Pathway Calcium atpase	1.2
1635934_at	spaghetti	1.2
1629696_a_at	CG30497 gene product from transcript CG30497-RA	1.2
1629371_at	Elongase 68beta	1.2

1627656_at	gurken	1.2
1641486_at	CG42588 gene product from transcript CG42588-RA	1.19
1632294_at	senseless	1.19
1631083_at	lethal (1) G0144	1.19
1624720_s_at	CG6043 gene product from transcript CG6043-RG	1.19
1624272_at	CG10618 gene product from transcript CG10618-RB	1.19
1638283_at	CG9799 gene product from transcript CG9799-RA	1.18
1633412_s_at	CG3249 gene product from transcript CG3249-RC	1.18
1628180_at	CG12909 gene product from transcript CG12909-RA	1.18
1627461_at	bicoid stability factor	1.18
1636941_at	CG9007 gene product from transcript CG9007-RA	1.17
1631611_at	obstructor-H	1.17
1628216_at	peter pan	1.17
1623537_at	cdna:novel chromosome:BDGP5:X:12776214:12784445:-	1.17
1639288_at	Mystery 45A	1.15
1638480_at	CG8161 gene product from transcript CG8161-RA	1.15
1631465_at	CG3919 gene product from transcript CG3919-RB	1.15
1631198_at	CG2173 gene product from transcript CG2173-RA	1.15
1625253_at	Plenty of SH3s	1.15
1623607_at	UDP-GlcNAc:a-3-D-mannoside-beta-1,2-N-acetylglucosan	1.15
1641297_at	hyperplastic discs	1.14
1640382_at	CG2691 gene product from transcript CG2691-RA	1.14
1640068_at	CG10286 gene product from transcript CG10286-RA	1.14
1637489_at	CG6133 gene product from transcript CG6133-RA	1.14
1629242_x_at	---	1.14
1624335_at	CG11188 gene product from transcript CG11188-RA	1.14
1634727_a_at	three rows	1.13
1632035_at	cdna:novel chromosome:BDGP5:3R:5233571:5233867:-1	1.13
1623998_at	CG10565 gene product from transcript CG10565-RB	1.13
1641081_at	obstructor-G	1.12
1640341_s_at	CG5729 gene product from transcript CG5729-RA	1.12
1637162_at	CG12054 gene product from transcript CG12054-RA	1.12
1636958_s_at	lethal (2) k01209	1.12
1636301_s_at	CG14065	1.12
1632728_at	CG1609 gene product from transcript CG1609-RA	1.12
1626347_at	CG15877 gene product from transcript CG15877-RA	1.12
1640562_at	CG30033 gene product from transcript CG30033-RB	1.11

1627778_a_at	Arginine methyltransferase 3	1.11
1626016_s_at	tropomodulin	1.11
1622906_at	Drosophila melanogaster MIP19391 full insert cDNA.	1.11
1641382_at	CG8169 gene product from transcript CG8169-RA	1.1
1641324_at	Laminin A	1.1
1627924_at	RNA polymerase I 135kD subunit	1.1
1641369_at	--- /// ---	1.09
1640191_a_at	CTP synthase	1.09
1636926_s_at	cactus	1.09
1634705_at	CG10341 gene product from transcript CG10341-RA	1.09
1632676_s_at	CG11897 gene product from transcript CG11897-RA	1.09
1631106_s_at	Isoleucyl-tRNA synthetase	1.09
1628807_at	CG5205 gene product from transcript CG5205-RA	1.09
1625758_s_at	pitchoune	1.09
1638964_at	CG7800 gene product from transcript CG7800-RA	1.08
1636513_a_at	kismet	1.08
1631433_at	CG3335 gene product from transcript CG3335-RA	1.08
1627641_s_at	CG17494 gene product from transcript CG17494-RA	1.08
1626933_s_at	CG2469 gene product from transcript CG2469-RB	1.08
1624412_at	apterous	1.08
1639671_at	eiger	1.07
1637468_at	lethal (2) 34Fd	1.07
1633466_at	CG7728 gene product from transcript CG7728-RA	1.07
1631822_at	mutagen-sensitive 205	1.07
1640143_at	CG10463 gene product from transcript CG10463-RA	1.06
1637125_at	CG2004 gene product from transcript CG2004-RA	1.06
1628767_s_at	Mediator complex subunit 26	1.06
1623612_at	Serpin 47C	1.06
1623432_s_at	plexin B	1.06
1633394_a_at	CG13900 gene product from transcript CG13900-RA	1.05
1640653_at	Eukaryotic initiation factor 4B	1.04
1636773_a_at	degringolade	1.04
1631093_at	CG11837 gene product from transcript CG11837-RA	1.04
1624660_at	Protein tyrosine phosphatase 10D	1.04
1637410_s_at	lethal (2) giant larvae	1.03
1633878_at	Misexpression suppressor of ras 4	1.03
1628884_at	Peptidoglycan recognition protein SA	1.03

1625130_at	CG8170 gene product from transcript CG8170-RB	1.03
1624780_at	CG2995 gene product from transcript CG2995-RA	1.03
1624267_at	CG7182 gene product from transcript CG7182-RA	1.03
1624141_at	CG4901 gene product from transcript CG4901-RA	1.03
1637494_at	CG3071 gene product from transcript CG3071-RA	1.02
1636468_a_at	CG5033 gene product from transcript CG5033-RA	1.02
1630823_at	l(3)76BDr	1.02
1629429_at	CG31388 gene product from transcript CG31388-RB	1.02
1626676_at	plexin B	1.02
1641026_a_at	Par-1 kinase	1.01
1639914_at	CG5961 gene product from transcript CG5961-RB	1.01
1639873_at	CG6745 gene product from transcript CG6745-RA	1.01
1637943_at	held out wings	1.01
1636869_at	Argonaute	1.01
1628240_at	CG4825 gene product from transcript CG4825-RA	1.01
1640915_at	CG3800 gene product from transcript CG3800-RA	1
1640214_at	Nicotinamide amidase	1
1627383_at	abnormal spindle	1
1625589_at	centrosomin's beautiful sister	1
1639731_at	CG7785 gene product from transcript CG7785-RA	-1
1637251_a_at	CG10622 gene product from transcript CG10622-RA	-1.01
1635473_at	diadenosine tetraphosphate hydrolase	-1.01
1626514_at	CG5013 gene product from transcript CG5013-RA	-1.01
1640298_at	CG6308 gene product from transcript CG6308-RA	-1.02
1637154_at	CG7470 gene product from transcript CG7470-RB	-1.02
1630229_at	CG9815 gene product from transcript CG9815-RB	-1.02
1628935_at	CG10962 gene product from transcript CG10962-RB	-1.02
1625477_a_at	CG4797 gene product from transcript CG4797-RA	-1.02
1624506_at	Jonah 25Biii	-1.02
1623632_s_at	CG6327 gene product from transcript CG6327-RD	-1.02
1634298_at	CG12375 gene product from transcript CG12375-RA	-1.03
1632378_at	no mechanoreceptor potential A	-1.03
1630523_at	CG12106 gene product from transcript CG12106-RA	-1.03
1640992_at	CG2811 gene product from transcript CG2811-RA	-1.04
1630908_at	CG13617 gene product from transcript CG13617-RA	-1.04
1626089_at	axotactin	-1.04
1625756_at	CG6656 gene product from transcript CG6656-RA	-1.04

1630450_s_at	CG1981 gene product from transcript CG1981-RA	-1.05
1623453_at	Nuclear factor Y-box B	-1.05
1623231_at	dynactin-subunit-p25	-1.05
1622908_a_at	CG10962 gene product from transcript CG10962-RB	-1.05
1640857_at	CG10208 gene product from transcript CG10208-RA	-1.06
1638000_at	spalt-adjacent	-1.06
1637510_s_at	Hexosaminidase 1	-1.06
1634609_at	CG31111 gene product from transcript CG31111-RA	-1.06
1624437_s_at	--- /// --- /// deltaTrypsin /// gammaTrypsin	-1.06
1637402_at	CG32109 gene product from transcript CG32109-RA	-1.07
1634199_at	CG15220 gene product from transcript CG15220-RA	-1.07
1631321_s_at	His1:CG31617 /// His1:CG33801 /// His1:CG33804 /// His1:CG33805	-1.07
1627460_at	CG18343 gene product from transcript CG18343-RA	-1.07
1622907_at	Drosophila melanogaster FI01425 full insert cDNA.	-1.07
1635223_at	Drosophila melanogaster GH07620 full insert cDNA.	-1.08
1629072_at	--- /// suppressor of white-apricot	-1.08
1628599_at	Psf2	-1.08
1625233_at	Phosphatidylinositol 3 kinase 68D	-1.08
1638504_s_at	Drosophila melanogaster LP09838 full insert cDNA.	-1.09
1633641_a_at	CG15611 gene product from transcript CG15611-RB	-1.09
1625644_at	CG2641 gene product from transcript CG2641-RA	-1.09
1632975_at	CG4398 gene product from transcript CG4398-RA	-1.1
1636168_s_at	CG13101 gene product from transcript CG13101-RA	-1.11
1632979_at	CG11784 gene product from transcript CG11784-RB	-1.11
1639515_at	CG7367 gene product from transcript CG7367-RB	-1.12
1633830_at	CG10195 gene product from transcript CG10195-RB	-1.12
1629973_at	GABA transporter /// ---	-1.12
1629520_at	CG8997 gene product from transcript CG8997-RA	-1.12
1625840_at	CG12001 gene product from transcript CG12001-RA	-1.12
1637063_at	CG33099 gene product from transcript CG33099-RA	-1.13
1633405_s_at	CG4288 gene product from transcript CG4288-RB	-1.13
1631101_at	CG6480 gene product from transcript CG6480-RA	-1.13
1628177_at	juvenile hormone acid methyltransferase	-1.13
1639951_at	CG2611 gene product from transcript CG2611-RA	-1.15
1637022_at	CG3532 gene product from transcript CG3532-RB	-1.15
1635222_at	CG1513 gene product from transcript CG1513-RA	-1.15
1631674_at	O-fucosyltransferase 1	-1.15

1636942_at	CG8498 gene product from transcript CG8498-RA	-1.16
1635398_at	--- /// Calexcitin	-1.16
1635031_s_at	CG11147 gene product from transcript CG11147-RA	-1.16
1629821_at	Drosophila melanogaster GM14547 full length cDNA.	-1.16
1629430_s_at	CG1803 gene product from transcript CG1803-RA	-1.16
1641360_at	CG10222 gene product from transcript CG10222-RA	-1.17
1636816_s_at	CG33090 gene product from transcript CG33090-RB	-1.18
1631784_at	CG13663 gene product from transcript CG13663-RA	-1.18
1636431_at	CG8768 gene product from transcript CG8768-RA	-1.19
1623953_at	CG11592 gene product from transcript CG11592-RA	-1.19
1636535_at	CG15912 gene product from transcript CG15912-RA	-1.2
1636196_s_at	--- /// ---	-1.2
1633801_s_at	CG9171 gene product from transcript CG9171-RC	-1.2
1640901_at	CG6753 gene product from transcript CG6753-RB	-1.21
1638661_at	yippee interacting protein 7	-1.21
1636121_at	CG12924 gene product from transcript CG12924-RA	-1.21
1640101_at	CG8152 gene product from transcript CG8152-RA	-1.22
1638031_at	CG14512 gene product from transcript CG14512-RA	-1.22
1638811_at	CG7334 gene product from transcript CG7334-RE	-1.23
1638417_at	CG31373 gene product from transcript CG31373-RA	-1.24
1637928_at	CG6070 /// Organic anion transporting polypeptide 58Db	-1.24
1635110_at	CG2397 gene product from transcript CG2397-RA	-1.24
1638975_at	CG13876 gene product from transcript CG13876-RA	-1.25
1635086_at	CG4666 gene product from transcript CG4666-RA	-1.25
1629875_a_at	Cytochrome P450-4d1	-1.25
1636742_at	--- /// --- /// nord	-1.26
1631252_a_at	CG12023 gene product from transcript CG12023-RA	-1.26
1639322_at	etaTrypsin	-1.27
1634925_at	Transport and Golgi organization 2	-1.27
1640561_at	CG5978 gene product from transcript CG5978-RA	-1.28
1628184_at	Tetraspanin 3A	-1.28
1625531_at	Odorant-binding protein 18a	-1.28
1632431_s_at	Angiotensin converting enzyme	-1.29
1640286_at	--- /// UDP-sugar transporter in 74C	-1.3
1634746_at	CG3589 gene product from transcript CG3589-RA	-1.3
1640658_at	CG10005 gene product from transcript CG10005-RA	-1.31
1628330_at	CG34116 gene product from transcript CG34116-RA	-1.31

1626524_at	Phaedra 1	-1.31
1635919_at	CG13255 gene product from transcript CG13255-RA	-1.33
1633789_at	CG18144 gene product from transcript CG18144-RA	-1.33
1630989_a_at	CG32442 gene product from transcript CG32442-RA	-1.33
1638844_s_at	CG3714 gene product from transcript CG3714-RC	-1.34
1634699_a_at	Peroxin 6	-1.34
1626204_at	CG42246 gene product from transcript CG42246-RA	-1.34
1631432_at	Drosophila melanogaster RE24790 full insert cDNA.	-1.36
1628682_at	CG5577 gene product from transcript CG5577-RA	-1.36
1625800_at	CG4074 gene product from transcript CG4074-RA	-1.36
1637097_at	CG7497 gene product from transcript CG7497-RB	-1.37
1637041_a_at	CG3332 gene product from transcript CG3332-RB	-1.37
1633880_s_at	Ionotropic receptor 76a	-1.37
1628314_a_at	CG6891 gene product from transcript CG6891-RA	-1.37
1641412_at	CG31809 gene product from transcript CG31809-RB	-1.38
1637469_at	presenilin enhancer	-1.38
1629199_at	Antigen 5-related 2	-1.38
1628345_at	Cytochrome P450-6a9	-1.39
1627744_at	CG15209 gene product from transcript CG15209-RA	-1.4
1630414_at	CG13603 gene product from transcript CG13603-RA	-1.41
1637346_at	CG33514 gene product from transcript CG33514-RA	-1.42
1633378_at	Galactose-specific C-type lectin	-1.43
1623883_at	CG18661 gene product from transcript CG18661-RA	-1.43
1637791_at	CG31922 gene product from transcript CG31922-RA	-1.45
1633707_at	CG12824 gene product from transcript CG12824-RA	-1.45
1626166_at	CG13082 gene product from transcript CG13082-RA	-1.45
1640665_at	CG14133 gene product from transcript CG14133-RB	-1.47
1636409_at	CG11034 gene product from transcript CG11034-RB	-1.47
1637403_at	CG7953 gene product from transcript CG7953-RA	-1.48
1636793_at	Cytochrome P450-4d2	-1.48
1634016_at	CG2781 gene product from transcript CG2781-RA	-1.48
1634628_at	CG30392 gene product from transcript CG30392-RA	-1.49
1633268_s_at	Na⁺/H⁺ hydrogen antiporter 1	-1.5
1632540_at	iotaTrypsin	-1.52
1624824_at	Jonah 74E	-1.52
1637309_a_at	CG14680 gene product from transcript CG14680-RC	-1.53
1636929_at	aveugle	-1.54

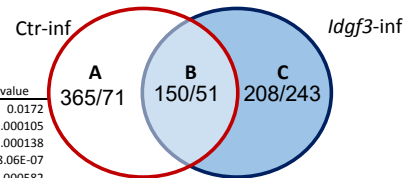
1635756_at	CG32039 gene product from transcript CG32039-RA	-1.54
1639049_at	CG17145 gene product from transcript CG17145-RA	-1.55
1637301_a_at	slowpoke	-1.55
1631387_at	CG30344 gene product from transcript CG30344-RA	-1.55
1629215_at	CG10723 gene product from transcript CG10723-RA	-1.55
1630528_at	CG17751 gene product from transcript CG17751-RB	-1.56
1629716_a_at	CG13284 gene product from transcript CG13284-RA	-1.56
1630957_s_at	slimfast	-1.57
1629897_a_at	CG6044 gene product from transcript CG6044-RA	-1.57
1625177_at	CG14182 gene product from transcript CG14182-RA	-1.57
1636973_at	Senescence marker protein-30	-1.58
1630467_a_at	Diuretic hormone 31	-1.58
1623620_a_at	rhomboid-6	-1.58
1636059_at	CG9689 gene product from transcript CG9689-RA	-1.59
1640244_at	CG33514 gene product from transcript CG33514-RA	-1.6
1631420_at	CG9509 gene product from transcript CG9509-RA	-1.6
1641190_at	Jonah 65Aii	-1.62
1639111_at	CG15362 gene product from transcript CG15362-RA	-1.62
1631266_a_at	CG5840 gene product from transcript CG5840-RB	-1.62
1639904_at	O-6-alkylguanine-DNA alkyltransferase	-1.64
1634607_at	CG14160 gene product from transcript CG14160-RA	-1.64
1637983_s_at	CG10365 gene product from transcript CG10365-RC	-1.65
1626022_at	CG14680 gene product from transcript CG14680-RC	-1.68
1623555_at	CG10131 gene product from transcript CG10131-RA	-1.68
1638473_at	CG4386 gene product from transcript CG4386-RA	-1.69
1627207_at	CG14352 gene product from transcript CG14352-RA	-1.69
1625304_s_at	CG34301 gene product from transcript CG34301-RA	-1.7
1637632_at	CG12194 gene product from transcript CG12194-RA	-1.73
1631277_at	alpha-Esterase-4	-1.74
1628907_at	Type III alcohol dehydrogenase	-1.74
1636392_at	Drosophila melanogaster IP21342 full insert cDNA.	-1.75
1635507_at	--- /// ---	-1.76
1633386_s_at	methuselah-like 8	-1.76
1631369_at	CG7567 gene product from transcript CG7567-RA	-1.78
1627741_at	CG13086 gene product from transcript CG13086-RA	-1.78
1625948_at	CG17633 gene product from transcript CG17633-RA	-1.78
1626689_at	CG1644 gene product from transcript CG1644-RA	-1.8

1635868_at	CG6295 gene product from transcript CG6295-RA	-1.81
1636736_s_at	--- /// Misexpression suppressor of KSR 4	-1.82
1623468_at	mitotic spindle density 5	-1.85
1636154_at	CG30090 gene product from transcript CG30090-RA	-1.87
1633783_a_at	CG5921 gene product from transcript CG5921-RD	-1.87
1637829_at	CG4020 gene product from transcript CG4020-RA	-1.88
1631285_at	Tetraspanin 5D	-1.88
1624670_at	CG7589 gene product from transcript CG7589-RA	-1.88
1628430_at	CG15704 gene product from transcript CG15704-RA	-1.89
1641664_at	CG10170 gene product from transcript CG10170-RA	-1.91
1637551_at	CG1887 gene product from transcript CG1887-RD	-1.92
1635975_s_at	Drosophila melanogaster RE54004 full length cDNA.	-1.92
1623728_at	CG13689 gene product from transcript CG13689-RA	-1.92
1626605_at	CG14075 gene product from transcript CG14075-RA	-1.93
1638973_s_at	CG11149 gene product from transcript CG11149-RD	-1.97
1626481_a_at	Tafazzin	-1.97
1626342_at	CG12115 gene product from transcript CG12115-RA	-1.98
1636470_at	CG34026 gene product from transcript CG34026-RA	-2.02
1634033_s_at	Drosophila melanogaster glucose transporter 1 (glut1) m	-2.02
1636193_at	CG13893 gene product from transcript CG13893-RA	-2.04
1633033_s_at	CG1732 gene product from transcript CG1732-RA	-2.04
1638775_at	Multi drug resistance 50	-2.05
1634143_at	CG8345 gene product from transcript CG8345-RA	-2.05
1632695_at	CG18585 gene product from transcript CG18585-RA	-2.05
1628896_a_at	CG4210 gene product from transcript CG4210-RC	-2.05
1638601_at	spookier	-2.08
1627657_at	CG16749 gene product from transcript CG16749-RA	-2.08
1624732_at	Glutathione S transferase E5	-2.1
1637291_at	CG18031 gene product from transcript CG18031-RA	-2.12
1624092_at	Jonah 99Ci	-2.14
1630886_at	CG6584 gene product from transcript CG6584-RI	-2.18
1634267_at	CG30495 gene product from transcript CG30495-RA	-2.19
1639338_at	CG11912 gene product from transcript CG11912-RA	-2.22
1631668_at	CG17147 gene product from transcript CG17147-RA	-2.25
1624171_at	CG13488 gene product from transcript CG13488-RB	-2.28
1624816_at	CG30283 gene product from transcript CG30283-RB	-2.29
1623256_at	Glutathione S transferase E1	-2.31

1637516_at	•	CG15449 gene product from transcript CG15449-RA	-2.35
1637561_at	•	CG16834 gene product from transcript CG16834-RB	-2.37
1637253_s_at	•	CG17570 gene product from transcript CG17570-RA	-2.43
1634323_at	•	CG17191 gene product from transcript CG17191-RA	-2.43
1625833_at	•	CG9896 gene product from transcript CG9896-RA	-2.47
1635254_at	•	CG17662 gene product from transcript CG17662-RB	-2.53
1640060_at	•	CG33096 gene product from transcript CG33096-RE	-2.58
1633411_s_at		--- /// ---	-2.62
1634076_at	•	CG12057 gene product from transcript CG12057-RA	-2.63
1639733_s_at	•	CG14275 gene product from transcript CG14275-RA	-2.64
1633050_at	•	Niemann-Pick type C-2d	-2.64
1625082_a_at	•	CG7882 gene product from transcript CG7882-RA	-2.78
1627946_at		shroud	-2.82
1640978_at	•	CG14567 gene product from transcript CG14567-RA	-2.85
1625487_at	•	CG6839 gene product from transcript CG6839-RA	-2.86
1632444_at	•	CG15170 gene product from transcript CG15170-RA	-2.95
1623559_s_at		---	-3.02
1641125_at	•	CG1942 gene product from transcript CG1942-RA	-3.11
1627120_at	•	CG1014 gene product from transcript CG1014-RA	-3.18
1624137_at	•	CG11911 gene product from transcript CG11911-RA	-3.2
1635952_at	•	lethal (2) essential for life	-3.23
1632045_at	•	CG5697 gene product from transcript CG5697-RA	-3.24
1633460_at	•	CG6034 gene product from transcript CG6034-RA	-3.25
1626028_at	•	CG4783 gene product from transcript CG4783-RA	-3.45
1640037_at	•	CG7798 gene product from transcript CG7798-RA	-3.52
1637590_at	•	CG42329 gene product from transcript CG42329-RA	-3.55
1629542_at	•	CG31821 gene product from transcript CG31821-RA	-3.6
1637986_at	•	CG15253 gene product from transcript CG15253-RA	-3.68
1629184_at	•	CG3819 gene product from transcript CG3819-RA	-3.75
1627499_at	•	CG2016 gene product from transcript CG2016-RB	-3.79
1625910_at	•	CG1773 gene product from transcript CG1773-RA	-3.89
1630619_at	•	Serine protease inhibitor 1	-3.92
1625739_at	•	CG3292 gene product from transcript CG3292-RA	-4
1627477_at		cdna:known chromosome:BDGP5:3R:3866970:3881259:1	-4.02
1640542_at	•	CG5892 gene product from transcript CG5892-RA	-4.16
1641715_at	•	CG11162 gene product from transcript CG11162-RA	-4.34
1635306_at	•	CG4650 gene product from transcript CG4650-RB	-4.62

1629324_at	•	CG6870 gene product from transcript CG6870-RA	-4.7
1630822_at	•	CG13078 gene product from transcript CG13078-RA	-5.26
1626031_at	•	CG12539 gene product from transcript CG12539-RA	-5.4

Analysis Type:	PANTHER Overrepresentation Test (release 20150430)
Annotation Version and Release Date:	GO Ontology database Released 2015-06-06
Reference List:	Drosophila melanogaster (all genes in database)
	Bonferroni correction for multiple testing



A - genes significantly changed only in infected control

GO biological process complete	#ref	#analyzed	expected	Fold Enrichment	+/-	P value
regulation of hippo signaling	16	6	0.44	>5	+	0.0172
negative regulation of Wnt signaling pathway	33	10	0.9	>5	+	0.000105
homophilic cell adhesion via plasma membrane adhesion molecules	34	10	0.93	>5	+	0.000138
regulation of Wnt signaling pathway	72	16	1.97	>5	+	8.06E-07
cell-cell adhesion via plasma-membrane adhesion molecules	62	12	1.7	>5	+	0.000582
establishment of ommatidial planar polarity	62	10	1.7	>5	+	0.0287
cell-cell adhesion	83	13	2.27	>5	+	0.00194
peripheral nervous system development	94	14	2.57	>5	+	0.00132
establishment of tissue polarity	91	12	2.49	4.81	+	0.0288
establishment of planar polarity	91	12	2.49	4.81	+	0.0288
chemotaxis	267	35	7.31	4.79	+	1.32E-10
brain development	125	16	3.42	4.67	+	0.00149
axonogenesis	291	37	7.97	4.64	+	6E-11
axon development	300	38	8.22	4.62	+	2.94E-11
morphogenesis of a polarized epithelium	103	13	2.82	4.61	+	0.0198
axon guidance	246	31	6.74	4.6	+	1.05E-08
neuron projection guidance	254	32	6.96	4.6	+	4.69E-09
neuron recognition	113	14	3.1	4.52	+	0.0109
taxis	325	40	8.9	4.49	+	1.42E-11
cell recognition	119	14	3.26	4.29	+	0.0195
cell morphogenesis involved in differentiation	478	55	13.09	4.2	+	1.27E-15
cell morphogenesis involved in neuron differentiation	434	49	11.89	4.12	+	2.72E-13
head development	151	17	4.14	4.11	+	0.00375
imaginal disc-derived appendage development	406	44	11.12	3.96	+	4.65E-11
appendage development	409	44	11.2	3.93	+	5.98E-11
wing disc morphogenesis	352	37	9.64	3.84	+	1.55E-08
imaginal disc-derived appendage morphogenesis	402	42	11.01	3.81	+	6.29E-10
imaginal disc-derived wing morphogenesis	346	36	9.48	3.8	+	4.02E-08
post-embryonic appendage morphogenesis	395	41	10.82	3.79	+	1.52E-09
appendage morphogenesis	405	42	11.09	3.79	+	7.99E-10
central nervous system development	233	24	6.38	3.76	+	0.000133
negative regulation of signal transduction	243	25	6.66	3.76	+	7.11E-05
regulation of neurogenesis	167	17	4.57	3.72	+	0.014
negative regulation of response to stimulus	296	30	8.11	3.7	+	3.91E-06
negative regulation of signaling	259	26	7.09	3.66	+	6.04E-05
negative regulation of cell communication	263	26	7.2	3.61	+	8.14E-05
neuron projection morphogenesis	527	52	14.44	3.6	+	6.4E-12
post-embryonic organ morphogenesis	459	45	12.57	3.58	+	7.2E-10
imaginal disc morphogenesis	459	45	12.57	3.58	+	7.2E-10
neuron projection development	541	53	14.82	3.58	+	4.46E-12
regulation of cell proliferation	184	18	5.04	3.57	+	0.0127
dendrite morphogenesis	195	19	5.34	3.56	+	0.00737
neuron development	664	64	18.19	3.52	+	7.41E-15
locomotion	564	54	15.45	3.5	+	5.95E-12
dendrite development	199	19	5.45	3.49	+	0.00982
compound eye development	326	31	8.93	3.47	+	9.05E-06
cell adhesion	200	19	5.48	3.47	+	0.0105
instar larval or pupal morphogenesis	474	45	12.98	3.47	+	2.13E-09
post-embryonic morphogenesis	485	46	13.29	3.46	+	1.2E-09
positive regulation of nucleobase-containing compound metabolic process	327	31	8.96	3.46	+	9.71E-06
post-embryonic organ development	517	49	14.16	3.46	+	1.96E-10
eye development	341	32	9.34	3.43	+	6.84E-06
metamorphosis	501	47	13.72	3.42	+	9.53E-10
tube morphogenesis	556	52	15.23	3.41	+	5.18E-11
open tracheal system development	215	20	5.89	3.4	+	0.00802
regulation of anatomical structure size	183	17	5.01	3.39	+	0.0448
positive regulation of macromolecule biosynthetic process	325	30	8.9	3.37	+	3.15E-05
wing disc development	466	43	12.76	3.37	+	1.77E-08
compound eye morphogenesis	250	23	6.85	3.36	+	0.00176
morphogenesis of an epithelium	642	59	17.59	3.35	+	1.54E-12
positive regulation of nitrogen compound metabolic process	349	32	9.56	3.35	+	1.18E-05
sensory organ morphogenesis	262	24	7.18	3.34	+	0.00108
eye morphogenesis	262	24	7.18	3.34	+	0.00108
epithelial tube morphogenesis	524	48	14.35	3.34	+	1.22E-09
positive regulation of RNA metabolic process	306	28	8.38	3.34	+	0.000118
tissue morphogenesis	656	60	17.97	3.34	+	1.04E-12
positive regulation of RNA biosynthetic process	299	27	8.19	3.3	+	0.000267
positive regulation of transcription, DNA-templated	299	27	8.19	3.3	+	0.000267
positive regulation of nucleic acid-templated transcription	299	27	8.19	3.3	+	0.000267
neuron differentiation	767	69	21.01	3.28	+	1E-14
biological adhesion	213	19	5.83	3.26	+	0.0253
cell projection morphogenesis	584	52	16	3.25	+	3.41E-10
respiratory system development	225	20	6.16	3.25	+	0.0156
positive regulation of transcription from RNA polymerase II promoter	215	19	5.89	3.23	+	0.0288
cell morphogenesis	681	60	18.65	3.22	+	5.42E-12
cell part morphogenesis	591	52	16.19	3.21	+	5.36E-10
positive regulation of cellular biosynthetic process	364	32	9.97	3.21	+	3.13E-05
positive regulation of biosynthetic process	364	32	9.97	3.21	+	3.13E-05
positive regulation of gene expression	342	30	9.37	3.2	+	9.57E-05
generation of neurons	883	77	24.19	3.18	+	4.48E-16
instar larval or pupal development	574	50	15.72	3.18	+	2.36E-09
cell projection organization	656	57	17.97	3.17	+	5.35E-11
regulation of transcription from RNA polymerase II promoter	441	38	12.08	3.15	+	2.14E-06
organ morphogenesis	758	65	20.76	3.13	+	1.09E-12
embryo development	502	43	13.75	3.13	+	1.81E-07
regulation of nervous system development	259	22	7.09	3.1	+	0.0109
imaginal disc development	636	54	17.42	3.1	+	6.99E-10
cellular component morphogenesis	801	68	21.94	3.1	+	3.31E-13
movement of cell or subcellular component	594	50	16.27	3.07	+	8.08E-09
tube development	767	64	21.01	3.05	+	6.74E-12
muscle structure development	240	20	6.57	3.04	+	0.0391
post-embryonic development	637	53	17.45	3.04	+	2.58E-09
cell fate commitment	478	39	13.09	2.98	+	5.69E-06
epithelial cell differentiation	360	29	9.86	2.94	+	0.000932
epithelium development	1005	80	27.53	2.91	+	1.5E-14
sensory organ development	455	36	12.46	2.89	+	5.29E-05
ovarian follicle cell development	283	22	7.75	2.84	+	0.0423
columnar/cuboidal epithelial cell development	284	22	7.78	2.83	+	0.0446
tissue development	1120	86	30.68	2.8	+	5.56E-15
cell development	1409	108	38.6	2.8	+	5.62E-20
regulation of cell differentiation	333	25	9.12	2.74	+	0.0202
positive regulation of cellular process	956	70	26.19	2.67	+	1.58E-10
oogenesis	605	44	16.57	2.66	+	1.54E-05
regulation of multicellular organismal development	455	33	12.46	2.65	+	0.00147
positive regulation of macromolecule metabolic process	513	37	14.05	2.63	+	0.000335
female gamete generation	612	44	16.76	2.62	+	2.15E-05

negative regulation of cellular process	1003	72	27.47	2.62	+	1.68E-10
organ development	1226	88	33.58	2.62	+	1.24E-13
regulation of cellular macromolecule biosynthetic process	936	67	25.64	2.61	+	1.69E-09
regulation of macromolecule biosynthetic process	938	67	25.69	2.61	+	1.86E-09
regulation of RNA biosynthetic process	842	60	23.06	2.6	+	3.99E-08
regulation of transcription, DNA-templated	842	60	23.06	2.6	+	3.99E-08
regulation of nucleic acid-templated transcription	842	60	23.06	2.6	+	3.99E-08
positive regulation of cellular metabolic process	537	38	14.71	2.58	+	0.00036
regulation of cellular biosynthetic process	987	69	27.04	2.55	+	2.12E-09
regulation of biosynthetic process	988	69	27.06	2.55	+	2.22E-09
anatomical structure morphogenesis	1634	114	44.76	2.55	+	4.11E-18
regulation of signal transduction	661	46	18.11	2.54	+	2.54E-05
regulation of RNA metabolic process	919	63	25.17	2.5	+	5.65E-08
nervous system development	1548	106	42.4	2.5	+	7.26E-16
regulation of nucleobase-containing compound metabolic process	968	66	26.52	2.49	+	2.17E-08
positive regulation of biological process	1087	74	29.78	2.49	+	9.51E-10
response to external stimulus	838	57	22.95	2.48	+	7.92E-07
regulation of developmental process	677	46	18.54	2.48	+	5.17E-05
cellular process involved in reproduction in multicellular organism	771	52	21.12	2.46	+	7.04E-06
neurogenesis	1397	94	38.27	2.46	+	4.62E-13
negative regulation of biological process	1133	76	31.04	2.45	+	8.82E-10
regulation of nitrogen compound metabolic process	1002	67	27.45	2.44	+	3.41E-08
response to chemical	869	58	23.8	2.44	+	1.09E-06
regulation of response to stimulus	904	60	24.76	2.42	+	6.43E-07
behavior	548	36	15.01	2.4	+	0.00433
regionalization	472	31	12.93	2.4	+	0.0236
pattern specification process	518	34	14.19	2.4	+	0.00869
positive regulation of metabolic process	611	40	16.74	2.39	+	0.0012
germ cell development	703	46	19.26	2.39	+	0.000155
developmental process involved in reproduction	810	53	22.19	2.39	+	1.34E-05
anatomical structure formation involved in morphogenesis	571	37	15.64	2.37	+	0.00422
negative regulation of cellular metabolic process	483	31	13.23	2.34	+	0.0367
regulation of signaling	735	47	20.13	2.33	+	0.000215
gamete generation	832	53	22.79	2.33	+	3.26E-05
system development	2180	138	59.72	2.31	+	2.46E-19
regulation of gene expression	1076	68	29.47	2.31	+	2.66E-07
regulation of cell communication	745	47	20.41	2.3	+	0.000318
single organism reproductive process	898	56	24.6	2.28	+	2.48E-05
negative regulation of metabolic process	564	35	15.45	2.27	+	0.0206
multicellular organismal reproductive process	940	58	25.75	2.25	+	1.88E-05
regulation of multicellular organismal process	618	38	16.93	2.24	+	0.0102
mitotic cell cycle	537	33	14.71	2.24	+	0.0459
cell differentiation	2204	133	60.37	2.2	+	1.58E-16
sexual reproduction	962	58	26.35	2.2	+	4.23E-05
multi-organism reproductive process	972	58	26.63	2.18	+	6.05E-05
regulation of primary metabolic process	1357	80	37.17	2.15	+	1.2E-07
cellular component assembly	748	44	20.49	2.15	+	0.00524
reproductive process	1037	61	28.41	2.15	+	4.13E-05
cellular developmental process	2272	133	62.24	2.14	+	2.18E-15
regulation of cellular metabolic process	1404	82	38.46	2.13	+	1.01E-07
regulation of macromolecule metabolic process	1407	82	38.54	2.13	+	1.12E-07
cell cycle	725	41	19.86	2.06	+	0.0303
single-organism organelle organization	1034	57	28.32	2.01	+	0.0011
regulation of metabolic process	1603	88	43.91	2	+	3.88E-07
regulation of biological quality	996	54	27.28	1.98	+	0.00382
multicellular organismal development	2731	148	74.81	1.98	+	8.85E-15
anatomical structure development	2966	160	81.25	1.97	+	1.94E-16
multi-organism process	1251	67	34.27	1.96	+	0.000256
multicellular organism reproduction	1139	61	31.2	1.96	+	0.00107
regulation of cellular process	2928	155	80.2	1.93	+	7.25E-15
single-organism developmental process	3249	170	89	1.91	+	1.26E-16
cellular component organization	2342	122	64.15	1.9	+	7.4E-10
developmental process	3273	170	89.65	1.9	+	2.77E-16
regulation of biological process	3143	162	86.09	1.88	+	9.36E-15
reproduction	1270	65	34.79	1.87	+	0.00203
cellular component organization or biogenesis	2403	122	65.82	1.85	+	4.46E-09
response to stimulus	2341	117	64.13	1.82	+	4.55E-08
biological regulation	3426	171	93.85	1.82	+	1.3E-14
single-multicellular organism process	3274	155	89.68	1.73	+	1.99E-10
organelle organization	1529	72	41.88	1.72	+	0.00952
multicellular organismal process	3716	167	101.79	1.64	+	1.07E-09
single-organism cellular process	4942	196	135.37	1.45	+	3.29E-07
single-organism process	6392	229	175.09	1.31	+	4.19E-05
cellular process	6179	218	169.26	1.29	+	0.000783
Unclassified	3088	73	84.59	0.86	-	0

B - Shared genes (present in both - in infected control and infected IdgF3 mutant)

GO biological process complete	#ref	#analyzed	expected	Fold Enrichment	+/-	P value
antibacterial humoral response	30	12	0.4	>5	+	4.96E-11
defense response to Gram-positive bacterium	40	10	0.54	>5	+	7.18E-07
antimicrobial humoral response	76	16	1.02	>5	+	3.75E-11
humoral immune response	95	19	1.28	>5	+	2.88E-13
immune response	197	21	2.65	>5	+	1.26E-09
defense response to other organism	223	19	3	>5	+	7.26E-07
response to external biotic stimulus	287	23	3.86	>5	+	2.85E-08
response to other organism	287	23	3.86	>5	+	2.85E-08
response to biotic stimulus	289	23	3.88	>5	+	3.26E-08
defense response to bacterium	181	14	2.43	>5	+	0.000565
immune system process	290	22	3.9	>5	+	2.31E-07
defense response	331	25	4.45	>5	+	1.19E-08
response to bacterium	201	15	2.7	>5	+	0.000324
response to external stimulus	838	30	11.26	2.66	+	0.00252
response to stress	1038	37	13.95	2.65	+	0.000118
multi-organism process	1251	40	16.81	2.38	+	0.000548
negative regulation of cellular process	1003	31	13.48	2.3	+	0.0321
response to stimulus	2341	61	31.46	1.94	+	0.000249
Unclassified	3088	48	41.5	1.16	+	0

C - genes significantly changed only in infected IdgF3 mutant

GO biological process complete	#ref	#analyzed	expected	Fold Enrichment	+/-	P value
rRNA processing	41	15	1.47	>5	+	1.35E-07
rRNA metabolic process	43	15	1.54	>5	+	2.58E-07
ribosome biogenesis	76	23	2.72	>5	+	4.97E-11
ribonucleoprotein complex biogenesis	113	23	4.04	>5	+	1.36E-07
ncRNA processing	100	18	3.58	>5	+	0.000107
cellular response to starvation	109	16	3.9	4.1	+	0.00819
cellular response to nutrient levels	110	16	3.94	4.06	+	0.00918
cellular response to external stimulus	117	17	4.19	4.06	+	0.00464
cellular response to extracellular stimulus	112	16	4.01	3.99	+	0.0115
ncRNA metabolic process	158	20	5.66	3.54	+	0.00469
response to starvation	159	20	5.69	3.51	+	0.00515
response to nutrient levels	176	20	6.3	3.17	+	0.0226
response to extracellular stimulus	178	20	6.37	3.14	+	0.0266
Unclassified	3088	120	110.53	1.09	+	0

#ref - total number of reference genes annotated for GO process
#analyzed - number of significantly regulated genes
expected - expected number of genes

GSEA of KEGG pathways

logFC cutoff 0.4 (TRUE), Q-VALUE cutoff 0.05

Hypergeometric test, genes deregulated in any direction	KEGG	name	#ref	#analyzed	Q value
Regulated in ctr upon infection (ctr1 x ctr):	dme04914	<i>Progesterone-mediated oocyte maturation</i>	30	13	0.00102
	dme03020	RNA polymerase	20	9	0.0404
Regulated in mutant upon infection (m3i x m3):	dme03008	Ribosome biogenesis in eukaryotes	52	28	5.07E-11

Hypergeometric test, UP-deregulated genes	KEGG	name	#ref	#analyzed	Q value
Regulated in ctr upon infection (ctr1 x ctr):	dme04914	<i>Progesterone-mediated oocyte maturation</i>	30	13	2.42E-05
	dme04310	Wnt signaling pathway	51	17	0.00467
	dme04120	Ubiquitin mediated proteolysis	63	17	0.00988
	dme04630	Jak-STAT signaling pathway	13	6	0.0197
	dme04340	Hedgehog signaling pathway	17	8	0.0197
	dme04320	Dorso-ventral axis formation	16	5	0.0209
Regulated in mutant upon infection (m3i x m3):	dme04512	ECM-receptor interaction	9	4	0.0276
	dme03008	Ribosome biogenesis in eukaryotes	52	28	1.74E-16
	dme03013	RNA transport	79	21	0.000831

Hypergeometric test, DOWN-deregulated genes	KEGG	name	#ref	#analyzed	Q value
Regulated in ctr upon infection (ctr1 x ctr):	dme03020	RNA polymerase	20	9	0.00887
	dme00240	Pyrimidine metabolism	51	15	0.0252
Regulated in mutant upon infection (m3i x m3):					ns

#ref - total number of reference genes annotated for KEGG process and present on Affymetrix microarray

#analyzed - number of significantly regulated genes

ns - no significant results

DAVID gene annotation chart KEGG

ctri x ctr

Category	Term	Count	%	PValue	Genes	Fold Enrichment
KEGG_PATHWAY	dme03020:RNA polymerase	10	0.569476	0.005545	RNA polymerase II 15kD subunit, CG31155, RNA polymerase II 215kD subunit, CG7339, CG11246, CG13773, RNA polymerase II 140kD subunit, CG33051, lethal (2) 37Cg, CG3756	2.807161
KEGG_PATHWAY	dme04310:Wnt signaling pathway	19	1.082005	0.005608	Ras-like GTP-binding protein Rho1, Smad on X, nejire, wingless, Van Gogh, seven in absentia, nemo, shifted, cAMP-dependent protein kinase 3, F-box-like/WD repeat-containing protein ebi, division abnormally delayed, Calcineurin B2, no receptor potential A, microtubule star, CG2185, arrow, APC-like, RING-box protein 1B, naked cuticle	1.946046
KEGG_PATHWAY	dme04630:Jak-STAT signaling pathway	8	0.455581	0.007743	Suppressor of cytokine signaling at 36E, hopscotch, nejire, Signal-transducer and activator of transcription protein at 92E, CG4141, Son of sevenless, CG7037, Suppressor of Cytokine Signaling at 16D	3.191299
KEGG_PATHWAY	dme00310:Lysine degradation	10	0.569476	0.01184	CG7144, CG9149, grappa, Glycosyltransferase 25 family member, Probable histone-lysine N-methyltransferase CG1716, CG9629, Histone-lysine N-methyltransferase pr-set7, Probable histone-lysine N-methyltransferase Mes-4, CG2995, Histone-lysine N-methyltransferase Suv4-20	2.526445
KEGG_PATHWAY	dme04120:Ubiquitin mediated proteolysis	22	1.252847	0.011878	CG6303, Elongin C, CG8711, CG5087, CG3356, CG10254, seven in absentia, CG8610, courtless, Ubiquitin conjugating enzyme 10, DNA damage-binding protein 1, CG2508, CG7037, morula, Ubiquitin conjugating enzyme, Probable E3 ubiquitin-protein ligase HERC2, abnormal oocyte, imaginal discs arrested, CG6759, guftagu, RING-box protein 1B, Anaphase Promoting Complex 4	1.719025

KEGG_PATHWAY	dme00240:Pyrimidine metabolism	19	1.082005	0.013043	Ribonucleoside diphosphate reductase large subunit, CG31155, mutagen-sensitive 201, CG8891, CG4827, CG13773, Probable deoxycytidylate deaminase, CG3756, RNA polymerase II 15kD subunit, Probable uridine-cytidine kinase; Uridine kinase, DNA polymerase epsilon, diadenosine tetraphosphate hydrolase, RNA polymerase II 215kD subunit, CG7339, CG11246, RNA polymerase II 140kD subunit, lethal (2) k01209, CG33051, lethal (2) 37Cg	1.800092
KEGG_PATHWAY	dme04914:Progesterone-mediated oocyte maturation	12	0.683371	0.013646	Cyclin B3, Bub1-related kinase; Bub1 homologue, Serine/threonine-protein kinase polo, Mitogen-activated protein kinase 14B, imaginal discs arrested, CG4141, CG8610, CG6759, cAMP-dependent protein kinase 3, CG2508, Anaphase Promoting Complex 4, morula	2.218342
KEGG_PATHWAY	dme04320:Dorso-ventral axis formation	9	0.512528	0.014841	cappuccino, encore, anterior open, egghead, Protein giant-lens, spire, squid, pointed, Son of sevenless	2.623616
KEGG_PATHWAY	dme04340:Hedgehog signaling pathway	8	0.455581	0.0298	discs overgrown, costa, wingless, decapentaplegic, cAMP-dependent protein kinase 3, fused, CG34352, cubitus interruptus	2.526445

m3i x m3

Category	Term	Count	%	PValue	Genes	Fold Enrichment
				ns		

ns - nothing significant

settings of analyses: counts = 2, p < 0.05

Genes with q < 0.05 counted as significant

Table S5. List of primers used in real-time RT-PCR.

Primer name	Sequence
rp49 fw	CTTCATCCGCCACCAGTC
rp49 rev	GGCGACGCACTCTGTTGT
Idgf3 fw	GATCTGCTGCTCAGTCTCACC
Idgf3 rev	TCGACGGGGGCATCATAGTA

Table S6. Genotypes and treatments of the lines used for the array study.

#	Name	Abbreviation	Genotypes	Infected by EPN*
1	Control	ctr	<i>w; Idgf3^{LL}/+; UAS-Idgf3-myc/+</i>	N
2	EPN infection in control	ctri	<i>w; Idgf3^{LL}/+; UAS-Idgf3-myc/+</i>	Y
3	Idgf3 mutant	m3	<i>w; Idgf3^{LL}/dac⁷; UAS-Idgf3-myc/+</i>	N
4	EPN infection in Idgf3 mutant	m3i	<i>w; Idgf3^{LL}/dac⁷; UAS-Idgf3-myc/+</i>	Y

* EPN infection lasts for 2 hours, larvae were analyzed 6 hours post infection.

4.3. Publication III

Jana Fleischmannova, Lucie Kucerova, Katerina Sandova, Veronika Steinbauerova, Vaclav Broz, Petr Simek and Michal Zurovec (2012) **Differential response of Drosophila cell lines to extracellular adenosine**. *Insect Biochemistry and Molecular Biology* 42: 321-331

Abstract:

Adenosine (Ado) is a crucial metabolite that affects a wide range of physiological processes. Key proteins regulating Ado signaling, transport and metabolism are conserved among vertebrates and invertebrates. It is well known that Ado influences proliferation of several vertebrate and invertebrate cells. Here we show that Ado negatively influences viability, changes morphology and mitochondrial polarity of the *Drosophila* imaginal disc cell line (Cl.8+) via a mechanism exclusively dependent on cellular Ado uptake. High transport of Ado is followed by phosphorylation and ATP production as a part of Ado salvation, which at higher concentrations may interfere with cellular homeostasis. In contrast, hematopoietic cell line Mbn2, which grows well in high Ado concentration, preferentially uses adenosine deaminase as a part of the purine catabolic pathway. Our results show that different types of *Drosophila* cell lines use different pathways for Ado conversion and suggest that such differences may be an important part of complex mechanisms maintaining energy homeostasis in the body.



Differential response of *Drosophila* cell lines to extracellular adenosine

Jana Fleischmannova^a, Lucie Kucerova^{a,b}, Katerina Sandova^b, Veronika Steinbauerova^b,
Vaclav Broz^{a,b}, Petr Simek^b, Michal Zurovec^{a,b,*}

^a Faculty of Sciences, Univ. of South Bohemia, Ceske Budejovice, Czech Republic

^b Biology Centre AS CR, Branisovska 31, 370 05 Ceske Budejovice, Czech Republic

ARTICLE INFO

Article history:

Received 1 December 2011

Received in revised form

31 December 2011

Accepted 2 January 2012

Keywords:

Adenosine recycling

Nucleoside transport

Mbn2

Cl.8+

ATP synthesis

CG11045

CG11778

CG8083

CG11255

ABSTRACT

Adenosine (Ado) is a crucial metabolite that affects a wide range of physiological processes. Key proteins regulating Ado signaling, transport and metabolism are conserved among vertebrates and invertebrates. It is well known that Ado influences proliferation of several vertebrate and invertebrate cells. Here we show that Ado negatively influences viability, changes morphology and mitochondrial polarity of the *Drosophila* imaginal disc cell line (Cl.8+) via a mechanism exclusively dependent on cellular Ado uptake. High transport of Ado is followed by phosphorylation and ATP production as a part of Ado salvation, which at higher concentrations may interfere with cellular homeostasis. In contrast, hematopoietic cell line Mbn2, which grows well in high Ado concentration, preferentially uses adenosine deaminase as a part of the purine catabolic pathway. Our results show that different types of *Drosophila* cell lines use different pathways for Ado conversion and suggest that such differences may be an important part of complex mechanisms maintaining energy homeostasis in the body.

© 2012 Elsevier Ltd. All rights reserved.

1. Introduction

Adenosine (Ado) affects a remarkable variety of key physiological processes in mammals, such as the rate of blood flow in the heart, skeletal muscle and brain, rate of lipolysis in adipose tissue and neurotransmission in the brain (Fredholm et al., 2011). Ado is capable of protecting tissues from ischemia-reperfusion injury, thrombosis and atherosclerosis and plays an important role in promoting wound healing and tissue repair (Burnstock, 2011; Feoktistov et al., 2009). A number of reports also indicated its general immunosuppressive and anti-inflammatory function (Ohta and Sitkovsky, 2009). Extracellular adenosine (Ado) also influences energy homeostasis and cell growth (Aymerich et al., 2006; Porkka-Heiskanen and Kalinchuk,

2011); however, the mechanism of Ado action on cell physiology has not been studied in detail despite its importance for understanding the cell type specific mechanisms underlying maintenance of metabolic homeostasis.

Physiological concentrations of Ado are relatively low (0.06–0.3 μ M in *Drosophila* and 0.05–0.4 μ M in human), however its concentration may locally increase to micromolar range under stressful conditions (Dolezelova et al., 2005; Matherne et al., 1990; Van Belle et al., 1987). Elevated concentration of extracellular Ado is connected to many serious diseases including congenital immunodeficiency, diabetic complications, lung inflammation and asthma (Ponnoth and Jamal Mustafa, 2011; Sakowicz-Burkiewicz et al., 2006; Sauer and Aiuti, 2009). *In vitro*, excessive extracellular Ado has been reported to negatively influence cell growth and cause cell death in several vertebrate as well as invertebrate cell lines (Ohana et al., 2001; Zurovec et al., 2002).

Ado physiological and pathophysiological roles are mediated mainly by the activation of specific G protein-coupled receptors. Four Ado receptors from the G protein-coupled receptor superfamily (A1, A2A, A2B, A3) are present in mammals recruiting different G protein subunits (G_{α} , $G_{i/o}$, G_q) (Hasko and Cronstein, 2004). A1 and A2A high-affinity receptor isoforms seem to be physiologically relevant, whereas low-affinity receptor isoforms

Abbreviations: Ado, adenosine; CHA, cyclohexyladenosine; Dipy, dipyrindamole; Itu, 5-iodotubercidine; CM, complete medium; MM, minimal medium; H3-Ado, tritium labeled adenosine; C14-Uro, radioactive labeled uridine; Ino, inosine; Uro, uridine; Guo, guanosine; ADGF, adenosine deaminase growth factor; Adk, adenosine kinase; MSI, Male-specific insect derived growth factor.

* Corresponding author. Biology Centre AS CR, Branisovska 31, 370 05 Ceske Budejovice, Czech Republic. Tel.: +420 387775283; fax: +420 385310354.

E-mail address: zurovec@entu.cas.cz (M. Zurovec).

A2B and A3 could play a crucial role under pathological (e.g. inflammatory) conditions (Nyce, 1999).

As mentioned above, under stressful conditions, such as hypoxia or hypercapnia, extracellular Ado levels dramatically raise up to μM concentrations (Linden, 2001) by the action of 5'-nucleotidases (EC 3.1.3.5) or ecto-phosphodiesterase (EC 3.1.4.1) that convert adenosine nucleotides (ATP, cAMP) released from cells to Ado (Fredholm et al., 2011; Jackson et al., 2007). Alternatively, Ado is formed intracellularly by sequential dephosphorylation of Ado nucleotides. The steady-state extracellular concentration of Ado is maintained by the rate of its production in the extracellular and/or intracellular space, and its reutilization for ATP synthesis (salvage pathway) due to rephosphorylation or catabolism by Ado deaminases (EC 3.5.4.4) to inosine and hypoxanthine.

Ado salvage pathway has a major impact for energy conservation because of the high energy requirements of Ado *de novo* synthesis. Key players of extracellular Ado recycling are nucleoside membrane transporters and Ado kinase (EC 2.7.1.20) rephosphorylating Ado to AMP (Park and Gupta, 2008). In most tissues and animals investigated, the K_m values of Ado kinase for Ado are between one and two orders of magnitude lower than those for the deaminase allowing effective Ado recycling under conditions of low extracellular Ado concentration (Arch and Newsholme, 1978).

Nucleoside membrane transport is mediated by two types of specialized transporter systems. Equilibrative nucleoside transporters facilitate the diffusion of nucleosides down their concentration gradient. High affinity concentrative nucleoside transporters can transport nucleosides into cytoplasm even against concentration gradient by co-transport of Na^+ (King et al., 2006). All equilibrative (Ent1–4 in mammals) and concentrative nucleoside transporters (Cnt1–3 in mammals) are able to effectively transport Ado and thus contribute to Ado signaling regulation. Moreover, it has recently been shown that nucleoside transporters might play important role in cellular metabolism independent of Ado receptor signaling (Huber-Ruano et al., 2010).

Ado functions seemed to have been highly conserved during evolution; genes encoding Ado receptor (*DmAdoR*), ecto-5-nucleotidases, Ado deaminases (*ADGF A-E*, *DmADA*, *MSI*), three equilibrative (*DmEnt1-3* - CG11907, CG11045, CG11010) and two concentrative nucleoside transporters (*DmCnt1*, 2 - CG11778, CG8083) and three putative Ado kinases (*DmAdk1-3* - CG3809, CG11255, CG1851) have been found in the fruit fly genome (Dolezal et al., 2003; Dolezelova et al., 2007; Fencikova et al., 2011; Sankar et al., 2002). Characterization of mutants in genes encoding *DmAdoR*, *DmEnt2* and *Drosophila* Ado deaminases revealed surprising conservation of Ado roles in mammals and the fruit fly, including the regulation of neuromuscular junction, memory, energy homeostasis and cell growth (Dolezal et al., 2005; Knight et al., 2010; Zuberova et al., 2010). Phenotypes of both *ADGF-A* and *DmEnt2* mutants indicate involvement of Ado in regulation of energy homeostasis via *DmAdoR*-dependent as well as independent mechanisms (mutant phenotypes can be only partially rescued by *DmAdoR* mutation) (Dolezal et al., 2005; Knight et al., 2010). The presence of alternative Ado metabolic mechanisms and tissue specificity of Ado action make the understanding of Ado roles *in vivo* difficult even in *Drosophila melanogaster*, a model organism with lower complexity of Ado regulation than mammals. In this study, we show that different types of *Drosophila* cell lines may significantly differ by their ability to reutilize Ado which has a dramatic effect on their energy homeostasis. We show that Cl.8+ cells are very effective in Ado recycling, however when the extracellular Ado concentration exceeds the physiological range it influences their viability, morphology, and mitochondrial polarity.

2. Material and methods

2.1. Reagents

Cell culture chemicals including cell culture media, insulin and antibiotics, as well as nucleosides, nucleotides, cyclohexyladenosine (CHA), dipyrindamole (Dipy), and iodotubercidine (Itu) were purchased from Sigma Aldrich CO (St. Louis, USA). Fetal bovine serum (FBS, cat. number 16140071) was purchased from Invitrogen (San Diego, CA, USA). [2,8- ^3H]-Ado (12.8 Ci/mmol) (H3-Ado) and [2- ^{14}C]-Uridine (50 mCi/mmol) (C14-Uro) were purchased from Moravsek Biochemicals (Brea, USA).

2.2. Cell culture

Drosophila imaginal disc cells (Cl.8+) and hematopoietic Mbn2 cells (Samakovlis et al., 1992) were used for the experiments. Cl.8+ cells were maintained in complete medium (CM), which was Shields and Sang medium (Shields and Sang, 1970), (Sigma Aldrich CO, catalog no. S 8398) supplemented with 2% FBS, 2.5% fly extract (Cullen and Milner, 1991), 125 U/l insulin, 1% penicillin/streptomycin (10000 U/10 mg). Cells were passaged every 2 days (without trypsinization) by transferring one quarter of the suspended cells to fresh medium (at approx. cell density $4 \times 10^5/\text{ml}$). Confluent cells at 90–110 passages after cell line initiation were used for all experiments.

Mbn2 cells were maintained in Shields and Sang medium supplemented with 10% FBS, 125 U/l insulin, 1% penicillin/streptomycin (10000 U/10 mg). Cells were passaged every 3 days.

Minimal medium (MM) used for experiments was Shields and Sang medium (prepared from Sigma cell culture tested grade chemicals) supplemented with 1% penicillin/streptomycin (1000 U/mg) and 125 U/l insulin, without FBS, fly extracts and yeast extracts. The supplements were omitted in order to keep the cells in chemically defined conditions (yeast extracts are rich source of Ado and dAdo, fly extracts and serum are sources of adenosine deaminases).

2.3. Proliferation rate analysis

Cells were plated at $4 \times 10^5/\text{ml}$ in MM/CM and treated as appropriate with nucleosides or other drugs. Cell proliferation was measured by directly counting the cells on digital photographs of identical areas taken every 24 h during a period of 3 days. Three replica plates, one field per plate, were evaluated.

2.4. TUNEL assay

The cells were exposed for 16 h to various Ado concentrations. After the treatment, Fluorescein-dUTP TUNEL assays were performed according to the manufacturer's directions (In Situ Cell Death detection kit, Fluorescein, Roche, Basel, Switzerland). The cells were fixed in 4% paraformaldehyde for 1 h at room temperature, permeabilized in 0.1% Triton X-100, and then incubated with TUNEL reaction mix 1 h at 37 °C in the dark.

2.5. TMRE mitochondrial staining

After the cells were treated with 30–100 μM Ado, Cl.8+ cells were incubated with 600 nM tetramethyl rhodamine ethyl ester (TMRE, Molecular Probes, Eugene, USA) for 30 min at 37 °C in culture medium. The dye was taken up by mitochondria and the mitochondrial staining was analyzed by flow cytometry. At least 10000 events were used for analysis.

2.6. Real-time RT-PCR

Total RNA from Cl.8+ and Mbn2 *Drosophila* cells was isolated using RNA Blue (Top-Bio, Prague, Czech Republic) and subsequently cleaned with NucleoSpin RNA II kit (Macherey–Nagel, Duren, Germany) including on-column digestion step with rDNase I. 1,000 ng of total RNA was applied for reverse transcription using PrimeScript Reverse Transcriptase (Takara) and oligo(dT) (17-mer). The obtained cDNA was diluted and used for the Syber Green PCR reaction in triplets. Each 20 μ l PCR reaction contained: Hot start ExTaq polymerase (Takara) 0.75 unit, ExTaq buffer 1x, dNTPs 200 μ M each, Syber green 1:25,000, primers 400 nM each. The amplification was carried out on a Rotor-Gene 3000 (Corbet Research, Sydney, Australia) for 40 or 50 cycles (94 °C for 20 s; 60 °C [62 °C for *DmAdoR*] for 30 s; 72 °C for 30 s) following an initial denaturation/Taq activation step (95 °C for 2 min). Primers (Table S1) were designed with Lasergene Primer Select Software (DNASTAR, Madison, USA) to assure that all amplicons are situated in a comparative distance from the end of transcription (1 kb maximum) so the effect of reverse transcription efficiency can be excluded from our results. The amplicons encompassed exon/intron boundary with the exception of *DmEnt3*, whose introns are too distant from the transcription end/polyA tail. Amplified product specificity was confirmed by melting analysis. Data were analyzed and quantified with the Rotor-Gene 6 analysis software. Relative values were either standardized to *DmRack1* gene or standardized to *DmRack1* and normalized to the *DmAdoR* expression level in Cl.8+ cells (Pfaffl, 2006). All results are presented with means and SEM from 2 independent biological samples.

2.7. Ado and Uro uptake assay

Cells were seeded at 5×10^5 /ml and cultured overnight. Fresh MM containing 2 μ Ci H3-Ado with unlabeled Ado at appropriate concentration was added to the cells. After incubation, cells were extensively washed in fresh MM and lysed in 1 M NaOH. Samples were neutralized using 5 M HCl, mixed with Triton/toluene/POPOP scintillation cocktail and the radioactivity was measured with a Packard 1500 TriCarb β -Counter.

To determine equilibrative Ado transport sodium-free MM was used with glutamic acid K⁺ salt and K₂HPO₄ instead of their corresponding Na⁺ salts. For competition experiments unlabeled nucleosides (Ino, Uro, Guo) at 10, 50, and 200 μ M concentration were added to 10 μ M labeled Ado. For inhibition experiments, 20 min pre-treatment with Dipy (1–20 μ M) was applied before addition of 10 μ M Ado.

For Uro transport measurements, different concentrations of Uro (labeled with 2.5 μ Ci of C14-Uro) were assayed for 1 h as described above for Ado transport. To see the effect of Ado on Uro transport, various Uro concentrations were assayed together with 50 μ M Ado.

2.8. RNA interference

RNA interference (RNAi) approach was applied to silence expression of selected Ado signaling and metabolism genes. PCR primers were designed and about 400 nt fragments were amplified from a single exon using genomic DNA template or from a cDNA of genes involved in Ado metabolism and signaling (for primers see Table S2). The fragments were subcloned into pGemTeasy plasmids (Promega, Madison, USA). The clones were used as templates for synthesis of plus and minus RNA strands *in vitro* by using MEGAscript[®] T7 Kit (Ambion, Leicestershire, UK). After annealing and checking the quality of dsRNA, these molecules were transfected into the Cl.8+ cells by using transfection

protocol of Lum et al. (2003). The cells were incubated in CM overnight and then treated with 40 μ M Ado for 16 h. The percentage of cells with characteristic elongated cell shape and pseudopodia was calculated from the digital photographs of identical areas (0.8 \times 0.8 mm). *DmCht5* gene that is not connected with Ado signaling or metabolism and mock transfected cells without Ado treatment were used as positive and negative controls, respectively.

2.9. Ado incorporation assay

5×10^5 cells were incubated overnight in MM, supplemented with 100 μ M Ado labeled with 10 μ Ci H3-Ado. After 2 h, cells were washed two times in PBS, lysed in liquid nitrogen and nucleosides and nucleotides were extracted with ice-cold acetonitrile 4:1, (v/v) and separated by HPLC coupled with a UV (254 nm) and electro-spray mass spectrometric detection as described earlier (Zuberova et al., 2010). Elution time of each compound was estimated by means of a standard solution mixture containing Ado, Ino, AMP, ADP, and ATP. From each cell lysate, particular fractions of the Ino (3.17 min), AMP (8.81 min), ADP (11.36 min), and ATP (12.96 min) peaks were collected manually after their elution from HPLC and their radioactivity was measured as described in the Ado uptake experiments (see 2.7).

2.10. ATP assay

ATP was measured by The CellTiter-Glo[®] Luminescent Cell Viability Assay (Promega, Madison, USA) according to manufacturer's directions. Cells (100 μ l aliquots at a concentration of 5×10^5 /ml) were seeded on 96-well plates and incubated overnight in the presence of different concentrations of Ado in CM. After cultivation, equal volume of CellTiter-Glo reagent was added and luminescence in cell lysates was detected by Luminometer Orion II (Berthold Technologies, Bad Wildbad, Germany).

2.11. Statistical analysis

All data are presented as means \pm SDs of 3 independent experiments (excerpt for RT-PCR analysis, which was performed with two independent biological samples and the results are presented as means \pm SEM). *T*-test or one-way analysis of variance (ANOVA) followed by a post hoc test were used for statistical evaluation of the data.

3. Results

3.1. Effect of Ado on Cl.8+ cell proliferation and survival

We have reported earlier that high concentration of Ado in growth media may be toxic for some *Drosophila* cells, including imaginal disc cell line - Cl.8+ (Zurovec et al., 2002). In this study, we further characterized mechanism of Ado toxicity in Cl.8+ cells. First we re-evaluated the effect of Ado on cell proliferation and apoptosis under different growth conditions. Ado dose proportionally decreased growth rate of the Cl.8+ cells (Fig. 1a,b), changed their typical elongated fibroblast-like cell shape to round cells (Fig. 2a, upper row) and at higher concentrations induced cell death. In MM, 10 μ M Ado substantially decreased cell growth rate (Fig. 1a) while concentrations higher than 100 μ M caused cell death. No significant increase in the number of apoptotic cells was detected after treatment with 30 μ M Ado (Fig. 2a, lower row), whereas the cells treated overnight with 100 μ M Ado showed reduced mitochondrial polarity (visualized by marked decrease of mitochondrial TMRE staining; Fig. 2b), typical apoptotic DNA fragmentation and the

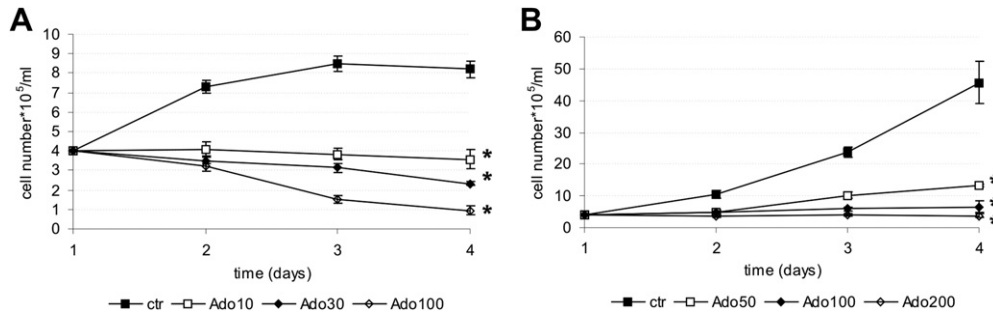


Fig. 1. Ado concentration-dependent decrease in proliferation rate of Cl.8+ cells grown in MM (A) and CM (B). Cells were incubated without Ado or with various Ado concentrations for 3 days. Cell numbers in defined areas were counted every 24 h. Values represent means \pm SD from three independent experiments. * $P < 0.05$ for whole data series compared with Ado untreated cells by Tukey's test.

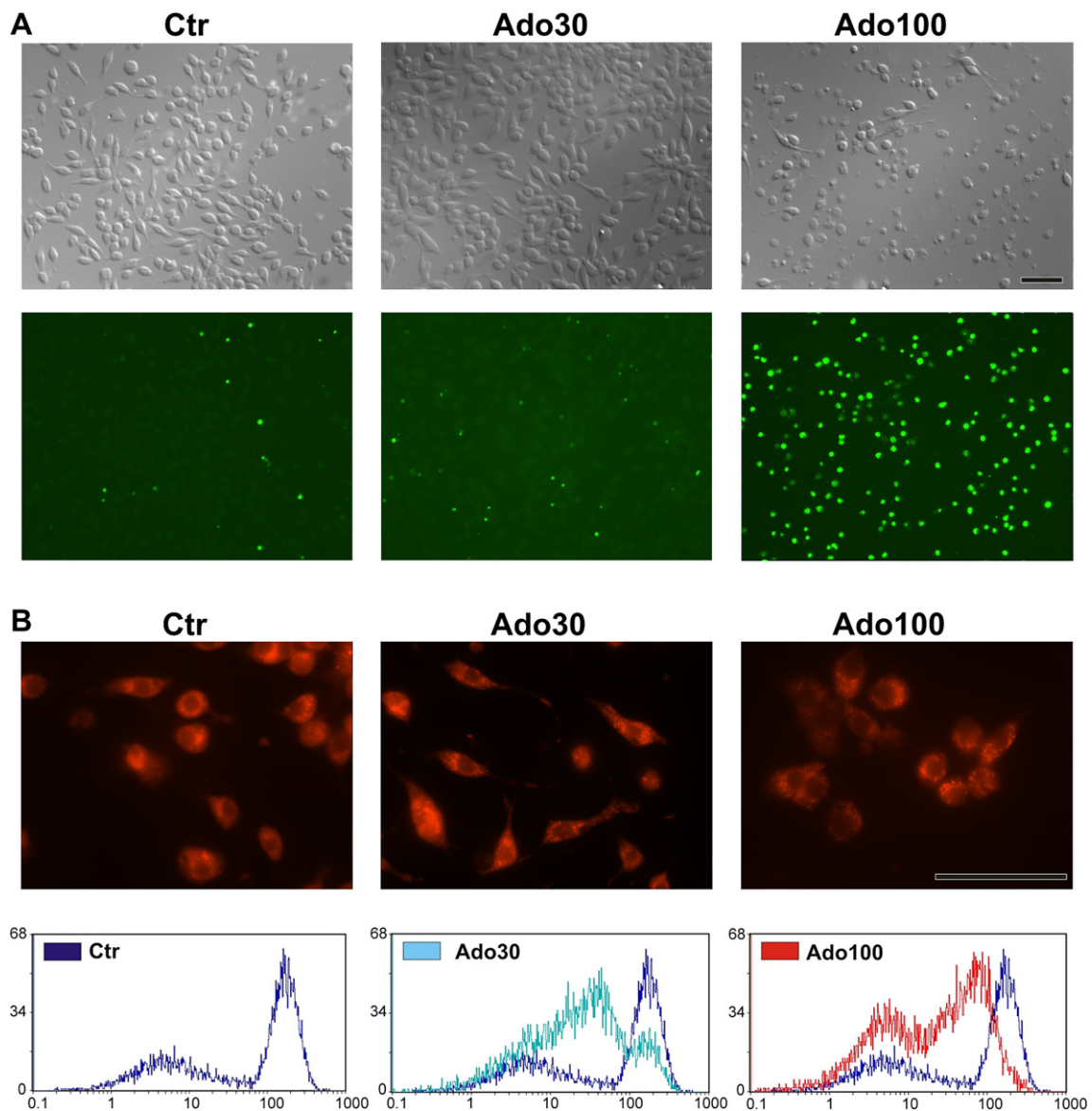


Fig. 2. Ado effect on cell morphology and apoptosis in Cl.8+ cells. Cells were treated with 30 or 100 μ M Ado in MM overnight. (A) Ado changed the typical fibroblast like morphology of Cl.8+ cells to round shape, decreased proliferation rate (upper row) and increased numbers of TUNEL positive cells (lower row) as documented on the micrographs. (B) Ado effect on mitochondrial membrane polarity visualized by decreased mitochondrial TMRE staining on micrographs (upper row) and flow cytometry plots (lower row). The channel number is shown on the x axis and the number of events on the y axis. ctr – control cells without Ado treatment, Ado30 – cells treated with 30 μ M Ado, Ado100 – cells cultured with 100 μ M Ado, bar 100 μ m.

partitioning of cytoplasm and nucleus into membrane bound-vesicles (apoptotic bodies) within 24–48 h. In CM (containing FBS, yeast extract, fly extract, and insulin), higher Ado doses were needed to inhibit cell proliferation (Fig. 1b) and the onset of cell death was substantially delayed. Only a minor decrease in TMRE staining was observed even after overnight cultivation with 200 μ M Ado probably because of presence of Ado deaminases in the media supplements.

3.2. Activation of *DmAdoR* in *Cl.8+* cells is not responsible for Ado growth inhibitory effect

Growth inhibitory effect of Ado may result from the activation of specific receptors or its uptake into the cytoplasm via nucleoside transporters respectively (Ohkubo et al., 2007). Specific pharmacological agents were exploited to distinguish between the receptor- and uptake- dependent Ado effect. A potent agonist of *DmAdoR* - cyclohexyladenosine (CHA) - that has been proven previously to activate cAMP response in *Drosophila* cells (data not shown) - was applied to the cells to see if it can mimic the Ado effect. The cells treated with 100 μ M CHA showed no difference in their growth rate compared to untreated control cells (Fig. 3a).

To further confirm that the effect of Ado is not mediated by *DmAdoR*, we reduced its expression using RNA interference and evaluated the effect of *DmAdoR* knock-down on the sensitivity of *Cl.8+* cells to Ado. Silencing of *DmCht5* and mock transfected cells without Ado treatment were used as positive and negative control, respectively. Proportion of cells lacking typical Ado-dependent morphological change (“healthy cells”) after 16 h cultivation with 40 μ M Ado was determined. In positive control cells with silenced *DmCht5* expression, Ado treatment decreased percentage of “healthy” cells to 16% of the non-treated mock transfected control cells. In agreement with CHA treatment, *DmAdoR* gene knock-down did not increase the percentage of “healthy” cells after Ado treatment (Fig. 3b).

3.3. Characterization of Ado transport in *Cl.8+* cells

The negative results of *DmAdoR* function elimination on Ado toxicity suggested that the effect of Ado might be uptake dependent. *Cl.8+* cells showed relatively high expression of *DmEnt2* and *DmEnt1* (Fig. 4a) and were able to transport significant amounts of Ado from the extracellular space to the cytoplasm. The uptake of H3-Ado (5–50 μ M) increased in time- (0–60 min interval) and concentration-dependent manner (Fig. 4b,c).

We investigated whether both concentrative and equilibrative transporters contribute to the total Ado uptake. The uptake of 10 μ M Ado was inhibited in direct proportion to the concentration of Dipy, a known inhibitor of equilibrative Ado transport in mammals. Maximum 70% inhibition was observed after treatment with 10 μ M Dipy (Fig. 4d). Involvement of concentrative Ado transport was tested in medium where Na^+ containing chemical components, mainly Na^+ glutamate and Na^+ phosphate, were replaced by their K^+ counterparts (see Material and Methods) to inhibit sodium-dependent concentrative nucleoside transporters. The level of Ado uptake in sodium-free medium (containing 90 mM K^+) ranged from 76 to 46% depending on the applied Ado concentration (Fig. 4e).

Since mammalian nucleoside transporters are known to transport broad spectrum of purine as well as pyrimidine nucleosides or nucleobases, we tested if common metabolites Ino, Uro, and Guo compete with Ado transport. Interestingly, even 20 times higher concentrations of these nucleosides did not inhibit transport of 10 μ M Ado (Fig. 4f). This indicates that Ado transport into *Cl.8+* cells is mediated via equilibrative and concentrative transporters not affected by other nucleosides.

3.4. Inhibition of Ado uptake rescues the Ado toxicity

To test if blocking of equilibrative Ado transport would be able to rescue the Ado-mediated growth arrest, Dipy was applied to the Ado treated cells in a concentration that maximally inhibited Ado uptake into cells. After 24 h, 10 μ M Dipy completely rescued growth inhibitory effect of 100 μ M Ado (Fig. 5a).

A presumed involvement of concentrative Ado transporters in Ado toxicity was tested in a medium with reduced Na^+ concentration. With respect to proliferation, *Cl.8+* cells tolerated a decrease in Na^+ concentration up to approximately 50% (approx. 60 mM K^+ , low sodium medium). When we applied Ado to the cells in the low sodium medium for 24 h, we observed partial rescue of the cell morphology (50 μ M Ado) without any beneficial effect on the cell growth rate (Fig. 5b,c).

RNA interference approach (as described in Section 3.2) was applied to further investigate the role of particular nucleoside transporters. RNA silencing of *DmEnt2*, and both *DmCnts* caused a significant increase in the number of healthy cells after an overnight 40 μ M Ado treatment compared to cells with silenced *DmCht5* gene. The silencing of Na^+ cotransporter *DmCnt1* (CG11778) showed almost complete rescue (98% cells with healthy morphology compared to negative control) followed by transporters *DmCnt2* CG8083 (75%) and *DmEnt2* (60%) (Fig. 5d).

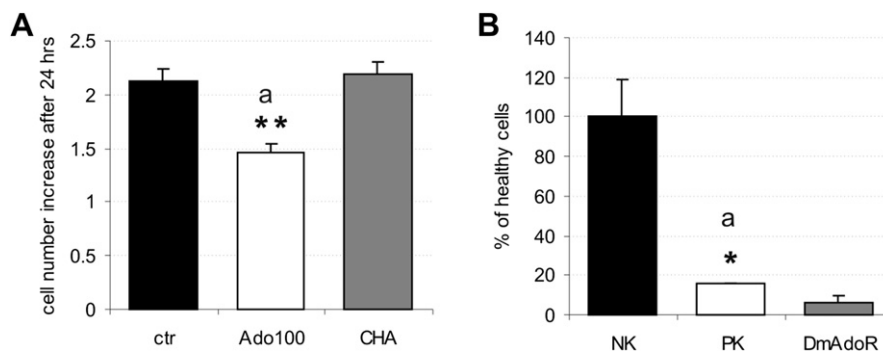


Fig. 3. Effect of pharmacological and genetic ablation of *DmAdoR* on Ado toxicity in *Cl.8+* cells. (A) Increase in cell number after 24 h after treatment with 100 μ M Ado and a previously characterized potent *DmAdoR* agonist CHA (100 μ M). (B) Rescue of cell morphology by RNAi. Cells were transfected with dsRNA fragments designed to silence *DmAdoR* expression. Data are expressed as a percentage of cells with Ado unaffected morphology (“healthy cells”) compared to mock transfected control. NK - mock transfected control without Ado treatment, PK - *DmCht5* transfected cells treated with Ado. * $P < 0.05$, ** $P < 0.01$, a – compared to NK.

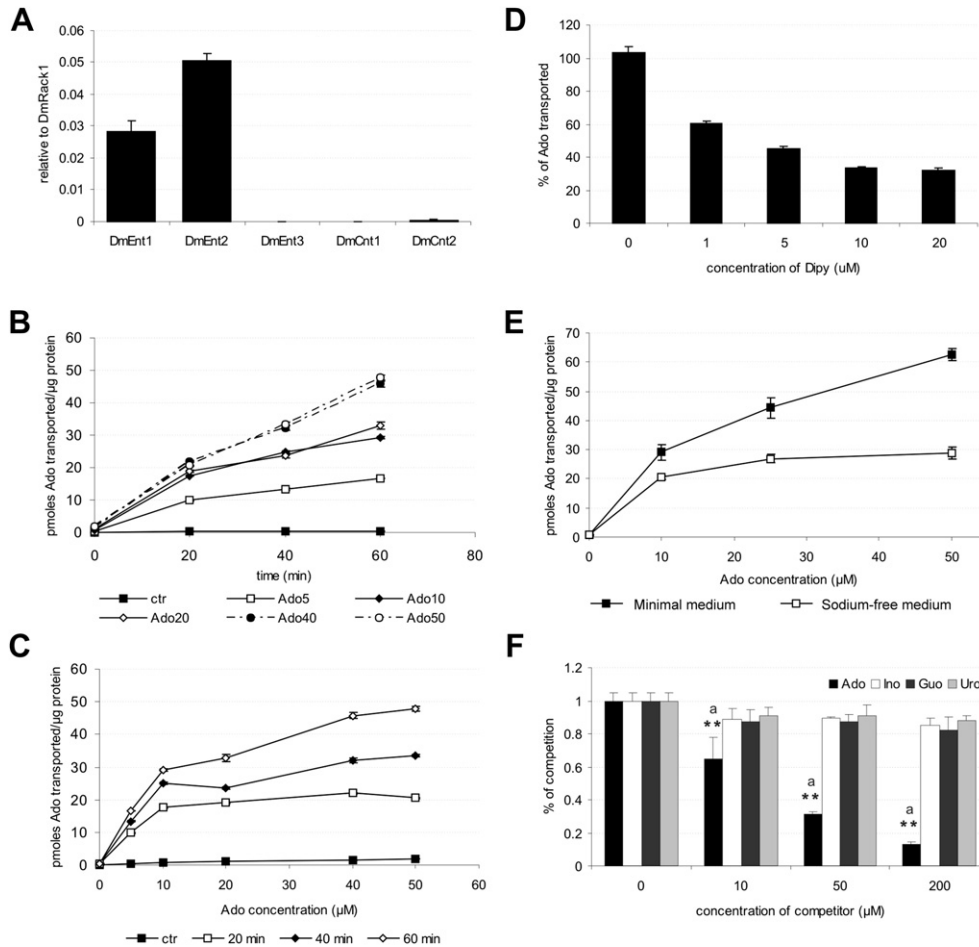


Fig. 4. Characterization of Ado uptake in Cl.8+ cells. (A) Expression of nucleoside transporters in Cl.8+ cells quantified by real time RT-PCR, relative expression values were standardized to *DmRack1* gene expression. (B) Time and (C) concentration dependency of Ado uptake into Cl.8+ cells. Cells were incubated with different concentrations of Ado (5–50 μM) for 20, 40 and 60 min. (D) Ado transport was inhibited by Dipy depending on the dose. The cells were treated with different Dipy concentrations and the uptake of 10 μM H3-Ado was measured as described in Materials and Methods. The data represent the relative uptake expressed in percent of the control 10 μM Ado transport with 0.05% DMSO. (E) Involvement of concentrative nucleoside transport in Ado uptake. Corresponding Ado concentrations were added to the cells in minimal and sodium-free medium, respectively and H3-Ado uptake was measured after 1 h. (F) Competition of Ado uptake by other nucleosides. Cells were incubated with 10 μM H3-Ado in the presence of different concentrations of other nucleosides (10–200 μM) with Ado used as control. Data are present as a decrease in Ado uptake compared to the control 10 μM Ado. Unless otherwise specified, all data are present as the amount of pmoles transported to the cytoplasm per μg of protein. Values are presented as means \pm SD of three independent experiments. $^{**}P < 0.01$, a – compared to control.

3.5. Ado uptake correlates with the increase of cellular ATP pool

In order to follow the metabolic fate of the H^3 -labeled Ado taken up into the Cl.8+ cells, we examined the distribution of the radioactive label in fractions corresponding to Ino, AMP, ADP, and ATP separated by HPLC. Radioactively labeled Ado (10 μCi , 100 μM) was added into the growth medium and the cells were incubated for 2 h and lysates than separated with HPLC. Our data showed that radioactivity predominantly accumulated in the fractions corresponding to Ino and ATP, both representing about the same radioactive label portion (44 and 42%, respectively). The amount of radioactivity in the AMP and ADP fractions was below 10% (Fig. 6a).

Detailed kinetics of Ado-dependent ATP production was measured by bioluminescent ATP kit that allowed simple and rapid non-radioactive quantification of ATP amount in cells compared to HPLC separation. Cells were cultured with different Ado concentrations (50, 100, 200 μM) for 1–12 h. Both dose and time dependent massive accumulation of ATP was observed in the initial 3–6 h interval resulting in up to 9x increase of ATP level in the case of 200 μM Ado treatment. Elevated level of ATP was maintained for at least 12 h (Fig. 6b). The concentration of ATP was directly

proportional to the dose of Ado over a wide range of concentrations suggesting the importance of Ado salvage in this cell type.

3.6. The Ado effect on Cl.8+ cells is rescued by Ado kinase inhibition but not by high Uro concentration

To further confirm the role of intracellular Ado phosphorylation in its toxicity, we applied a known inhibitor of Ado kinase, Itu, to the Ado treated cells. After 24 h, the number of cells cotreated with Itu and Ado was significantly higher than the number of Ado treated cells, and was similar to the control (Fig. 7b). RNAi experiments performed with constructs designed to silence all three *Drosophila* genes coding for proteins with Ado kinase activity (CG3809, CG11255, CG1851) revealed that the most abundant Ado kinase CG11255 was responsible for the Ado toxicity in Cl.8+ cells (Fig. 7a,c).

Excessive phosphorylation of Ado has been reported previously to interfere with *de novo* synthesis of pyrimidines that may result in growth arrest or even cell death (Ohkubo et al., 2007). Ado-induced pyrimidine starvation is reportedly possible to overcome by media supplementation with an alternative source of pyrimidines, such as

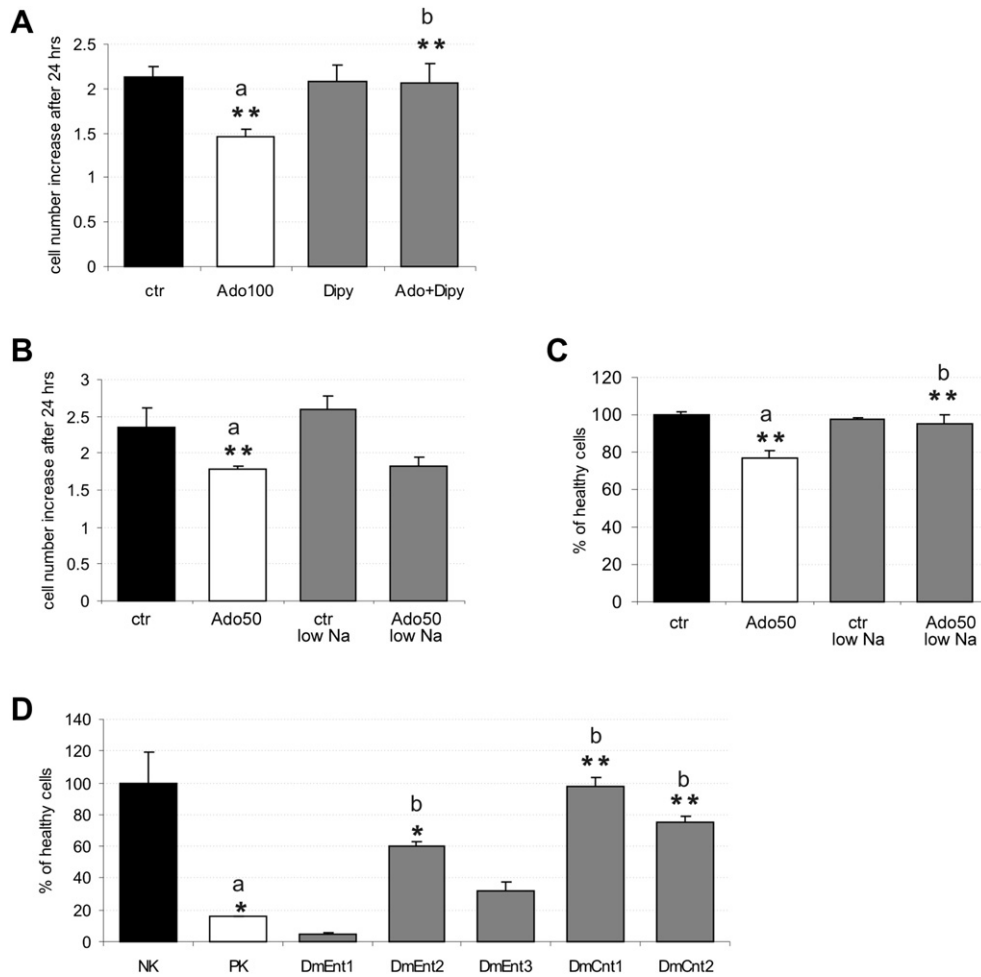


Fig. 5. Effect of pharmacological and genetic ablation of Ado uptake on Ado toxicity in Cl.8+ cells. (A) Effect of equilibrative transport inhibitor Dipy (10 μ M) on Ado mediated inhibition of cell growth in Cl.8+ cells, cell number increase after 24 h was quantified. (B) Effect of low sodium medium on cell proliferation and morphology (C) after Ado treatment. Cells were treated with 50 μ M Ado for 24 h in CM or low sodium medium respectively. The number and morphology of cells were assessed. (D) Genetic ablation of particular nucleoside transporters using RNAi approach. Data are expressed as a percentage of cells with Ado unaffected morphology ("healthy cells") compared to mock transfected control. NK - mock transfected control without Ado treatment, PK - *DmCht5* transfected cells treated with Ado. Values are presented as means \pm SD of three independent experiments. * $P < 0.05$, ** $P < 0.01$, a - compared to untreated control, b - compared to control Ado treatment.

Uro. We have shown that Cl.8+ cells can efficiently transport Uro even in the presence of 50 or 100 μ M Ado (Fig. S1). However, the co-treatment of Cl.8+ cells with Uro, even in 4x higher doses, did not rescue cell proliferation after Ado treatment (Fig. 7d). It suggests that Ado toxicity is directly connected to the massive ATP production independent of pyrimidine starvation.

3.7. Ado-tolerant Mbn2 cells do not accumulate such high concentration of ATP upon Ado treatment

To see if such a high level of ATP accumulation is specific for Ado-sensitive cell lines, we compared Ado uptake and ATP production in Cl.8+ cells with Mbn2 cells that seem to be tolerant to high concentrations of Ado (Fig. 8a). Interestingly, real-time RT PCR analysis of Mbn2 cells showed similar pattern of nucleoside transporter genes expression as did the Cl.8+ cells (Fig. 9). However, the rate of Ado uptake in Mbn2 cells ranged from 40 to 50% of that observed in Cl.8+ cells for all time points and concentrations tested (5–50 μ M ado, 20–60 min) (Fig. 8b). It probably resulted from higher activity of extracellular deamination by ADGF-A, which is more expressed in Mbn2 compared to Cl.8+ cells (Fig. 9).

ATP accumulation in Mbn2 cells was much lower than in Cl.8+ cells and maximum ATP content was reached after a shorter time

period. In Mbn2 cells, maximum ATP level was approximately 3–4.5x lower than in Cl.8+ cells depending on the applied Ado concentration (50, 100, 200 μ M) reached within the initial 1–4 h of Ado cultivation in contrast to the 3–6 h-long linear increase of ATP level observed in Cl.8+ cells (Fig. 8c,d). Lower incorporation of Ado into ATP was also confirmed also by radioactive labeling (18% radioactivity in the fraction corresponding to ATP in Mbn2 vs. 42% in Cl.8+ cells) (Fig. 8e). Lower radioactivity in the ATP fraction corresponded to higher level of labeled Ino in Mbn2 cell lysates (58 vs. 43% in Cl.8+ cells) corresponding to higher expression of DmADA and MSI genes in Mbn2 cells coding proteins with cytosolic Ado deaminase activity (Fig. 9). Interestingly, in addition to higher radioactivity in the Ino fraction, Mbn2 cells showed slightly, but still significantly higher levels of labeled AMP (8.5 vs. 6%) and ADP (15 vs. 9%) (Fig. 8e).

4. Discussion

Here we report that the adverse Ado effect on cell morphology, growth and viability in *Drosophila* Cl.8+ cells results from an excessive Ado uptake leading to massive ATP accumulation, whereas other cell lines including Mbn2 cells, Bg2-c2 neuroblasts and embryonic S2 cell line seem to be more Ado-tolerant.

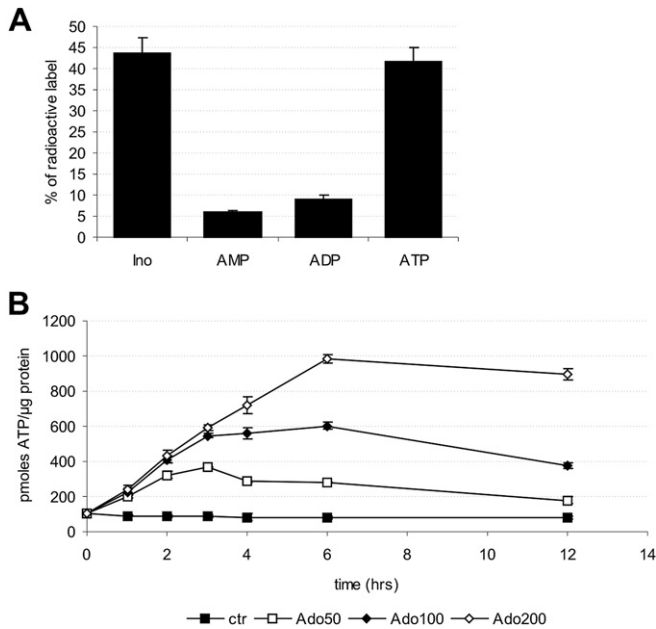


Fig. 6. ATP accumulation after Ado treatment in Cl.8+ cells. (A) Cells were incubated in 100 μ M H3-Ado for 2 h and lysed, the lysates were separated by HPLC and the percentage of radioactivity in each fraction corresponding to Ino, AMP, ADP, and ATP was determined using scintillation counting. (B) Time-course study of Ado-induced increase in ATP amount in Cl.8+ cells. The cells were incubated in CM containing indicated Ado concentrations (50 μ M, 100 μ M, 200 μ M). The amount of ATP was monitored in regular intervals for 12 h. Each data point represents mean \pm SD of three independent experiments.

Comparison of *Drosophila* Cl.8+ and Mbn2 cell lines showed that Ado-tolerant Mbn2 cells utilize Ado deamination as the preferred metabolic pathway to cope with increased level of extracellular Ado.

There is a large body of literature reporting Ado-induced growth arrest or cell death (Henderson and Scott, 1980; Merighi et al., 2002; Ohkubo et al., 2007; Peyot et al., 2000; Schrier et al., 2001). Mammalian receptor subtypes were shown to have anti-proliferative and, apoptotic, as well as prosurvival function depending on the cell type and applied Ado concentration (Ohana et al., 2001). Activation of AdoR may negatively influence cell survival via activation of cAMP, Ca²⁺, or MAP kinase cascades (Kizaki et al., 1990; Merighi et al., 2005; Szondy, 1994). On the other hand, anti-proliferative role of Ado is, in many cases, independent of its receptor activation since it can be blocked by nucleoside transport inhibitors such as Dipy (Ohkubo et al., 2007; Wu et al., 2006). Moreover, synergistic effect of both Ado uptake and signaling in apoptosis induction has also been reported in some cell lines (Dilorio et al., 2002).

Our results demonstrate that Ado signaling through the DmAdoR plays negligible role in Ado toxicity in Cl.8+ cells. Involvement of *DmAdoR* in this phenomenon may be excluded based on both RNAi knock-down and pharmacological experiments. The expression of DmAdoR in Cl.8+ cells was very low and its agonist CHA did not mimic Ado effect on cell proliferation. In agreement with these results, RNAi of DmAdoR did not rescue Ado toxicity in Cl.8+ cells. Recently, we have tested DmAdoR signaling in various *Drosophila* cell lines and showed that Ado is not able to recruit detectable levels of cAMP or Ca²⁺ second messengers in Cl.8+ cells (data not shown).

We have several lines of evidence that Ado anti-proliferative role in Cl.8+ cell line is caused exclusively by intracellular Ado uptake. We have shown that Ado is efficiently taken up into Cl.8+

cells, in a way that is not inhibited by other nucleosides and involves both equilibrative and concentrative transporters, since Ado toxicity can be rescued by Dipy treatment or Na⁺ depletion as well as knocking down the expression of *DmEnt2*, and both *DmCnts*. Previously, functional characteristics of DmENTs were studied by Machado et al. (2007) who expressed particular DmENTs in *Xenopus* oocytes and measured their capability to transport Uro, which is believed to be universal permeant of mammalian Ents. In agreement with our findings, they showed that only *DmEnt2* was capable of transporting Uro and broad scale of other nucleosides and nucleobases - including Ado - from the extracellular space, however they were not able to block Uro transport by classical mammalian equilibrative transport inhibitors (Dipy, Diazep, NBTI). These discrepancies might be caused by separate transporters for Ado and Uro in flies (as suggested by Fig. S1) or by methodological differences between the two studies.

Once taken up into cells, Ado is rapidly metabolized. It was shown in some mammalian cells that accompanying increase in AMP and S-adenosylhomocysteine concentration may contribute to Ado cytotoxicity causing pyrimidine starvation and hypomethylation, respectively (Green and Chan, 1973; Skinner et al., 1986). In accordance we found that the inhibitor of adenosine kinase Itu prevented Ado-induced growth retardation of Cl.8+ cells pointing to the involvement of Ado phosphorylation in its toxic effect. Despite the fact that Adk inhibitor Itu was able to block Adk enzymatic activity in cell lysates (data not shown), we can not exclude the fact that the Itu effect on living cells was caused by blockade of NTs, which was also reported to be an Itu target (Sinclair et al., 2001). However, further support for the involvement of Ado phosphorylation was received from RNAi silencing of DmAdoK2 (CG11255), which was able to rescue cells from Ado toxicity.

In Cl.8+ cells, Ado phosphorylation is connected to the massive accumulation of ATP. The contribution of extracellular Ado to the elevation of adenine nucleotide pool was earlier observed both *in vitro* and *ex vivo* in mammalian muscle cells, in which virtually all transported Ado was rapidly converted to ATP (95% after 30 min) (Barron and Gu, 2000; Hellsten and Frandsen, 1997). We found that elevated level of Ado-induced multiple increment of cellular ATP level (see Fig. 6). Such massive ATP pool enhancement is believed to cause pyrimidine starvation. Excessive Ado phosphorylation to AMP causes negative feedback inhibition of PRPP (5-phosphoribosyl-1-pyrophosphate) synthase, which produces an intermediate PRPP necessary for both pyrimidine and purine *de novo* biosynthesis (Seetulsingh-Goorah, 2006). Resulting depletion of the pyrimidine nucleotides pool interferes with DNA synthesis and ultimately causes growth arrest and cell death (Green and Chan, 1973). Inhibition of pyrimidine *de novo* synthesis can be compensated by the addition of Uro, a substrate of pyrimidine salvage pathway. However, in our conditions Uro was not able to rescue the Ado toxicity in the same way as described for some other cell types (Seetulsingh-Goorah, 2006). This indicates that a mechanism other than pyrimidine starvation is involved in Ado toxicity in Cl.8+ cells.

It has been reported that Ado can specifically increase the nuclear compartment pools of ATP and nuclear ATP/ADP ratio, such increase inhibits DNA synthesis in mouse fibroblasts (Rapaport et al., 1979). Alternatively, activation of AMP kinase has been reported to cause cell death after Ado treatment in intestinal rat epithelial cells, HUVEC and human gastric cancer cells (Aymerich et al., 2006; da Silva et al., 2006; Saitoh et al., 2004). However, we were not able to detect any increase in AMPK phosphorylation after Ado treatment (data not shown) probably because of the increased ATP/AMP ratio that is not favorable for AMP kinase activation (Hardie, 2004).

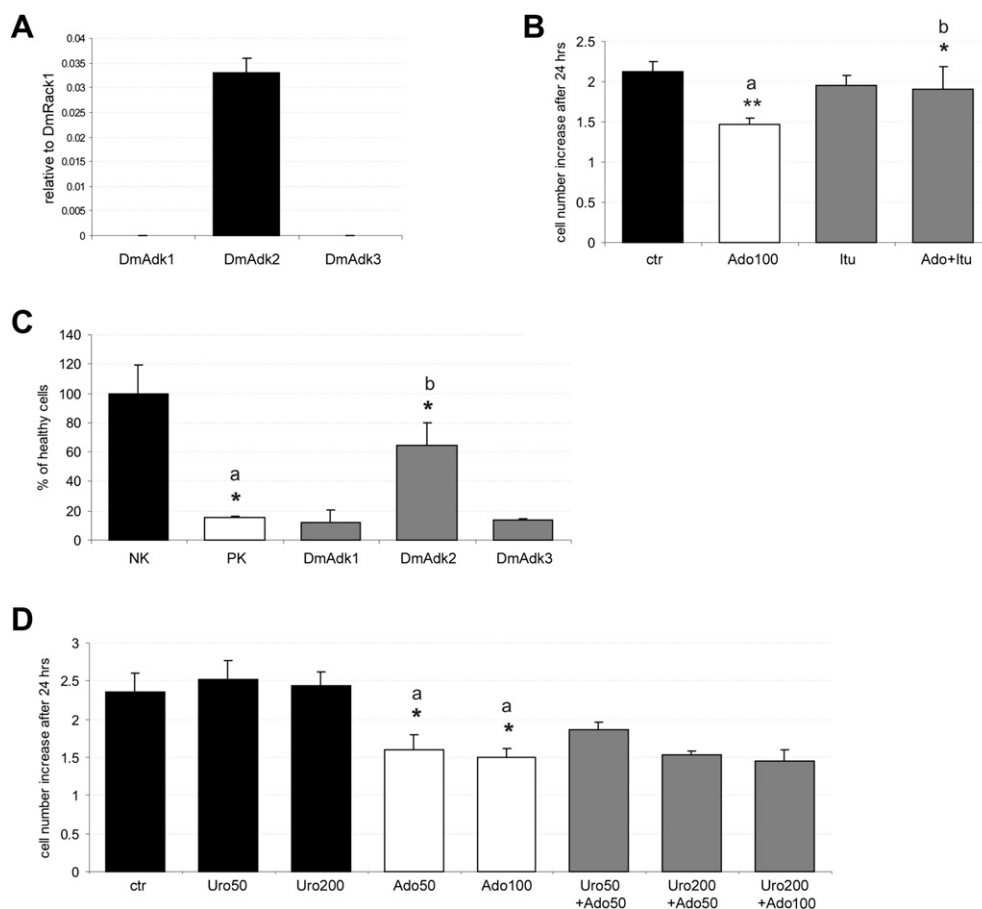


Fig. 7. Involvement of Ado phosphorylation and pyrimidine starvation in Ado toxicity. (A) Expression of three known *Drosophila* Ado kinases in Cl.8+ cells quantified by real time RT-PCR, relative expression values were standardized to *DmRack1* gene expression. (B) Effect of Adk inhibitor Itu (200 nM) on Ado mediated inhibition of cell growth in Cl.8+ cells, cell number increase after 24 h was quantified. (C) Genetic ablation of particular Adks using RNAi approach. Data are expressed as a percentage of cells with Ado unaffected morphology ("healthy cells") compared to mock transfected control. NK - mock transfected control without Ado treatment, PK - DmCht5 transfected cells treated with Ado. (D) Lack of Uro effect on Ado toxicity. Cells were treated with 50 μ M and 100 μ M Ado in the presence of various Uro concentrations. The number of cells per well after 24 h incubation is shown in the graph. Each data point represents mean \pm SD of three independent experiments. Data were analyzed by one-way ANOVA and Tukey's test. * $P < 0.05$, ** $P < 0.01$, a – compared to untreated control, b – compared to Ado treatment.

Crucial role of ATP production in Ado toxicity is supported by the observation that Ado resistant *Drosophila* cell lines, including Mbn2 cells, do not show such massive accumulation of ATP. Ado taken up into the cytoplasm is in these cells converted to ATP to a much lower extent than in Cl.8+ cells (see Fig. 8). Ado resistance in insect cells has mainly been connected to extracellular Ado deaminases (Zurovec et al., 2002). This was supported by our results indicating that both extra and intracellular adenosine deaminations are major pathways of Ado metabolism in Mbn2 cells. However, lower uptake of Ado and not as high levels of AMP and ADP in Mbn2 cells compared to Cl.8+ cells indicate that in addition to the higher Ado deaminase activity, less effective transport of Ado, and its phosphorylation to AMP and ADP contribute to Mbn2 resistance to Ado. In this context it is worth noting that the inhibition of AMP deaminase induces Ado toxicity in mammalian cell lines (Barry and Lind, 2000).

The differences in Ado metabolism, among different cell types at the level of its deamination, uptake and phosphorylation suggest elaborate regulation of Ado homeostasis in the *Drosophila* body that might be important especially during the period of tissue remodeling. Critical importance of Ado homeostasis during metamorphosis is supported by the fact that both null mutants in *DmENT2* as well as *ADGF-A* are lethal during late larval/early pupal stages (Dolezal et al., 2003; Knight et al., 2010). Mutants in several *de novo* synthesis pathway genes including *Prat*, *Ade2*, *Ade3*, and

Ade5 display pupal lethality (Ji and Clark, 2006). The key enzyme in the *de novo* purine synthesis - PRAT is not expressed in a large excess over the level necessary for normal development (Clark and MacAfee, 2000). *Drosophila* depends on purines derived from food (Burnet and Sang, 1963) supporting the important role of Ado recycling and redistribution (Henikoff et al., 1986).

For both vertebrates and invertebrates it has been previously shown that the Km value of Ado kinase for Ado was one to two orders of magnitude lower than that for Ado deaminase (Arch and Newsholme, 1978). Based on these findings we presume that Ado uptake and its effective phosphorylation even in relatively low Ado concentrations allows effective Ado redistribution and reutilization in newly formed tissues and organs, while high level of extracellular Ado deaminase enzymes in the hemolymph prevent major local Ado level fluctuations and keep the extracellular Ado below dangerous levels. Thus the maximum possible amount of Ado would be recycled in newly formed tissues (e.g. imaginal discs) while the tissues with slower growth/lower metabolic activity would have their Ado-recycling capacity limited due to high expression of both extracellular and intracellular deaminases.

We conclude that unlike the ATP production in Mbn2 cells (and other cell types, unpublished results), the amount of ATP produced in Cl.8+ cells is directly proportional to the level of extracellular Ado and is limited only by the metabolic capacity of the cells. In the

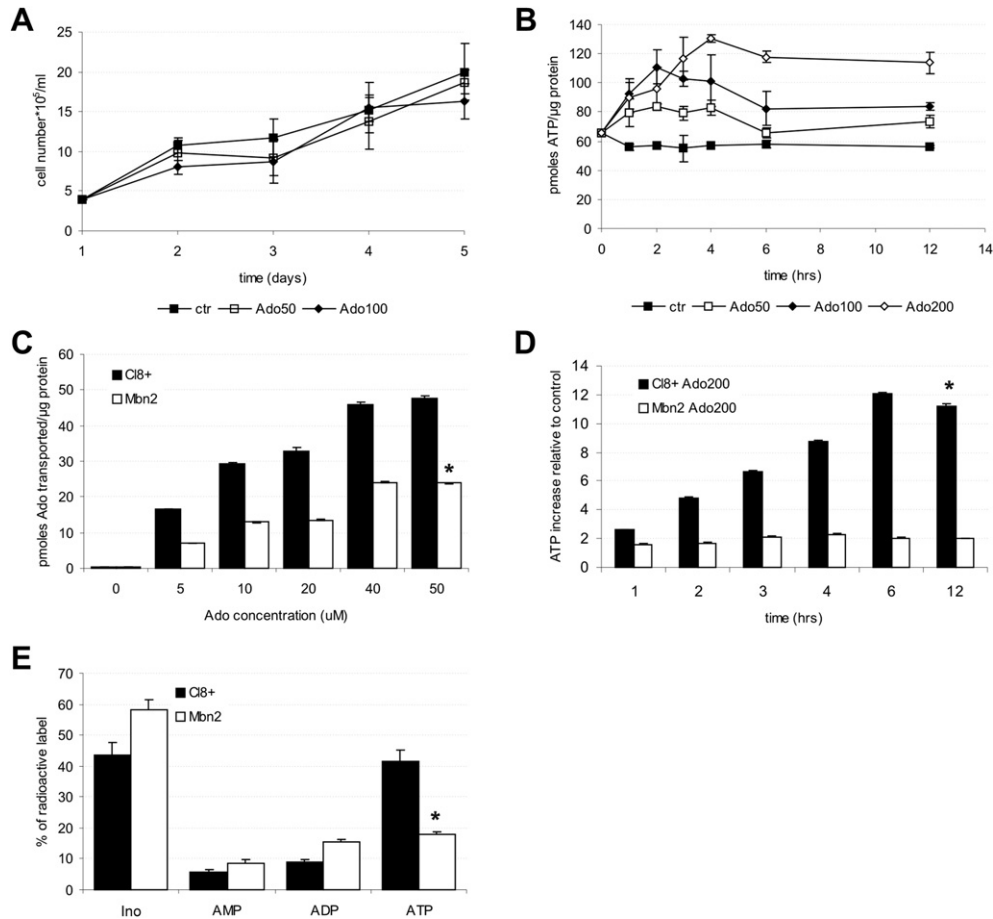


Fig. 8. Comparison of Ado response in Cl8+ and Mbn2 cells. (A) Effect of Ado on Mbn2 cells proliferation. Cells were incubated in CM without Ado or with indicated Ado concentrations for 3 days. Cell numbers were counted every 24 h using images of the same area of Petri dish. (B) Comparison of Ado uptake in Mbn2 and Cl8+ cells. Mbn2 cells were incubated with different concentrations of H3-Ado (5–50 μ M) for an hour and the data were compared with Cl8+ cells. Data are expressed as the amount of pmoles transported to the cytoplasm per μ g of protein. (C) ATP production in Mbn2 cells treated by Ado. The cells were incubated in CM medium containing various Ado concentrations (50 μ M, 100 μ M, 200 μ M). The amount of ATP (pmoles ATP per μ g protein) was monitored in regular intervals for 12 h. (D) Comparison of ATP increase after Ado treatment of Mbn2 and Cl8+ cells. Cells were treated with 200 μ M Ado for 12 h. Data are present as relative increase in ATP level compared to control. (E) Comparison of Ado incorporation into cellular Ado metabolites pool. Cells were incubated in 100 μ M H3-Ado for 2 h and lysed, the lysates were separated by HPLC and the percentage of radioactivity in each fraction corresponding to Ino, AMP, ADP, and ATP was determined using scintillation counting. Each point represents mean \pm SD of three independent experiments. * $P < 0.05$ for whole data series compared with corresponding value for Cl8+ cells by Tukey's test.

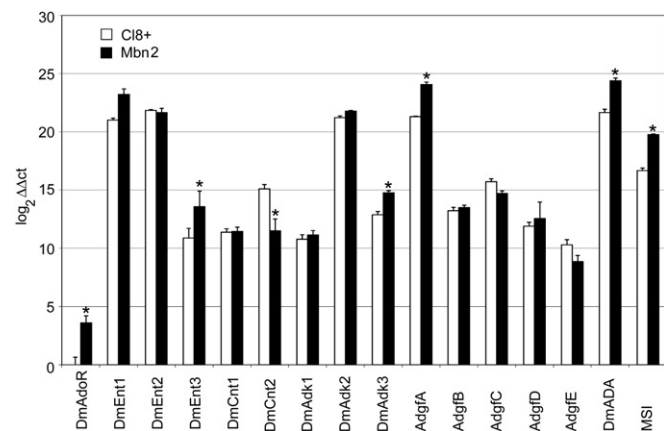


Fig. 9. RT-PCR analysis of expression profile of genes involved in Ado signaling and metabolism in Cl8+ and Mbn2 cell lines. The relative gene expression is presented as \log_2 ratios to the least abundant transcript ($\log_2 \Delta \Delta ct$). Data were normalized to internal control gene *Rack1*. Values represent averages from two independent biological samples. Bars indicate SEM. * $P < 0.05$ compared with corresponding value for Cl8+ cells by Tukey's test.

other words, these cells may lack an endogenous feedback mechanism that would protect them from the excessive ATP production that at higher doses of Ado results in the depletion of cell supplies, growth arrest, and eventually cell death. The exact nature of metabolic changes causing Ado-mediated growth arrest and cell death, however, will require further studies.

Acknowledgments

We would like to thank Dr. Anna Zaloudikova and Pavla Kruzberska for technical assistance. We are also grateful to Dr. Vladimir Dolezal for critical reading of the manuscript. The study was supported by the Grant Agency of Czech Academy of Sciences (KJB501410801) and by Research Center Program MSMT - LC06077. The presented work also used the infrastructure build with the help of European Community's Seventh Framework Programme (FP7/2007–2013) under grant agreement no. 229518.

Appendix. Supplementary material

Supplementary material associated with this article can be found, in the online version, at doi:10.1016/j.ibmb.2012.01.002.

References

- Arch, J.R., Newsholme, E.A., 1978. Activities and some properties of 5'-nucleotidase, adenosine kinase and adenosine deaminase in tissues from vertebrates and invertebrates in relation to the control of the concentration and the physiological role of adenosine. *Biochem. J.* 174, 965–977.
- Aymerich, I., Foufelle, F., Ferre, P., Casado, F.J., Pastor-Anglada, M., 2006. Extracellular adenosine activates AMP-dependent protein kinase (AMPK). *J. Cell Sci.* 119, 1612–1621.
- Barron, J.T., Gu, L., 2000. Energetic effects of adenosine on vascular smooth muscle. *Am. J. Physiol. Heart Circ. Physiol.* 278, H26–H32.
- Barry, C.P., Lind, S.E., 2000. Adenosine-mediated killing of cultured epithelial cancer cells. *Cancer Res.* 60, 1887–1894.
- Burnet, B., Sang, J.H., 1963. Dietary Utilization of DNA and its derivatives by *Drosophila-melanogaster* (Meig). *J. Insect Physiol.* 9, 553–562.
- Burnstock, G., 2011. Introductory overview of purinergic signalling. *Front. Biosci.* 3, 896–900. Elite ed.
- Clark, D.V., MacAfee, N., 2000. The purine biosynthesis enzyme PRAT detected in proenzyme and mature forms during development of *Drosophila melanogaster*. *Insect Biochem. Mol. Biol.* 30, 315–323.
- Cullen, C.F., Milner, M.J., 1991. Parameters of growth in primary cultures and cell lines established from *Drosophila* imaginal discs. *Tissue Cell* 23, 29–39.
- da Silva, C.G., Jarzyna, R., Specht, A., Kaczmarek, E., 2006. Extracellular nucleotides and adenosine independently activate AMP-activated protein kinase in endothelial cells: involvement of P2 receptors and adenosine transporters. *Circ. Res.* 98, e39–47.
- Di Iorio, P., Kleywegt, S., Ciccarelli, R., Traversa, U., Andrew, C.M., Crocker, C.E., Werstiuik, E.S., Rathbone, M.P., 2002. Mechanisms of apoptosis induced by purine nucleosides in astrocytes. *Glia* 38, 179–190.
- Dolezal, T., Dolezelova, E., Zurovec, M., Bryant, P.J., 2005. A role for adenosine deaminase in *Drosophila* larval development. *Plos Biol.* 3, e201.
- Dolezal, T., Gazi, M., Zurovec, M., Bryant, P.J., 2003. Genetic analysis of the ADGF multigene family by homologous recombination and gene conversion in *Drosophila*. *Genetics* 165, 653–666.
- Dolezelova, E., Nothacker, H.P., Civelli, O., Bryant, P.J., Zurovec, M., 2007. A *Drosophila* adenosine receptor activates cAMP and calcium signaling. *Insect Biochem. Mol. Biol.* 37, 318–329.
- Dolezelova, E., Zurovec, M., Dolezal, T., Simek, P., Bryant, P.J., 2005. The emerging role of adenosine deaminases in insects. *Insect Biochem. Mol. Biol.* 35, 381–389.
- Fenckova, M., Hobizalova, R., Fric, Z.F., Dolezal, T., 2011. Functional characterization of ecto-5'-nucleotidases and apyrases in *Drosophila melanogaster*. *Insect Biochem. Mol. Biol.* 41, 956–967.
- Feoktistov, I., Biaggioni, I., Cronstein, B.N., 2009. Adenosine receptors in wound healing, fibrosis and angiogenesis. *Handbook Exp. Pharmacol.*, 383–397.
- Fredholm, B.B., Johansson, S., Wang, Y.Q., 2011. Adenosine and the regulation of metabolism and body temperature. *Adv. Pharmacol.* 61, 77–94.
- Green, H., Chan, T., 1973. Pyrimidine starvation induced by adenosine in fibroblasts and lymphoid cells: role of adenosine deaminase. *Science* 182, 836–837.
- Hardie, D.G., 2004. AMP-activated protein kinase: a key system mediating metabolic responses to exercise. *Med. Sci. Sports Exerc.* 36, 28–34.
- Hasko, G., Cronstein, B.N., 2004. Adenosine: an endogenous regulator of innate immunity. *Trends Immunol.* 25, 33–39.
- Hellsten, Y., Frandsen, U., 1997. Adenosine formation in contracting primary rat skeletal muscle cells and endothelial cells in culture. *J. Physiol.* 504 (Pt 3), 695–704.
- Henderson, J.F., Scott, F.W., 1980. Inhibition of animal and invertebrate cell growth by naturally occurring purine bases and ribonucleosides. *Pharmacol. Ther.* 8, 539–571.
- Henikoff, S., Nash, D., Hards, R., Bleskan, J., Woolford, J.F., Naguib, F., Patterson, D., 1986. Two *Drosophila melanogaster* mutations block successive steps of de novo purine synthesis. *Proc. Natl. Acad. Sci. USA.* 83, 3919–3923.
- Huber-Ruano, I., Pinilla-Macua, I., Torres, G., Casado, F.J., Pastor-Anglada, M., 2010. Link between high-affinity adenosine concentrative nucleoside transporter-2 (CNT2) and energy metabolism in intestinal and liver parenchymal cells. *J. Cell Physiol.* 225, 620–630.
- Jackson, E.K., Mi, Z., Dubey, R.K., 2007. The extracellular cAMP-adenosine pathway significantly contributes to the in vivo production of adenosine. *J. Pharmacol. Exp. Ther.* 320, 117–123.
- Ji, Y., Clark, D.V., 2006. The purine synthesis gene *Prat2* is required for *Drosophila* metamorphosis, as revealed by inverted-repeat-mediated RNA interference. *Genetics* 172, 1621–1631.
- King, A.E., Ackley, M.A., Cass, C.E., Young, J.D., Baldwin, S.A., 2006. Nucleoside transporters: from scavengers to novel therapeutic targets. *Trends Pharmacol. Sci.* 27, 416–425.
- Kizaki, H., Suzuki, K., Tadakuma, T., Ishimura, Y., 1990. Adenosine receptor-mediated accumulation of cyclic AMP-induced T-lymphocyte death through internucleosomal DNA cleavage. *J. Biol. Chem.* 265, 5280–5284.
- Knight, D., Harvey, P.J., Iliadi, K.G., Klose, M.K., Iliadi, N., Dolezelova, E., Charlton, M.P., Zurovec, M., Boulianne, G.L., 2010. Equilibrative nucleoside transporter 2 regulates associative learning and synaptic function in *Drosophila*. *J. Neurosci.* 30, 5047–5057.
- Linden, J., 2001. Molecular approach to adenosine receptors: receptor-mediated mechanisms of tissue protection. *Annu. Rev. Pharmacol. Toxicol.* 41, 775–787.
- Lum, L., Yao, S., Mozer, B., Rovescalli, A., Von Kessler, D., Nirenberg, M., Beachy, P.A., 2003. Identification of Hedgehog pathway components by RNAi in *Drosophila* cultured cells. *Science* 299, 2039–2045.
- Machado, J., Abdulla, P., Hanna, W.J., Hilliker, A.J., Coe, I.R., 2007. Genomic analysis of nucleoside transporters in Diptera and functional characterization of DmENT2, a *Drosophila* equilibrative nucleoside transporter. *Physiol. Genomics* 28, 337–347.
- Matherne, G.P., Headrick, J.P., Coleman, S.D., Berne, R.M., 1990. Interstitial transudate purines in normoxic and hypoxic immature and mature rabbit hearts. *Pediatr. Res.* 28, 348–353.
- Merighi, S., Benini, A., Mirandola, P., Gessi, S., Varani, K., Leung, E., MacLennan, S., Borea, P.A., 2005. A3 adenosine receptor activation inhibits cell proliferation via phosphatidylinositol 3-kinase/Akt-dependent inhibition of the extracellular signal-regulated kinase 1/2 phosphorylation in A375 human melanoma cells. *J. Biol. Chem.* 280, 19516–19526.
- Merighi, S., Mirandola, P., Milani, D., Varani, K., Gessi, S., Klotz, K.N., Leung, E., Baraldi, P.G., Borea, P.A., 2002. Adenosine receptors as mediators of both cell proliferation and cell death of cultured human melanoma cells. *J. Invest. Dermatol.* 119, 923–933.
- Nyce, J.W., 1999. Insight into adenosine receptor function using antisense and gene-knockout approaches. *Trends Pharmacol. Sci.* 20, 79–83.
- Ohana, G., Bar-Yehuda, S., Barer, F., Fishman, P., 2001. Differential effect of adenosine on tumor and normal cell growth: focus on the A3 adenosine receptor. *J. Cell Physiol.* 186, 19–23.
- Ohkubo, S., Nagata, K., Nakahata, N., 2007. Adenosine uptake-dependent C6 cell growth inhibition. *Eur. J. Pharmacol.* 577, 35–43.
- Ohta, A., Sitkovsky, M., 2009. The adenosinergic immunomodulatory drugs. *Curr. Opin. Pharmacol.* 9, 501–506.
- Park, J., Gupta, R.S., 2008. Adenosine kinase and ribokinase—the RK family of proteins. *Cell. Mol. Life Sci.* 65, 2875–2896.
- Peyot, M.L., Gadeau, A.P., Dandre, F., Belloc, I., Dupuch, F., Desgranges, C., 2000. Extracellular adenosine induces apoptosis of human arterial smooth muscle cells via A(2b)-purinoceptor. *Circ. Res.* 86, 76–85.
- Pfaffl, M.W., 2006. Real-time PCR. Taylor & Francis, New York.
- Ponnoth, D.S., Jamal Mustafa, S., 2011. Adenosine receptors and vascular inflammation. *Biochim. Biophys. Acta* 1808, 1429–1434.
- Porkka-Heiskanen, T., Kalinchuk, A.V., 2011. Adenosine, energy metabolism and sleep homeostasis. *Sleep Med. Rev.* 15, 123–135.
- Rapaport, E., Garcia-Blanco, M.A., Zamecnik, P.C., 1979. Regulation of DNA replication in S phase nuclei by ATP and ADP pools. *Proc. Natl. Acad. Sci. USA* 76, 1643–1647.
- Saitoh, M., Nagai, K., Nakagawa, K., Yamamura, T., Yamamoto, S., Nishizaki, T., 2004. Adenosine induces apoptosis in the human gastric cancer cells via an intrinsic pathway relevant to activation of AMP-activated protein kinase. *Biochem. Pharmacol.* 67, 2005–2011.
- Sakowicz-Burkiewicz, M., Kocbuch, K., Grden, M., Szutowicz, A., Pawelczyk, T., 2006. Diabetes-induced decrease of adenosine kinase expression impairs the proliferation potential of diabetic rat T lymphocytes. *Immunology* 118, 402–412.
- Samakovlis, C., Asling, B., Boman, H.G., Gateff, E., Hultmark, D., 1992. In vitro induction of cecropin genes—an immune response in a *Drosophila* blood cell line. *Biochem. Biophys. Res. Commun.* 188, 1169–1175.
- Sankar, N., Machado, J., Abdulla, P., Hilliker, A.J., Coe, I.R., 2002. Comparative genomic analysis of equilibrative nucleoside transporters suggests conserved protein structure despite limited sequence identity. *Nucleic Acids Res.* 30, 4339–4350.
- Sauer, A.V., Aiuti, A., 2009. New insights into the pathogenesis of adenosine deaminase-severe combined immunodeficiency and progress in gene therapy. *Curr. Opin. Allergy Clin. Immunol.* 9, 496–502.
- Seetulsingh-Goorah, S.P., 2006. Mechanisms of adenosine-induced cytotoxicity and their clinical and physiological implications. *Biofactors* 27, 213–230.
- Shields, G., Sang, J.H., 1970. Characteristics of five cell types appearing during in vitro culture of embryonic material from *Drosophila melanogaster*. *J. Embryol. Exp. Morphol.* 23, 53–69.
- Schrier, S.M., van Tilburg, E.W., van der Meulen, H., Ijzerman, A.P., Mulder, G.J., Nagelkerke, J.F., 2001. Extracellular adenosine-induced apoptosis in mouse neuroblastoma cells: studies on involvement of adenosine receptors and adenosine uptake. *Biochem. Pharmacol.* 61, 417–425.
- Sinclair, C.J., Powell, A.E., Xiong, W., LaRiviere, C.G., Baldwin, S.A., Cass, C.E., Young, J.D., Parkinson, F.E., 2001. Nucleoside transporter subtype expression: effects on potency of adenosine kinase inhibitors. *Br. J. Pharmacol.* 134, 1037–1044.
- Skinner, M.A., Ho, H.J., Chan, V.L., 1986. Inhibition of methylation of DNA and tRNA by adenosine in an adenosine-sensitive mutant of the baby hamster kidney cell line. *Arch. Biochem. Biophys.* 246, 725–732.
- Szondy, Z., 1994. Adenosine stimulates DNA fragmentation in human thymocytes by Ca(2+)-mediated mechanisms. *Biochem. J.* 304 (Pt 3), 877–885.
- Van Belle, H., Goossens, F., Wynants, J., 1987. Formation and release of purine catabolites during hypoperfusion, anoxia, and ischemia. *Am. J. Physiol.* 252, H886–H893.
- Wu, L.F., Li, G.P., Feng, J.L., Pu, Z.J., 2006. Molecular mechanisms of adenosine-induced apoptosis in human HepG2 cells. *Acta Pharmacol. Sin.* 27, 477–484.
- Zuberova, M., Fenckova, M., Simek, P., Janeckova, L., Dolezal, T., 2010. Increased extracellular adenosine in *Drosophila* that are deficient in adenosine deaminase activates a release of energy stores leading to wasting and death. *Dis. Model. Mech.* 3, 773–784.
- Zurovec, M., Dolezal, T., Gazi, M., Pavlova, E., Bryant, P.J., 2002. Adenosine deaminase-related growth factors stimulate cell proliferation in *Drosophila* by depleting extracellular adenosine. *Proc. Natl. Acad. Sci. USA.* 99, 4403–4408.

Supplementary information

Figure S1. Uridine transport in the Cl.8+ cells. Concentration dependency of Uro transport in presence or absence of 50 μ M Ado. Data are present as the amount of pmoles transported to the cytoplasm per μ g of protein. Values are presented as means \pm SD of three independent experiments.

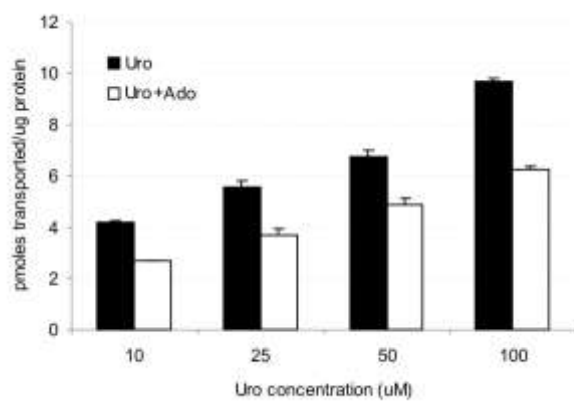


Table S1: List of primers used for the real time RT-PCR amplification of Ado signalling and metabolism genes.

Gene	Sequence
DmEnt1-fw	TCCCTGCGCACCAAGAT
DmEnt1-rev	ATAAACTCGGAGGGAAATAGACC
DmEnt2-fw	CGTGTGCAACGGCATCTAC
DmEnt2-rev	GTTGGAGCCCAGGACGAC
DmEnt3-fw	CATCGCTCTGGGCATCAC
DmEnt3-rev	CCACCGTCAGACCAACATTAT
DmCnt1-fw	GGGGGCTTATGTGTCCTTC
DmCnt1-rev	GGCCGCATCCAAAATAGA
DmCnt2-fw	CTTTGCCAATCCCAGTTCC
DmCnt2-rev	TAGTTCGCCCCGCTCGTC
DmAdoR-fw	CCCATCTGAACTCGGCGGTAAATC
DmAdoR-rev	GCCTCCTGCTGCTGCCTCAAC
DmAdk1-fw	GGTCAGTGGGCAAGGATAAG
DmAdk1-rev	AGAAAGAAGCCCGTAAAGTAGAA
DmAdk2-fw	CAACAAGGCTCTGGTGGATAA
DmAdk2-rev	AATGGTGCGCTGAGGTTC
DmAdk3-fw	GGGCTCCAAGGGTGAAC
DmAdk3-rev	ACGGCGCCAAAGAAGAG
AdgfA-fw	AGGCTCATCCAGATTTTCATTG
AdgfA-rev	CGGGTACTTTTCCTTTATTTGTT
AdgfB-fw	GCTGACCATTTCGGGACAC

AdgfB-rev	CAACTAGATCAAAGCCAACCAT
AdgfC-fw	TGTACACAGAGATTCGGACCAG
AdgfC-rev	TAGACGGCCATAATGACTTTGA
AdgfD-fw	CTGACCACCACCAATAATCTGTA
AdgfD-rev	AGCGCTCCCAAATCTTCTT
AdgfE-fw	ATCGCGCTGGAGGTGTG
AdgfE-rev	CAGAAAGGCCATGTAGAAGTCA
DrADA-fw	GACAGTGGCGTTTTTGATACC
DrADA-rev	CGCTGGCGAATGAATGAT
MSI-fw	CGCCCGATCTGGAGTGAA
MSI-rev	ATATTTGGCAGCGAGGAACG
DmRack1-fw	CCCGTGACAAGACCCTGAT
DmRack1-rev	TAGTTGCCATCGGAGGAGAG

Table S2: List of primers used in RNAi silencing of Ado signalling and metabolism genes.

Gene	Sequence
DmCht5-fw	ACGCAGTGTGGTACGCTTTATGAA
DmCht5-rev	CGCCGCCTGCCTCCTTATT
DmAdoR-fw	GCTAGTGGGCGCATTGGGTATTC
DmAdoR-rev	CGGAGGCGGGGTTCATCGTA
DmEnt1-fw	ATCTCGAGCAGATGTCTCTTGAAAAGC
DmEnt1-rev	ATTCTAGAATGACTGCTCCTCGAACG
DmEnt2-fw	ATCTCGAGTAATCCCGAAATCAGAGTGC
DmEnt2-rev	ATCTCGAGTAATCCCGAAATCAGAGTGC
DmEnt3-fw	ATCTCGAGTGTGAATAATCCGCCAGAGG
DmEnt3-rev	ATTCTAGATGTAGTCCCAGAAATAGTGG
DmCnt1-fw	GAGAAGCCAGTGCCAGAGGTTA
DmCnt1-rev	AAGGGGAGGCGCAGGCAGAGTAT
DmCnt2-fw	GCGCATAGTCATCACGGGAATC
DmCnt2-rev	GCGGGAGCTGCCATCACC
DmAdk2-fw	GCCGCCGGACTGGATGTTCACTAC
DmAdk2-rev	CGCGTCGGGTTTTTCTTCTCCA
DmAdk3-fw	GCGGGTTTTTGGCCTCAGTAT
DmAdk3-rev	CATCGGATTTGGCCCTCTTTTC
DmAdk1-fw	CGGTGGAGCGCAAGCAAATC
DmAdk1-rev	GAATCCGGCCACAAAAGCATCTC

4.4. Publication IV

Lucie Kucerova, Vaclav Broz, Jana Fleischmannova, Roman Sidorov, Vladimir Dolezal and Michal Zurovec (2012) **Effects of adenosine analogs on *Drosophila* adenosine receptor: the effect of adenosine analogs on cAMP signaling in *Drosophila* cells and their utility for in vivo experiments.** Journal of Neurochemistry 121: 383–395

Abstract:

Adenosine receptors (AR) belonging to the G protein-coupled receptor family influence a wide range of physiological processes. Recent elucidation of the structure of human A2AR revealed the conserved amino acids necessary for contact with the Ado moiety. However, the selectivity of Ado analogs for AR subtypes is still not well understood. We have shown previously that the *Drosophila* adenosine receptor (DmAdoR) evokes an increase in cAMP and calcium concentration in heterologous cells. In this study, we have characterized the second-messenger stimulation by endogenous DmAdoR in a *Drosophila* neuroblast cell line and examined a number of Ado analogs for their ability to interact with DmAdoR. We show that Ado can stimulate cAMP but not calcium levels in *Drosophila* cells. We found one full and four partial DmAdoR agonists, as well as four antagonists. The employment of the full agonist, 2-chloroadenosine, in flies mimicked in vivo the phenotype of DmAdoR over-expression, whereas the antagonist, SCH58261, rescued the flies from the lethality caused by DmAdoR over-expression. Differences in pharmacological effect of the tested analogs between DmAdoR and human A2AR can be partially explained by the dissimilarity of specific key amino acid residues disclosed by the alignment of these receptors.

ORIGINAL
ARTICLECharacterization of the *Drosophila* adenosine receptor: the effect of adenosine analogs on cAMP signaling in *Drosophila* cells and their utility for *in vivo* experiments

Lucie Kucerova,* Vaclav Broz,* Jana Fleischmannova,* Eva Santruckova,† Roman Sidorov,* Vladimir Dolezal† and Michal Zurovec*

*Biology Centre Czech Acad. Sci. and Faculty of Science, University of South Bohemia, Ceske Budejovice, Czech Republic

†Department of Neurochemistry, Institute of Physiology, Czech Acad. Sci., Videnska Praha 4, Czech Republic

Abstract

Adenosine receptors (AR) belonging to the G protein-coupled receptor family influence a wide range of physiological processes. Recent elucidation of the structure of human A2AR revealed the conserved amino acids necessary for contact with the Ado moiety. However, the selectivity of Ado analogs for AR subtypes is still not well understood. We have shown previously that the *Drosophila* adenosine receptor (DmAdoR) evokes an increase in cAMP and calcium concentration in heterologous cells. In this study, we have characterized the second-messenger stimulation by endogenous DmAdoR in a *Drosophila* neuroblast cell line and examined a number of Ado analogs for their ability to interact with DmAdoR. We show that Ado can

stimulate cAMP but not calcium levels in *Drosophila* cells. We found one full and four partial DmAdoR agonists, as well as four antagonists. The employment of the full agonist, 2-chloroadenosine, in flies mimicked *in vivo* the phenotype of DmAdoR over-expression, whereas the antagonist, SCH58261, rescued the flies from the lethality caused by DmAdoR over-expression. Differences in pharmacological effect of the tested analogs between DmAdoR and human A2AR can be partially explained by the dissimilarity of specific key amino acid residues disclosed by the alignment of these receptors.

Keywords: AdoR, calcium, CG9753, cyclic AMP, GloSensor, GPCR.

J. Neurochem. (2012) **121**, 383–395.

Adenosine (Ado) is a key cellular metabolite that physiologically regulates energy and oxygen homeostasis, neural functions, adipose tissue metabolism, immune reactions, and sleep (Jacobson and Gao 2009). Ado signaling is also involved in a variety of pathological conditions, including neurological, cardiovascular and inflammatory diseases as well as cancer (Trincavelli *et al.* 2010). Its concentration in cells and tissue fluids ranges under normal conditions from 20 to 200 nM and can rise during stressful events into the micromolar range (Fredholm 2010). The release and uptake of Ado requires nucleoside membrane transport. Half-life of Ado in the circulation is very short, usually between 1 and 10 s (Jacobson and Gao 2009). As Ado is a part of many metabolic pathways, it is always present both inside and outside of cells (Fredholm 2010).

Extracellular Ado mediates most of its effects through the activation of adenosine receptor (AR). Four subtypes of AR

were identified in mammals displaying an overall amino acid identity of 31–46% (Piirainen *et al.* 2011). They belong to the G protein-coupled receptor family and are positively (A2A and A2B) or negatively (A1 and A3) coupled to adenylyl cyclase (van Calker *et al.* 1979; Fredholm *et al.*

Received January 30, 2012; revised manuscript received February 6, 2012; accepted February 16, 2012.

Address correspondence and reprint requests to Michal Zurovec, Biology Centre Czech Acad. Sci., Branisovska 31, 37005 Ceske Budejovice, Czech Republic. E-mail: zurovec@entu.cas.cz

Abbreviations used: AR, adenosine receptor; CADo, 2-chloroadenosine; CCPA, 2-chloro-*N*(6)-cyclopentyladenosine; CHA, *N*(6)-cyclohexyladenosine; CHO, Chinese hamster ovary; CPA, *N*(6)-cyclopentyladenosine; DmAdoR, *Drosophila* adenosine receptor; DMSO, dimethylsulfoxide; DPCPX, 1,3-dipropyl-8-cyclopentylxanthine; IB-MECA, *N*(6)-(3-iodobenzyl)adenosine-5'-*N*-methyluronamide; NECA, 5'-*N*-ethylcarboxamidoadenosine; TM, transmembrane; XAC, xanthine amine congener.

1994; Linden 1994). The expression of AR is widely spread in various tissues and Ado responses are highly dependent on the level of receptor expression in a particular cell type. Mice carrying null mutations in different adenosine receptor subtypes display only subtle phenotypic effects (Fredholm *et al.* 2005). The receptor knockouts pointed to clusters of activities related to the cardiovascular and the nervous systems, whose physiology is either reduced or enhanced upon specific receptor deletion (Hasko *et al.* 2008). Despite progress in the elucidation of the pathophysiology of Ado signaling, there are potential problems with compensatory mechanisms and receptor redundancy, which are not understood (Johansson *et al.* 2007). Further understanding of Ado signaling requires the combination of pharmacological and genetic approaches and multiple adenosine receptor subtype deficiency studies (Yaar *et al.* 2005).

A number of AR ligands displaying much better metabolic stability than Ado and selectivity for individual receptor subtypes were characterized. A detailed structure of the human A2AR has been solved and co-crystallization was performed with its antagonist ZM241385 and agonists UK-432097, Ado and 5'-*N*-ethylcarboxamidoadenosine (NECA; Jaakola *et al.* 2008; Lebon *et al.* 2011; Xu *et al.* 2011). Contact amino acid residues for binding of these Ado analogs were elucidated. At least three residues were crucial for binding of all mentioned analogs: F5.29 (amino acid residue 168 in A2AR primary sequence) in the extracellular loop 2, I7.39 and N6.55, which bind to the adenine core. In addition, co-crystallization of A2AR with the agonist UK-432097 suggested important roles of H7.43 and S7.42, which create hydrogen bonds with the OH groups of the ribose ring (Xu *et al.* 2011). Three more amino acid residues, including V3.32, L6.51 and W6.48, were implicated to bind ribose moiety by the recent study of Lebon *et al.* (2011). These contact amino acids are well conserved among all four human isoforms (see Fig. 1). Further information is needed to specify the role of other amino acid residues responsible for ligand binding differences of each specific receptor subtype.

A single AR was found in *Drosophila* (DmAdoR) based on its homology to the human ARs (Brody and Cravchik 2000; Broeck 2001; Dolezelova *et al.* 2007). The closest homolog of *Drosophila* DmAdoR in human is A2AR. It has about 38.3% identity in the 350 base long N-terminal part. Other ARs show following rank order of amino acid conservation: A1 having 36.2%, A2B – 35.2% and A3 – 34.5% identity with DmAdoR. DmAdoR is expressed mainly in the optic lobes of the brain, ring gland, imaginal discs and salivary glands of the third instar *Drosophila* larvae. In adults, the expression is higher in the head than in the rest of the body (Dolezelova *et al.* 2007). *Drosophila* DmAdoR null mutant flies are viable but exhibit reduced associative learning and defects in synaptic transmission (Knight *et al.* 2010). Ectopic expression of DmAdoR

results in complex pleiotropic phenotypes ranging from slight wing morphology abnormalities to lethality depending on expression level and the tissue specificity of its expression.

Drosophila provides an advantage of lower complexity model system (three equilibrative nucleoside transporters and only single adenosine receptor), with the opportunity to use genetic approaches not possible in higher organisms. We previously found that a null mutant in *DmAdoR*, as well as a hypomorph in *DmEnt2*, a major *Drosophila* equilibrative nucleoside transporter (Machado *et al.* 2007), display changes in synaptic function (i.e. plasticity and pre-synaptic calcium influx) and altered behavioural responses (Knight *et al.* 2010). Interestingly, the phenotypes of both mutants were remarkably similar and suggest extensive adaptive responses to extracellular levels of Ado (Knight *et al.* 2010). Unraveling the relationship between the Ado transport and the receptor signaling will greatly improve our understanding of Ado function. The importance of the equilibrative nucleoside transporters for Ado receptor signaling was demonstrated earlier in mice carrying mutation in *ENT1*, which exhibited a reduced inhibitory tonus mediated by endogenous Ado (Choi *et al.* 2004). In the mammalian CNS, the inhibitory effect of Ado on cellular and synaptic activity appears to be primarily mediated by A1 receptors (Dunwiddie 1980; Greene and Haas 1991).

Our previous study showed a concentration-dependent accumulation of cAMP and calcium in Ado-treated Chinese hamster ovary (CHO) cells expressing recombinant *Drosophila* DmAdoR (Dolezelova *et al.* 2007). We re-examined the second messenger responses in native *Drosophila* cells and showed that the naturally expressed DmAdoR primarily stimulates the increase in cAMP synthesis. We also provide data on the ability of a number of the subtype selective analogs of human AR to stimulate or block DmAdoR. This study provides important information about the biological role of DmAdoR in flies *in vivo* and brings new insight into the role of specific amino acid residues in the mammalian Ado receptors.

Materials and methods

Chemicals

Ado, inosine, guanosine, deoxyadenosine, NECA, *N*(6)-(3-iodobenzyl)adenosine-5'-*N*-methyluronamide (IB-MECA), *N*(6)-cyclohexyladenosine (CHA), 2-chloro-*N*(6)-cyclopentyladenosine (CCPA), CGS 21680, *N*(6)-cyclopentyladenosine (CPA), 2-chloro-adenosine (CADO), caffeine, theophylline, xanthine amine congener (XAC), CGS 15943, SCH58261, 1,3-dipropyl-8-cyclopentylxanthine (DPCPX) and forskolin were obtained from Sigma-Aldrich (St Louis, MO, USA); CV1808, ZM241385 and pentostatin (deoxycoformycin) were purchased from Tocris Bioscience (Bristol, UK); 2-phenylaminoadenosine (ADAC) and SCH442416 were from

Cell culture

Four different *Drosophila* cell lines were used for the experiments, including imaginal disc cells Cl.8+ (Peel and Milner 1990), hematopoietic cells Mbn2 (Samakovlis *et al.* 1992), embryonic cells S2 (Schneider 1971) and neuroblasts Bg2-c2 (Ui *et al.* 1994). All cells were maintained in Shields and Sang medium (Sigma, S 8398) with different supplements as described previously (Zurovec *et al.* 2002). The growth media of Cl.8+ cells were supplemented with 2% fetal bovine serum, 2.5% fly extract, and 0.125 IU/mL insulin. Embryonic S2 cells and hematopoietic Mbn2 cells were maintained in Shields and Sang medium with 10% FBS and 0.125 IU/mL insulin, whereas the medium for Bg2-c2 cells contained 10% fetal bovine serum, yeast extract (1 g/L), pepton (2.5 g/L) and 0.3 IU/mL insulin.

Measurement of Ado-induced cAMP increase

The coding sequence for a chimeric firefly luciferase carrying a cAMP-binding moiety protein was PCR amplified from the *pGloSensor-20F* plasmid (Promega, Madison, WI, USA) and subcloned into the commercial *Drosophila* expression vector *pAC5.1/V5-His* (Invitrogen), which is under a *Drosophila* actin *V* promoter. The following primers were used, both incorporating EcoRI site (underlined) at its 5' ends: GsF: TTGAATTCGAAATGCCTGGCGCAGTAGGCAAGG and GsR: GTTGAATTCAGAGTTTAAACCCCTTCTGGAG.

The ability of the construct to emit light upon cAMP binding was first confirmed by transient transfection of the pAC-GloSensor plasmid into *Drosophila* Cl.8+ cells and treatment by forskolin (an activator of adenylyl cyclase). The cAMP responses in *Drosophila* cells were detected by luminescence readout (see the procedure below). Forskolin (20 μ M) induced about three times higher level of luciferase activity than the control-uninduced cells (see Results). Ado responses were measured with or without inhibitors of adenosine deaminases (deoxycoformycin) and we did not observe any significant effect on cAMP responses.

The *Drosophila* Bg2-c2 or S2 cells were seeded into 60-mm dishes at a density of 1×10^6 cells/mL in 3 mL medium. The pAC-GloSensor plasmid (1 μ g) was then transiently transfected into the cells by using the Effectene reagent (Qiagen, Hilden, Germany). After 18 h of transfection, the cells were washed with 2 mL of complete medium and 3 mL of fresh complete medium was added to the cells and incubated for an additional 24 h. A bioluminescence-based cAMP assay was conducted using the GloSensor cAMP assay kit (Promega) following manufacturer's instructions (Fan *et al.* 2008). The cells were pre-equilibrated for 2 h with the GloSensor cAMP reagent and dispensed into 96-well plates (2×10^6 cells per mL). After loading, the cells were treated with ligands and luminescence was measured on a Berthold Orion II Microplate luminometer using the kinetic protocol (a maximum cAMP signal was reached in 8–11 min.). The results represent the average of three experiments.

Measurement of Ado-induced calcium release

The fluorescent calcium indicator Fura-2 was employed to monitor changes in intracellular calcium ion concentration (Grynkiewicz *et al.* 1985) with modifications according to (Torfs *et al.* 2000). Cells were resuspended in insect Elliot buffer (129.7 mM NaCl, 5.44 mM KCl, 1.2 mM MgCl₂·6H₂O, 4.2 mM NaHCO₃, 7.3 mM NaH₂PO₄, 20 mM HEPES, 63 mM saccharose; pH 6.2) supple-

mented with 1 mM CaCl₂, 4 mg/mL Fura-2 acetoxymethyl ester (Molecular Probes, Eugene, OR, USA), 10 mM glucose, and 1 mM probenecid and incubated in the dark for 30 min at 22°C. Then a coverslip with the attached cells was washed in fresh medium, inserted into a recording chamber and placed on a stage of an inverted fluorescence microscope (Nikon, Tokyo, Japan). The cells were alternatively illuminated at 340 nm and 380 nm and the emitted light was recorded at 510 nm using the Hammamatsu CCD camera. The cells were kept in 0.5 mL of the basal medium and were stimulated by adding 0.5 mL of the medium containing Ado. The recording chamber was kept at 25°C.

Real-time RT-PCR

Total RNA from *Drosophila* cells was isolated using the RNA Blue reagent (Top-Bio, Prague, Czech Republic). The RNA was further purified by NucleoSpin RNA II kit (Macherey-Nagel, Duren, Germany) including on-column digestion step with rDNase I. One microgram of total RNA was reversely transcribed at 42°C using oligo(dT)₁₇ and PrimeScript Reverse Transcriptase (Takara Bio Inc., Shiga, Japan).

The PCR reaction volume was 20 μ L, containing 10 μ L of diluted cDNA and reaction mix [Hot start ExTaq polymerase (Takara) 0.75 unit, ExTaq buffer, dNTPs 200 μ M each, Syber green 1 : 25 000, primers 400 nM each]. The amplification was carried out on a Rotor-Gene 3000 (Corbet Research, Sydney, Australia) for 50 cycles (94°C for 20 s; 62°C for 30 s; 72°C for 30 s) following an initial denaturation/Taq activation step (95°C for 2 min). Each sample was analyzed in triplicate. Primers (sequences shown in Table 1) were designed with Lasergene PrimerSelect Software (DNASTAR, Madison, WI, USA) to assure that each amplicon encompassed an exon/intron boundary. The product size was confirmed by melting analysis. Data were analyzed and quantified with the Rotor-Gene 6 analysis software. Relative values were normalized to the *Rack1* cDNA and standardized to the Cl.8+ sample. All results are presented with means and SEM from four independent biological samples.

Fly strains and survival experiments

Transgenic fly strains *w; UAS-DmAdoR* and *w; DmAdoR¹* were described previously (Dolezelova *et al.* 2007); other strains, including *yw; UAS-GFP; act-gal4:PR* (Rogulja and Irvine 2005) and *w¹¹¹⁸* were provided by the Bloomington Stock Center (Indiana University, Bloomington). Mutant *w; DmAdoR¹* was isogenized to *w¹¹¹⁸* for eight generations. Flies were kept on a cornmeal–yeast–agar–sugar diet supplemented with the mold inhibitor methylparaben at 25°C. After hatching, first instar larvae of isogenized *w; DmAdoR¹* or *w¹¹¹⁸* were collected and transferred to vials containing

Table 1 List of primers used in real-time RT-PCR

Primer name	Sequence
DmRack1-fw	CCC GTG ACA AGA CCC TGA T
DmRack1-rev	TAG TTG CCA TCG GAG GAG AG
DmAdoR-fw	CCC ATC TGA ACT CGG CGG TAA ATC
DmAdoR-rev	GCC TCC TGC TGC TGC CTC AAC

3 mL of fly food with or without the addition of Ado or its analog CADO (final concentration 500 µg/mL). Numbers of pupae were counted twice a day around the 120-h time point (when the first larvae start to pupariate). 150 larvae per sample were analyzed. Late third instar larvae containing *wP; UAS-DmAdoR/act-gal4:PR* (or control flies without *UAS-DmAdoR*) were injected with 50 nL of Ringer's solution containing 170 µM SCH58261 and 0.6% DMSO or 0.6% DMSO alone, respectively. The injection volume was approximately 5% of the total larval volume. Injected larvae were transferred into vials with cornmeal–yeast–agar–sugar diet at 25°C (30 injected larvae per vial). Numbers of pupae were counted and compared with numbers of eclosed flies.

Sequence alignment, amino acid numbering, GenBank accession numbers

The alignment of several G protein-coupled receptors was performed using the MEGA 4 software (Tamura *et al.* 2007). To simplify the identification of corresponding residues in human and *Drosophila* AR, we used the index system established by Ballesteros and Weinstein (1995). The numbering is based on the relative position of each amino acid residue to the most conserved residue in each transmembrane (TM) segment (the most conserved residue in each TM domain is designated x.50, where x is the TM helix number). The GenBank accession numbers of ARs used in this paper are: no. NP_651772 (*DmAdoR*); no. NP_000665 (human A1R), no. NP_000666 (human A2AR), no. NP_000667 (human A2BR) and no. CAA54288 (human A3R).

Statistical methods

Data are presented as means ± SEM of the number of independent experiments indicated in Figure legends. In concentration–response experiments, EC₅₀ (half maximal effective concentration) was determined by non-linear regression using Graphpad Prism v5.0 software (GraphPad, San Diego, CA, USA).

Results

DmAdoR –mediated stimulation of cAMP in *Drosophila* cells

We first tried to detect the Ado-induced cAMP responses in *Drosophila* imaginal disc Cl8+ cells, but we did not obtain any response. We therefore examined the *DmAdoR* mRNA levels and found that these cells demonstrate rather low endogenous receptor mRNA expression (Fig. 2). We tried to over-express *DmAdoR* in these cells, however, the transfection and over-expression of recombinant *DmAdoR* did not improve the outcome of the Ado signaling assays. As the transfection was cytotoxic, the cells grew poorly, and the level of expressed *DmAdoR* mRNA remained very low.

To find another cell line with a higher endogenous level of *DmAdoR* expression, we employed real-time RT PCR and examined several *Drosophila* cell lines of different tissue origin, including embryonic S2, hematopoietic Mbn2, and neuroblast Bg2-c2 cells. We also compared the mRNA concentrations in these cell lines with the levels of *DmAdoR* mRNA in adult fly body parts. As is shown in Fig. 2, the expression of *DmAdoR* varies substantially among the cell

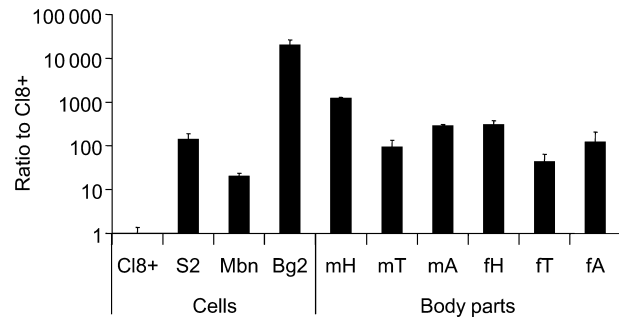


Fig. 2 Expression of *DmAdoR* mRNA in *Drosophila* cell lines and imago body parts. Real-time RT PCR was performed in order to compare the expression of *DmAdoR* in four cell types (Cl8+, S2, Mbn2, Bg2-c2) and adult male (m) and female (f) body parts including head (H), thorax (T) and abdomen (A). *Rack1* mRNA was used as an internal control. Ordinate: The level of mRNA is expressed as a log of ratio relative to Cl8+ cells.

lines and tissues examined. Bg2-c2 cells displayed the highest level of *DmAdoR* mRNA expression, which was about 10 times higher than the natural receptor mRNA level found in heads of male flies. The level of receptor mRNA in S2 cells was about 10 times lower than that in the heads of male flies and comparable to other parts of the fly examined (female heads, thorax and abdomen of both male and female flies) but still about 100 times higher than in Cl8+ cells. The Bg2-c2 and the S2 cells were therefore used in most of the subsequent experiments.

The examination of Ado-stimulated cAMP induction in Bg2-c2 and S2 cells transiently transfected with pGloSensor reporter showed a concentration dependent Ado-specific increase in the cAMP readout (Fig. 3a and b). This response was strong and robust in Bg2-c2 cells (about 200% induction) and, in line with the smaller *DmAdoR* mRNA expression, much lower in S2 cells (about 50% induction, Fig. 3a). The estimated EC₅₀ values were 4.2 (95% confidence interval 3.7–4.8 µM) and 55 µM (95% confidence interval 13–236 µM) in Bg2-c2 and S2 cells, respectively (Fig. 3a and b).

Lack of adenosine receptor-mediated calcium responses in *Drosophila* cells

The intracellular free calcium release upon Ado stimulation of Fura-2-loaded Bg2-c2 and S2 cells was investigated by digital imaging fluorescence microscopy. Application of the calcium ionophore, ionomycin was used as a positive control to demonstrate that the calcium detection system worked properly. As shown in Fig. 4, the resting calcium concentration was very stable and the addition of ionomycin to the cells in the presence of extracellular calcium caused the expected maximal increase in the signal. However, Ado failed to stimulate a detectable increase in the concentration of calcium in both S2 and Bg2-c2 cells (Fig. 4a and b). Marginal calcium responses (just above the detection limit) were observed only in some samples of Bg2-c2 cells treated

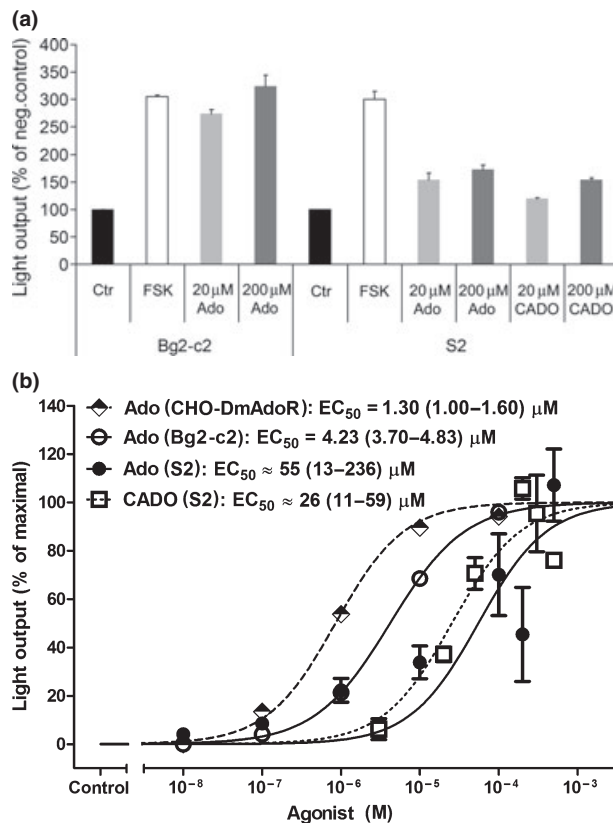


Fig. 3 The responses of Bg2-c2, and S2 cells to Ado and CADO. (a) The cells were treated with 20 or 200 μM Ado, 20 or 200 μM 2-chloroadenosine (CADO) and 20 μM forskolin (FSK). The cAMP production induced by Ado (ordinate, expressed in percent of control) was proportional to the level of adenosine receptor mRNA while forskolin-induced comparable responses in both cell types. (b) Comparison of Ado-induced cAMP accumulation in Bg2-c2 (open circles) and S2 cells (closed circles). The CADO-induced cAMP accumulation in S2 cells is also included (open square). Concentration–response curves of cAMP production in response to extracellular Ado in Bg2-c2 and S2 cells is expressed as percent of calculated maximal response (ordinate) in individual experiments. Values represent the mean ± SEM of four values obtained in one experiment for Bg2-c2 cells and 3–9 values from two independent experiments for S2 cells. Abscissa: molar concentration of analogs. The EC_{50} values of Ado and CADO with 95% confidence limit are shown in graph. For comparison, the dotted line with diamond symbols illustrates the concentration–response curve of DmAdoR over-expressed in Chinese hamster ovary cells, published earlier by Dolezelova *et al.* (2007). Sigmoidal concentration–response equation was fitted to normalized data.

with a high (100 μM) concentration of Ado. We conclude that there is no or very little calcium signal in response to Ado in the *Drosophila* cells examined.

Determining ligand specificity and pharmacological profile of DmAdoR

The ability of potential physiologically relevant natural ligands to activate DmAdoR was examined using cAMP

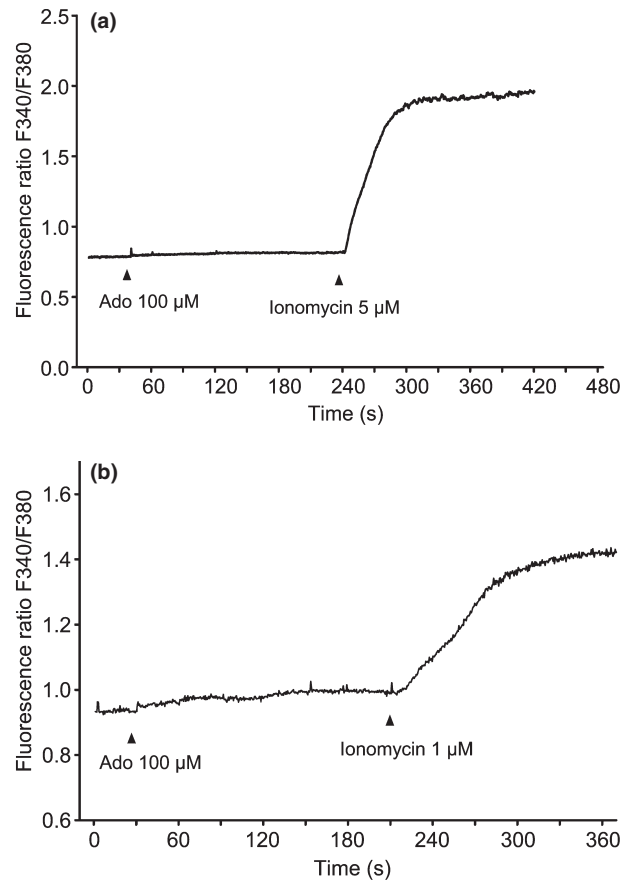


Fig. 4 Determination of intracellular calcium in response to Ado stimulation in *Drosophila* S2 and Bg2-c2 cells. The calcium level is unaffected by Ado treatment in S2 cells (a) and has at best a marginal effect in Bg2-c2 cells (b). Ionomycin in the presence of extracellular calcium elicits a maximal signal in both cell lines. Ordinate: fluorescence emission ratio recorded at 510 nm after alternating excitation at 340 and 380 nm.

functional assays and Bg2-c2 cells. We examined deoxyadenosine (dAdo), inosine and guanosine and found that inosine and guanosine do not activate DmAdoR and dAdo has only a marginal effect (Fig. 5a).

To further characterize the ligand sensitivity of the DmAdoR, we assayed various structural Ado analogs, including CHA, CPA, CCPA, CADO, IB-MECA, ADAC, CV1808, CGS 21680 and NECA. In the first set of experiments these ligands were tested in Bg2-c2 cells for downstream signaling (cAMP production) at two concentrations – 10 and 100 μM. The results showed that a number of analogs displayed an increase in cAMP levels, including CADO, CHA, CPA, CCPA, CV1808 and ADAC (Fig. 5b). In the next set of experiments, concentration–response relationship of ADO, CADO, CV1808, and CHA (Figs 3b and 5c, Table 2) was determined. The rank order of the tested agonist potency was CHA > ADO > CADO = CV1808 and the efficacy CADO > CV1808 = ADO > CHA. At an equi-

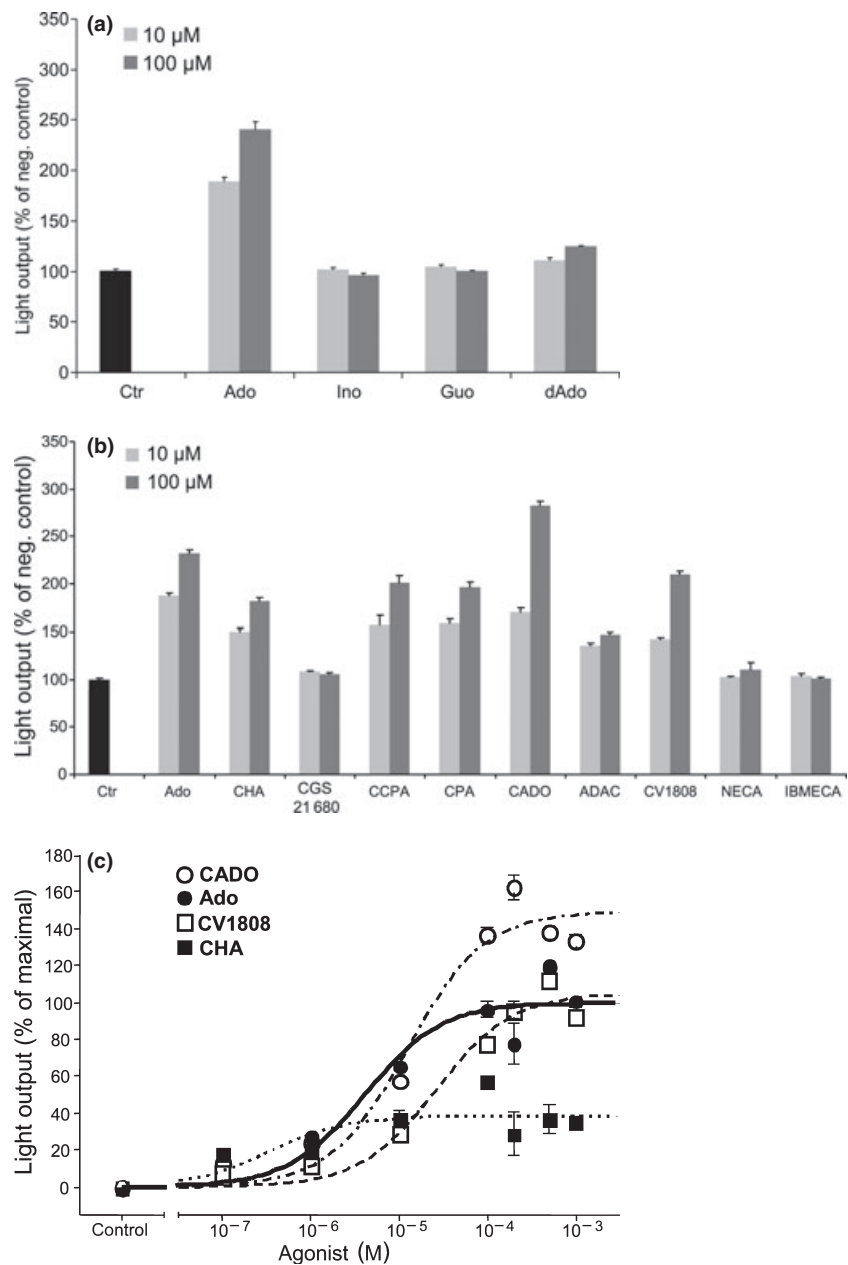


Fig. 5 Effects of AdoR agonists on cAMP accumulation in Bg2-c2 cells. (a, b) The cell responses to 10 and 100 μM concentration of Ado, or indicated potential AdoR agonists. The increase in cAMP concentration is expressed as a percentage of the basal level. (c) Concentration–response curves of cAMP accumulation in response to extracellular Ado and adenosine receptor agonist CADO, CV1808, and CHA. Individual points are expressed as a percentage of the maximal Ado response (ordinate) and represent mean \pm SEM of 3–6 values. Abscissa: molar concentration of agonist. Sigmoidal concentration–response equation was fitted to normalized data. Parameters of fits are given in Table 2.

Table 2 Parameters of concentration–response curves (shown in Fig. 5C) of agonist-induced cAMP accumulation in Bg2-c2 cells

Agonist	EC ₅₀ (log M)	E _{max} (% of Ado)
Ado	-5.39 \pm 0.23	100 \pm 7
CADO	-4.91 \pm 0.17	150 \pm 8
CV1808	-4.58 \pm 0.16	105 \pm 6
CHA	-6.47 \pm 0.47	38 \pm 5

molar 100 μM concentration, the CCPA, CPA, and ADAC reached 76, 73, and 46 percent of the Ado effect, respectively, while CGS21680 and other analogs including

NECA and IB-MECA had no effect (Fig. 5b). The potency of CADO-induced cAMP response was slightly higher in Bg2-c2 cells (12 μM) than in S2 cells (26 μM), as shown in Figs 3b and 5c.

We also examined activity of various antagonists on DmAdoR by assaying their ability to inhibit an Ado-stimulated cAMP response. The Bg2-c2 cells pre-loaded with GloSensor reagent were pre-incubated with 1 μM and 10 μM concentrations of antagonist for 5 minutes, followed by an addition of 10 μM concentration of Ado. As shown in Fig. 6a, the following order of potency was observed: SCH442416 \geq ZM241385 \geq SCH58261 > XAC > CGS15943. Pre-incubation with 1 and 10 μM SCH442416, 10 μM

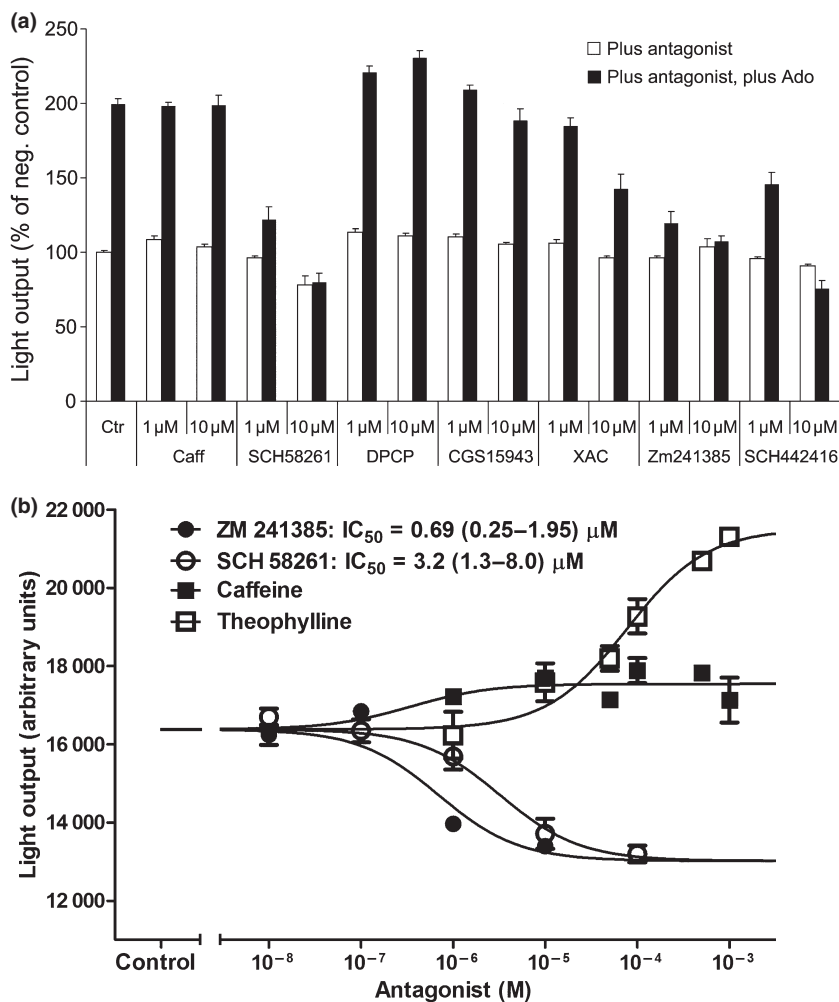


Fig. 6 Effects of AdoR antagonists on Ado-stimulated cAMP accumulation in Bg2-c2 cells. (a) The Bg2-c2 cells were pre-incubated for 5 min with 1 or 10 μM antagonist. The cells were then treated with 10 μM Ado and the cAMP accumulation was measured using the pGloSensor assay. The left chart (empty) columns are data prior to Ado treatment, the right chart (filled) columns are the records, taken after 10 μM Ado treatment. Ctr indicates control without the addition of antagonist. Columns represent mean ± SEM of 3–6 values. (b) Concentration–response curves of cAMP accumulation in response to DmAdoR antagonists. The Bg2-c2 cells were pre-incubated for 5 min with various concentrations of antagonists and then cells treated with 10 μM Ado. Individual points are expressed in arbitrary units (ordinate) and represent mean ± SEM of three values. The 50% effective concentrations of SCH 582261 and ZM 241385 (IC_{50} value with 95% confidence limits) are shown in graph.

SCH58261, and 10 μM ZM241385 completely prevented Ado-stimulated cAMP accumulation (Fig. 6a). XAC at a 10 μM concentration inhibited the increase of cAMP by about 50% but higher XAC concentrations did not cause full inhibition. Interestingly, simple xanthines like caffeine, theophylline and DPCPX failed to antagonize DmAdoR signaling (Fig. 6a and b). Slight increase in cAMP signal induced by high caffeine and theophylline concentrations (Fig. 6b), may not be receptor specific and results rather from phosphodiesterases inhibition.

To study the functional diversity of AR, we tried to find a correlation of the differences in the ligand selectivity and sequence variations among the DmAdoR and human ARs. We aligned DmAdoR with human A2AR and several AR-like sequences found in GenBank. We found that amino acids involved in contact with the Ado are perfectly conserved in *Drosophila* AdoR and these amino acid residues might be used as an important character to recognize AR orthologs in distant species. They include amino acid residues N6.55, F5.29, I.7.39, S7.42, H7.43, L6.51 and W 6.48 (Fig. 1 and Figure S1). Similarly, 6 of the 11 A2AR

amino acid residues, which make contact with the antagonist ZM241385, were conserved between A2AR and DmAdoR (Figure S2).

Function of adenosine receptor analogs *in vivo*

The ectopic expression of DmAdoR in flies was shown earlier to cause gain of function phenotypes ranging from melanotic tumors to lethality, depending on the level and tissue specificity of over-expression (Dolezelova *et al.* 2007). To verify the effect of DmAdoR antagonists *in vivo*, we examined the ability of SCH58261 to rescue the lethal effect of DmAdoR over-expression. We administered the SCH58261 both by feeding and microinjection. Virtually no eclosed adults over-expressing DmAdoR under *act-gal4:PR* driver emerged in untreated (control) flies. We did not observe any influence of the Ado receptor antagonists SCH58261 in the fed flies probably because of its low water solubility. However, the microinjection at the dosage of 50 nL of 170 μM SCH58261 in Ringer's solution into the third instar larvae partially rescued the lethality and led to the emergence of approximately 20% of adult flies (Fig. 7a). The

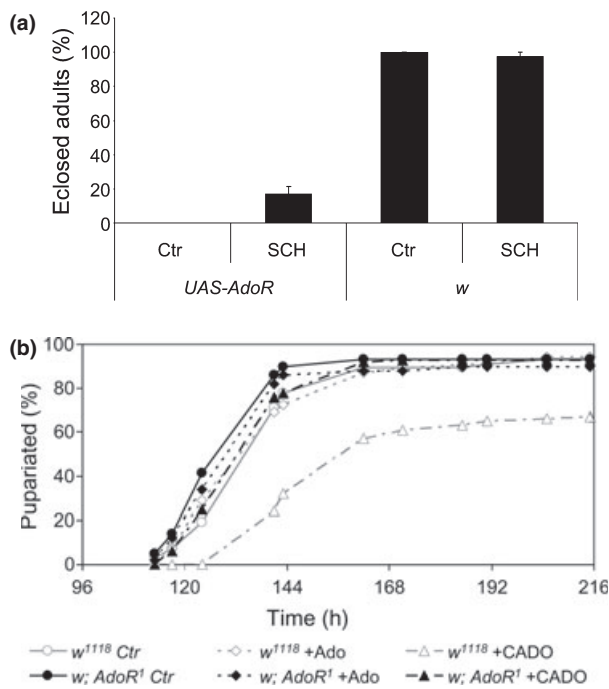


Fig. 7. *In vivo* effect of DmAdoR agonists and antagonists. (a) Antagonist SCH58261 rescues pupal lethality of DmAdoR over-expressing flies. (Ctrl) Control L3 larvae injected with 50 nL of vehicle (0.6% DMSO in Ringer solution), (SCH) L3 larvae injected with 50 nL of 170 μ M SCH58261. Fly genotypes: “UAS-AdoR” - *w*; UAS-DmAdoR/act-gal4:PR; “*w*” - control genotype, *w*; +/act-gal4:PR (b) Stable Ado agonist CADO causes larval lethality and developmental delay in *wt* flies but not in *DmAdoR* null mutants. First instar larvae were transferred to control fly food (Ctrl) or fly food containing 500 μ g/mL of CADO or Ado.

dosage of 55 μ M SCH58261 was already too low to rescue the phenotype. Consistently, the administration of XAC, which is a less potent DmAdoR antagonist, did not show any rescue of flies (not shown). Our survival assay thus confirmed the utility of SCH58261 for *in vivo* experiments in flies.

We also tested if agonist treatment in *wt* flies results in the lethality characteristic for DmAdoR over-expression and whether *null* mutants in the *DmAdoR* gene (*DmAdoR*₁) are resistant to the treatment. Indeed, the feeding of *wt* flies with CADO led to developmental delays as well as larval and pupal lethality observed previously with DmAdoR over-expression (Dolezelova *et al.* 2007). Consistent with this result, *DmAdoR*₁ mutants were resistant to CADO treatment (Fig. 7b), confirming that the CADO effect is mediated by DmAdoR. Ado administered at the same dosage in food did not show any effect, most likely due to Ado degradation in the gut.

Discussion

Our previous results on the activation of second messenger pathways in heterologous CHO cells over-expressing

DmAdoR showed a concentration-dependent increase in both intracellular cAMP and calcium (Dolezelova *et al.* 2007). Now, we confirmed that Ado activation of endogenous DmAdoRs in *Drosophila* cells induces cAMP accumulation. The Bg2-c2 and S2 cells responded to Ado by an increase in intracellular cAMP level in a concentration-dependent manner, with EC₅₀ values of approximately 4 and 55 μ M, respectively (Fig. 3a and b). There was an influence of the Ado solvent DMSO, which slightly interfered with the measurements, affecting especially low responses of S2 cells. The EC₅₀ value received for Ado in S2 cells is therefore very approximate and had to be confirmed with metabolically more stable agonist CADO (the responses of Bg2-c2 and S2 cells to CADO showed EC₅₀ values of approximately 12 and 26 μ M, respectively; Figs 3b and 5c). The different potency of the same Ado receptor response can be explained by either the dissimilarity of cells in which the receptor is expressed or the level of receptor expression. Our results are consistent with the latter explanation. Ado at 200 μ M concentration increased cAMP level 3 times in Bg2-c2 cells but only 1.5 times in S2 cells (Fig. 3a). This difference cannot be explained by unequal ability to produce cAMP because the direct activator of adenylyl cyclase forskolin had the same effect in Bg2-c2 and S2 cells. S2 cells also seem to have similar amount of G α s subunits (Figure S3) and low level of adenosine deaminase activity (Zurovec *et al.* 2002) when compared with Bg2-c2 cells. However, this divergence fits well with the receptor mRNA expression level, which is about 100 times higher in Bg2-c2 cells than in S2 cells (Fig. 2). Considering also the lack of Ado-induced cAMP response in Cl.8+ cells, which demonstrate about 10 times lesser receptor gene expression level than S2 cells, we conclude that the level of the Ado-induced cAMP response is proportional to that of *DmAdoR* mRNA expression and the naturally expressed receptor in the tested cells demonstrates low or no receptor reserve.

In contrast to our previous results obtained using CHO cells over-expressing *Drosophila* DmAdoRs (Dolezelova *et al.* 2007), we observed no effect of Ado on the concentration of free intracellular calcium in either of the tested *Drosophila* cell types. This discrepancy can also be explained by the high level of receptor expression in CHO cells. The EC₅₀ value for Ado-induced cAMP accumulation was about three to four times lesser in previous experiments (see dotted trace in Fig. 3b) than the one found in this study for Bg2-c2 cells. This result suggests the presence of a receptor reserve, which when activated can interact with a non-preferential signaling pathway(s). Our results are in line with reports showing that other heterologously over-expressed G protein-coupled receptors interact with multiple G-protein subunits (Robb *et al.* 1994; Reale *et al.* 1997; Jakubik *et al.* 2006; Michal *et al.* 2007), including mammalian ARs (Fredholm *et al.* 2007), and that activation of non-preferential G-protein signaling depends on receptor

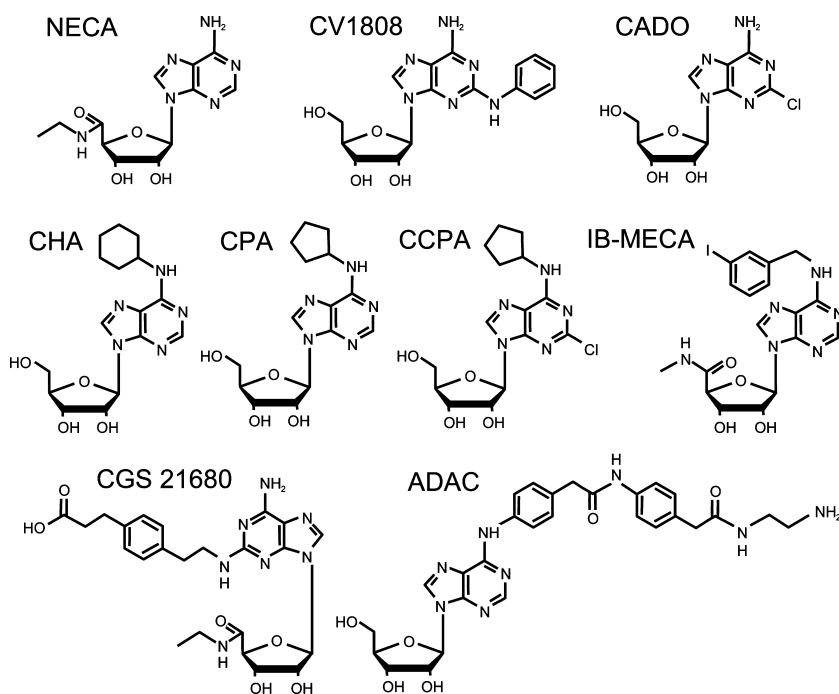


Fig. 8 Adenosine receptor agonists used in this study.

expression level (Michal *et al.* 2001). Our results thus demonstrate that in *Drosophila* cells cAMP is the preferred physiological second messenger in DmAdoR signaling.

Establishing a general pharmacological profile of the receptor is a key step towards the molecular characterization of DmAdoR signaling. From the functional point of view (stimulation of cAMP synthesis) DmAdoR resembles A2 isoforms in mammals. Recent studies on human A2A structure (Kim *et al.* 2003; Jaakola *et al.* 2008; Lebon *et al.* 2011; Xu *et al.* 2011) have described contact amino acid residues needed for ligand binding. These residues are highly conserved among human isoforms but the differences in selectivity of various Ado analogs binding and receptor activation are not yet well understood.

Most agonists of human AR carry substitutions in the C2 or N6 positions of the adenine ring or in the 5' position of the ribose (Yan *et al.* 2003) (Fig. 8). The agonists NECA and UK-432097 used for the A2AR co-crystallization (Lebon *et al.* 2011; Xu *et al.* 2011) share the 5' carboxyl substitutions of ribose while UK-432097 contains the two additional substitutions in the adenine ring (see Figure S1). According to these studies, the amino acid residues H6.52 and T3.36 are involved in interactions between the receptor and the 5' carboxyl substituted Ado analog. We found that unlike human receptor subtypes DmAdoR does not tolerate the 5' carboxyl substitutions of ribose. The difference between DmAdoR and mammalian ARs may be due to the difference in residues H6.52 and T3.36 which are conserved in mammalian receptors but replaced by Y and C, respectively, in DmAdoR. We examined three 5'-substituted Ado analogs including the non-selective human ARs agonist NECA, A3R

selective agonist IB-MECA, and A2AR selective agonist CGS 21680. Regardless of the presence or absence of substitutions in the C2 or N6 positions of the adenine ring they did not activate DmAdoR. Earlier study (Kim *et al.* 1995) reported that the point mutation of H6.52 for Y in A2AR strongly reduced binding affinity of certain agonists. However, this reduction was much less pronounced for the 5'-carboxyl substituted analog NECA and CGS. As DmAdoR carries the same amino acid replacement it seems that the difference between mutated human A2AR and DmAdoR is due to the difference of the amino acid residues at position 3.36 (T is replaced by C in DmAdoR) or another alternative interaction.

The most efficacious agonists at DmAdoR were C2-substituted adenine analogs. The non-selective (with respect to mammalian AR) agonist CADO carrying a relatively small chlorine atom at the C2 position is an even more potent DmAdoR agonist than Ado itself. Our results show that DmAdoR can tolerate even larger C2 substituents including a phenylamino group of CV1808 (see Fig. 8), making its pharmacological profile more similar to human A2R. The N6 substituted analogs of Ado are selective agonists of the human A1R (Jacobson 2009). We found that all tested N6 substituted analogs CHA, CPA, and ADAC are weak agonists of DmAdoR. We searched for the difference in binding site between A2AR and A1R, which is shared with DmAdoR. Such difference is in the 7.35 position which is occupied by M in A2AR but bears a substitution M → T in both A1R and DmAdoR (Fig. 1). The M7.35 residue was previously implicated in the direct interaction of A2AR with the antagonist ZM241385 (Jaakola *et al.* 2008) (Figure S2)

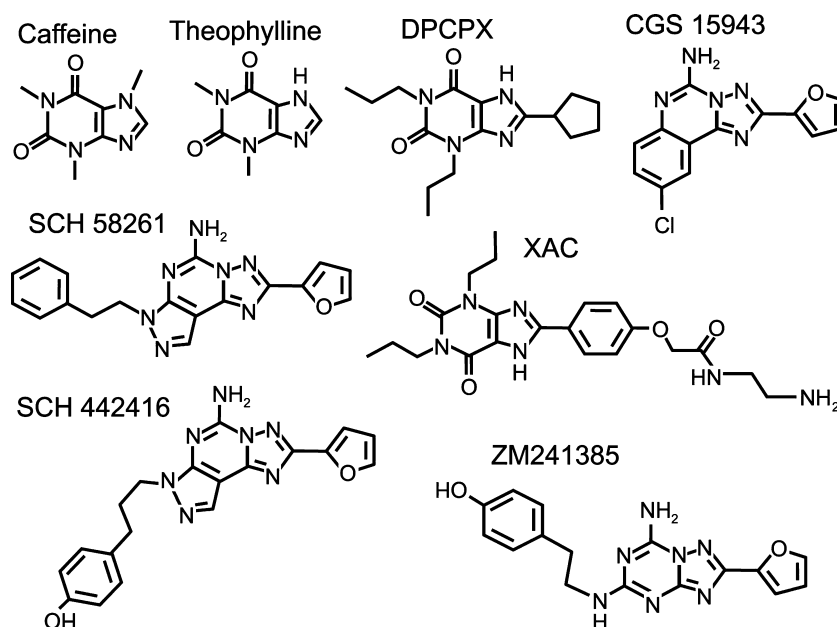


Fig. 9 Adenosine receptor antagonists used in this study.

and we suggest that T7.35 plays a role in the N6-substituted agonist selectivity of A1R and activation of DmAdoR.

The key feature that differentiates agonists from corresponding antagonists is the presence of the ribose ring (Xu *et al.* 2011) (Fig. 9). The most common weak non-selective AR antagonists are xanthines. Interestingly, simple xanthines including caffeine and theophylline, which bind to all human AR subtypes with submicromolar affinity and more potent A1R selective derivative DPCPX did not prevent Ado-induced DmAdoR activation (Fig. 6a). In addition, non-xanthine human AR antagonist CGS 15943 with affinity range 1–30 nM in human AR subtypes also showed no inhibition of DmAdoR. A marginal antagonistic activity was detected only for the non-selective antagonist XAC.

The best DmAdoR antagonists were non-xanthine polyheterocycles, which also all work as human A2AR-selective antagonists (Muller and Jacobson 2011). They include ZM241385, SCH58261 and SCH442416. The structural analysis of the A2AR-ZM241385 complex reported earlier (Jaakola *et al.* 2008) showed that 11 amino acid residues were crucial for the antagonist-receptor contacts. Interestingly, five of the 11 human A2AR amino acid residues that make contact with the ligand are conserved between A2AR and DmAdoR (Figure S2). The substitution of V5.30 for a E5.30 in human A3R was predicted to contribute to the low affinity of ZM241385 for A3AR (Pirainen *et al.* 2011). However, the same difference in DmAdoR does not eliminate the antagonistic activity of ZM241385 in DmAdoR.

Differences in pharmacological effect of some of the tested Ado analogs between DmAdoR and human A2AR can be partially explained by replacement of specific key amino acid residues disclosed by alignment of these two receptors.

Based on the pharmacological profile, sequence similarity and cAMP-linked signaling, the most closely related human subtype appears to be A2AR, while the high EC₅₀ values are more reminiscent of A2B receptor.

The availability of new drugs will accelerate research of Ado signaling in *Drosophila* and other insects. Synthetic AR agonists typically persist in the body much longer than Ado. The employment of the most efficacious agonist, CADO, in flies *in vivo* mimicked the phenotype of DmAdoR over-expression, whereas the most potent antagonist, SCH58261, rescued the flies from the lethality caused by DmAdoR over-expression (Fig. 7a). CADO is more stable in the organism than Ado but does not affect DmAdoR₁ mutant flies (Fig. 7b). This observation proves that CADO effect is mediated by native DmAdoR. Our *in vivo* experiments show that both the CADO and SCH58261, by stimulating or inhibiting the DmAdoR-mediated cAMP response, mimic the phenotypes of the DmAdoR receptor over-expression or knockout. As Ado also influences physiology of all cells via Ado transport, the pharmacological approach will allow separating the effects of signaling through AR from the effects on Ado transport in physiological experiments.

The involvement of Ado in many distinct physiological functions such as neuromodulation, defense responses, metabolic stress responses, and even altered regulation of lipolysis and lipogenesis in *Drosophila* has been demonstrated (Dolezal *et al.* 2005; Knight *et al.* 2010; Zuberova *et al.* 2010). These physiological functions of Ado confirm an ancient origin of Ado signaling. In addition, they show a great deal of similarity with responses in mammals where Ado effects are mediated by four AdoR subtypes (for a review, see Wei *et al.* 2011). It points to the importance of

studies on molecular mechanisms and physiological outcomes of DmAdoR activation. The confirmation of the DmAdoR coupling with cAMP signaling and the establishment of DmAdoR pharmacological profile are important steps towards understanding the complexity of Ado responses in this genetically tractable organism and constitute a necessary background for understanding evolution of Ado signaling.

Acknowledgements

This research was supported by grant P305/10/2406 from the Grant Agency of the Czech Republic, by Research Center Program MSMT – LC06077 and by grant KJB501410801 from the Grant Agency of the Academy of Sciences of Czech Republic. VD a ES were supported by projects AV0Z50110509 and MSMT LC554. This work was also supported by the infrastructure built with funding from the European Community's Seventh Framework Programme (FP7/2007-2013) under grant agreement no. 229518. We gratefully acknowledge the help of Vladimír Rudajev with western blottings and Helena Janíčková with binding experiments. The authors declare no conflict of interest.

Supporting information

Additional supporting information may be found in the online version of this article:

Figure S1. Schematic representation of interactions between A2AR and agonists – Adenosine (black lines), NECA (black and blue lines) and UK-432097 (black, blue and grey lines) according to Xu *et al.* (2011) and Lebon *et al.* (2011).

Figure S2. Schematic representation of the interactions (orange dashed lines) between A2AR and antagonist ZM241385 (according to Jaakola *et al.* 2008 and Piirainen *et al.* 2011).

Figure S3. Western blotting of cell lysates (25 µg) probed with anti-Gαs/olf antibody (C-18, cat. no. sc-383; Santa Cruz Biotechnology) including S2 cells (lines 1–4), Cl.8+ cells (line 5) and Bg2-c2 cells (lines 6–8).

As a service to our authors and readers, this journal provides supporting information supplied by the authors. Such materials are peer-reviewed and may be re-organized for online delivery, but are not copy-edited or typeset. Technical support issues arising from supporting information (other than missing files) should be addressed to the authors.

References

- Ballesteros J. A. and Weinstein H. (1995) Integrated Methods for Modeling G-Protein Coupled Receptors. *Methods Neurosci* **25**, 366–428.
- Brody T. and Cravchik A. (2000) *Drosophila melanogaster* G protein-coupled receptors. *J. Cell Biol.* **150**, F83–88.
- Broeck J. V. (2001) Insect G protein-coupled receptors and signal transduction. *Arch. Insect Biochem. Physiol.* **48**, 1–12.
- van Calker D., Muller M. and Hamprecht B. (1979) Adenosine regulates via two different types of receptors, the accumulation of cyclic AMP in cultured brain cells. *J. Neurochem.* **33**, 999–1005.
- Choi D. S., Cascini M. G., Mailliard W., Young H., Paredes P., McMahon T., Diamond I., Bonci A. and Messing R. O. (2004) The type 1 equilibrative nucleoside transporter regulates ethanol intoxication and preference. *Nat. Neurosci.* **7**, 855–861.
- Dolezal T., Dolezelova E., Zurovec M. and Bryant P. J. (2005) A role for adenosine deaminase in *Drosophila* larval development. *PLoS Biol.* **3**, e201.
- Dolezelova E., Nothacker H. P., Civelli O., Bryant P. J. and Zurovec M. (2007) A *Drosophila* adenosine receptor activates cAMP and calcium signaling. *Insect Biochem. Mol. Biol.* **37**, 318–329.
- Dunwiddie T. V. (1980) Endogenously released adenosine regulates excitability in the in vitro hippocampus. *Epilepsia* **21**, 541–548.
- Fan F., Binkowski B. F., Butler B. L., Stecha P. F., Lewis M. K. and Wood K. V. (2008) Novel genetically encoded biosensors using firefly luciferase. *ACS Chem. Biol.* **3**, 346–351.
- Fredholm B. B. (2010) Adenosine receptors as drug targets. *Exp. Cell Res.* **316**, 1284–1288.
- Fredholm B. B., Abbracchio M. P., Burnstock G., Daly J. W., Harden T. K., Jacobson K. A., Leff P. and Williams M. (1994) Nomenclature and classification of purinoceptors. *Pharmacol. Rev.* **46**, 143–156.
- Fredholm B. B., Chen J. F., Masino S. A. and Vaugeois J. M. (2005) Actions of adenosine at its receptors in the CNS: insights from knockouts and drugs. *Annu. Rev. Pharmacol. Toxicol.* **45**, 385–412.
- Fredholm B. B., Chern Y., Franco R. and Sitkovsky M. (2007) Aspects of the general biology of adenosine A2A signaling. *Prog. Neurobiol.* **83**, 263–276.
- Greene R. W. and Haas H. L. (1991) The electrophysiology of adenosine in the mammalian central nervous system. *Prog. Neurobiol.* **36**, 329–341.
- Grynkiewicz G., Poenie M. and Tsien R. Y. (1985) A new generation of Ca²⁺ indicators with greatly improved fluorescence properties. *J. Biol. Chem.* **260**, 3440–3450.
- Hasko G., Linden J., Cronstein B. and Pacher P. (2008) Adenosine receptors: therapeutic aspects for inflammatory and immune diseases. *Nat Rev Drug Discov* **7**, 759–770.
- Jaakola V. P., Griffith M. T., Hanson M. A., Cherezov V., Chien E. Y., Lane J. R., Ijzerman A. P. and Stevens R. C. (2008) The 2.6 angstrom crystal structure of a human A2A adenosine receptor bound to an antagonist. *Science* **322**, 1211–1217.
- Jacobson K. A. (2009) *Introduction to Adenosine receptors as Therapeutic Targets, Vol 193*. Springer-Verlag, Berlin, Heidelberg.
- Jacobson K. A. and Gao Z. G. (2009) Adenosine, in *Intercellular communication in the nervous system* (Malenka R. C., ed.), pp. 627–638. Elsevier, Boston, MA.
- Jakubik J., El-Fakahany E. E. and Dolezal V. (2006) Differences in kinetics of xanomeline binding and selectivity of activation of G proteins at M(1) and M(2) muscarinic acetylcholine receptors. *Mol. Pharmacol.* **70**, 656–666.
- Johansson S. M., Yang J. N., Lindgren E. and Fredholm B. B. (2007) Eliminating the antilipolytic adenosine A1 receptor does not lead to compensatory changes in the antilipolytic actions of PGE2 and nicotinic acid. *Acta Physiol (Oxf)* **190**, 87–96.
- Kim J., Wess J., van Rhee A. M., Schoneberg T. and Jacobson K. A. (1995) Site-directed mutagenesis identifies residues involved in ligand recognition in the human A2a adenosine receptor. *J. Biol. Chem.* **270**, 13987–13997.
- Kim S. K., Gao Z. G., Van Rompaey P., Gross A. S., Chen A., Van Calenbergh S. and Jacobson K. A. (2003) Modeling the adenosine receptors: comparison of the binding domains of A2A agonists and antagonists. *J. Med. Chem.* **46**, 4847–4859.
- Knight D., Harvey P. J., Iliadi K. G., Klose M. K., Iliadi N., Dolezelova E., Charlton M. P., Zurovec M. and Boulianne G. L. (2010) Equilibrative nucleoside transporter 2 regulates associative learn-

- ing and synaptic function in *Drosophila*. *J. Neurosci.* **30**, 5047–5057.
- Lebon G., Warne T., Edwards P. C., Bennett K., Langmead C. J., Leslie A. G. and Tate C. G. (2011) Agonist-bound adenosine A2A receptor structures reveal common features of GPCR activation. *Nature* **474**, 521–525.
- Linden J. (1994) Cloned adenosine A3 receptors: pharmacological properties, species differences and receptor functions. *Trends Pharmacol. Sci.* **15**, 298–306.
- Machado J., Abdulla P., Hanna W. J., Hilliker A. J. and Coe I. R. (2007) Genomic analysis of nucleoside transporters in Diptera and functional characterization of DmENT2, a *Drosophila* equilibrative nucleoside transporter. *Physiol. Genomics* **28**, 337–347.
- Michal P., Lysikova M. and Tucek S. (2001) Dual effects of muscarinic M(2) acetylcholine receptors on the synthesis of cyclic AMP in CHO cells: dependence on time, receptor density and receptor agonists. *Br. J. Pharmacol.* **132**, 1217–1228.
- Michal P., El-Fakahany E. E. and Dolezal V. (2007) Muscarinic M2 receptors directly activate Gq/11 and Gs G-proteins. *J. Pharmacol. Exp. Ther.* **320**, 607–614.
- Muller C. E. and Jacobson K. A. (2011) Recent developments in adenosine receptor ligands and their potential as novel drugs. *Biochim. Biophys. Acta* **1808**, 1290–1308.
- Peel D. J. and Milner M. J. (1990) The diversity of cell morphology in cloned cell lines derived from *Drosophila* imaginal discs. *Roux's Arch. Dev. Biol.* **198**, 479–482.
- Piirainen H., Ashok Y., Nanekar R. T. and Jaakola V. P. (2011) Structural features of adenosine receptors: from crystal to function. *Biochim. Biophys. Acta* **1808**, 1233–1244.
- Reale V., Hannan F., Midgley J. M. and Evans P. D. (1997) The expression of a cloned *Drosophila* octopamine/tyramine receptor in *Xenopus* oocytes. *Brain Res.* **769**, 309–320.
- Robb S., Cheek T. R., Hannan F. L., Hall L. M., Midgley J. M. and Evans P. D. (1994) Agonist-specific coupling of a cloned *Drosophila* octopamine/tyramine receptor to multiple second messenger systems. *EMBO J.* **13**, 1325–1330.
- Rogulja D. and Irvine K. D. (2005) Regulation of cell proliferation by a morphogen gradient. *Cell* **123**, 449–461.
- Samakovlis C., Asling B., Boman H. G., Gateff E. and Hultmark D. (1992) In vitro induction of cecropin genes—an immune response in a *Drosophila* blood cell line. *Biochem. Biophys. Res. Commun.* **188**, 1169–1175.
- Schneider I. (1971) Embryonic cell lines of *D. melanogaster*. *Drosophila Inform. Serv.* **46**, 111.
- Tamura K., Dudley J., Nei M. and Kumar S. (2007) MEGA4: Molecular Evolutionary Genetics Analysis (MEGA) software version 4.0. *Mol. Biol. Evol.* **24**, 1596–1599.
- Torfs H., Shariatmadari R., Guerrero F., Parmentier M., Poels J., Van Poyer W., Swinnen E., De Loof A., Akerman K. and Vanden Broeck J. (2000) Characterization of a receptor for insect tachykinin-like peptide agonists by functional expression in a stable *Drosophila* Schneider 2 cell line. *J. Neurochem.* **74**, 2182–2189.
- Trincavelli M. L., Daniele S. and Martini C. (2010) Adenosine receptors: what we know and what we are learning. *Curr. Top. Med. Chem.* **10**, 860–877.
- Ui K., Nishihara S., Sakuma M., Togashi S., Ueda R., Miyata Y. and Miyake T. (1994) Newly established cell lines from *Drosophila* larval CNS express neural specific characteristics. *In Vitro Cell. Dev. Biol.* **30A**, 209–216.
- Wei C. J., Li W. and Chen J. F. (2011) Normal and abnormal functions of adenosine receptors in the central nervous system revealed by genetic knockout studies. *Biochim. Biophys. Acta* **1808**, 1358–1379.
- Xu F., Wu H., Katritch V., Han G. W., Jacobson K. A., Gao Z. G., Cherezov V. and Stevens R. C. (2011) Structure of an agonist-bound human A2A adenosine receptor. *Science* **332**, 322–327.
- Yaar R., Jones M. R., Chen J. F. and Ravid K. (2005) Animal models for the study of adenosine receptor function. *J. Cell. Physiol.* **202**, 9–20.
- Yan L., Burbiel J. C., Maass A. and Muller C. E. (2003) Adenosine receptor agonists: from basic medicinal chemistry to clinical development. *Expert Opin Emerg Drugs* **8**, 537–576.
- Zuberova M., Fenckova M., Simek P., Janeckova L. and Dolezal T. (2010) Increased extracellular adenosine in *Drosophila* that are deficient in adenosine deaminase activates a release of energy stores leading to wasting and death. *Dis Model Mech* **3**, 773–784.
- Zurovec M., Dolezal T., Gazi M., Pavlova E. and Bryant P. J. (2002) Adenosine deaminase-related growth factors stimulate cell proliferation in *Drosophila* by depleting extracellular adenosine. *Proc Natl Acad Sci USA* **99**, 4403–4408.

Supplementary material:

Figure S1

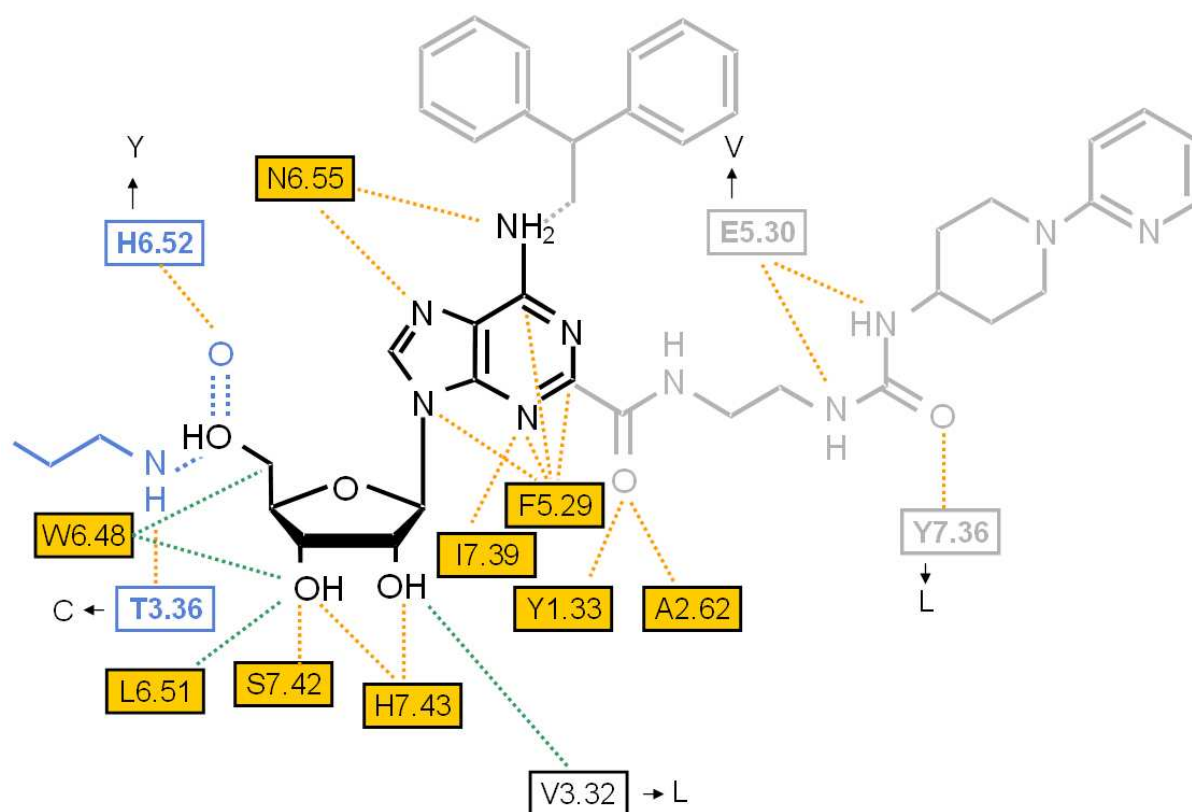


Figure S1. Schematic representation of interactions between A2AR and agonists - Adenosine (black lines), NECA (black and blue lines) and UK-432097 (black, blue and grey lines) according to Xu et al. (2011) and Lebon et al. (2011). Amino acid residues involved in contact with agonists are shown in boxes. The interactions described first by Xu et al. (2011) are shown as orange dashed lines, additional interactions of W6.48, L6.51 and V3.32 described by Lebon et al. (2011) are shown as green dashed lines. Residues conserved between A2AR and DmAdoR are highlighted by yellow boxes. Amino acid replacements in nonconserved positions are indicated by arrows and uppercase letters.

Figure S2

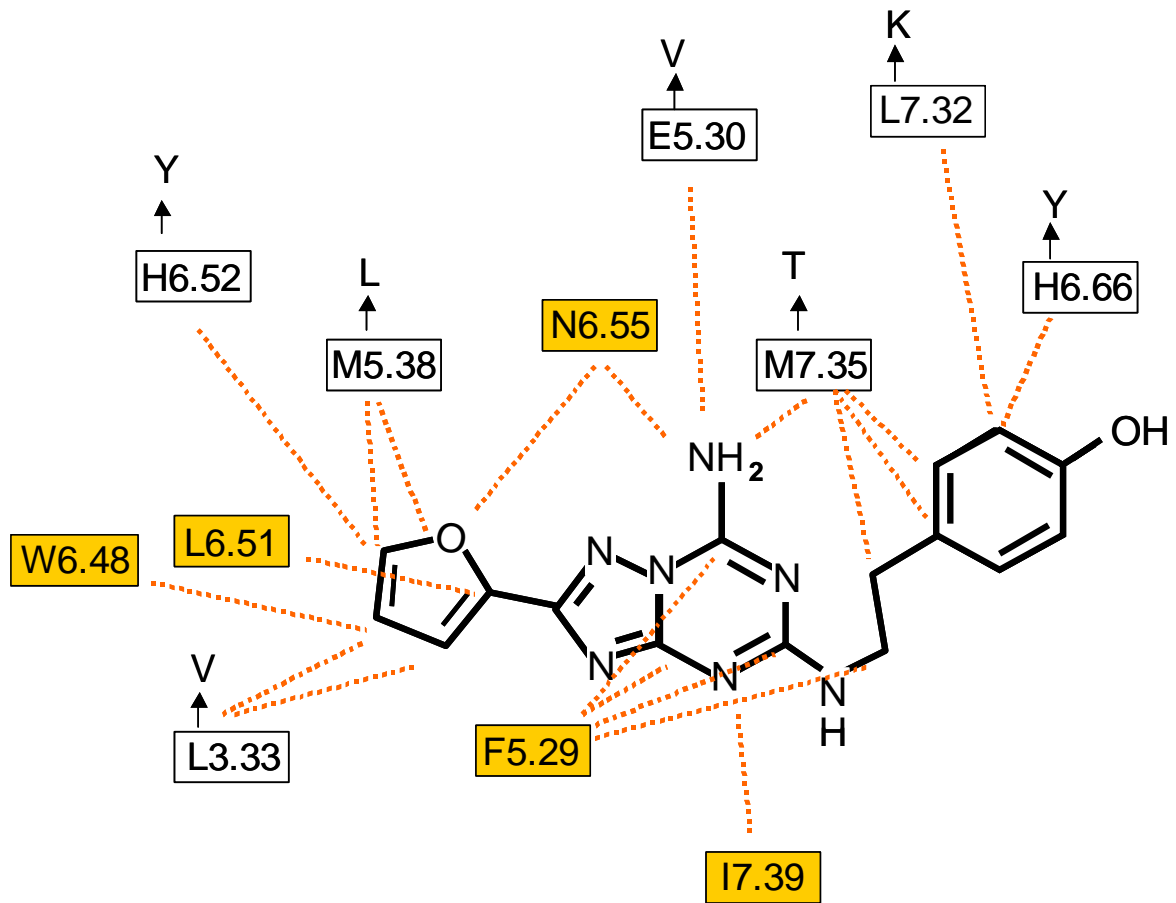


Figure S2: Schematic representation of the interactions (orange dashed lines) between A2AR and antagonist ZM241385 (according to Yaakola et al. 2008 and Piirainen et al. 2011). Amino acid residues involved in contact with ZM241385 are shown in boxes. Amino acid residues conserved between A2AR and DmAdoR are highlighted by yellow boxes. Amino acid replacements in nonconserved positions are indicated by arrows and uppercase letters.

Figure S3

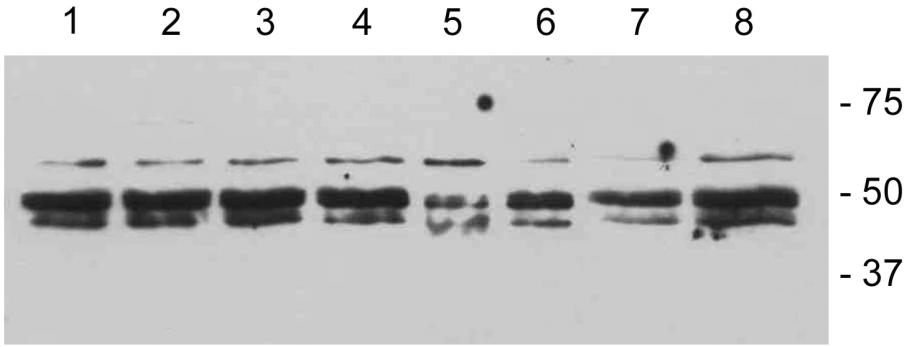


Figure S3: Western blotting of cell lysates (25 μ g) probed with anti-G α s/olf antibody (C-18, cat. No. sc-383, Santa Cruz Biotechnology) including S2 cells (lines 1-4), Cl.8+ cells (line 5) and Bg2-c2 cells (line 6-8). Position of molecular weight markers is shown on the right side of the figure.

5. Conclusion and future perspectives

This Ph.D. thesis significantly extends the knowledge of two important *Drosophila* growth regulators, the IDGF proteins and extracellular adenosine. The author of this thesis is the first author on the first publication and a co-author on the other three. The main conclusions are as follows:

- We determined the concentration of native IDGF2 in *Drosophila* hemolymph.
- We showed that recombinant IDGF2 has dose dependent effect on the cell viability of Cl.8+ cells in SFM
- We demonstrated that IDGF2 at physiologically relevant concentrations can protect the Cl.8+ cells from the toxic effect of some metabolites and xenobiotics.
- We showed that the cytoprotective effects of IDGF2 on Cl.8+ cells are independent on insulin and that IDGF2 has distinct effect on mitochondrial membrane potential than insulin and is also unable to activate insulin downstream targets (dS6K and dAkt).
- We conducted a transcriptional analysis of IDGF2-treated Cl.8+ cells and showed the up-regulation of genes connected with the Imd immune pathway and also some detoxification pathways.
- Based on our experiments we found that *Idgf2* is up-regulated in *Drosophila* larvae *in vivo* by aseptic or septic injury, but not in adults.
- We demonstrated that the highest concentration of IDGF2 protein *in vivo* is in *Drosophila* nephrocytes (pericardial and garland cells).
- We showed that *Idgf3* mutants have hemolymph clotting defects after wounding, the wound healing is significantly delayed and the mutant flies are more susceptible to microbial and nematode infection.
- We found that the flies overexpressing *Idgf3* have over-clotting problems.
- Based on our genome-wide transcriptional analysis of *Idgf3* mutant flies we showed that IDGF3 is involved in the regulation of innate defense mechanisms and signal pathways connected to wound healing as well as regenerative processes.
- We studied the response of several *Drosophila* cell lines to extracellular adenosine. We found that the wing imaginal disc Cl.8+ cells are most sensitive to high Ado concentration.
- From our experiments we concluded that Ado toxicity in Cl.8+ cells is exclusively dependent on the adenosine uptake. Adenosine induces massive ATP production and causes the loss of mitochondrial membrane potential followed by apoptosis.
- We found that IDGF2 can protect the Cl.8+ cells from the loss of mitochondrial membrane potential caused by high level of extracellular Ado, suggesting that Ado and IDGFs can interact *in vivo*.

- We show that endogenous AdoR in *Drosophila* cells *in vitro* stimulates cAMP second messenger pathway, but not calcium, as reported previously for the heterologous system of CHO cells.
- We identified more stable adenosine agonists and antagonists able to mimic or rescue the AdoR overexpression phenotype.

There are still many unsolved problems about IDGFs and adenosine signaling. In future I would like to focus on solving these questions:

- to test the crosstalk between Ado and IDGFs
- to test the effect of IDGFs and Ado on the activation of signaling pathways involved in cell division and stress, including ERK, JNK, p38, dS6K and dAkt with the help of commercially available antibodies
- to examine the effects of other recombinant IDGF proteins on cell growth
- to find the importance of glycosylation of IDGF proteins
- to find IDGF binding partners and exact glycoproteins to which IDGFs can bind
- to generate mutants in all IDGF genes
- to study the different IDGF2 isoforms detected by Vierstrate et al. with the help of mass spectrometry
- to find the exact role of IDGFs in immune response

6. References

- Arakane, Y., Muthukrishnan, S., 2010. Insect chitinase and chitinase-like proteins. *Cell Mol Life Sci* 67, 201-216.
- Arias, E.B., Verhage, H.G., Jaffe, R.C., 1994. Complementary deoxyribonucleic acid cloning and molecular characterization of an estrogen-dependent human oviductal glycoprotein. *Biol Reprod* 51, 685-694.
- Badariotti, F., Lelong, C., Dubos, M.P., Favrel, P., 2007. Characterization of chitinase-like proteins (Cg-Clp1 and Cg-Clp2) involved in immune defence of the mollusc *Crassostrea gigas*. *FEBS J* 274, 3646-3654.
- Badariotti, F., Lelong, C., Dubos, M.P., Favrel, P., 2011. Identification of three singular glycosyl hydrolase family 18 members from the oyster *Crassostrea gigas*: Structural characterization, phylogenetic analysis and gene expression. *Comp Biochem Physiol B Biochem Mol Biol* 158, 56-63.
- Baeg, G.H., Zhou, R., Perrimon, N., 2005. Genome-wide RNAi analysis of JAK/STAT signaling components in *Drosophila*. *Genes Dev* 19, 1861-1870.
- Barankiewicz, J., Danks, A.M., Abushanab, E., Makings, L., Wiemann, T., Wallis, R.A., Pragnacharyulu, P.V., Fox, A., Marangos, P.J., 1997. Regulation of adenosine concentration and cytoprotective effects of novel reversible adenosine deaminase inhibitors. *J Pharmacol Exp Ther* 283, 1230-1238.
- Barry, W.E., Thummel, C.S., 2016. The *Drosophila* HNF4 nuclear receptor promotes glucose-stimulated insulin secretion and mitochondrial function in adults. *Elife* 5.
- Bharadwaj, A.G., Kovar, J.L., Loughman, E., Elowsky, C., Oakley, G.G., Simpson, M.A., 2009. Spontaneous Metastasis of Prostate Cancer Is Promoted by Excess Hyaluronan Synthesis and Processing. *Am J Pathol* 174, 1027-1036.
- Bigg, H.F., Wait, R., Rowan, A.D., Cawston, T.E., 2006. The mammalian chitinase-like lectin, YKL-40, binds specifically to type I collagen and modulates the rate of type I collagen fibril formation. *J Biol Chem* 281, 21082-21095.
- Blanco, E., Ruiz-Romero, M., Beltran, S., Bosch, M., Punset, A., Serras, F., Corominas, M., 2010. Gene expression following induction of regeneration in *Drosophila* wing imaginal discs. Expression profile of regenerating wing discs. *BMC Dev Biol* 10, 94.
- Boison, D., Scheurer, L., Zumsteg, V., Rulicke, T., Litynski, P., Fowler, B., Brandner, S., Mohler, H., 2002. Neonatal hepatic steatosis by disruption of the adenosine kinase gene. *Proc Natl Acad Sci U S A* 99, 6985-6990.
- Buchon, N., Silverman, N., Cherry, S., 2014. Immunity in *Drosophila melanogaster*--from microbial recognition to whole-organism physiology. *Nat Rev Immunol* 14, 796-810.
- Coutinho, P.M., Henrissat, B., 1999. Carbohydrate-active enzymes: an integrated database approach, in: Gilbert, H.H., Davies, G.J., Henrissat, H., Svensson, B. (Eds.), *Recent advances in carbohydrate bioengineering*. Royal Soc. Chemistry, Cambridge, UK, pp. 3-12.
- Currie, D.A., Milner, M.J., Evans, C.W., 1988. The growth and differentiation in vitro of leg and wing imaginal disc cells from *Drosophila melanogaster*. *Development* 102, 805-814.
- D'Ambrosio, M.V., Vale, R.D., 2010. A whole genome RNAi screen of *Drosophila* S2 cell spreading performed using automated computational image analysis. *J Cell Biol* 191, 471-478.

- De Gregorio, E., Spellman, P.T., Rubin, G.M., Lemaitre, B., 2001. Genome-wide analysis of the *Drosophila* immune response by using oligonucleotide microarrays. *Proc Natl Acad Sci U S A* 98, 12590-12595.
- De Gregorio, E., Spellman, P.T., Tzou, P., Rubin, G.M., Lemaitre, B., 2002. The Toll and Imd pathways are the major regulators of the immune response in *Drosophila*. *EMBO J* 21, 2568-2579.
- Di Iorio, P., Kleywegt, S., Ciccarelli, R., Traversa, U., Andrew, C.M., Crocker, C.E., Werstiuk, E.S., Rathbone, M.P., 2002. Mechanisms of apoptosis induced by purine nucleosides in astrocytes. *Glia* 38, 179-190.
- Dolezal, T., Dolezelova, E., Zurovec, M., Bryant, P.J., 2005. A role for adenosine deaminase in *Drosophila* larval development. *Plos Biology* 3, e201.
- Dolezal, T., Gazi, M., Zurovec, M., Bryant, P.J., 2003. Genetic analysis of the ADGF multigene family by homologous recombination and gene conversion in *Drosophila*. *Genetics* 165, 653-666.
- Dolezelova, E., Nothacker, H.P., Civelli, O., Bryant, P.J., Zurovec, M., 2007. A *Drosophila* adenosine receptor activates cAMP and calcium signaling. *Insect Biochem Mol Biol* 37, 318-329.
- Dolezelova, E., Zurovec, M., Dolezal, T., Simek, P., Bryant, P.J., 2005. The emerging role of adenosine deaminases in insects. *Insect Biochem Mol Biol* 35, 381-389.
- Ellison, P.T., 2001. Reproductive ecology and human evolution. Aldine de Gruyter, New York.
- Ely, S.W., Berne, R.M., 1992. Protective effects of adenosine in myocardial ischemia. *Circulation* 85, 893-904.
- Fenckova, M., Hobizalova, R., Fric, Z.F., Dolezal, T., 2011. Functional characterization of ecto-5'-nucleotidases and apyrases in *Drosophila melanogaster*. *Insect Biochem Mol Biol* 41, 956-967.
- Fleischmannova, J., Kucerova, L., Sandova, K., Steinbauerova, V., Broz, V., Simek, P., Zurovec, M., 2012. Differential response of *Drosophila* cell lines to extracellular adenosine. *Insect Biochem Mol Biol* 42, 321-331.
- Foley, E., O'Farrell, P.H., 2004. Functional dissection of an innate immune response by a genome-wide RNAi screen. *PLoS Biol* 2, E203.
- Fredholm, B.B., 2010. Adenosine receptors as drug targets. *Exp Cell Res* 316, 1284-1288.
- Fredholm, B.B., Johansson, S., Wang, Y.Q., 2011. Adenosine and the regulation of metabolism and body temperature. *Adv Pharmacol* 61, 77-94.
- Funkhouser, J.D., Aronson, N.N., Jr., 2007. Chitinase family GH18: evolutionary insights from the genomic history of a diverse protein family. *BMC Evol Biol* 7, 96.
- Fusetti, F., Pijning, T., Kalk, K.H., Bos, E., Dijkstra, B.W., 2003. Crystal structure and carbohydrate-binding properties of the human cartilage glycoprotein-39. *J Biol Chem* 278, 37753-37760.
- Gupta, G.S., Gupta, A., Gupta, R.K., 2012. Animal lectins : form, function and clinical applications. Springer, Vienna ; New York.
- Hamid, R., Khan, M.A., Ahmad, M., Ahmad, M.M., Abdin, M.Z., Musarrat, J., Javed, S., 2013. Chitinases: An update. *J Pharm Bioallied Sci* 5, 21-29.
- Harbison, S.T., Chang, S., Kamdar, K.P., Mackay, T.F., 2005. Quantitative genomics of starvation stress resistance in *Drosophila*. *Genome Biol* 6, R36.
- He, C.H., Lee, C.G., Dela Cruz, C.S., Lee, C.M., Zhou, Y., Ahangari, F., Ma, B., Herzog, E.L., Rosenberg, S.A., Li, Y., Nour, A.M., Parikh, C.R., Schmidt, I., Modis, Y., Cantley, L., Elias, J.A., 2013. Chitinase 3-like 1 regulates cellular and tissue responses via IL-13 receptor alpha2. *Cell Rep* 4, 830-841.

- Henderson, J.F., Scott, F.W., 1980. Inhibition of animal and invertebrate cell growth by naturally occurring purine bases and ribonucleosides. *Pharmacol Ther* 8, 539-571.
- Hirsh, A.J., Stonebraker, J.R., van Heusden, C.A., Lazarowski, E.R., Boucher, R.C., Picher, M., 2007. Adenosine deaminase 1 and concentrative nucleoside transporters 2 and 3 regulate adenosine on the apical surface of human airway epithelia: implications for inflammatory lung diseases. *Biochemistry* 46, 10373-10383.
- Irving, P., Ubeda, J.M., Doucet, D., Troxler, L., Lagueux, M., Zachary, D., Hoffmann, J.A., Hetru, C., Meister, M., 2005. New insights into *Drosophila* larval haemocyte functions through genome-wide analysis. *Cell Microbiol* 7, 335-350.
- Jaakola, V.P., Griffith, M.T., Hanson, M.A., Cherezov, V., Chien, E.Y., Lane, J.R., Ijzerman, A.P., Stevens, R.C., 2008. The 2.6 angstrom crystal structure of a human A2A adenosine receptor bound to an antagonist. *Science* 322, 1211-1217.
- Johansen, J.S., Cintin, C., Jorgensen, M., Kamby, C., Price, P.A., 1995. Serum YKL-40: a new potential marker of prognosis and location of metastases of patients with recurrent breast cancer. *Eur J Cancer* 31A, 1437-1442.
- Karlsson, C., Korayem, A.M., Scherfer, C., Loseva, O., Dushay, M.S., Theopold, U., 2004. Proteomic analysis of the *Drosophila* larval hemolymph clot. *J Biol Chem* 279, 52033-52041.
- Kawamura, K., Shibata, T., Saget, O., Peel, D., Bryant, P.J., 1999. A new family of growth factors produced by the fat body and active on *Drosophila* imaginal disc cells. *Development* 126, 211-219.
- Kirkpatrick, R.B., Matico, R.E., McNulty, D.E., Strickler, J.E., Rosenberg, M., 1995. An abundantly secreted glycoprotein from *Drosophila melanogaster* is related to mammalian secretory proteins produced in rheumatoid tissues and by activated macrophages. *Gene* 153, 147-154.
- Kizaki, H., Suzuki, K., Tadakuma, T., Ishimura, Y., 1990. Adenosine receptor-mediated accumulation of cyclic AMP-induced T-lymphocyte death through internucleosomal DNA cleavage. *J Biol Chem* 265, 5280-5284.
- Kleino, A., Myllymaki, H., Kallio, J., Vanha-aho, L.M., Oksanen, K., Ulvila, J., Hultmark, D., Valanne, S., Ramet, M., 2008. Pirk is a negative regulator of the *Drosophila* Imd pathway. *J Immunol* 180, 5413-5422.
- Knight, D., Harvey, P.J., Iliadi, K.G., Klose, M.K., Iliadi, N., Dolezelova, E., Charlton, M.P., Zurovec, M., Boulianne, G.L., 2010. Equilibrative nucleoside transporter 2 regulates associative learning and synaptic function in *Drosophila*. *J Neurosci* 30, 5047-5057.
- Kuranda, M.J., Aronson, N.N., 1986. A Di-N-Acetylchitinase Activity Is Involved in the Lysosomal Catabolism of Asparagine-Linked Glycoproteins in Rat-Liver. *Journal of Biological Chemistry* 261, 5803-5809.
- Kzhyshkowska, J., Mamidi, S., Gratchev, A., Kremmer, E., Schmuttermaier, C., Krusell, L., Haus, G., Utikal, J., Schledzewski, K., Scholtze, J., Goerdts, S., 2006. Novel stabilin-1 interacting chitinase-like protein (SI-CLP) is up-regulated in alternatively activated macrophages and secreted via lysosomal pathway. *Blood* 107, 3221-3228.
- Lebon, G., Warne, T., Edwards, P.C., Bennett, K., Langmead, C.J., Leslie, A.G., Tate, C.G., 2011. Agonist-bound adenosine A2A receptor structures reveal common features of GPCR activation. *Nature* 474, 521-525.
- Leopold, P., Perrimon, N., 2007. *Drosophila* and the genetics of the internal milieu. *Nature* 450, 186-188.

- Malette, B., Paquette, Y., Merlen, Y., Bleau, G., 1995. Oviductins possess chitinase- and mucin-like domains: a lead in the search for the biological function of these oviduct-specific ZP-associating glycoproteins. *Mol Reprod Dev* 41, 384-397.
- Meng, G., Zhao, Y., Bai, X., Liu, Y., Green, T.J., Luo, M., Zheng, X., 2010. Structure of human stabilin-1 interacting chitinase-like protein (SI-CLP) reveals a saccharide-binding cleft with lower sugar-binding selectivity. *J Biol Chem* 285, 39898-39904.
- Merighi, S., Benini, A., Mirandola, P., Gessi, S., Varani, K., Leung, E., Maclennan, S., Borea, P.A., 2005. A3 adenosine receptor activation inhibits cell proliferation via phosphatidylinositol 3-kinase/Akt-dependent inhibition of the extracellular signal-regulated kinase 1/2 phosphorylation in A375 human melanoma cells. *J Biol Chem* 280, 19516-19526.
- Merighi, S., Mirandola, P., Milani, D., Varani, K., Gessi, S., Klotz, K.N., Leung, E., Baraldi, P.G., Borea, P.A., 2002. Adenosine receptors as mediators of both cell proliferation and cell death of cultured human melanoma cells. *J Invest Dermatol* 119, 923-933.
- Michaut, L., Flister, S., Neeb, M., White, K.P., Certa, U., Gehring, W.J., 2003. Analysis of the eye developmental pathway in *Drosophila* using DNA microarrays. *P Natl Acad Sci USA* 100, 4024-4029.
- Ohana, G., Bar-Yehuda, S., Barer, F., Fishman, P., 2001. Differential effect of adenosine on tumor and normal cell growth: focus on the A3 adenosine receptor. *J Cell Physiol* 186, 19-23.
- Ohkubo, S., Nagata, K., Nakahata, N., 2007. Adenosine uptake-dependent C6 cell growth inhibition. *Eur J Pharmacol* 577, 35-43.
- Pandey, U.B., Nichols, C.D., 2011. Human disease models in *Drosophila melanogaster* and the role of the fly in therapeutic drug discovery. *Pharmacol Rev* 63, 411-436.
- Pastor-Anglada, M., Errasti-Murugarren, E., Aymerich, I., Casado, F.J., 2007. Concentrative nucleoside transporters (CNTs) in epithelia: from absorption to cell signaling. *J Physiol Biochem* 63, 97-110.
- Pesch, Y.Y., Riedel, D., Patil, K.R., Loch, G., Behr, M., 2016. Chitinases and Imaginal disc growth factors organize the extracellular matrix formation at barrier tissues in insects. *Sci Rep* 6, 18340.
- Peyot, M.L., Gadeau, A.P., Dandre, F., Belloc, I., Dupuch, F., Desgranges, C., 2000. Extracellular adenosine induces apoptosis of human arterial smooth muscle cells via A(2b)-purinoceptor. *Circ Res* 86, 76-85.
- Ranok, A., Wongsantichon, J., Robinson, R.C., Suginta, W., 2015. Structural and Thermodynamic Insights into Chitooligosaccharide Binding to Human Cartilage Chitinase 3-like Protein 2 (CHI3L2 or YKL-39). *Journal of Biological Chemistry* 290, 2617-2629.
- Rathore, A.S., Gupta, R.D., 2015. Chitinases from Bacteria to Human: Properties, Applications, and Future Perspectives. *Enzyme Res* 2015, 791907.
- Samakovlis, C., Asling, B., Boman, H.G., Gateff, E., Hultmark, D., 1992. In vitro induction of cecropin genes--an immune response in a *Drosophila* blood cell line. *Biochem Biophys Res Commun* 188, 1169-1175.
- Shao, Y.Y., Lin, Z.Z., Hsu, C., Shen, Y.C., Hsu, C.H., Cheng, A.L., 2010. Early alpha-fetoprotein response predicts treatment efficacy of antiangiogenic systemic therapy in patients with advanced hepatocellular carcinoma. *Cancer* 116, 4590-4596.
- Schimpl, M., Rush, C.L., Betou, M., Eggleston, I.M., Recklies, A.D., van Aalten, D.M., 2012. Human YKL-39 is a pseudo-chitinase with retained chitooligosaccharide-binding properties. *Biochem J* 446, 149-157.
- Schneider, I., 1971. Embryonic cell lines of *Drosophila melanogaster*. *Drosoph. Inform. Serv.* 46, 111.

- Schrier, S.M., van Tilburg, E.W., van der Meulen, H., Ijzerman, A.P., Mulder, G.J., Nagelkerke, J.F., 2001. Extracellular adenosine-induced apoptosis in mouse neuroblastoma cells: studies on involvement of adenosine receptors and adenosine uptake. *Biochem Pharmacol* 61, 417-425.
- Sun, Y.J., Chang, N.C., Hung, S.I., Chang, A.C., Chou, C.C., Hsiao, C.D., 2001. The crystal structure of a novel mammalian lectin, Ym1, suggests a saccharide binding site. *J Biol Chem* 276, 17507-17514.
- Szondy, Z., 1994. Adenosine stimulates DNA fragmentation in human thymocytes by Ca(2+)-mediated mechanisms. *Biochem J* 304 (Pt 3), 877-885.
- Ui, K., Nishihara, S., Sakuma, M., Togashi, S., Ueda, R., Miyata, Y., Miyake, T., 1994. Newly established cell lines from *Drosophila* larval CNS express neural specific characteristics. *In Vitro Cell Dev Biol Anim* 30A, 209-216.
- Varela, P.F., Llera, A.S., Mariuzza, R.A., Tormo, J., 2002. Crystal structure of imaginal disc growth factor-2. A member of a new family of growth-promoting glycoproteins from *Drosophila melanogaster*. *J Biol Chem* 277, 13229-13236.
- Vierstraete, E., Cerstiaens, A., Baggerman, G., Van den Bergh, G., De Loof, A., Schoofs, L., 2003. Proteomics in *Drosophila melanogaster*: first 2D database of larval hemolymph proteins. *Biochem Biophys Res Commun* 304, 831-838.
- Wang, H.B., Sakudoh, T., Kawasaki, H., Iwanaga, M., Araki, K., Fujimoto, H., Takada, N., Iwano, H., Tsuchida, K., 2009. Purification and expression analysis of imaginal disc growth factor in the silkworm, *Bombyx mori*. *J Insect Physiol* 55, 1065-1071.
- Watanabe, T., Oyanagi, W., Suzuki, K., Ohnishi, K., Tanaka, H., 1992. Structure of the gene encoding chitinase D of *Bacillus circulans* WL-12 and possible homology of the enzyme to other prokaryotic chitinases and class III plant chitinases. *J Bacteriol* 174, 408-414.
- Wu, L.F., Li, G.P., Feng, J.L., Pu, Z.J., 2006. Molecular mechanisms of adenosine-induced apoptosis in human HepG2 cells. *Acta Pharmacol Sin* 27, 477-484.
- Wu, M.N., Ho, K., Crocker, A., Yue, Z., Koh, K., Sehgal, A., 2009. The effects of caffeine on sleep in *Drosophila* require PKA activity, but not the adenosine receptor. *J Neurosci* 29, 11029-11037.
- Xu, F., Wu, H., Katritch, V., Han, G.W., Jacobson, K.A., Gao, Z.G., Cherezov, V., Stevens, R.C., 2011. Structure of an agonist-bound human A2A adenosine receptor. *Science* 332, 322-327.
- Zhou, Y., Peng, H., Sun, H., Peng, X., Tang, C., Gan, Y., Chen, X., Mathur, A., Hu, B., Slade, M.D., Montgomery, R.R., Shaw, A.C., Homer, R.J., White, E.S., Lee, C.M., Moore, M.W., Gulati, M., Geun Lee, C., Elias, J.A., Herzog, E.L., 2014. Chitinase 3-like 1 suppresses injury and promotes fibroproliferative responses in Mammalian lung fibrosis. *Sci Transl Med* 6, 240ra276.
- Zhu, Q., Arakane, Y., Banerjee, D., Beeman, R.W., Kramer, K.J., Muthukrishnan, S., 2008. Domain organization and phylogenetic analysis of the chitinase-like family of proteins in three species of insects. *Insect Biochem Mol Biol* 38, 452-466.
- Zurovec, M., Dolezal, T., Gazi, M., Pavlova, E., Bryant, P.J., 2002. Adenosine deaminase-related growth factors stimulate cell proliferation in *Drosophila* by depleting extracellular adenosine. *Proc Natl Acad Sci U S A* 99, 4403-4408.

7. Curriculum vitae

Václav Brož

PERSONAL DETAILS:

date and place of birth: 6 March 1983, Plzen

nationality: Czech

email: vasa.broz@centrum.cz

WORK EXPERIENCE:

2009 – present **Research Scientist**
Biology Centre CAS, Institute of Entomology, Branisovska 31,
Ceske Budejovice 370 05, CZ.

EDUCATION:

From 2009 **PhD Student**
PhD programme in Molecular and Cell Biology and Genetics, Faculty of
Sciences, University of South Bohemia, Ceske Budejovice, CZ.
PhD thesis topic: Role of IDGFs and adenosine signaling in cell survival and
energy homeostasis, under the supervision of Prof. Michal Zurovec

2007 -2009 **MSc.**
Genetics and Genetic Engineering program, Faculty of Biological Sciences,
University of South Bohemia, Ceske Budejovice, CZ.
Thesis: Purification and characterization of protein IDGF2, under the supervision of
Prof. Michal Zurovec

2003 – 2007 **BSc.**
Developmental and Cell Biology program, Faculty of Biological Sciences,
University of South Bohemia, Ceske Budejovice, CZ.
Thesis: Isolation of homologs of Drosophila IDGF family from a distant
Dipteran, under the supervision of Dr. Martina Zurovcova

TEACHING ACTIVITIES:

2009 – 2011 Practices in Molecular genetics of model organisms. Faculty of Biological
Sciences, University of South Bohemia, Ceske Budejovice, CZ.

PUBLICATIONS:

Vaclav Broz, Lucie Kucerova, Lenka Rouhova, Jana Fleischmannova, Hynek Strnad, Peter J. Bryant & Michal Zurovec (2017) ***Drosophila* imaginal disc growth factor 2 is a trophic factor involved in energy balance, detoxification, and innate immunity** . *Scientific Reports*. 7:43273

Lucie Kucerova, Vaclav Broz, Arefin B, Maaroufi HO, Hurychova J, Strnad H, Zurovec M, Theopold U. (2015) **The *Drosophila* Chitinase-Like Protein IDGF3 Is Involved in Protection against Nematodes and in Wound Healing**. *Journal of Innate Immunity* 8(2):199-210

Jana Fleischmannova, Lucie Kucerova, Katerina Sandova, Veronika Steinbauerova, Vaclav Broz, Petr Simek and Michal Zurovec (2012) **Differential response of *Drosophila* cell lines to extracellular adenosine**. *Insect Biochemistry and Molecular Biology* 42: 321-331

Lucie Kucerova, Vaclav Broz, Jana Fleischmannová, Roman Sidorov, Vladimir Dolezal and Michal Zurovec (2012) **Effects of adenosine analogs on *Drosophila* adenosine receptor: the effect of adenosine analogs on cAMP signaling in *Drosophila* cells and their utility for in vivo experiments**. *Journal of Neurochemistry* 121: 383–395

CONFERENCES:

Vaclav Broz, Lucie Kucerova, David Smith, Richard David Cumingsem and Michal Zurovec (2013) **IDGF2 protects cells from toxic agents through its ability to bind specific carbohydrate moiety**. 54th Annual *Drosophila* Research Conference

ORGANIZATION OF WORKSHOPS:

Molecular Methods in Insect Physiology, České Budějovice, June 3-5, 2015

Invertebrate Innate Immunity – České Budějovice, June 3-4, 2013.

Engineered nucleases and genome editing - České Budějovice, May 21-25, 2012

STAY ABROAD:

2010 Two months stay in Prof. D. Carroll laboratory. University of Utah, Salt Lake City, USA

© for non-published parts Václav Brož

vasa.broz@centrum.cz

Role of IDGFs and adenosine signaling in cell survival and energy homeostasis

Ph.D. Thesis 2017

All rights reserved

For non-commercial use only

University of South Bohemia in České Budějovice
Faculty of Science
Branišovská 31
370 05 České Budějovice, Czech Republic

Phone: +420 387 772 244

www.prf.jcu.cz, e-mail: sekret@prf.jcu.cz